HUMAN EMBRYONIC STEM CELL MODELS OF HUNTINGTON'S DISEASE

Jonathan Christos Niclis

Bachelor of Science (Honours)

Department of Anatomy and Development
Monash University
Victoria, Australia

August 2013

**Submitted in total fulfilment of the requirements for the degree of
Doctor of Philosophy**

Notice 2

I certify that I have made all reasonable efforts to secure copyright permissions for third-party content included in this thesis and have not knowingly added copyright content to my work without the owner's permission.

Table of Contents

Chapter 3: Robust Serum Free Forebrain Differentiation Of Human Pluripotent Stem Cells

Chapter 4: Characterisation Of Forebrain Neurons Derived From Late-Onset Huntington's Disease Human Embryonic Stem Cell Lines

Chapter 5: General Discussion

Appendix I

Abstract

Huntington's Disease (HD) is a devastating neurodegenerative disorder that typically strikes during the fourth or fifth decade of life causing fatal atrophy of the striatum and other brain regions. A rare feature of this neurodegenerative disorder is the dominant inheritance pattern due to a CAG repeat expansion in exon 1 of the Huntingtin gene. The discovery that ≥35 repeats underlies HD pathology rapidly led to tremendous advances in our understanding of this complex disorder, with the identification from animal models of numerous pathological mechanisms including perturbation of anterograde and retrograde transport, neuronal activity, mitochondrial function, neurotrophic factor production, cholesterol biosynthesis and gene expression. Nonetheless, many disease mechanisms and the interplay between each remain ill defined in HD and particularly within a human cellular environment. As such there exists a need for novel *in vitro* human models to address these concerns and continue to decipher the etiology of HD.

This thesis describes the investigation and detailed characterisation of two human embryonic stem cell (hESC) lines carrying CAG_{37} and CAG_{51} repeat expansions to determine whether disease hallmarks are present in undifferentiated or neural differentiated human cells carrying HD mutations. To achieve this, a novel neural differentiation protocol was optimised for the precise comparison of genetically distinct human pluripotent stem cell lines in a high-throughput and chemically defined platform. The application of this protocol revealed HD hESCs possess the capacity to differentiate to various neural lineages with comparable efficiency to wildtype cells consistent with typical neurodevelopment, however, CAG repeat instability, minor gene dysregulation and importantly neuronal functional perturbations were identified. Consequently, HD hESCs carrying typical onset CAG repeat expansions are likely a valid and valuable tool for investigating the pathological events leading to disease onset and elucidating the hierarchical relationship between disease mechanisms. Human neuronal HD cultures additionally provide a promising resource for high-throughput *in vitro* screening of candidate therapeutics for the advancement of clinical treatment options.

General Declaration

In accordance with Monash University Doctorate Regulation 17 Doctor of Philosophy and Research Master's regulations the following declarations are made:

I hereby declare that this thesis contains no material which has been accepted for the award of any other degree or diploma at any university or equivalent institution except where declared below, and that, to the best of my knowledge and belief, this thesis contains no material previously published or written by another person, except where due reference is made in the text of the thesis.

This thesis includes 3 original papers published in peer reviewed journals and 0 unpublished publications. The core theme of the thesis is the *in vitro* modeling of Huntington's disease using human embryonic stem cells. The ideas, development and writing of all papers in thesis chapters were the principal responsibility of myself, the candidate, working within the Department of Anatomy and Developmental Biology under the supervision of Dr David S. Cram.

In the case of chapters 2, 4 and Appendix I, my contribution to the work involved the following:

With reference to Chapter 2, the pluripotent cell culture work, neural differentiation and PCRs were performed by myself while Dr Andrew Ellisdon assisted with western blot assays. Figures 1, 3 and 4 were obtained during my undergraduate (Honours) degree, and it must be noted these are reflective of approximately 25% of the total experimental contribution within this publication. The manuscript was written by myself, with guidance from Dr David Cram. Chapter 4 was predominantly my own work. Ms Anita Pinar provided raw data for Figure 1, 6 and 7 with assistance and supervision from myself. Dr John Haynes provided functional data for Figure 5. Dr Robert Jenny and Mr Walaa Alsanie assisted with neural differentiation experiments under my supervision. The experimental design and manuscript preparation was largely executed by myself. I generated data with neural differentiation and
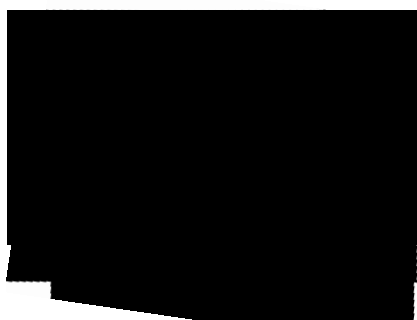
immunocytochemistry assays for Figure 4 of Appendix I and furthermore, I assisted with the preparation of this manuscript.

Overall, my contribution to the work included in this thesis was greater than 90%.

Thesis Chapter	Publication title	Publication status*	Nature and extent of candidate's contribution
2	Human embryonic stem cell models of Huntington's disease	Published	Writing of manuscript, optimization, procurement of data, analysis.
4	Characterisation of forebrain neurons derived from late-onset Huntington's disease human embryonic stem cell lines	Published	Writing of manuscript, experimental design, optimization, procurement of data, analysis.
Appendix I	Generation of induced pluripotent stem cells from human kidney mesangial cells	Published	Involved in the generation of data and manuscript preparation.

I have not renumbered sections of submitted or published papers in order to generate a consistent presentation within the thesis.

Signed: …………………………………

Date: ………20.04.2014………………………

Acknowledgments

I wish to take this opportunity to remind the reader that the technology, methods, equipment and assays utilised within this study were only possible after centuries of effort to evolve a mode of thought based upon rational and objective principles underpinned by empirical data. All scientists and members of society are indebted to the early pioneers Aristotle, Democritus, Ptolemy, Ibn al-Haytham (Alhazen), Francis Bacon, Galileo Galilei, Charles Darwin, Louis Pasteur, Gregor Mendel, Edward Jenner, Baruch Spinoza, Bertrand Russell, Francis Crick and James Watson (to name but a few). These individuals laid the groundwork for modern freethought, science, and key disciplines, often in the face of vitriol, ignorance and dogmatic resistance.

We exist during a most exciting chapter of human history where the deployment of the scientific method coupled with phenomenal technological prowess has rapidly advanced the frontiers of our knowledge. I hope this thesis plays its own small role in this process, to reveal a little more of the unknown.

All who endure difficult trials are cognisant of the immense support required from close friends and family to ensure your objectives and goals are realised. This support was often the only force keeping me fixed on the long windy road that was my PhD, out in the woods at Monash. As such what remains clearly in my mind at the end of all of this, are the many important individuals who aided me throughout my thesis years and I wish to thank them here.

I will begin firstly by thanking my parents, Nick and Ann Niclis. Both of you have been as supportive as any son could wish. I cannot thank you both enough for the scrumptious home cooked meals and generous financial support while I was a poor student. Throughout the years you provided me with all the motivation, encouragement, love and metal support I needed to become who I am today and close this chapter of my life. To my brother James, thanks for teaching me what good music should sound like to keep me energised during the many nights studying at work as well as general encouragement at home. Kat, my sister, thanks too for being supportive of me throughout the years and for the times spent going for drinks that

helped me to unwind. And to my siblings, mum and dad, thanks for tolerating my argumentative and sometimes overbearing diatribes during discussions on many a random topics.

To my partner Leona, I cannot thank you enough for all your love and support. I greatly appreciate your tolerance of the many nights I spent complaining about the tough experimental and political times through my turbulent PhD. Your help in navigating through all the trials as well as love and warmth at home were invaluable. While I may have many regrets about the PhD itself, it was what put us both in the same place and time and enabled us to meet in the first place, and for that alone I'd do it all over again.

I would also like to thank the extended members of my family for all their interest and encouragement over the years, and particularly my grandparents for continually supporting my educational aspirations and trying their best to understand what I do despite language and generational differences.

To my primary supervisor Dr David Cram, thank you for your enthusiasm and encouragement over the years. It has been a long and arduous journey but I think we're both glad it is now complete and has come off as successful as we could have hoped! There have been plenty of stressful moments but they have prepared me well for a future in science. Your guidance not only in the tough moments but throughout the PhD has given me valuable insight into what it means to be a researcher and how to be resilient and competitive. Thanks also to my secondary supervisor Prof Claude Bernard for your advice and help whenever I sought it. Also to my original secondary supervisor, Prof Alan Trounson, you were an inspiration to me when I began my research career during my honours and early PhD at Monash. The enthusiasm you have for the altruistic and boundary-breaking aims of our profession are a key reason I've fallen in love with and chosen to continue on this path.

To Profs Ed Stanley and Andrew Elefanty, I cannot stress how far beyond the call of duty you both went to support me and my research project. The experimental planning, reagents and career advice you gave me was indispensible and will never be

forgotten. I hope that I will repay this debt by adhering to all your advice and providing my assistance to future young acolytes of science. To another mentor of mine I am extremely grateful. Dr Mirella Dottori generously donated many hours (whenever I requested them) over several years to helping me plan neural differentiation experiments and her sage guidance was invaluable to preventing me from being lost in the rabbit hole that is differentiation protocol development! To Dr Steve Petratos, similar thanks for helping me to navigate and learn the basics of neural development whenever I asked. And to Dr Clare Parish, your willingness to give me a go, entrust me with major responsibility, push me as a scientist and build my skills and knowledge at the Florey after my PhD has immensely boosted my confidence and provided me with the motivation to complete this thesis.

Numerous other scientists, far more wiser than I, such as Elizabeth Ng, Phil Heraud Sharon Ricardo, Richard Boyd, Chris Siatskas and Mark Malin (Marky Mark), all provided me with an array of assistance that I could not have done without over the years, whether it be technical lab assistance, helping me navigate the politics of our field, or giving my career a boost by helping me with experiments or engaging me for collaborations locally and abroad. There were also many other students and staff over the years, Payal, Bi, Raf, Jurbs, Julie, Jen, Chew-li, Melly, Dave Elliott, Vanta, the Greeks (Koula, Maggie and Kathy) who've all provided support, advice and relief from work and to all of you thanks for your help. In particular I must mention Dr Chris Siatskas who gave me advice whenever I needed it, thank you so much for never hesitating to spend 15 or 150 minutes to help a struggling PhD student out and keep my head on straight. You were an invaluable mentor, with your advice ranging from the technical to the emotional and I'll never forget the unconditional help you gave me mate!

Most importantly, in the time of one's PhD there is a close group of fellow ~~slaves~~ PhD students that share so many of the horrible experiences and exciting moments. For me this was Mali, Marco, Christina, Robbie, Timmy, Andy and Sean. I still laugh at the memories of our expeditions to source dumplings/Nandos/Thai yim/Indian late at night, the long debates on the merit of each option, and the strange phenomenon where despite agreeing we would take a quick break from work, our food runs invariably went on for a couple of hours longer than anticipated! … odd but I think a

similar thing happened with our coffee breaks, bitch session breaks etc etc. I'll also never forget the fun Marco and I had scaring Mali in the lab late at night! Thanks to Timmy for the FACS help, Marco for his intellectual debates on any scientific topic (whether related to our projects or not), Mali for her continual advice from the year ahead of me which helped keep me in check and grounded (even if she didn't realise it) and to and Chrissy for some cool heavy metal rock tunes to hear float across from her neighbouring office late at night as well as thesis preparation help. After all those years, all the fun and support we lent each other, I think we bonded as siblings and in many ways I'm truly sad that those days are behind us. I hope we'll all stay connected in the years ahead. To another student who joined the lab to the end of my PhD time, Walaa, I am greatly appreciative of the support you gave in helping me cope with the political dynamics of our group, without an insider to lean on and 'discuss' with I think we both couldn't have lasted! Cheers for the unrestrained hospitality in Saudi too!

I also wish to acknowledge the role close friends of mine have played in helping me maintain a connection to the real world during the years of my PhD. I don't know how I could have made it through without the many moments of pensive universal reflection and contemplation, robust political discourse and holidays together with Diaco and Boris, and of late, Walaa too. Thanks to Pete and Marco for the many gym sessions at the height of my PhD woes that provided me with an apt outlet for my frustration and a 15kg boost to my muscle mass! (which I promptly lost after leaving Monash hahaha). To Boris, Diaco, Ash, Nik R, Pete, Nick T, Dean and Zaf I cheers for the numerous laid back coffee catch-ups at Glenny and many nights I can't remember across Melbourne's clubs, bars, pubs, festivals and the most hipster dive bars we could find!

So that does it, finally finished, this was the last thing I had to write! I suppose if you're still reading I'll leave you with one last thought: The gradual and methodical charting of the vast, hidden ocean of knowledge is the key to humanity's mastery of the universe, and as I've found, it's an exhilarating pleasure and I hope to never stop discovering!

Research Output

Manuscripts

- **Niclis JC**, Pinar A, Haynes JM, Alsanie W, Jenny R, Dottori M, Cram DS (2013). Characterisation of forebrain neurons derived from late-onset Huntington's Disease human embryonic stem cell lines. <u>Frontiers in Cellular Neuroscience</u>, 7:1-13.

- Alsanie WF, **Niclis JC**, Petratos S (2013) Human embryonic stem cell derived oligodendrocytes: Protocols and perspectives. <u>Stem Cells and Development</u>. ePublication ahead of print: April 2013.

- Song B, **Niclis JC**, Alikhan MA, Sakkal S, Sylvain A, Kerr PG, Laslett AL, Bernard CA, Ricardo SD (2011). Generation of induced pluripotent stem cells from human kidney mesangial cells. <u>Journal of the American Society of Nephrology</u>, **22**(7):1213-1220.

- **Niclis** JC, Trounson AO, Dottori M, Ellisdon AM, Bottomley SP, Verlinsky Y, Cram DS. (2009). Human Embryonic Stem Cell Models of Huntington's Disease, <u>Reproductive Biomedicine Online</u>, **19**(1):106-113.

- **Niclis** JC and Murphy S, Parkinson D, Amr Z, Knoechel C, Le Gross M, Larabelle C, Cram DS, Heraud P (*in preparation*). Tomographic Reconstruction of Human Stem Cells using Transmission X-Ray Microscopy, <u>Journal of Biophotonics.</u>

- **Niclis JC**, Stanley EG, Elefanty AG, Cram DS, Ricardo, SD, Dottori M (*in preparation*). Robust neural differentiation of human pluripotent stem cells to define early neural precursor subsets.

Invited Seminars

International

- "Human embryonic stem cell biology: Techniques and Frontiers," Taif University, Saudi Arabia – June 2011

National

- "Huntington's Disease: The Potential Of Human Embryonic Stem Cell Modelling," 2nd Annual Australia-China Stem Cells Workshop**,** Melbourne, Australia – November 2009

Conference Poster Presentations

International

- Song B, **Niclis JC**, Alikhan MA, Sakkal S, Sylvain A, Kerr PG, Laslett AL, Bernard CA, Ricardo SD. (2011). Generation of induced pluripotent stem cells from human kidney mesangial cells. World Congress of Nephrology, Vancouver, Canada

- **Niclis JC**, Trounson AO, Dottori M, Ellisdon AM, Bottomley SP, Verlinsky Y, Cram DS. (2009). Human Embryonic Stem Cell Models of Huntington's Disease. International Society of Stem Cell Research 7th Annual Meeting, Barcelona, Spain

- **Niclis JC**, Trounson AO, Dottori M, Ellisdon AM, Bottomley SP, Verlinsky Y, Cram DS. (2007). Human Embryonic Stem Cell Models of Huntington's Disease. International Society of Stem Cell Research 5th Annual Meeting, Cairns, Australia

National

- Fernando CV, Blakely BD, Bye CR, **Niclis JC**, Turner BJ, Kele J, Stenman J, Arenas E, Parish CL. (2012). Diverse roles for Wnt7a in ventral midbrain neurogenesis and dopaminergic axon morphogenesis. Australasian Society for Stem Cell Research 5th Annual Meeting, Adelaide, South Australia

- **Niclis JC**, Stanley EG, Elefanty AG, Ricardo SD, Cram DS. (2011). High Throughput Neuronal Differentiation of Human Pluripotent Stem Cells in Serum Free & Feeder Free Conditions. Australasian Society for Stem Cell Research 4th Annual Meeting, Blue Mountains, New South Wales

- **Niclis JC**, Trounson AO, Dottori M, Ellisdon AM, Bottomley SP, Verlinsky Y, Cram DS. (2010). Human Embryonic Stem Cell Models of Huntington's Disease. Australasian Society for Stem Cell Research 3rd Annual Meeting, Melbourne, Victoria

- **Niclis JC**, Trounson AO, Dottori M, Ellisdon AM, Bottomley SP, Verlinsky Y, Cram DS. (2008). Human Embryonic Stem Cell Models of Huntington's Disease.

Australasian Society for Stem Cell Research 1st Annual Meeting, Brisbane, Queensland

- **Niclis JC**, Trounson AO, Dottori M, Ellisdon AM, Bottomley SP, Verlinsky Y, Cram DS. (2007). Human Embryonic Stem Cell Models of Huntington's Disease. International Brain Research Organization Huntington's Disease Satellite Meeting, Melbourne, Victoria

Awards

- Best 4th /5th year PhD student award, MISCL Annual Student Symposium - 2011
- Travel award from the Australasian Society of Stem Cell Research to attend the 4th Annual ASSCR Meeting – 2011
- Successful competitive research proposal approval for beam-time on the Advanced Light Source synchrotron (Berkeley, California) – 2010
- Australian Synchrotron Travel Funding Grant - 2010
- Best Scientific Poster Presentation, 5th Annual ISSCR Meeting – 2007
- Travel award from the ASCC to attend the 5th Annual ISSCR Meeting – 2007
- Australian Postgraduate Award – 2007

Abbreviations

7-DHCR	Dehydrocholesterol Reductase	mRNA	Messenger Ribonucleic Acid
BDNF	Brain Derived Neurotrophic Factor	miRNA	Micro Ribonucleic Acid
BM-MSC	Bone Marrow Mesenchymal Stem Cell	MRI	Magnetic Resonance Imaging
BMP	Bone Morphogenic Protein	MSN	Medium Spiny Neuron
CNS	Central Nervous System	NBM	Neurobasal Media
DMEM	Dulbecco's Modified Eagle Medium	NCAM	Neural Cell Adhesion Molecule
DMSO	Dimethyl sulfoxide	NDEB	Neural Directed Embryoid Body
DNA	Deoxyribonucleic Acid	NMDAR	N-methyl-D-aspartate Receptor
DRD2	Dopamine Receptor D2	NPC	Neural Precursor Cell
DRP1	Dynamin-1-like protein	NSC	Neural Stem Cell
DMD	Duchenne Muscular Dystrophy	OCT4	Octamer-Binding Transcription Factor 4
EB	Embryoid Body		
EGF	Epithelial Growth Factor	OLIG2	Oligodendrocyte Transcription Factor
EpCAM	Epithelial Cell Adhesion Moleculue		
FBS / FCS	Fetal Bovine/Calf Serum	OTX2	Orthodenticle Homeobox 2
FOXG1	Forkhead Box G1	P/S	Penicillin/Streptomycin
F-PCR	Fluorescent PCR	PAX6	Paired Box Protein 6
FACS	Flow Activated Cell Sorting	PDGFa	Platelet Derived Growth Factor a
FGF2/b	Fibroblast Growth Factor basic/2	PENK	Proenkephalin
GABA	Gamma Aminobutyric Acid	PFA	Paraformaldehyde
GAD67	Glutamic Acid Decarboxylase 67	PGC-1a	Peroxisome Proliferator-Activated Receptor g, Coactivator 1 a
GFAP	Glial Fibrillary Acidic Protein		
GFP	Green Fluorescent Protein	PGD	Pre-implantation Genetic Diagnosis
HAP1	Huntingtin Associated Protein 1		
HD	Huntington's Disease	PolyQ	Poly Glutamine
hECC	Human embryonic carcinoma cells	PVA	Polyvinyl Alcohol
HEPES	(4-(2-hydroxyethyl)-1-piperazineethanesulfonic acid)	qRT-PCR	Quantitative Real Time PCR
		REST	RE1-Silencing Transcription Factor
hESC	Human Embryonic Stem Cell	RILP	REST-interacting LIM domain protein
hiPSC	Human Induced Pluripotent Stem Cell		
HMGCoAR	3-hydroxy-3-methylglutaryl CoA Reductase	RISC	RNA-induced silencing complex
		RNA	Ribonucleic Acid
hPSC	Human Pluripotent Stem Cell	ROCK	Rho-Associated Protein Kinase
HTT	Huntingtin (protein)	RT-PCR	Reverse Transcription PCR
HTT	Huntingtin (transcript)	SHH	Sonic Hedgehog
ICM	Inner Cell Mass	SMAD	Mothers Against Decapentaplegic
ITS-X	Insulin Transferrin Selenium-X	SOX2	Sex determining region Y-box 2
IVF	In Vitro Fertilisation	SREBP1	Sterol Regulatory Element-Binding Protein 1
KSR	Knockout Serum Replacement		
MAP2	Microtubule Associated Protein 2	SSEA1	Stage Specific Embryonic Antigen 1
MD	Muscular Dystrophy	SSEA3	Stage Specific Embryonic Antigen 3
MEF	Mouse Embryonic Fibroblast	SSEA4	Stage Specific Embryonic Antigen 4
mESC	Mouse Embryonic Stem Cell	TFEB	Transcription Factor EB
mGluR	Metabotropic Glutamate Receptor	UPS	Ubiquitin-Proteasome System
mHTT	Mutant Huntingtin (protein)		

CHAPTER 1

Literature Review

1.0 Huntington's Disease

Huntington's Disease (HD) is an autosomal dominant neurological disorder that affects approximately 1 in 10, 000 individuals worldwide. HD is a late onset disease that typically manifests between the 4th and 5th decade of life and is caused solely by a single genetic mutation. A groundbreaking international collaboration between 58 scientists, forming the Huntington's Disease Collaborative Research Group, first identified the location of the culprit mutation at the genomic location of 4p16.3 and renamed the gene huntingtin (THDCRG, 1993).

In HD individuals, a trinucleotide CAG repeat tract within exon 1 is extended, and disease alleles ($CAG_{\geq 35}$) exhibit an age dependent penetrance. The lowest disease range (CAG_{36-39}) is associated with a later age of onset than typically reported (Snell et al., 1993;McNeil et al., 1997). CAG_{40+} alleles are associated with full penetrance and once reaching extreme expansion lengths (CAG_{60+}) result in juvenile or infantile onset that are characterised by egregious symptoms (Squitieri et al., 2006). The correlation between the CAG repeat and age of onset is approximately 50%, with further influence due to environmental and genetic factors (Andrew et al., 1993;Wexler et al., 2004). Genetic contributors include polymorphisms within the *HTT* gene that may alter the age of onset (Andrew et al., 1993;Snell et al., 1993;Vuillaume et al., 1998;Rubinsztein and Carmichael, 2003) and multiple loci revealed by genomic investigations such as the HD-MAPS study (Li et al., 2003;Li et al., 2006;Gayan et al., 2008).

Clinical symptoms gradually worsen from the age of onset and include broad motor dysfunctions, both involuntary movements and abnormalities of voluntary movements, and were the basis for the early diagnosis of HD as *chorea*, a derivation of Greek word 'dance'. Patients also present with psychiatric disturbances and impairment of higher cognitive functions such as reasoning and memory (Zuccato et al., 2010). Patients eventually lose the ability to talk and require full time care before succumbing 10-20 years after onset, predominantly to aspiration pneumonia from swallowing difficulties (Zuccato et al., 2010). No cure presently exists and the few available treatments fail to target the underlying causes of pathology.

1.1 Wildtype Huntingtin

HTT is a 350kDa protein encoded by 67 exons that is ubiquitously expressed within humans, mice and rats with the highest concentrations in CNS neurons (DiFiglia et al., 1995;Trottier et al., 1995;Ferrante et al., 1997). HTT exhibits an extensive subcellular distribution, associating with numerous organelles including mitochondria, vesicles, the nucleus and endoplasmic reticulum, as well as exhibiting neural specific association with microtubules and vesicles within neurites and synapses (DiFiglia et al., 1995;Velier et al., 1998;Hoffner et al., 2002).

HTT is highly conserved across vertebrate species with 80% sequence homology between *Homo sapiens* and *Fugu* fish (Zuccato et al., 2010). Expression of HTT is critical during development, with embryonic lethality in *HTT$^{-/-}$* knockout mice at embryonic day 8.5 before gastrulation begins (Duyao et al., 1995;Nasir et al., 1995). Homologous *HTT* genes are found outside the subphylum Vertebrata, although appear to play a less critical developmental role with *HTT$^{-/-}$ Drosophila* embryos able to reach maturity, albeit with survival and neurological complications (Zhang et al., 2009). The discrepancy between rodent and *Drosophila* null mutants may be explained by the acquisition of novel neuronal activities by the *HTT* gene in dueterostomes and particularly vertebrates and mammals (Cattaneo et al., 2005).

HTT engages in unique roles within neuronal cells that may account for the CNS specificity of pathology. HTT expression is concentrated within the brain, but even more so within cortical neurons of layers III and V which project to the striatum to provide the neurotrophic factor BDNF (Fusco et al., 1999). Further, BDNF (and numerous other neural genes) are regulated in part by HTT interactions with a master transcriptional repressor and this complex becomes destabilised by mutant length polyglutamine tracts. Additionally, HTT has been shown to play a role in axonal transport in *Drosophila* (Gunawardena et al., 2003) and mice (Trushina et al., 2004).

HTT also contributes to synaptic activity by interacting with proteins essential to endo- and exocytosis, vital processes for the release and re-absorption of neurotransmitters at the synaptic cleft (Smith et al., 2005). Further, HTT interacts

with synaptic transmission proteins (Smith et al., 2005) and neurotransmitter receptor proteins (Sun et al., 2001), and these may be aberrantly modulated in a disease state. The promiscuous involvement of wildtype HTT in the CNS implies a multifaceted and essential function in neuronal activity.

Additionally, studies indicate decreased levels of wildtype protein in itself represents a component of neurodegeneration. HTT involvement in *Drosophila* and mouse axonal transport were discovered after reductions in wildtype protein levels caused perturbation of anterograde and retrograde transport (Gunawardena et al., 2003;Trushina et al., 2004). Further, merely increasing or depleting wildtype HTT expression alters levels of important REST regulated neural genes (Zuccato et al., 2007). In addition, homozygous patients exhibit increased disease severity (Squitieri et al., 2003), and some HD mouse models exhibit exacerbated disease phenotypes in homozygous littermates (Reddy et al., 1998). Further, YAC128 mice crossed with another strain to produce offspring that also carry two or zero copies of endogenous wildtype *Htt* alleles, show increases in the severity of neurodegeneration, motor and behavioural dysfunction in the YAC128 + $Htt^{-/-}$ littermates (Van Raamsdonk et al., 2005). Further emphasising this proposition, overexpression of wildtype huntingtin in YAC128 mice reduces some aspects of neurodegeneration (Van Raamsdonk et al., 2006).

1.2 Huntingtin Disease Mechanisms and Cellular Pathologies

The pernicious activity of mutant HTT (mHTT) is a complex phenomenon, involving the disruption of multiple components of the cellular machinery in concert. Decades of investigative analysis have not decoded the sequence of disease mechanisms. The following sections describe mechanisms that are proposed to contribute greatest to the development of clinical pathology and decline.

1.2.1 Gene expression chaos

1.2.1.1 Protein coding gene dysregulation

Postmortem human brain samples assessed with *in situ* hybridization provided the first observations of altered mRNA transcript levels in HD, specifically those encoding signalling neuropeptides (i.e. enkephalin, substance P, somatostatin) and neurotransmitter receptors (NMDAR subunits, Dopamine D1 and D2 receptors) (Augood et al., 1996;Norris et al., 1996;Arzberger et al., 1997;Augood et al., 1997). Gene expression studies following these initial findings confirmed widespread neurotransmitter transcript alterations (Cha et al., 1998) and were followed by comprehensive mRNA microarray probing of the transcriptome.

Rodent models of HD have proven a principal focus for central nervous system (CNS) microarray analyses, identifying transcript alterations more commonly decreased than increased compared to wildtype controls, with some alterations initiating pre-onset stages and steadily enhanced with disease progression (Luthi-Carter et al., 2000;Fossale et al., 2002;Luthi-Carter et al., 2002a;Luthi-Carter et al., 2002b;Sipione et al., 2002). Predictably, altered transcripts were typically observed to encode genes involved in pathways associated with HD symptoms including neurotransmitter receptors, synaptic transmission, calcium homeostasis, intracellular signalling, transcriptional processes, neuroinflammation, vesicle trafficking, cholesterol biosynthesis and cytoskeletal proteins (Luthi-Carter et al., 2000;Chan et al., 2002;Fossale et al., 2002;Luthi-Carter et al., 2002a;Luthi-Carter et al., 2002b;Sipione et al., 2002;Crocker et al., 2006;Cha, 2007;Hodges et al., 2008). The first elucidation of the mechanistic process by which mHTT exert transcriptional dysregulation came from observations that polyglutamine tracts may directly bind and sequester transcriptional co-factors, such as the ubiquitous activator Sp1, to inhibit downstream promoter binding to the dopamine receptor D2 gene promoter (Dunah et al., 2002). The centrality of transcriptomic dysregulation in HD is highlighted HD-inducible striatal cell models that demonstrate mRNA alterations within 12 hours of mHTT expression (Sipione et al., 2002) and further show characteristic striatal neurodegeneration is mirrored by unique transcript dysregulation throughout this structure (Cha, 2000;Luthi-Carter et al., 2000;Luthi-Carter et al., 2002b). Intriguingly,

recent investigations have revealed that cellular transcriptome disruption is not restricted to the CNS as discussed later in this section.

1.2.1.2 Non-protein coding gene dysregulation

Non-coding RNAs are divided into numerous sub-categories of which the most understood are micro-RNAs (miRNAs) of which over 900 have now been identified (miRBase release 18.0, http://microrna.sanger.ac.uk). Gene regulation by miRNAs involves the transportation of mature miRNA fragments within RNA-induced silencing complexes (RISCs) to processing bodies (P-bodies) where miRNAs bind to target mRNAs and either degrade targets or inhibit transcription (Bartel, 2004;Kosik, 2006).

The CNS expresses significant numbers of miRNAs that are essential during development and adulthood, some of which are ubiquitously expressed or restricted to specific neural cell types or sub-populations (Sempere et al., 2004;Kosik, 2006;Bak et al., 2008). Further, miRNAs are also found at presynaptic terminals where they have been found to regulate BDNF and promote dendrite growth (Vo et al., 2005;Klein et al., 2007). Changes in miRNA expression have been linked in a correlative or causative manner to numerous degenerative disorders including schizophrenia, Tourette's syndrome, DiGeorge syndrome and general neuropathology in animal models (Buckley et al., 2010).

Emerging studies are linking dysfunction of the complex miRNA regulatory system with HD etiology. Firstly, wildtype HTT performs a stabilising role in the miRNA biogenesis pathway itself, between Argonaute proteins (core components of the RISC) and P-bodies. Polyglutamine expansions in HTT perturb this interaction, reducing P-bodies and overall activity of this regulatory system (Savas et al., 2008). Secondly, mHTT interacts with miRNA regulators, such as p53 and RE1-Silencing Transcription Factor (REST), resulting in aberrant modulation of downstream miRNA expression in HD (Marti et al., 2010). Interestingly, miRNAs that exhibit brain region specific alterations in HD provided an additional explanation for the regional selectivity of this disorder (Johnson et al., 2008;Johnson and Buckley, 2009).

The master regulator REST controls numerous miRNAs including miR-7, -9, -124, -129, -132, -137 and -184, that experience altered expression levels in HD (Johnson et al., 2008;Packer et al., 2008;Johnson and Buckley, 2009). Interestingly, miR-9 is a bi-functional miRNA that dually silences REST and a co-repressor (CoREST), generating a double negative feedback loop, that is disrupted by aberrant mHTT influence on REST (Packer et al., 2008). Changes in individual miRNAs can have dramatic implications, for example, miR-124 contributes to the maintenance of neuronal cell fate by silencing large numbers of non-neuronal genes (Conaco et al., 2006;Visvanathan et al., 2007) and miR-124 targets are enriched among HD upregulated gene lists (Johnson and Buckley, 2009).

1.2.2 Striatal starvation of BDNF

The role of BDNF in HD has been explored since initial observations of MSNs dependency on cortical anterograde shuttling of BDNF (Altar et al., 1997) and the finding that BDNF knockout mice present with motor abnormalities reflective of HD transgenic and knockin models (Baquet, 2004). Significant *in vitro* reduction of BDNF expression in an immortalized CNS line, and of *in vivo* levels within the cortex and striatum of HD transgenic mice, was demonstrated definitively for the first time by Elena Cattaneo's laboratory at the University of Milan (Zuccato, 2001). Corroborating these findings are reductions in BDNF levels within the cerebral cortex of HD post-mortem patient tissues by ~50% (Zuccato et al., 2008) and numerous animal models that demonstrate BDNF downregulation immediately after onset (Zuccato et al., 2005;Zuccato and Cattaneo, 2007).

Wildtype neural cells exhibit cytoplasmic sequestration of the transcriptional repressor REST in a complex that includes proteins such as Huntingtin Associated Protein 1 (HAP1), REST-interacting LIM domain protein (RILP) and HTT itself (**Figure 1.1**; Shimojo and Hersh, 2006). Expanded polyQ tracts of mHTT proteins destabilise this complex and REST translocates to the nucleus, binding to a RE1 element within BDNF promoter II to repress transcription (Zuccato et al., 2007;Zuccato and Cattaneo 2007). Intriguingly, REST regulates approximately 2400 principally neural genes (Johnson et al., 2006;Johnson et al., 2008) and the preferential downregulation of

REST mediated neural genes is consistent with HD CNS microarray expression studies (Johnson and Buckley, 2009). The involvement of REST in non-coding RNA and epigenetic regulation exacerbates the complexity of this pathological mechanism; themes extensively reviewed in conjunction with targeted therapeutic strategies previously (Buckley et al., 2010).
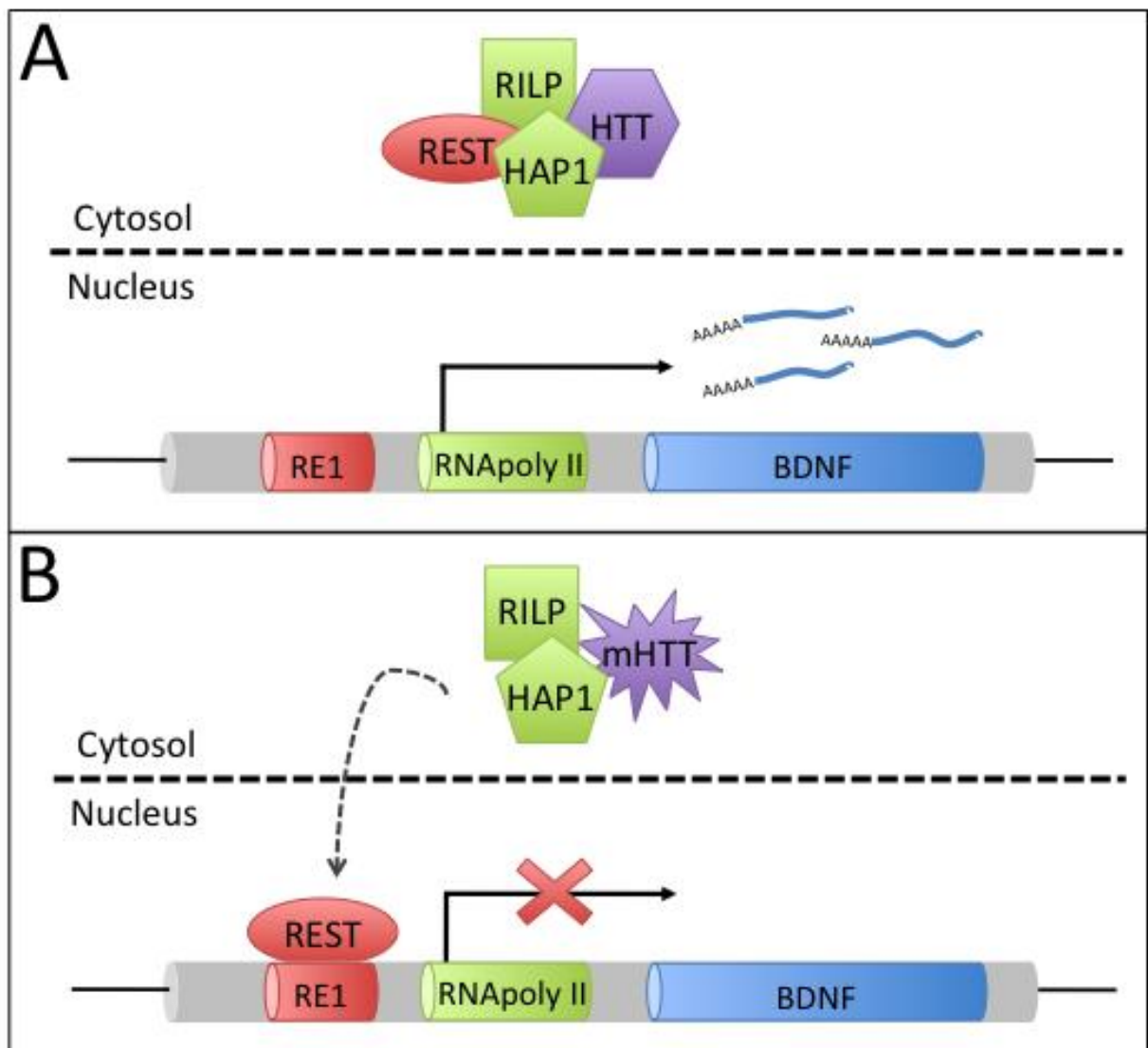
Figure 1.1: Transcriptional dysregulation of BDNF as a consequence of mHTT. In neural cells the master regulator REST exists within a complex also comprising HTT, sequestering this transcription factor within the cytosol **(A)**. PolyQ expansions of mHTT destabilise this complex, enabling REST to translocate to the nucleus and repress >100 genes containing target RE1 binding sequences, including the prominent neurotrophic factor, BDNF **(B)**.

1.2.3 Cholesterol dysfunction

Approximately 25% of total human cholesterol is contained within the brain (Dietschy and Turley, 2004) and almost three quarters of this produced locally by oligodendrocytes, predominantly during development (Jurevics and Morell, 1995). Cholesterol is contained within neuronal membranes and lipid rafts where they are required for the functional properties of ion channels and transmitter receptors, playing a crucial role in the initiation, propagation and maintenance of signal transduction (Pfrieger, 2003;Allen et al., 2007). Further, cholesterol promotes neurite outgrowth during development (Hayashi et al., 2004) and supports synaptogenesis (Mauch et al., 2001;Goritz et al., 2005).

Evidence of disrupted cholesterol biosynthesis within HD model systems is emerging and may contribute significantly to disease development. Sterol regulatory element binding-proteins (SREBPs) regulate numerous cholesterol biosynthesis genes that are downregulated in HD rodent cell lines (Sipione et al., 2002) and the striatum and cortex of R6/2 mice (Valenza et al., 2005). Two cholesterol precursors and both the gene expression and functional activity of a rate-limiting enzyme, 3-hydroxy-3-methylglutaryl CoA reductase (HMGCoAR), are decreased in R6/2 mice, and this is even observed before disease onset (Valenza et al., 2007b). Similar observations from the same research group led by Elena Cattaneo were made in the CNS and blood of a separate HD model, YAC128 mice (Valenza et al., 2007a). Further supporting a role for cholesterol in HD, whole body metabolism of this lipid is impaired in HD patients at pre-onset and post-onset stages, who exhibit reduced cholesterol precursor and metabolite levels in CNS and blood samples (Duane and Javitt, 1999;Leoni et al., 2011) as well as decreased total cholesterol in plasma samples (Markianos et al., 2008). Reductions in cholesterol synthesis may represent an avenue for potential therapeutic intervention and one targetable before disease onset.

1.2.4 Mitochondrial dysfunction

Neurons consume substantial levels of ATP for normal cellular function placing considerable demands on mitochondria, and any disruption of cellular energy production rapidly perturbs neuronal homeostasis. Mitochondrial dysfunction occurs

in HD and thus is considered a key contributor to disease pathology (Lin and Beal, 2006;Bossy-Wetzel et al., 2008).

Several pathways of mitochondrial dysfunction are activated by mHTT, even disruption of the core pathway of ATP production, the electron transport chain, by reducing activity of enzymes within the oxidative phosphoryation mitochondrial component (Zuccato et al., 2010). Further mitochondrial alterations in HD are the fission and fusion cycles that are mediated by large GTPases of the dynamin family, with fission regulated by DRP1 and fusion by Mitofusin. Expanded polyQ tracts increase mHTT and DRP1 binding in the mitochondria which subsequently disrupts the delicate fission-fusion balance in favour of the former, compromising cellular activity (Song et al., 2011). Corroborating this mechanistic theory are reports of increased fission and small sized mitochondria, particularly within striatal MSNs of HD post-mortem tissue samples, which are linked to increased expression of the protein DRP1 (Kim et al., 2010;Shirendeb et al., 2011). Increased mitochondrial fission, which occurs in a poly-Q dependent manner, also perturbs anterograde and retrograde transport velocities to aggravate neuronal degeneration in both knockin mice and human patients (Song et al., 2011). These events occur before aggregate formation and apoptosis and interactions between DRP1 and mHTT are even seen to occur before disease onset in mice (Song et al., 2011).

Mitochondrial biogenesis is also disrupted in HD, and due in part to mHTT interactions with the promoter sequence of the mitochondrial transcription regulator peroxisome proliferator-activated receptor-α co-activator-1α (PGC-1α), which is itself down regulated (Cui et al., 2006). The potential centrality of PGC-1 α to regional specific neuronal degeneration is demonstrated by findings that striatal MSNs exhibit a positive correlation between PGC-1α down regulation and disease severity (Kim et al., 2010), and further knockout PGC-1α mice exhibit the highest levels of neuropathology within the striatum (Lin et al., 2004;Leone et al., 2005). Reinforcing this supposition, HTT knockin and PGC-1α knockout crossed mice present with egregious striatal degeneration and motor abnormalities (Cui et al., 2006).

The calcium uptake capacity of mitochondria is also impaired in neural cells of HD mice and is detectable months before disease onset (Panov et al., 2002) and is also observed in non-CNS tissue of patients and HD mouse models, including lymphoblasts and skeletal muscles (Panov et al., 2002;Gizatullina et al., 2006). In line with other pathological mechanisms, striatal neurons appear particularly sensitive to this deficit (Brustovetsky et al., 2005), however, the precise impact of perturbed calcium homeostasis is unclear.

1.2.5 Excitotoxicity at the corticostriatal junction

Glutamate release from the cortex to striatal neurons constitutes a key survival cue and is significantly disrupted in HD. Glutamate NMDAR receptors are reduced in concomitance with decreased receptor binding affinities in patients (London et al., 1981;Young et al., 1988;DiFiglia, 1990;Dure et al., 1991), and this represents a significant hallmark that is also measurable before onset (Albin et al., 1990). Further, glutamate agonists, most commonly quinolinic acid, injected into the striatum of wildtype mice (Schwarcz et al., 1984;Beal et al., 1986;Sanberg et al., 1989) and primates (Hantraye et al., 1990;Ferrante et al., 1993) cause a phenotype akin to HD. HD induced disruption of striatal NMDAR activity and increased NMDA sensitivity to excitotoxicity is partially due to decreases in levels of a striatal enriched NMDAR subunit isoform NR2B, a consequence of attenuated transcription and abnormally high proteolysis (Arzberger et al., 1997;Zeron et al., 2002;Cowan et al., 2008). Glutamate excitotoxicity may be exacerbated further by decreases in metabotropic glutamate receptor, mGluR2, identified in mouse models (Cha et al., 1998;Luthi-Carter et al., 2000).

Glial uptake of neurotransmitters at the synaptic cleft maintains neuronal microenvironments and appears dysregulated in HD, implicating non-neuronal cells in pathology. Removal of glutamate from the extracellular space is impaired due to downregulation of the glial neurotransmitter transporter GLT-1 both within animal HD models and post-mortem patient samples (Arzberger et al., 1997;Shin et al., 2005;Hassel et al., 2008;Estrada-Sanchez et al., 2009). This impairment of glutamate

clearance from the synaptic cleft causes excitotoxicity, and is partially abrogated by increasing GLT1 expression in R6/2 mice (Miller et al., 2008).

1.2.6 Intransigent mHTT and the vexing role of aggregates

HD belongs to a distinct group of approximately nine neurodegenerative disorders, including several spinocerebellar ataxias, all of which share an expanded CAG repeat region and polyglutamine (polyQ) tract in various proteins, and a common hallmark of all these disorders are aggregates of the respective mutant proteins.

Early studies identified aggregates in neurons from all cortical layers and the striatum of HD postmortem tissue samples (DiFiglia et al., 1997). Aggregates exist in both the nucleus and cytoplasm, with mostly N-terminal mHTT fragments associated with the former and both N-terminal and full-length mHTT with the latter (Cooper et al., 1998;Hackam et al., 1998;Martindale et al., 1998). However, whether aggregates are indicative of toxicity or represent a protective countermeasure still remains highly controversial.

Early theories purported a toxic role of HD aggregates, which are targeted for, yet resilient to, degradation by the ubiquitin-proteasome system (UPS). Although and aggregates are readily ubiquitinated and arise before onset in some mouse models (Davies et al., 1997;Bence et al., 2001;Waelter et al., 2001), the UPS has difficulties in clearing them (Bence et al., 2001;Verhoef et al., 2002;Holmberg et al., 2004). Aggregates also sequester numerous subunits and chaperones of the UPS impairing the function of this clearance system (Jana et al., 2001;Sakahira et al., 2002). UPS dysfunction is exhibited predominantly within neurons, as opposed to glia, and may account for observed preferential susceptibility (Tydlacka et al., 2008). Further, the addition of proteasome inhibitors (i.e. lactacystin) increases aggregate formation (Martín-Aparicio et al., 2001;Ravikumar et al., 2002;Zhou et al., 2003;Fukui and Moraes, 2007), whereas overexpression of components of the UPS reduces aggregation and provides physiological benefits in HD animal models (Carmichael et al., 2000;Klettner, 2004;Vacher et al., 2005;Seo et al., 2007). It is clear however that the UPS does clear mHTT but the rate is below that of production, as shown with conditional knockout HD mouse models that eliminate aggregates and reverse

neuropathology in response to the silencing of *mHTT* expression, a recovery that is prevented by the proteasome inhibitor lactacystin (Yamamoto et al., 2000;Martín-Aparicio et al., 2001). UPS dysfunction extends to the synapses of neurons, and provides another mechanism for the CNS specificity of HD (Wang et al., 2008).

Aggregates of mHTT contain numerous other proteins containing polyQ tracts, including wildtype HTT and transcription factors and regulators (Cha, 2007), which may facilitate the correlation between aggregate formation and apoptosis in cultured cells (Hackam et al., 1998). The sequestration of motor proteins important in anterograde and retrograde axonal transport by mHTT aggregates may additionally exert a toxic effect (Li et al., 2001;Gunawardena et al., 2003).

Conversely, recent studies identified an opposite correlation between aggregates and cell susceptibility to undermine the toxicity theory of aggregate formation, as demonstrated by several animal models where neuropathology is observed without aggregates or normal cellular functions are exhibited in the presence of aggregates. One HD mouse model presents with CNS aggregates and no neurological dysfunction or apoptosis (Slow et al., 2005), and the YAC128 model exhibits behavioural abnormalities appear at 3 months when neuronal aggregates are not present (Van Raamsdonk et al., 2005). These findings are corroborated in the BACHD transgenic mouse line that presents reduced and smaller aggregates in the striatum and cortex at the age of onset (Gray et al., 2008).

Consolidating a shift away from the aggregate-toxicity paradigm was an *in vitro* study tracking individual neurons over time in rat striatal cultures transfected with exon 1 *HTT* fragments. This study found that aggregates may arise as a coping response to mHTT as aggregate formation correlated with improved cellular survival (Arrasate et al., 2004). Additionally, promoting aggregate formation within HD cell cultures lines, been shown to lessen rather than advance cellular pathology (Bodner et al., 2006).

Reports arguing for a protective role of mHTT aggregates frequently attribute toxicity instead to diffuse intracellular mHTT monomers that may possess a propensity for disruptive activities and that aggregates sequester these toxic monomers (Arrasate et

al., 2004;Bodner et al., 2006). Further, as the proteasomal degradation of mHTT fragments downstream from the polyglutamine residue appear to continue, concentrations of toxic monomers increases to fuel pathology (Venkatraman et al., 2004). The theory that aggregates form in response to monomeric fragments to inhibit their toxic effect is supported by observations that aggregation formation is faster in response to short N-terminal fragments compared to full length mHTT proteins (Hackam et al., 1998). Nevertheless, after extensive research the role of aggregates in HD remains contentions.

1.2.7 CAG repeat instability

Instability of the CAG repeat expansion in HD cells is a clear signature of disease state. Wildtype alleles of <35 CAGs are stable *in vivo* and instability appears to initiate upon CAG repeats reaching disease inducing lengths of 35 CAGs or more. CAG instability predominantly manifests as expansions, and the male germ line is particularly susceptible in contrast to the female germ line that predominantly exhibits small-scale contractions (Telenius et al., 1993;Telenius et al., 1994;Leeflang et al., 1995). Consequently, a phenomenon known as anticipation, where the age of onset decreases in successive generations corollary to gradual increases in CAG repeat length, occurs via paternal disease transmission.

Somatic cells, particularly those in the brain, also exhibit a propensity for CAG expansion in a tissue and cell specific manner. Expansions have been detected preferentially in affected brain regions of HD patients and extreme expansions over 1000 repeats in length have been recorded (Telenius et al., 1994;Kennedy et al., 2003). Analysis of individual laser captured micro-dissected somatic brain cells has observed CAG repeat length gains to correlate with neuronal susceptibility (Shelbourne et al., 2007). Mechanisms of trinucleotide repeat instability have not been solved, but may result from hairpin loop formations during the repair of single strand breaks that then interfere with DNA recombination, repair and cellular replication machinery (Mirkin, 2006;Mcmurray, 2010).

1.3 HD – A Late Onset Disorder?

While HD patients do not generally display overt phenotypic changes until onset around 40 or 50 years of age, all possess culprit mutations at conception. Therefore it is plausible that disease mechanisms gestate before onset, and indeed pathological observations within pre-onset HD individuals are emerging to support this notion. A recent commentary by Sandrine Humbert even goes so far as to frame HD as a developmental disorder (Humbert, 2010).

The two overarching causes of HD pathology, a reduction in wildtype HTT and gain of negative functions from an expanded polyQ tract, produce fundamental changes to cellular systems and components critical throughout the totality of an individual's life. Insight into the mechanistic actions of these causes does not preclude the possibility that, consistent with other late onset neurodegenerative disorders, overt disease manifestation represents a 'crossing of the Rubicon' corollary to progressive and cumulative degeneration over a preceding period, concomitant with a failure of compensatory mechanisms.

Evidence is beginning to accumulate revealing alterations before disease onset, including mitochondrial dysfunction, gene expression changes, excitotoxicity and cholesterol biosynthesis perturbation. For example, aggregate formation, one of the principle HD hallmarks, is detectable before onset across numerous model systems (Weiss et al., 2008). This section will detail the research into pre-onset changes and will place these in the context of their potential for exploiting early symptoms as disease markers to monitor disease progression, consistent with the principle focus of pre-onset researcher initiatives.

Markers are urgently required to provide quantitative, sensitive, objective and replicable measurements of HD progression to evaluate therapeutic treatment efficacies, as opposed to the existing standard of the Unified Huntington Disease Rating Scale which is restricted to motor, cognitive and behavioural evaluations that despite uniform criteria are inconsistent in pre-onset carriers and are of low

sensitivity (Paulsen et al., 2006). Markers can be classified into imaging methodologies and molecular biomarkers.

1.3.1 Imaging methodologies

Abnormalities in the CNS of pre-onset HD carriers have been recorded using an array of imaging techniques, with early studies employing structural Magnetic Resonance Imaging (MRI) to reveal significant volume decreases in the basal ganglia, particularly within the striatum, and reduced neural blood flows (Harris et al., 1999;Thieben et al., 2002).

Large cohort structural MRI studies involving several hundred subjects representing a wide spectrum of HD pathological states from pre- to post-onset demonstrated definitively neurological alterations before overt phenotypic changes arise particularly within the basal ganglia (Paulsen et al., 2008;Tabrizi et al., 2009;Nopoulos et al., 2010a;Nopoulos et al., 2010b). The sensitivity of this technology is highlighted by the detection of decreases in striatal volume approximately two decades before onset (Paulsen et al., 2008). Overall, intracranial brain volume decreases, regional grey and white matter differences and cortical thinning are observable in pre-onset individuals often with normal motor scores, and these degenerative changes are exacerbated in parallel with aging as predicted (Tabrizi et al., 2009;Nopoulos et al., 2010a;Nopoulos et al., 2010b). Functional MRI, which enables measurements to be taken over time and in combination with neural stimulation with cognitive or motor tasks, corroborates findings from standard MRI techniques, and has identified striatal changes many years before disease onset (Zimbelman et al., 2007). Beyond the striatum, neurodegenerative changes have also observed with imaging technologies, including cortical thinning across numerous studies indicating HD pathological symptoms can be identified throughout many CNS regions (Rosas et al., 2002;Rosas et al., 2005;Nopoulos et al., 2010a).

1.3.2 Molecular biomarkers

Identification of blood borne biomarkers linked to early physiological alterations represents an approach amenable to regular sampling and easy access. For example, pre-onset patients exhibit weight loss in conjunction with disruption of the circadian rhythm, sexual behaviour alterations and increased energy metabolism (Petersen and Bjorkqvist, 2006;Petersen et al., 2009), all potentially due to hypothalamic dysfunction (Politis et al., 2008). Weight loss represents a potential target for developing early biomarkers of HD and two studies attest to this theory recording decreased levels of branched chain amino acids in pre-onset carrier blood samples (Underwood et al., 2006;Mochel et al., 2007).

Microglia are the counterparts of macrophages in the CNS and their correlation with disease progression and activation in HD subjects at pre- and post-onset stages were the first signs of a possible immune component in HD (Shin et al., 2005;Pavese et al., 2006;Tai et al., 2007). Further, the immune protein clusterin and immune signalling pathway regulating IL-6 release are altered in HD (Khoshnan et al., 2004;Dalrymple et al., 2007). Proteomic profiling of human plasma identified signs of these phenomenon, with increased levels of interleukin-6 (IL-6) in pre-manifest carriers 16 years before disease onset on average, and this stands as the earliest HD alteration detectable in blood samples to date (Bjorkqvist et al., 2008).

Transcriptional dysregulation arguably represents the strongest hallmark of HD and array based studies have accurately measured hundreds of changes simultaneously between HD and wildtype samples. This presents a rich reservoir of potential disease biomarkers, either the transcripts themselves or downstream protein products. Particular focus has been paid to mHTT disruption of master regulators REST and SREBP that control BDNF expression and cholesterol biosynthesis respectively; even at stages preceding onset.

Biomarker studies have probed for changes in peripheral tissues and identified alterations in skeletal muscles from R6/2 mice and HD patients (Strand, 2005). Recent focus has shifted to peripheral blood mRNA microarray analysis, first performed by Borovecki and others and applied to a cohort of 62 HD subjects (including early 9 pre-onset, 21 late pre-onset and 32 post-onset patients) against 53 age matched controls

(Borovecki et al., 2005). Over three hundred transcripts were shown to be differentially expressed between HD and control groups, with 7 of the 12 most statistically significant additionally dysregulated in caudate tissue samples of postmortem HD patients (Borovecki et al., 2005). Notably a subset of 3 transcripts could distinguish stages of disease beginning at an early pre-onset phase (22.5 ± 2.6 years) (Borovecki et al., 2005). Corroborating these findings, two miRNAs have been reported as differentially expressed within human *in vitro* models of HD and this alteration is detectable for one (miR-34b) in the blood plasma of pre- but not post-onset HD patients and controls (Gaughwin et al., 2011).

Confounding the transcriptome dysregulation findings from Borovecki et al., 2005 is a replicative mRNA array study enrolling more patients that failed to identify any changes in all but one gene (immediate early response 3; IER3) between HD and control groups despite profiling lymphocyte samples, whole or peripheral blood (Runne et al., 2007). The utility of blood mRNA screens presently requires further interrogation and validation.

1.4 Disease Modelling

1.4.1 *In vivo* modelling

Human CNS disorders pose a challenging research environment if studied *in vivo*, being opaque to most detailed molecular, biochemical and cellular assays due to the invasive nature of such techniques; human studies are therefore largely limited to neuroimaging or human post-mortem tissue analysis as previously described.

Cellular and animal models provide alternative options with HD induced within common model organisms such as *Caenorhabditis elegans*, *Drosophila melanogaster* and *Danio rerio*. These model systems have demonstrated some of the central phenotypes of human HD including correlations with CAG repeat length and neurodegeneration severity (Faber et al., 1999;Parker et al., 2001;Gunawardena et al., 2003;Marsh and Thompson, 2006). These organisms complement rodent models and provide a platform for *in vivo* studies on a larger scale.

HD model organism studies have primarily focused on rodent models that provide a mammalian system in combination with relatively quick generation cycles. Early studies of non-genetic models of HD provided early insights into protective and restorative treatments in mice and rats. Such models are generated by intrastriatal injections of glutamate agonists such as Quinolinic Acid to induce excitotoxicity and mimic selective striatal neurodegeneration, however, these methods do not enable the dissection of the stepwise pathological process caused by an expanded CAG repeat tract (Beal et al., 1986).

Perhaps the most widely studied HD model is the R6/2 mouse line, also the first transgenic HD line that harbours a 1.9 kb insertion carrying 144 CAG repeats within exon 1 of the human huntingtin under the endogenous human promoter (Mangiarini et al., 1996). The extreme number of CAG repeats within this model translates to juvenile onset in human patients, and indeed R6/2 mice exhibit severe symptoms and an early onset at ≈3.5 weeks of age (Carter et al., 1999). Pathological qualities of R6/2 mice do however mirror those within humans, including atrophy of the brain and specifically the striatum, the precipitation of nuclear mutant HTT inclusions in neurons and a decrease in striatal dendritic dopamine D1 and D2 receptors (Mangiarini et al., 1996;Davies et al., 1997;Cha et al., 1998).

Models that more closely parallel typical human onset timeframes include the mouse strains R6/1, BACHD, YAC128 and a transgenic rats strain (Mangiarini et al., 1996;von Horsten et al., 2003;Slow et al., 2005;Gray et al., 2008). Not surprisingly these later onset models often carry fewer CAG repeats within exogenous genes as well as fewer transgene copies than R6/2 mice. Transgenic HD rodent lines are not without limitations and drawbacks. All contain an additional copy of a full or partial fragment of a huntingtin gene and protein. This result in a higher load of huntingtin proteins in total and a higher dose of wildtype endogenous proteins may attenuate disease phenotypes that would be evident with a knock-in model. Further artefacts may arise where artificial promoters are used to overexpress the exogenous huntingtin gene and concerns are magnified where randomly integrating transgenic systems are created

that possibly disturb the activity of host genes or result in multiple insertion sites as seen in the R6/2 strain.

In contrast, knock-in models express mutant huntingtin at the correct genomic loci under the endogenous promoter to produce 'normal' physiological concentrations of the disease protein. Two strategies exist for generating knock-in mice, either replacing the endogenous mouse exon 1 with a human equivalent containing a pathological CAG repeat tract (Ishiguro et al., 2001;Menalled et al., 2003) or inserting additional CAG repeats into the existing mouse repeat tract (Shelbourne et al., 1999;Lin et al., 2001). Unfortunately, knock-in lines generally exhibit a mild pathological phenotype, possibly limiting the utility of such models to understanding the stages of pre-onset or early post-onset HD.

A transgenic non-human primate model of HD was recently developed where an exon 1 fragment of the human huntingtin gene hosting 84 CAG repeats was expressed in rhesus macaques (Yang et al., 2008). This model displays hallmark behavioural abnormalities of HD including choria and dystonia in combination with molecular signs of neurodegeneration and may substantially progress the understanding of HD etiology (Yang et al., 2008).

1.4.2 *In vitro* animal modelling

In vivo animal studies possess numerous logistical and financial complexities, and are impractical for high-throughput drug screening to identify candidates for blocking and reversing mHTT toxicity. *In vitro* HD models derived from mice and rats provide an alternative platform and include inducible systems (Sipione et al., 2002), knockin (Trettel et al., 2000) and transgenic lines (Petersen et al., 2001). These systems have been successfully utilised to dissect numerous disease mechanisms including transcriptional dysregulation, aggregates and mitochondrial alterations, as well as demonstrating that mHTT promotes neural death in primary striatal cultures (Petersen et al., 2001;Hermel et al., 2004;Zeron et al., 2004;Zala et al., 2005); and neural stem cell cultures (Chu-LaGraff et al., 2001). Indeed, *in vitro* HD rodent cultures have progressed sufficiently enough for their utility in high-throughput drug

screening studies from which candidates that block and reverse mHTT toxicity have been found (Bodner et al., 2006).

Both *in vitro* and *in vivo* animal models have and will continue to contribute invaluable knowledge to our understanding of HD pathogenesis; however, none to date accurately recapitulates the full repertoire of human HD pathology. This may stem from significant biological differences caused by wide evolutionary distances between each model organism and *Homo sapiens*, or from novel pathological pathways corollary to genetic manipulation such as the insertion of additional mutant genes and overexpression above normal levels.

1.4.3 Human pluripotent disease models: A good match for HD?

hPSCs represent enormous possibilities for regenerative medicine by possessing the capacity to produce the entire repertoire of cellular types, a scenario that has ignited a cavalcade of ethical discourse, but most importantly, scientific pursuit.

Two categories of hPSCs exist, the first derived from the inner cell mass (ICM) and second upon the reprogramming of somatic cells and were first identified by research groups led by James Thomson and Shinya Yamanaka respectively (**Figure 1.2**; (Thomson, 1998;Takahashi et al., 2007). The isolation of hESCs from the ICM occurs in the early blastocyst before gastrulation at E14 and are characterised by numerous criteria, including the expression of key cell surface antigens linked to pluripotency including SSEA-3, SSEA-4, TRA-1-60, TRA-1-81 and GCTM2, as well as critical pluripotency transcription factors OCT4 and Nanog (Nichols et al., 1998;Chambers et al., 2003). An innovative alternative class of pluripotent cells, iPSCs, were first derived from mouse fibroblasts by overexpressing the key genes c-MYC, OCT4, SOX2 and KLF4 using retroviral vectors (Takahashi and Yamanaka, 2006). Reprogramming has now been performed on human cells and can be achieved with numerous vector systems, including non-integrative mRNA, episomal or protein mediated techniques that do not disrupt endogenous genomic DNA, generating cell lines highly analogous to hESC counterparts (**Figure 1.2**; Takahashi et al., 2007).

Utilising starting cells that possess genomic mutations correlating to a specific disease ostensibly enables the generation of diseased hPSC lines, and is achieved by access to either PGD embryos for hESCs or diseased patients for hiPSCs. The conflation of a pluripotent human system with genetic mutations corresponding to specific disorders opens the possibility of deriving the specific adult cell types that are susceptible for *in vitro* human modelling. This is particularly valuable in a neurological context, as live human neural tissue at any stage of disease is inaccessible for research and only available post-mortem.

The *in vitro* neural differentiation of hPSCs carrying the genetic insults of neurodegenerative disorders, such as Alzheimer's disease, Parkinson's disease and particularly full penetrance genetic disorders such as HD, represent priceless tools for deciphering the pathological cascades involved in disease development and high throughput drug screening for therapeutic agents.
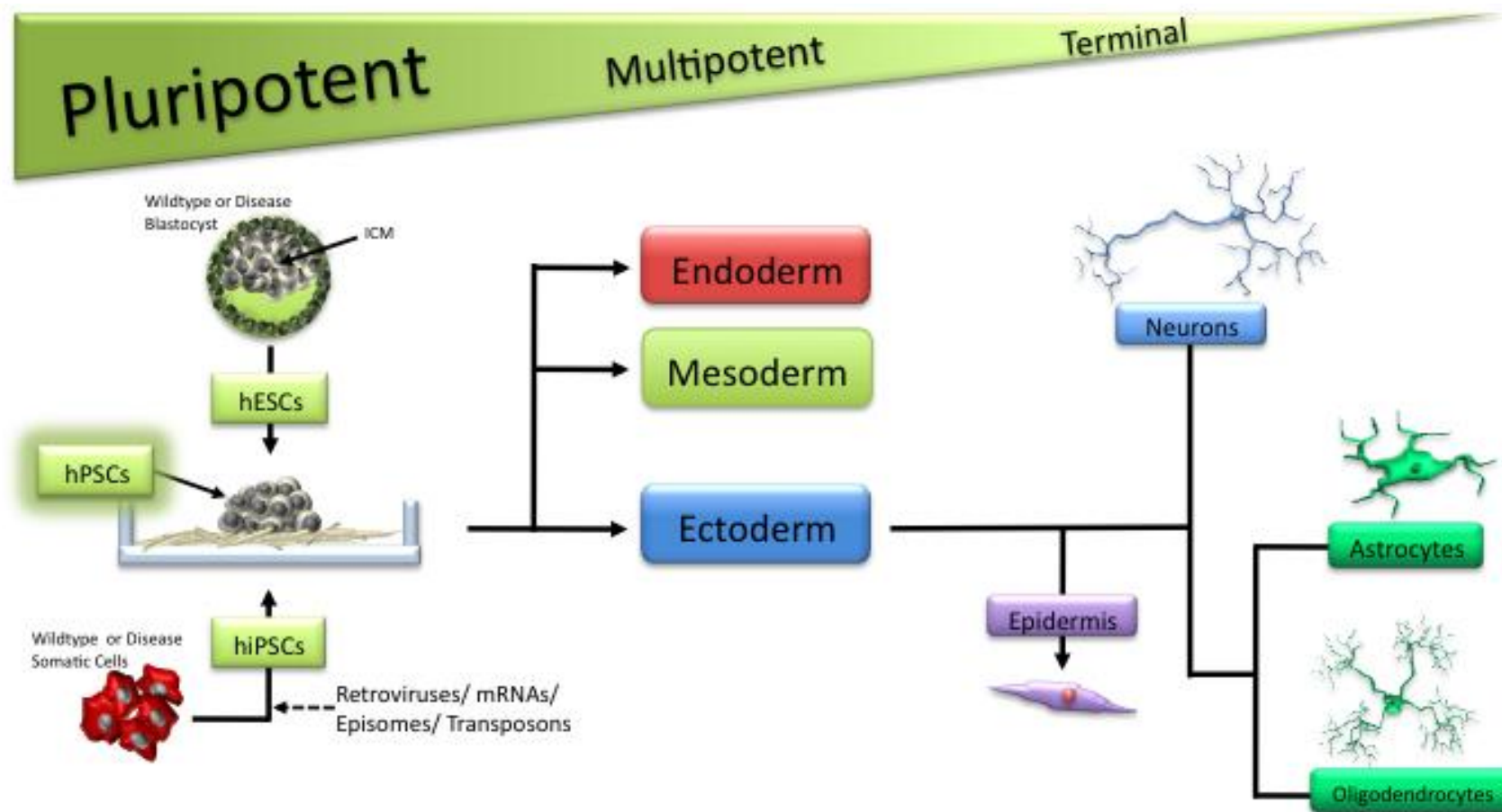
Figure 1.2: hPSCs are sourced from either the inner cell mass of the developing blastocyst or via the reprogramming of somatic cell types. hPSCs are pluripotent, capable of generating all cells of the human body, and may be directed to differentiate along germ layer pathways under specialised conditions. As differentiation progresses, cells move from a pluripotent state to a multipotent state with restricted differentiation capabilities, and continue until cells become terminally differentiated into adult cell types.

24

Indeed, hPSC lines have been generated for numerous neurodegenerative disorders and in many cases differentiated to neurons with a variety of protocols, however, observations of pathology are scarce and frequently in conflict **(Table 1.1)**. Fortunately, a disproportionate number of hPSC lines have been generated carrying HD mutations and promisingly these very recent publications are providing tantalising observation of some disease phenotypes **(Table 1.1)**. Several concerns are envisaged when modelling neurological disorders in hPSC models, namely that typically decades are required to develop phenotypes and they are often the consequence of complex and ill defined genetic and environmental interactions. However, of all neurological disorders, HD is clearly a superior choice for interrogation using hPSCs, as HD pathology is determined by a single clearly identified genetic mutation. These hPSC models also provide a unique opportunity to study pre-onset disease stages in human cells.

A study from Lund University was the first to demonstrate the feasibility of an *in vitro* pluripotent model system of HD, with the generation of transgenic human embryonic carcinoma cells (hECCs) overexpressing human *HTT* exon 1 with 23, 73 or 145 CAG repeats (Gaughwin et al., 2011). A subset of key HD features common to animal models and patients were recapitulated in undifferentiated and neural differentiated human cultures of hECCs, and in particular miRNA microarrays identified significant upregulation of two novel candidates (miR-34b and miR-1285) that were corroborated in patient blood samples. Further, previously unreported pro-survival effects of mHTT were discovered in undifferentiated cultures, and neual toxicity of mHTT confirmed in neurons derived from these hECCs (Gaughwin et al., 2011).

In reference to HD pluripotent models, it is also important to mention the work from Elena Cattaneo's laboratory, despite the derivation being made from R6/2 mouse fibroblasts, as it produced the first bona fide pluripotent model that recapitulated facets of HD pathology (Castiglioni et al., 2012). Aggregates, which were not present in the source fibroblasts or pluripotent iPSCs, began to sporadically appear after 10 days of neuronal differentiation of R6/2 iPSCs. Further, transcriptomic comparisons identified reduced expression of the cholesterol biosynthesis gene *7dhcr* and those of the autophagy-lysosomal system which is disrupted in HD (Sardiello et al., 2009), with

transcription Factor EB (TFEB, a master regulator) and its targets *Tpp1, Ctsf* and *Lamp1*, altered in undifferentiated R6/2 iPSCs and neural derrivatives. While the R6/2 iPSC model system provides a valuable biological tool for investigating HD *in vitro*, drawbacks remain including those associated with transgene insertion and uncertainty in the degree to which pathological phenotypes are faithfully reproduced in rodent systems.

Quite recently several studies have emerged of hiPSC lines carrying CAG repeat expansions. Intriguingly, all of these lines possess mutations representative of rare HD subsets, carrying either egregious expansions (CAG_{60+}) that clinically correlate to juvenile or infantile onset, or homozygous mutations that induce symptoms with greater severity (Gaughwin et al., 2011;Camnasio et al., 2012;Castiglioni et al., 2012;HDIPSCC, 2012;Jeon et al., 2012). However, a range of HD phenotypes have been identified across these studies, including HTT aggregates, CAG repeat instability, gene dysregulation and lysosomal dysfunction. Intriguingly, these studies confoundingly report conflicting observations and rarely is a single disease phenotype correlated across multiple studies. Potentially these discrepancies arise because these cell lines operate within the ranges of rare and poorly studied HD subtypes, or are a consequence of the variable reprogramming techniques employed, or even effects of the reprogramming process itself on diseased somatic cells that have been exposed to considerable periods of mHTT production.

Alternatively, HD hESC lines have been generated from PGD embryos, providing an alternative and 'natural' platform to interrogate HD in the absence of the aforementioned cellular reprogramming concerns (Mateizel, 2005;Verlinsky et al., 2005;Park et al., 2008;Niclis et al., 2009;Bradley et al., 2010). While these reports indicate HD embryos generate hESC lines with efficiencies equivalent to wildtype controls, limited investigation of their pluripotent dynamics, neuronal differentiation capacities or the presence of disease phenotypes have been performed. In order to address these fundamental questions and make sense of the nascent and conflicting literature surrounding HD hiPSC lines, there is an urgent need to investigate HD hESC lines, particularly those carrying mutations equivalent to archetypal late-onset phenotypes.

Table 1.1: Compilation of reported of human pluripotent stem cell lines carrying mutations in relevant disease genes and/or derived from individuals with specific disorders. * fibroblasts refer to patient dermal fibroblasts; ** for iPSC studies numbers reflect how many genetically distinct lines were generated; *** number of disease relevant genes dysregulated are shown in brackets.

Authors	Disease	Generation Technique *	Classific-ation	Disease Lines **	Undifferentiated Phenotype	Neural Differentiation Phenotype ***
Yagi et al... Suzuki 2011	**Alzheimer's (familial)**	Retroviral reprogramming of fibroblasts	hiPSCs	4	None reported	- Increased amyloid b42 - Pharmacological amelioration
Israel et al...Goldstein 2012	**Alzheimer's (sporadic & familial)**	Retroviral reprogramming of fibroblasts	hiPSCs	2 (Spor.) 2 (Famil.)	None reported	- High levels of pathological markers amyloid-b, phospho-tau, active glycogen synthase kinase-3b - Early endosome formation
Dimos et al... Eggan 2008	**Amyotrophic Lateral Sclerosis**	Retroviral reprogramming of fibroblasts	hiPSCs	1	None reported	None reported
Mitne-Neto et al... Zata 2011	**Amyotrophic Lateral Sclerosis (ALS8)**	Retroviral reprogramming of fibroblasts	hiPSCs	4	- Decreased levels of *VAPB*	- Decreased levels of *VAPB*
Nayler et al... Wolvetang 2012	**Ataxia-Telangiectasia**	Lentiviral reprogramming of fibroblasts	hiPSCs	2	- Reprogramming inefficiency - Defective DNA damage response - Cell cycle perturbations - Gene dysregulation	- Defective DNA damage response
Briggs et al... Wolvetang 2012	**Down Syndrom**	Episomal reprogramming of patient fibroblasts	hiPSCs	2	- Gene (>1000) dysregulation	- Gene (>1000) dysregulation - Differentiation bias - Oxidative stress senstivity
Mateizel et al... Stierteghem 2005	**Huntington's Disease & Mytonic Dystrophy**	ICM from PGD embryos	hESCs	HD (1) MD (1)	None reported	None reported (Only EB & teratoma assays performed)

27

Verlinsky et al… Kuliev 2005; and Niclis et al… Cram 2009 Niclis et al… Cram 2013	**Huntington's Disease**	ICM from PGD embryos	hESCs	2	None reported		- CAG instability - Neuronal calcium dysfunction - Gene expression
Park et al… Daley 2008	**HD, Duchenne MD, Parkinson's, Down Syndrome**	Retroviral reprogramming of fibroblasts or BM-MSCs	hiPSCs	HD (1) DMD (1) PD (1) DS (1)	None reported		None reported (Only EB & teratoma assays performed)
Bradley et al…Stojanov 2010	**Huntington's Disease**	ICM from PGD embryos	hESCs	4	None reported		- Potential impairment of ectodermal differentiation
Seriola et al… Sermon 2010	**Huntington's Disease & Mytonic Dystrophy**	ICM from PGD embryos	hESCs	HD (1) MD (3)	- None reported (HD) - CAG repeat instability (MD)		- CAG repeat instability (MD)
Gaughwin et al… Bjorkqvist 2011	**Huntington's Disease**	Transgene (CAG73 & 145) insertion	Embryonic Carcinoma Lines	1	- miRNA upregulation - Gene (1) downregulation - Increased survival		- miRNA upregulation - Impaired neural survivability/differentiation
Jeon et al… Song 2012	**Huntington's Disease**	Retroviral reprogramming of patient fibroblasts	hiPSCs (early onset)	1	- None reported		- HTT aggregates
Castiglioni et al… and Cattaneo 2012	**Huntington's Disease**	Retroviral reprogramming of R6/2 fibroblasts	miPSCs	1	- Cholesterol biosythesis gene dysregulation (3) - Lysosome gene (3) dysregulation		- Lysosome gene (3) dysregulation - HTT aggregates
Camnasio et al… Cattaneo 2012	**Huntington's Disease**	Retroviral reprogramming of patient fibroblasts	hiPSCs (early onset)	3	- Lysosome activity perturbation		- Lysosome activity perturbation
The HD iPSC Consortium	**Huntington's Disease**	Lentiviral & episomal reprogramming of patient fibroblasts	hiPSCs (early onset)	3	None reported		- CAG repeat instability - Altered NP cell adhesion - Neuronal vulnerability - Gene (>100) dysregulation

Lee et al… and Studer, 2009	**Familial Dysautonomia**	Lentiviral reprogramming of fibroblasts	hiPSCs	3	None reported	- Gene (89) dysregulation - Decreased neurogenesis - Impaired cell migration - Pharmacological amelioration
Eiges et al… Ben-Yosef 2007	**Fragile X**	ICM from PGD embryos	hESCs	1	None reported	- Hallmark *FMR1* epigentic inactivation
Urbach et al… Benvenisty 2010	**Fragile X**	Retroviral reprogramming of fibroblasts	hiPSCs	3	- Inactivation of *FMR1*	None reported
Soldner et al… Jaenisch 2009	**Parkinson's (idiopathic)**	Excisable lentiviral reprogramming of fibroblasts	hiPSCs	5	None reported	None reported
Nguyen et al… Pera 2011	**Parkinson's (*LRRK2* mutant)**	Retroviral reprogramming of fibroblasts	hiPSCs	1	None reported	- Increased expression of oxidative stress-response genes - Increased expression of a-synuclein - Increased susceptibility to stressors
Brennand et al… Gage 2011	**Schizophrenia**	Lentiviral reprogramming of fibroblasts	hiPSCs	5	None reported	- Decreased neurite numbers - Decreased neuronal connectivity - Gene (149) dysregulation - Pharmacological amelioration

1.5 Summary And Scope Of Study

The immense capacity for hPSCs to differentiate into the full repertoire of adult somatic cell types and neuronal cells relevant to HD offers the possibly of a live human context to dissect pathological pathways in a way previously unattainable. Investigations of unadulterated HD hESCs are severely limited and do not progress far beyond initial characterisation. Whether *in vitro* hESC HD models expressing mHTT under endogenous promoters will reveal signs of pathology is not clear, despite evidence for widespread mHTT dysfunction before disease onset.

A human HD cellular milieu may provide insights as to how rodent pathology differs and provide answers to remaining questions about human HD etiology. Such models can be deployed to identify novel disease pathways, separate the hierarchical relationship between copious disease mechanisms and identify those which contribute most significantly to clinical pathology. HD hESC lines with typical late onset mutations may further provide a window into the early stages of disease development and further complement these goals. Consequently, hPSC models may enable therapeutic strategies to target the most relevant mechanisms in a system amenable to high-throughput screening with the goal to finally provide useful treatment options for HD sufferers.

Subsequent chapters of this dissertation describe the detailed characterisation of numerous wildtype control hESC lines with two HD hESC lines generated from PGD embryos, SI-186 and SI-187, carrying (CAG_{37}) and (CAG_{51}) alleles equivalent to typical late onset phenotypes. In the course of these investigations, the development of a robust, novel neuronal differentiation protocol was achieved and utilised to assess the forebrain differentiation capabilities of HD hESC and generate neural and neuronal cell types for the pursuit of disease phenotypes. This overall aim of the study was to establish whether hESCs carrying clinically relevant HD mutations constitute a valid human *in vitro* model system of HD.

1.6 References

Albin, R.L., Young, A.B., Penney, J.B., Handelin, B., Balfour, R., Anderson, K.D., Markel, D.S., Tourtellotte, W.W., and Reiner, A. (1990). Abnormalities of striatal projection neurons and N-methyl-D-aspartate receptors in presymptomatic Huntington's disease. *The New England journal of medicine* 322**,** 1293-1298.

Allen, J.A., Halverson-Tamboli, R.A., and Rasenick, M.M. (2007). Lipid raft microdomains and neurotransmitter signalling. *Nature reviews. Neuroscience* 8**,** 128-140.

Altar, C.A., Cai, N., Bliven, T., Juhasz, M., Conner, J.M., Acheson, A.L., Lindsay, R.M., and Wiegand, S.J. (1997). Anterograde transport of brain-derived neurotrophic factor and its role in the brain. *Nature* 389**,** 856-860.

Andrew, S.E., Goldberg, Y.P., Kremer, B., Telenius, H., Theilmann, J., Adam, S., Starr, E., Squitieri, F., Lin, B., Kalchman, M.A., and Et Al. (1993). The relationship between trinucleotide (CAG) repeat length and clinical features of Huntington's disease. *Nature genetics* 4**,** 398-403.

Arrasate, M., Mitra, S., Schweitzer, E.S., Segal, M.R., and Finkbeiner, S. (2004). Inclusion body formation reduces levels of mutant huntingtin and the risk of neuronal death. *Nature* 431**,** 805-810.

Arzberger, T., Krampfl, K., Leimgruber, S., and Weindl, A. (1997). Changes of NMDA receptor subunit (NR1, NR2B) and glutamate transporter (GLT1) mRNA expression in Huntington's disease--an in situ hybridization study. *Journal of neuropathology and experimental neurology* 56**,** 440-454.

Augood, S.J., Faull, R.L., and Emson, P.C. (1997). Dopamine D1 and D2 receptor gene expression in the striatum in Huntington's disease. *Annals of neurology* 42**,** 215-221.

Augood, S.J., Faull, R.L., Love, D.R., and Emson, P.C. (1996). Reduction in enkephalin and substance P messenger RNA in the striatum of early grade Huntington's disease: a detailed cellular in situ hybridization study. *Neuroscience* 72**,** 1023-1036.

Bak, M., Silahtaroglu, A., Moller, M., Christensen, M., Rath, M.F., Skryabin, B., Tommerup, N., and Kauppinen, S. (2008). MicroRNA expression in the adult mouse central nervous system. *RNA* 14**,** 432-444.

Baquet, Z.C. (2004). Early Striatal Dendrite Deficits followed by Neuron Loss with Advanced Age in the Absence of Anterograde Cortical Brain-Derived Neurotrophic Factor. *Journal of Neuroscience* 24**,** 4250-4258.

Bartel, D.P. (2004). MicroRNAs: genomics, biogenesis, mechanism, and function. *Cell* 116**,** 281-297.

Beal, M.F., Kowall, N.W., Ellison, D.W., Mazurek, M.F., Swartz, K.J., and Martin, J.B. (1986). Replication of the neurochemical characteristics of Huntington's disease by quinolinic acid. *Nature* 321**,** 168-171.

Bence, N.F., Sampat, R.M., and Kopito, R.R. (2001). Impairment of the ubiquitin-proteasome system by protein aggregation. *Science* 292**,** 1552-1555.

Bjorkqvist, M., Wild, E.J., Thiele, J., Silvestroni, A., Andre, R., Lahiri, N., Raibon, E., Lee, R.V., Benn, C.L., Soulet, D., Magnusson, A., Woodman, B., Landles, C., Pouladi, M.A., Hayden, M.R., Khalili-Shirazi, A., Lowdell, M.W., Brundin, P., Bates, G.P., Leavitt, B.R., Moller, T., and Tabrizi, S.J. (2008). A novel pathogenic pathway of

immune activation detectable before clinical onset in Huntington's disease. *Journal of Experimental Medicine* 205**,** 1869-1877.

Bodner, R.A., Outeiro, T.F., Altmann, S., Maxwell, M.M., Cho, S.H., Hyman, B.T., Mclean, P.J., Young, A.B., Housman, D.E., and Kazantsev, A.G. (2006). Pharmacological promotion of inclusion formation: a therapeutic approach for Huntington's and Parkinson's diseases. *Proceedings of the National Academy of Sciences of the United States of America* 103**,** 4246-4251.

Borovecki, F., Lovrecic, L., Zhou, J., Jeong, H., Then, F., Rosas, H.D., Hersch, S.M., Hogarth, P., Bouzou, B., Jensen, R.V., and Krainc, D. (2005). Genome-wide expression profiling of human blood reveals biomarkers for Huntington's disease. *Proceedings of the National Academy of Sciences of the United States of America* 102**,** 11023-11028.

Bossy-Wetzel, E., Petrilli, A., and Knott, A.B. (2008). Mutant huntingtin and mitochondrial dysfunction. *Trends in neurosciences* 31**,** 609-616.

Bradley, C.K., Scott, H.A., Chami, O., Peura, T.T., Dumevska, B., Schmidt, U., and Stojanov, T. (2010). Derivation of Huntington's Disease-Affected Human Embryonic Stem Cell Lines. *Stem cells and development.*

Brennand, K.J., Simone, A., Jou, J., Gelboin-Burkhart, C., Tran, N., Sangar, S., Li, Y., Mu, Y., Chen, G., Yu, D., Mccarthy, S., Sebat, J., and Gage, F.H. (2011). Modelling schizophrenia using human induced pluripotent stem cells. *Nature* 473**,** 221-225.

Briggs JA, Sun J, Shepherd J, Ovchinnikov DA, Chung TL, Nayler SP, Kao LP, Morrow CA, Thakar NY, Soo SY, Peura T, Grimmond SM, Wolvetang EJ. (2012). Integration-free iPS cells identify genetic and neural developmental features of Down syndrome etiology. *Stem Cells*, 31, 467-478.

Brustovetsky, N., Lafrance, R., Purl, K.J., Brustovetsky, T., Keene, C.D., Low, W.C., and Dubinsky, J.M. (2005). Age-dependent changes in the calcium sensitivity of striatal mitochondria in mouse models of Huntington's Disease. *Journal of neurochemistry* 93**,** 1361-1370.

Buckley, N.J., Johnson, R., Zuccato, C., Bithell, A., and Cattaneo, E. (2010). The role of REST in transcriptional and epigenetic dysregulation in Huntington's disease. *Neurobiology of disease* 39**,** 28-39.

Camnasio, S., Carri, A.D., Lombardo, A., Grad, I., Mariotti, C., Castucci, A., Rozell, B., Riso, P.L., Castiglioni, V., Zuccato, C., Rochon, C., Takashima, Y., Diaferia, G., Biunno, I., Gellera, C., Jaconi, M., Smith, A., Hovatta, O., Naldini, L., Di Donato, S., Feki, A., and Cattaneo, E. (2012). The first reported generation of several induced pluripotent stem cell lines from homozygous and heterozygous Huntington's disease patients demonstrates mutation related enhanced lysosomal activity. *Neurobiol Dis* 46**,** 41-51.

Carmichael, J., Chatellier, J., Woolfson, A., Milstein, C., Fersht, A.R., and Rubinsztein, D.C. (2000). Bacterial and yeast chaperones reduce both aggregate formation and cell death in mammalian cell models of Huntington's disease. *Proceedings of the National Academy of Sciences of the United States of America* 97**,** 9701-9705.

Carter, R.J., Lione, L.A., Humby, T., Mangiarini, L., Mahal, A., Bates, G.P., Dunnett, S.B., and Morton, A.J. (1999). Characterization of progressive motor deficits in mice transgenic for the human Huntington's disease mutation. *The Journal of neuroscience : the official journal of the Society for Neuroscience* 19**,** 3248-3257.

Castiglioni, V., Onorati, M., Rochon, C., and Cattaneo, E. (2012). Induced pluripotent stem cell lines from Huntington's disease mice undergo neuronal

differentiation while showing alterations in the lysosomal pathway. *Neurobiology of Disease* 46**,** 30-40.

Cattaneo, E., Zuccato, C., and Tartari, M. (2005). Normal huntingtin function: an alternative approach to Huntington's disease. *Nature reviews. Neuroscience* 6**,** 919-930.

Cha, J.-H.J. (2000). Transcriptional dysregulation in Huntington's disease. *Trends in Neuroscience***,** 1-6.

Cha, J.-H.J. (2007). Transcriptional signatures in Huntington's disease. *Progress in neurobiology* 83**,** 228-248.

Cha, J.H., Kosinski, C.M., Kerner, J.A., Alsdorf, S.A., Mangiarini, L., Davies, S.W., Penney, J.B., Bates, G.P., and Young, A.B. (1998). Altered brain neurotransmitter receptors in transgenic mice expressing a portion of an abnormal human huntington disease gene. *Proceedings of the National Academy of Sciences of the United States of America* 95**,** 6480-6485.

Chambers, I., Colby, D., Robertson, M., Nichols, J., Lee, S., Tweedie, S., and Smith, A. (2003). Functional expression cloning of Nanog, a pluripotency sustaining factor in embryonic stem cells. *Cell* 113**,** 643-655.

Chan, E.Y.W., Luthi-Carter, R., Strand, A., Solano, S.M., Hanson, S.A., Dejohn, M.M., Kooperberg, C., Chase, K.O., Difiglia, M., Young, A.B., Leavitt, B.R., Cha, J.-H.J., Aronin, N., Hayden, M.R., and Olson, J.M. (2002). Increased huntingtin protein length reduces the number of polyglutamine-induced gene expression changes in mouse models of Huntington's disease. *Human molecular genetics* 11**,** 1939-1951.

Chu-Lagraff, Q., Kang, X., and Messer, A. (2001). Expression of the Huntington's disease transgene in neural stem cell cultures from R6/2 transgenic mice. *Brain research bulletin* 56**,** 307-312.

Conaco, C., Otto, S., Han, J.J., and Mandel, G. (2006). Reciprocal actions of REST and a microRNA promote neuronal identity. *Proceedings of the National Academy of Sciences of the United States of America* 103**,** 2422-2427.

Cooper, J.K., Schilling, G., Peters, M.F., Herring, W.J., Sharp, A.H., Kaminsky, Z., Masone, J., Khan, F.A., Delanoy, M., Borchelt, D.R., Dawson, V.L., Dawson, T.M., and Ross, C.A. (1998). Truncated N-terminal fragments of huntingtin with expanded glutamine repeats form nuclear and cytoplasmic aggregates in cell culture. *Human molecular genetics* 7**,** 783-790.

Cowan, C.M., Fan, M.M., Fan, J., Shehadeh, J., Zhang, L.Y., Graham, R.K., Hayden, M.R., and Raymond, L.A. (2008). Polyglutamine-modulated striatal calpain activity in YAC transgenic huntington disease mouse model: impact on NMDA receptor function and toxicity. *The Journal of neuroscience : the official journal of the Society for Neuroscience* 28**,** 12725-12735.

Crocker, S.F., Costain, W.J., and Robertson, H.A. (2006). DNA microarray analysis of striatal gene expression in symptomatic transgenic Huntington's mice (R6/2) reveals neuroinflammation and insulin associations. *Brain research* 1088**,** 176-186.

Cui, L., Jeong, H., Borovecki, F., Parkhurst, C.N., Tanese, N., and Krainc, D. (2006). Transcriptional Repression of PGC-1α by Mutant Huntingtin Leads to Mitochondrial Dysfunction and Neurodegeneration. *Cell* 127**,** 59-69.

Dalrymple, A., Wild, E.J., Joubert, R., Sathasivam, K., Bjorkqvist, M., Petersen, A., Jackson, G.S., Isaacs, J.D., Kristiansen, M., Bates, G.P., Leavitt, B.R., Keir, G., Ward, M., and Tabrizi, S.J. (2007). Proteomic profiling of plasma in Huntington's

disease reveals neuroinflammatory activation and biomarker candidates. *Journal of proteome research* 6**,** 2833-2840.

Davies, S.W., Turmaine, M., Cozens, B.A., Difiglia, M., Sharp, A.H., Ross, C.A., Scherzinger, E., Wanker, E.E., Mangiarini, L., and Bates, G.P. (1997). Formation of neuronal intranuclear inclusions underlies the neurological dysfunction in mice transgenic for the HD mutation. *Cell* 90**,** 537-548.

Dietschy, J.M., and Turley, S.D. (2004). Thematic review series: brain Lipids. Cholesterol metabolism in the central nervous system during early development and in the mature animal. *Journal of lipid research* 45**,** 1375-1397.

Difiglia, M. (1990). Excitotoxic injury of the neostriatum: a model for Huntington's disease. *Trends in neurosciences* 13**,** 286-289.

Difiglia, M., Sapp, E., Chase, K., Schwarz, C., Meloni, A., Young, C., Martin, E., Vonsattel, J.P., Carraway, R., Reeves, S.A., and Et Al. (1995). Huntingtin is a cytoplasmic protein associated with vesicles in human and rat brain neurons. *Neuron* 14**,** 1075-1081.

Difiglia, M., Sapp, E., Chase, K.O., Davies, S.W., Bates, G.P., Vonsattel, J.P., and Aronin, N. (1997). Aggregation of huntingtin in neuronal intranuclear inclusions and dystrophic neurites in brain. *Science* 277**,** 1990-1993.

Dimos, J.T., Rodolfa, K.T., Niakan, K.K., Weisenthal, L.M., Mitsumoto, H., Chung, W., Croft, G.F., Saphier, G., Leibel, R., Goland, R., Wichterle, H., Henderson, C.E., and Eggan, K. (2008). Induced Pluripotent Stem Cells Generated from Patients with ALS Can Be Differentiated into Motor Neurons. *Science* 321**,** 1218-1221.

Duane, W.C., and Javitt, N.B. (1999). 27-hydroxycholesterol: production rates in normal human subjects. *Journal of lipid research* 40**,** 1194-1199.

Dunah, A.W., Jeong, H., Griffin, A., Kim, Y.-M., Standaert, D.G., Hersch, S.M., Mouradian, M.M., Young, A.B., Tanese, N., and Krainc, D. (2002). Sp1 and TAFII130 transcriptional activity disrupted in early Huntington's disease. *Science* 296**,** 2238-2243.

Dure, L.S.T., Young, A.B., and Penney, J.B. (1991). Excitatory amino acid binding sites in the caudate nucleus and frontal cortex of Huntington's disease. *Annals of neurology* 30**,** 785-793.

Duyao, M.P., Auerbach, A.B., Ryan, A., Persichetti, F., Barnes, G.T., Mcneil, S.M., Ge, P., Vonsattel, J.P., Gusella, J.F., Joyner, A.L., and Et Al. (1995). Inactivation of the mouse Huntington's disease gene homolog Hdh. *Science* 269**,** 407-410.

Eiges, R., Urbach, A., Malcov, M., Frumkin, T., Schwartz, T., Amit, A., Yaron, Y., Eden, A., Yanuka, O., Benvenisty, N., and Ben-Yosef, D. (2007). Developmental Study of Fragile X Syndrome Using Human Embryonic Stem Cells Derived from Preimplantation Genetically Diagnosed Embryos. *Cell stem cell* 1**,** 568-577.

Estrada-Sanchez, A.M., Montiel, T., Segovia, J., and Massieu, L. (2009). Glutamate toxicity in the striatum of the R6/2 Huntington's disease transgenic mice is age-dependent and correlates with decreased levels of glutamate transporters. *Neurobiology of disease* 34**,** 78-86.

Faber, P.W., Alter, J.R., Macdonald, M.E., and Hart, A.C. (1999). Polyglutamine-mediated dysfunction and apoptotic death of a Caenorhabditis elegans sensory neuron. *Proceedings of the National Academy of Sciences of the United States of America* 96**,** 179-184.

Ferrante, R.J., Kowall, N.W., Cipolloni, P.B., Storey, E., and Beal, M.F. (1993). Excitotoxin lesions in primates as a model for Huntington's disease: histopathologic and neurochemical characterization. *Experimental neurology* 119**,** 46-71.

Ferrante, R.J., Gutekunst, C.A., Persichetti, F., Mcneil, S.M., Kowall, N.W., Gusella, J.F., Macdonald, M.E., Beal, M.F., and Hersch, S.M. (1997). Heterogeneous topographic and cellular distribution of huntingtin expression in the normal human neostriatum. *The Journal of neuroscience : the official journal of the Society for Neuroscience* 17**,** 3052-3063.

Fossale, E., Wheeler, V.C., Vrbanac, V., Lebel, L.-A., Teed, A., Mysore, J.S., Gusella, J.F., Macdonald, M.E., and Persichetti, F. (2002). Identification of a presymptomatic molecular phenotype in Hdh CAG knock-in mice. *Human molecular genetics* 11**,** 2233-2241.

Fukui, H., and Moraes, C.T. (2007). Extended polyglutamine repeats trigger a feedback loop involving the mitochondrial complex III, the proteasome and huntingtin aggregates. *Human molecular genetics* 16**,** 783-797.

Fusco, F.R., Chen, Q., Lamoreaux, W.J., Figueredo-Cardenas, G., Jiao, Y., Coffman, J.A., Surmeier, D.J., Honig, M.G., Carlock, L.R., and Reiner, A. (1999). Cellular localization of huntingtin in striatal and cortical neurons in rats: lack of correlation with neuronal vulnerability in Huntington's disease. *The Journal of neuroscience : the official journal of the Society for Neuroscience* 19**,** 1189-1202.

Gaughwin, P.M., Ciesla, M., Lahiri, N., Tabrizi, S.J., Brundin, P., and Bjorkqvist, M. (2011). Hsa-miR-34b is a plasma-stable microRNA that is elevated in pre-manifest Huntington's disease. *Hum Mol Genet* 20**,** 2225-2237.

Gayan, J., Brocklebank, D., Andresen, J.M., Alkorta-Aranburu, G., Zameel Cader, M., Roberts, S.A., Cherny, S.S., Wexler, N.S., Cardon, L.R., and Housman, D.E. (2008). Genomewide linkage scan reveals novel loci modifying age of onset of Huntington's disease in the Venezuelan HD kindreds. *Genetic epidemiology* 32**,** 445-453.

Gizatullina, Z.Z., Lindenberg, K.S., Harjes, P., Chen, Y., Kosinski, C.M., Landwehrmeyer, B.G., Ludolph, A.C., Striggow, F., Zierz, S., and Gellerich, F.N. (2006). Low stability of Huntington muscle mitochondria against Ca2+ in R6/2 mice. *Annals of neurology* 59**,** 407-411.

Goritz, C., Mauch, D.H., and Pfrieger, F.W. (2005). Multiple mechanisms mediate cholesterol-induced synaptogenesis in a CNS neuron. *Molecular and cellular neurosciences* 29**,** 190-201.

Gray, M., Shirasaki, D.I., Cepeda, C., Andre, V.M., Wilburn, B., Lu, X.H., Tao, J., Yamazaki, I., Li, S.H., Sun, Y.E., Li, X.J., Levine, M.S., and Yang, X.W. (2008). Full-length human mutant huntingtin with a stable polyglutamine repeat can elicit progressive and selective neuropathogenesis in BACHD mice. *The Journal of neuroscience : the official journal of the Society for Neuroscience* 28**,** 6182-6195.

Gunawardena, S., Her, L.S., Brusch, R.G., Laymon, R.A., Niesman, I.R., Gordesky-Gold, B., Sintasath, L., Bonini, N.M., and Goldstein, L.S. (2003). Disruption of axonal transport by loss of huntingtin or expression of pathogenic polyQ proteins in Drosophila. *Neuron* 40**,** 25-40.

Hackam, A.S., Singaraja, R., Wellington, C.L., Metzler, M., Mccutcheon, K., Zhang, T., Kalchman, M., and Hayden, M.R. (1998). The influence of huntingtin protein size on nuclear localization and cellular toxicity. *The Journal of Cell Biology* 141**,** 1097-1105.

Hantraye, P., Riche, D., Maziere, M., and Isacson, O. (1990). A primate model of Huntington's disease: behavioral and anatomical studies of unilateral excitotoxic lesions of the caudate-putamen in the baboon. *Experimental neurology* 108**,** 91-104.

Harris, G.J., Codori, A.M., Lewis, R.F., Schmidt, E., Bedi, A., and Brandt, J. (1999). Reduced basal ganglia blood flow and volume in pre-symptomatic, gene-tested persons at-risk for Huntington's disease. *Brain : a journal of neurology* 122 (Pt 9)**,** 1667-1678.

Hassel, B., Tessler, S., Faull, R.L., and Emson, P.C. (2008). Glutamate uptake is reduced in prefrontal cortex in Huntington's disease. *Neurochemical Research* 33**,** 232-237.

Hayashi, H., Campenot, R.B., Vance, D.E., and Vance, J.E. (2004). Glial lipoproteins stimulate axon growth of central nervous system neurons in compartmented cultures. *The Journal of biological chemistry* 279**,** 14009-14015.

Hdipscc (2012). Induced pluripotent stem cells from patients with Huntington's disease show CAG-repeat-expansion-associated phenotypes. *Cell Stem Cell* 11**,** 264-278.

Hermel, E., Gafni, J., Propp, S.S., Leavitt, B.R., Wellington, C.L., Young, J.E., Hackam, A.S., Logvinova, A.V., Peel, A.L., Chen, S.F., Hook, V., Singaraja, R., Krajewski, S., Goldsmith, P.C., Ellerby, H.M., Hayden, M.R., Bredesen, D.E., Ellerby, L.M. (2004). Specific caspase interactions and amplification are involved in selective neuronal vulnerability in Huntington's disease. *Cell Death and Differentiation* 11, 424-438.

Hodges, A., Hughes, G., Brooks, S., Elliston, L., Holmans, P., Dunnett, S.B., and Jones, L. (2008). Brain gene expression correlates with changes in behavior in the R6/1 mouse model of Huntington's disease. *Genes, Brain and Behavior* 7**,** 288-299.

Hoffner, G., Kahlem, P., and Djian, P. (2002). Perinuclear localization of huntingtin as a consequence of its binding to microtubules through an interaction with beta-tubulin: relevance to Huntington's disease. *Journal of cell science* 115**,** 941-948.

Holmberg, C.I., Staniszewski, K.E., Mensah, K.N., Matouschek, A., and Morimoto, R.I. (2004). Inefficient degradation of truncated polyglutamine proteins by the proteasome. *The EMBO Journal* 23**,** 4307-4318.

Humbert, S. (2010). Is Huntington disease a developmental disorder? *EMBO reports* 11**,** 899.

Ishiguro, H., Yamada, K., Sawada, H., Nishii, K., Ichino, N., Sawada, M., Kurosawa, Y., Matsushita, N., Kobayashi, K., Goto, J., Hashida, H., Masuda, N., Kanazawa, I., and Nagatsu, T. (2001). Age-dependent and tissue-specific CAG repeat instability occurs in mouse knock-in for a mutant Huntington's disease gene. *Journal of Neuroscience Research* 65**,** 289-297.

Israel, M.A., Yuan, S.H., Bardy, C., Reyna, S.M., Mu, Y., Herrera, C., Hefferan, M.P., Van Gorp, S., Nazor, K.L., Boscolo, F.S., Carson, C.T., Laurent, L.C., Marsala, M., Gage, F.H., Remes, A.M., Koo, E.H., and Goldstein, L.S.B. (2012). Probing sporadic and familial Alzheimer's disease using induced pluripotent stem cells. *Nature***,** 1-7.

Jana, N.R., Zemskov, E.A., Gh, W., and Nukina, N. (2001). Altered proteasomal function due to the expression of polyglutamine-expanded truncated N-terminal huntingtin induces apoptosis by caspase activation through mitochondrial cytochrome c release. *Human molecular genetics* 10**,** 1049-1059.

Jeon, I., Lee, N., Li, J.Y., Park, I.H., Park, K.S., Moon, J., Shim, S.H., Choi, C., Chang, D.J., Kwon, J., Oh, S.H., Shin, D.A., Kim, H.S., Do, J.T., Lee, D.R., Kim, M., Kang, K.S., Daley, G.Q., Brundin, P., and Song, J. (2012). Neuronal properties, in vivo effects, and pathology of a Huntington's disease patient-derived induced pluripotent stem cells. *Stem Cells* 30**,** 2054-2062.

Johnson, R., and Buckley, N.J. (2009). Gene dysregulation in Huntington's disease: REST, microRNAs and beyond. *NeuroMolecular Medicine* 11**,** 183-199.

Johnson, R., Gamblin, R.J., Ooi, L., Bruce, A.W., Donaldson, I.J., Westhead, D.R., Wood, I.C., Jackson, R.M., and Buckley, N.J. (2006). Identification of the REST regulon reveals extensive transposable element-mediated binding site duplication. *Nucleic Acids Research* 34**,** 3862-3877.

Johnson, R., Zuccato, C., Belyaev, N.D., Guest, D.J., Cattaneo, E., and Buckley, N.J. (2008). A microRNA-based gene dysregulation pathway in Huntington's disease. *Neurobiology of disease* 29**,** 438-445.

Jurevics, H., and Morell, P. (1995). Cholesterol for synthesis of myelin is made locally, not imported into brain. *Journal of neurochemistry* 64**,** 895-901.

Kennedy, L., Evans, E., Chen, C.-M., Craven, L., Detloff, P.J., Ennis, M., and Shelbourne, P.F. (2003). Dramatic tissue-specific mutation length increases are an early molecular event in Huntington disease pathogenesis. *Human molecular genetics* 12**,** 3359-3367.

Khoshnan, A., Ko, J., Watkin, E.E., Paige, L.A., Reinhart, P.H., and Patterson, P.H. (2004). Activation of the IkappaB kinase complex and nuclear factor-kappaB contributes to mutant huntingtin neurotoxicity. *The Journal of neuroscience : the official journal of the Society for Neuroscience* 24**,** 7999-8008.

Kim, J., Moody, J.P., Edgerly, C.K., Bordiuk, O.L., Cormier, K., Smith, K., Beal, M.F., and Ferrante, R.J. (2010). Mitochondrial loss, dysfunction and altered dynamics in Huntington's disease. *Human molecular genetics* 19**,** 3919-3935.

Klein, M.E., Lioy, D.T., Ma, L., Impey, S., Mandel, G., and Goodman, R.H. (2007). Homeostatic regulation of MeCP2 expression by a CREB-induced microRNA. *Nature Neuroscience* 10**,** 1513-1514.

Klettner, A. (2004). The induction of heat shock proteins as a potential strategy to treat neurodegenerative disorders. *Drug news & perspectives* 17**,** 299-306.

Kosik, K.S. (2006). The neuronal microRNA system. *Nature Reviews Neuroscience* 7**,** 911-920.

Leeflang, E.P., Zhang, L., Tavare, S., Hubert, R., Srinidhi, J., Macdonald, M.E., Myers, R.H., De Young, M., Wexler, N.S., Gusella, J.F., and Et Al. (1995). Single sperm analysis of the trinucleotide repeats in the Huntington's disease gene: quantification of the mutation frequency spectrum. *Human molecular genetics* 4**,** 1519-1526.

Leone, T.C., Lehman, J.J., Finck, B.N., Schaeffer, P.J., Wende, A.R., Boudina, S., Courtois, M., Wozniak, D.F., Sambandam, N., Bernal-Mizrachi, C., Chen, Z., Holloszy, J.O., Medeiros, D.M., Schmidt, R.E., Saffitz, J.E., Abel, E.D., Semenkovich, C.F., and Kelly, D.P. (2005). PGC-1alpha deficiency causes multi-system energy metabolic derangements: muscle dysfunction, abnormal weight control and hepatic steatosis. *PLoS biology* 3**,** e101.

Leoni, V., Mariotti, C., Nanetti, L., Salvatore, E., Squitieri, F., Bentivoglio, A.R., Bandettini Di Poggio, M., Piacentini, S., Monza, D., Valenza, M., Cattaneo, E., and Di Donato, S. (2011). Whole body cholesterol metabolism is impaired in Huntington's disease. *Neuroscience letters* 494**,** 245-249.

Li, H., Li, S.H., Yu, Z.X., Shelbourne, P., and Li, X.J. (2001). Huntingtin aggregate-associated axonal degeneration is an early pathological event in Huntington's disease mice. *The Journal of neuroscience : the official journal of the Society for Neuroscience* 21**,** 8473-8481.

Li, J.L., Hayden, M.R., Almqvist, E.W., Brinkman, R.R., Durr, A., Dode, C., Morrison, P.J., Suchowersky, O., Ross, C.A., Margolis, R.L., Rosenblatt, A., Gomez-Tortosa, E., Cabrero, D.M., Novelletto, A., Frontali, M., Nance, M., Trent, R.J., Mccusker, E., Jones, R., Paulsen, J.S., Harrison, M., Zanko, A., Abramson, R.K., Russ, A.L., Knowlton, B., Djousse, L., Mysore, J.S., Tariot, S., Gusella, M.F., Wheeler, V.C.,

Atwood, L.D., Cupples, L.A., Saint-Hilaire, M., Cha, J.H., Hersch, S.M., Koroshetz, W.J., Gusella, J.F., Macdonald, M.E., and Myers, R.H. (2003). A genome scan for modifiers of age at onset in Huntington disease: The HD MAPS study. *American journal of human genetics* 73**,** 682-687.

Li, J.L., Hayden, M.R., Warby, S.C., Durr, A., Morrison, P.J., Nance, M., Ross, C.A., Margolis, R.L., Rosenblatt, A., Squitieri, F., Frati, L., Gomez-Tortosa, E., Garcia, C.A., Suchowersky, O., Klimek, M.L., Trent, R.J., Mccusker, E., Novelletto, A., Frontali, M., Paulsen, J.S., Jones, R., Ashizawa, T., Lazzarini, A., Wheeler, V.C., Prakash, R., Xu, G., Djousse, L., Mysore, J.S., Gillis, T., Hakky, M., Cupples, L.A., Saint-Hilaire, M.H., Cha, J.H., Hersch, S.M., Penney, J.B., Harrison, M.B., Perlman, S.L., Zanko, A., Abramson, R.K., Lechich, A.J., Duckett, A., Marder, K., Conneally, P.M., Gusella, J.F., Macdonald, M.E., and Myers, R.H. (2006). Genome-wide significance for a modifier of age at neurological onset in Huntington's disease at 6q23-24: the HD MAPS study. *BMC medical genetics* 7**,** 71.

Lin, C.H., Tallaksen-Greene, S., Chien, W.M., Cearley, J.A., Jackson, W.S., Crouse, A.B., Ren, S., Li, X.J., Albin, R.L., and Detloff, P.J. (2001). Neurological abnormalities in a knock-in mouse model of Huntington's disease. *Human molecular genetics* 10**,** 137-144.

Lin, J., Wu, P.H., Tarr, P.T., Lindenberg, K.S., St-Pierre, J., Zhang, C.Y., Mootha, V.K., Jager, S., Vianna, C.R., Reznick, R.M., Cui, L., Manieri, M., Donovan, M.X., Wu, Z., Cooper, M.P., Fan, M.C., Rohas, L.M., Zavacki, A.M., Cinti, S., Shulman, G.I., Lowell, B.B., Krainc, D., and Spiegelman, B.M. (2004). Defects in adaptive energy metabolism with CNS-linked hyperactivity in PGC-1alpha null mice. *Cell* 119**,** 121-135.

Lin, M.T., and Beal, M.F. (2006). Mitochondrial dysfunction and oxidative stress in neurodegenerative diseases. *Nature* 443**,** 787-795.

London, E.D., Yamamura, H.I., Bird, E.D., and Coyle, J.T. (1981). Decreased receptor-binding sites for kainic acid in brains of patients with Huntington's disease. *Biological psychiatry* 16**,** 155-162.

Luthi-Carter, R., Hanson, S.A., Strand, A.D., Bergstrom, D.A., Chun, W., Peters, N.L., Woods, A.M., Chan, E.Y., Kooperberg, C., Krainc, D., Young, A.B., Tapscott, S.J., and Olson, J.M. (2002a). Dysregulation of gene expression in the R6/2 model of polyglutamine disease: parallel changes in muscle and brain. *Human molecular genetics* 11**,** 1911-1926.

Luthi-Carter, R., Strand, A., Peters, N.L., Solano, S.M., Hollingsworth, Z.R., Menon, A.S., Frey, A.S., Spektor, B.S., Penney, E.B., Schilling, G., Ross, C.A., Borchelt, D.R., Tapscott, S.J., Young, A.B., Cha, J.H., and Olson, J.M. (2000). Decreased expression of striatal signaling genes in a mouse model of Huntington's disease. *Human molecular genetics* 9**,** 1259-1271.

Luthi-Carter, R., Strand, A.D., Hanson, S.A., Kooperberg, C., Schilling, G., La Spada, A.R., Merry, D.E., Young, A.B., Ross, C.A., Borchelt, D.R., and Olson, J.M. (2002b). Polyglutamine and transcription: gene expression changes shared by DRPLA and Huntington's disease mouse models reveal context-independent effects. *Human molecular genetics* 11**,** 1927-1937.

Mangiarini, L., Sathasivam, K., Seller, M., Cozens, B., Harper, A., Hetherington, C., Lawton, M., Trottier, Y., Lehrach, H., Davies, S.W., and Bates, G.P. (1996). Exon 1 of the HD gene with an expanded CAG repeat is sufficient to cause a progressive neurological phenotype in transgenic mice. *Cell* 87**,** 493-506.

Markianos, M., Panas, M., Kalfakis, N., and Vassilopoulos, D. (2008). Low plasma total cholesterol in patients with Huntington's disease and first-degree relatives. *Molecular genetics and metabolism* 93**,** 341-346.

Marsh, J.L., and Thompson, L.M. (2006). Drosophila in the study of neurodegenerative disease. *Neuron* 52**,** 169-178.

Marti, E., Pantano, L., Banez-Coronel, M., Llorens, F., Minones-Moyano, E., Porta, S., Sumoy, L., Ferrer, I., and Estivill, X. (2010). A myriad of miRNA variants in control and Huntington's disease brain regions detected by massively parallel sequencing. *Nucleic Acids Research* 38**,** 7219-7235.

Martín-Aparicio, E., Yamamoto, A., Hernández, F., Hen, R., Avila, J., and Lucas, J.J. (2001). Proteasomal-dependent aggregate reversal and absence of cell death in a conditional mouse model of Huntington's disease. *The Journal of neuroscience : the official journal of the Society for Neuroscience* 21**,** 8772-8781.

Martindale, D., Hackam, A., Wieczorek, A., Ellerby, L., Wellington, C., Mccutcheon, K., Singaraja, R., Kazemi-Esfarjani, P., Devon, R., Kim, S.U., Bredesen, D.E., Tufaro, F., and Hayden, M.R. (1998). Length of huntingtin and its polyglutamine tract influences localization and frequency of intracellular aggregates. *Nature genetics* 18**,** 150-154.

Mateizel, I. (2005). Derivation of human embryonic stem cell lines from embryos obtained after IVF and after PGD for monogenic disorders. *Human Reproduction* 21**,** 503-511.

Mauch, D.H., Nagler, K., Schumacher, S., Goritz, C., Muller, E.C., Otto, A., and Pfrieger, F.W. (2001). CNS synaptogenesis promoted by glia-derived cholesterol. *Science* 294**,** 1354-1357.

Mcmurray, C.T. (2010). Mechanisms of trinucleotide repeat instability during human development. *Nature reviews Genetics* 11**,** 786-799.

Mcneil, S.M., Novelletto, A., Srinidhi, J., Barnes, G., Kornbluth, I., Altherr, M.R., Wasmuth, J.J., Gusella, J.F., Macdonald, M.E., and Myers, R.H. (1997). Reduced penetrance of the Huntington's disease mutation. *Human molecular genetics* 6**,** 775-779.

Menalled, L.B., Sison, J.D., Dragatsis, I., Zeitlin, S., and Chesselet, M.F. (2003). Time course of early motor and neuropathological anomalies in a knock-in mouse model of Huntington's disease with 140 CAG repeats. *The Journal of comparative neurology* 465**,** 11-26.

Miller, B.R., Dorner, J.L., Shou, M., Sari, Y., Barton, S.J., Sengelaub, D.R., Kennedy, R.T., and Rebec, G.V. (2008). Up-regulation of GLT1 expression increases glutamate uptake and attenuates the Huntington's disease phenotype in the R6/2 mouse. *Neuroscience* 153**,** 329-337.

Mirkin, S.M. (2006). DNA structures, repeat expansions and human hereditary disorders. *Current opinion in structural biology* 16**,** 351-358.

Mochel, F., Charles, P., Seguin, F., Barritault, J., Coussieu, C., Perin, L., Le Bouc, Y., Gervais, C., Carcelain, G., Vassault, A., Feingold, J., Rabier, D., and Durr, A. (2007). Early energy deficit in Huntington disease: identification of a plasma biomarker traceable during disease progression. *PloS one* 2**,** e647.

Nasir, J., Floresco, S.B., O'kusky, J.R., Diewert, V.M., Richman, J.M., Zeisler, J., Borowski, A., Marth, J.D., Phillips, A.G., and Hayden, M.R. (1995). Targeted disruption of the Huntington's disease gene results in embryonic lethality and behavioral and morphological changes in heterozygotes. *Cell* 81**,** 811-823.

Nichols, J., Zevnik, B., Anastassiadis, K., Niwa, H., Klewe-Nebenius, D., Chambers, I., Scholer, H., and Smith, A. (1998). Formation of pluripotent stem cells in the mammalian embryo depends on the POU transcription factor Oct4. *Cell* 95**,** 379-391.

Niclis, J.C., Trounson, A.O., Dottori, M., Ellisdon, A.M., Bottomley, S.P., Verlinsky, Y., and Cram, D.S. (2009). Human embryonic stem cell models of Huntington disease. *Reproductive biomedicine online* 19, 106-113.

Nopoulos, P.C., Aylward, E.H., Ross, C.A., Johnson, H.J., Magnotta, V.A., Juhl, A.R., Pierson, R.K., Mills, J., Langbehn, D.R., and Paulsen, J.S. (2010a). Cerebral cortex structure in prodromal Huntington disease. *Neurobiology of disease* 40, 544-554.

Nopoulos, P.C., Aylward, E.H., Ross, C.A., Mills, J.A., Langbehn, D.R., Johnson, H.J., Magnotta, V.A., Pierson, R.K., Beglinger, L.J., Nance, M.A., Barker, R.A., Paulsen, J.S., and Group, T.P.-H.I.a.C.O.T.H.S. (2010b). Smaller intracranial volume in prodromal Huntington's disease: evidence for abnormal neurodevelopment. *Brain : a journal of neurology* 134, 137-142.

Norris, P.J., Waldvogel, H.J., Faull, R.L., Love, D.R., and Emson, P.C. (1996). Decreased neuronal nitric oxide synthase messenger RNA and somatostatin messenger RNA in the striatum of Huntington's disease. *Neuroscience* 72, 1037-1047.

Packer, A.N., Xing, Y., Harper, S.Q., Jones, L., and Davidson, B.L. (2008). The bifunctional microRNA miR-9/miR-9* regulates REST and CoREST and is downregulated in Huntington's disease. *The Journal of neuroscience : the official journal of the Society for Neuroscience* 28, 14341-14346.

Panov, A.V., Gutekunst, C.A., Leavitt, B.R., Hayden, M.R., Burke, J.R., Strittmatter, W.J., and Greenamyre, J.T. (2002). Early mitochondrial calcium defects in Huntington's disease are a direct effect of polyglutamines. *Nature Neuroscience* 5, 731-736.

Park, I.-H., Arora, N., Huo, H., Maherali, N., Ahfeldt, T., Shimamura, A., Lensch, M.W., Cowan, C., Hochedlinger, K., and Daley, G.Q. (2008). Disease-specific induced pluripotent stem cells. *Cell* 134, 877-886.

Parker, J.A., Connolly, J.B., Wellington, C., Hayden, M., Dausset, J., and Neri, C. (2001). Expanded polyglutamines in Caenorhabditis elegans cause axonal abnormalities and severe dysfunction of PLM mechanosensory neurons without cell death. *Proceedings of the National Academy of Sciences of the United States of America* 98, 13318-13323.

Paulsen, J.S., Langbehn, D.R., Stout, J.C., Aylward, E., Ross, C.A., Nance, M., Guttman, M., Johnson, S., Macdonald, M., Beglinger, L.J., Duff, K., Kayson, E., Biglan, K., Shoulson, I., Oakes, D., and Hayden, M. (2008). Detection of Huntington's disease decades before diagnosis: the Predict-HD study. *Journal of neurology, neurosurgery, and psychiatry* 79, 874-880.

Paulsen, J.S., Magnotta, V.A., Mikos, A.E., Paulson, H.L., Penziner, E., Andreasen, N.C., and Nopoulos, P.C. (2006). Brain structure in preclinical Huntington's disease. *Biological psychiatry* 59, 57-63.

Pavese, N., Gerhard, A., Tai, Y.F., Ho, A.K., Turkheimer, F., Barker, R.A., Brooks, D.J., and Piccini, P. (2006). Microglial activation correlates with severity in Huntington disease: a clinical and PET study. *Neurology* 66, 1638-1643.

Petersen, A., and Bjorkqvist, M. (2006). Hypothalamic-endocrine aspects in Huntington's disease. *The European journal of neuroscience* 24, 961-967.

Petersen, A., Hult, S., and Kirik, D. (2009). Huntington's disease - new perspectives based on neuroendocrine changes in rodent models. *Neuro-degenerative diseases* 6, 154-164.

Petersen, A., Larsen, K.E., Behr, G.G., Romero, N., Przedborski, S., Brundin, P., and Sulzer, D. (2001). Expanded CAG repeats in exon 1 of the Huntington's disease

gene stimulate dopamine-mediated striatal neuron autophagy and degeneration. *Human molecular genetics* 10**,** 1243-1254.

Pfrieger, F.W. (2003). Outsourcing in the brain: do neurons depend on cholesterol delivery by astrocytes? *BioEssays : news and reviews in molecular, cellular and developmental biology* 25**,** 72-78.

Politis, M., Pavese, N., Tai, Y.F., Tabrizi, S.J., Barker, R.A., and Piccini, P. (2008). Hypothalamic involvement in Huntington's disease: an in vivo PET study. *Brain : a journal of neurology* 131**,** 2860-2869.

Ravikumar, B., Duden, R., and Rubinsztein, D.C. (2002). Aggregate-prone proteins with polyglutamine and polyalanine expansions are degraded by autophagy. *Human molecular genetics* 11**,** 1107-1117.

Reddy, P.H., Williams, M., Charles, V., Garrett, L., Pike-Buchanan, L., Whetsell, W.O., Jr., Miller, G., and Tagle, D.A. (1998). Behavioural abnormalities and selective neuronal loss in HD transgenic mice expressing mutated full-length HD cDNA. *Nature genetics* 20**,** 198-202.

Rosas, H.D., Hevelone, N.D., Zaleta, A.K., Greve, D.N., Salat, D.H., and Fischl, B. (2005). Regional cortical thinning in preclinical Huntington disease and its relationship to cognition. *Neurology* 65**,** 745-747.

Rosas, H.D., Liu, A.K., Hersch, S., Glessner, M., Ferrante, R.J., Salat, D.H., Van Der Kouwe, A., Jenkins, B.G., Dale, A.M., and Fischl, B. (2002). Regional and progressive thinning of the cortical ribbon in Huntington's disease. *Neurology* 58**,** 695-701.

Rubinsztein, D.C., and Carmichael, J. (2003). Huntington's disease: molecular basis of neurodegeneration. *Expert reviews in molecular medicine* 5**,** 1-21.

Runne, H., Kuhn, A., Wild, E.J., Pratyaksha, W., Kristiansen, M., Isaacs, J.D., Régulier, E., Delorenzi, M., Tabrizi, S.J., and Luthi-Carter, R. (2007). Analysis of potential transcriptomic biomarkers for Huntington's disease in peripheral blood. *Proceedings of the National Academy of Sciences of the United States of America* 104**,** 14424-14429.

Sakahira, H., Breuer, P., Hayer-Hartl, M.K., and Hartl, F.U. (2002). Molecular chaperones as modulators of polyglutamine protein aggregation and toxicity. *Proceedings of the National Academy of Sciences of the United States of America* 99 Suppl 4**,** 16412-16418.

Sanberg, P.R., Calderon, S.F., Giordano, M., Tew, J.M., and Norman, A.B. (1989). The quinolinic acid model of Huntington's disease: locomotor abnormalities. *Experimental neurology* 105**,** 45-53.

Sardiello, M., Palmieri, M., Di Ronza, A., Medina, D.L., Valenza, M., Gennarino, V.A., Di Malta, C., Donaudy, F., Embrione, V., Polishchuk, R.S., Banfi, S., Parenti, G., Cattaneo, E., and Ballabio, A. (2009). A gene network regulating lysosomal biogenesis and function. *Science* 325**,** 473-477.

Savas, J.N., Makusky, A., Ottosen, S., Baillat, D., Then, F., Krainc, D., Shiekhattar, R., Markey, S.P., and Tanese, N. (2008). Huntington's disease protein contributes to RNA-mediated gene silencing through association with Argonaute and P bodies. *Proceedings of the National Academy of Sciences of the United States of America* 105**,** 10820-10825.

Schwarcz, R., Foster, A.C., French, E.D., Whetsell, W.O., Jr., and Kohler, C. (1984). Excitotoxic models for neurodegenerative disorders. *Life sciences* 35**,** 19-32.

Sempere, L.F., Freemantle, S., Pitha-Rowe, I., Moss, E., Dmitrovsky, E., and Ambros, V. (2004). Expression profiling of mammalian microRNAs uncovers a subset of brain-expressed microRNAs with possible roles in murine and human neuronal differentiation. *Genome biology* 5**,** R13.

Seo, H., Sonntag, K.-C., Kim, W., Cattaneo, E., and Isacson, O. (2007). Proteasome activator enhances survival of Huntington's disease neuronal model cells. *PloS one* 2**,** e238.

Shelbourne, P.F., Keller-Mcgandy, C., Bi, W.L., Yoon, S.-R., Dubeau, L., Veitch, N.J., Vonsattel, J.P., Wexler, N.S., Group, U.-V.C.R., Arnheim, N., and Augood, S.J. (2007). Triplet repeat mutation length gains correlate with cell-type specific vulnerability in Huntington disease brain. *Human molecular genetics* 16**,** 1133-1142.

Shelbourne, P.F., Killeen, N., Hevner, R.F., Johnston, H.M., Tecott, L., Lewandoski, M., Ennis, M., Ramirez, L., Li, Z., Iannicola, C., Littman, D.R., and Myers, R.M. (1999). A Huntington's disease CAG expansion at the murine Hdh locus is unstable and associated with behavioural abnormalities in mice. *Human molecular genetics* 8**,** 763-774.

Shimojo, M., and Hersh, L.B. (2006). Characterization of the REST/NRSF-interacting LIM domain protein (RILP): localization and interaction with REST/NRSF. *Journal of neurochemistry* 96**,** 1130-1138.

Shin, J.Y., Fang, Z.H., Yu, Z.X., Wang, C.E., Li, S.H., and Li, X.J. (2005). Expression of mutant huntingtin in glial cells contributes to neuronal excitotoxicity. *The Journal of Cell Biology* 171**,** 1001-1012.

Shirendeb, U., Reddy, A.P., Manczak, M., Calkins, M.J., Mao, P., Tagle, D.A., and Hemachandra Reddy, P. (2011). Hugging tight in Huntington's. *Human molecular genetics* 20**,** 1438-1455.

Sipione, S., Rigamonti, D., Valenza, M., Zuccato, C., Conti, L., Pritchard, J., Kooperberg, C., Olson, J.M., and Cattaneo, E. (2002). Early transcriptional profiles in huntingtin-inducible striatal cells by microarray analyses. *Human molecular genetics* 11**,** 1953-1965.

Slow, E.J., Graham, R.K., Osmand, A.P., Devon, R.S., Lu, G., Deng, Y., Pearson, J., Vaid, K., Bissada, N., Wetzel, R., Leavitt, B.R., and Hayden, M.R. (2005). Absence of behavioral abnormalities and neurodegeneration in vivo despite widespread neuronal huntingtin inclusions. *Proceedings of the National Academy of Sciences of the United States of America* 102**,** 11402-11407.

Smith, R., Brundin, P., and Li, J.Y. (2005). Synaptic dysfunction in Huntington's disease: a new perspective. *Cellular and molecular life sciences : CMLS* 62**,** 1901-1912.

Snell, R.G., Macmillan, J.C., Cheadle, J.P., Fenton, I., Lazarou, L.P., Davies, P., Macdonald, M.E., Gusella, J.F., Harper, P.S., and Shaw, D.J. (1993). Relationship between trinucleotide repeat expansion and phenotypic variation in Huntington's disease. *Nature genetics* 4**,** 393-397.

Song, W., Chen, J., Petrilli, A., Liot, G., Klinglmayr, E., Zhou, Y., Poquiz, P., Tjong, J., Pouladi, M.A., Hayden, M.R., Masliah, E., Ellisman, M., Rouiller, I., Schwarzenbacher, R., Bossy, B., Perkins, G., and Bossy-Wetzel, E. (2011). Mutant huntingtin binds the mitochondrial fission GTPase dynamin-related protein-1 and increases its enzymatic activity. *Nature Medicine***,** 1-7.

Squitieri, F., Frati, L., Ciarmiello, A., Lastoria, S., and Quarrell, O. (2006). Juvenile Huntington's disease: does a dosage-effect pathogenic mechanism differ from the classical adult disease? *Mechanisms of ageing and development* 127**,** 208-212.

Squitieri, F., Gellera, C., Cannella, M., Mariotti, C., Cislaghi, G., Rubinsztein, D.C., Almqvist, E.W., Turner, D., Bachoud-Levi, A.C., Simpson, S.A., Delatycki, M., Maglione, V., Hayden, M.R., and Donato, S.D. (2003). Homozygosity for CAG

mutation in Huntington disease is associated with a more severe clinical course. *Brain : a journal of neurology* 126**,** 946-955.

Strand, A.D. (2005). Gene expression in Huntington's disease skeletal muscle: a potential biomarker. *Human molecular genetics* 14**,** 1863-1876.

Sun, Y., Savanenin, A., Reddy, P.H., and Liu, Y.F. (2001). Polyglutamine-expanded huntingtin promotes sensitization of N-methyl-D-aspartate receptors via post-synaptic density 95. *The Journal of biological chemistry* 276**,** 24713-24718.

Tabrizi, S.J., Langbehn, D.R., Leavitt, B.R., Roos, R.A., Durr, A., Craufurd, D., Kennard, C., Hicks, S.L., Fox, N.C., Scahill, R.I., Borowsky, B., Tobin, A.J., Rosas, H.D., Johnson, H., Reilmann, R., Landwehrmeyer, B., Stout, J.C., and Investigators, T.T.-H. (2009). Biological and clinical manifestations of Huntington's disease in the longitudinal TRACK-HD study: cross-sectional analysis of baseline data. *The Lancet Neurology* 8**,** 791-801.

Tai, Y.F., Pavese, N., Gerhard, A., Tabrizi, S.J., Barker, R.A., Brooks, D.J., and Piccini, P. (2007). Imaging microglial activation in Huntington's disease. *Brain research bulletin* 72**,** 148-151.

Takahashi, K., Tanabe, K., Ohnuki, M., Narita, M., Ichisaka, T., Tomoda, K., and Yamanaka, S. (2007). Induction of pluripotent stem cells from adult human fibroblasts by defined factors. *Cell* 131**,** 861-872.

Takahashi, K., and Yamanaka, S. (2006). Induction of Pluripotent Stem Cells from Mouse Embryonic and Adult Fibroblast Cultures by Defined Factors. *Cell* 126**,** 663-676.

Telenius, H., Kremer, B., Goldberg, Y.P., Theilmann, J., Andrew, S.E., Zeisler, J., Adam, S., Greenberg, C., Ives, E.J., and Clarke, L.A. (1994). Somatic and gonadal mosaicism of the Huntington disease gene CAG repeat in brain and sperm. *Nature genetics* 6**,** 409-414.

Telenius, H., Kremer, H.P., Theilmann, J., Andrew, S.E., Almqvist, E., Anvret, M., Greenberg, C., Greenberg, J., Lucotte, G., Squitieri, F., and Et Al. (1993). Molecular analysis of juvenile Huntington disease: the major influence on (CAG)n repeat length is the sex of the affected parent. *Human molecular genetics* 2**,** 1535-1540.

Thdcrg (1993). A novel gene containing a trinucleotide repeat that is expanded and unstable on Huntington's disease chromosomes. The Huntington's Disease Collaborative Research Group. *Cell* 72**,** 971-983.

Thieben, M.J., Duggins, A.J., Good, C.D., Gomes, L., Mahant, N., Richards, F., Mccusker, E., and Frackowiak, R.S. (2002). The distribution of structural neuropathology in pre-clinical Huntington's disease. *Brain : a journal of neurology* 125**,** 1815-1828.

Thomson, J.A. (1998). Embryonic Stem Cell Lines Derived from Human Blastocysts. *Science* 282**,** 1145-1147.

Trettel, F., Rigamonti, D., Hilditch-Maguire, P., Wheeler, V.C., Sharp, A.H., Persichetti, F., Cattaneo, E., and Macdonald, M.E. (2000). Dominant phenotypes produced by the HD mutation in STHdh(Q111) striatal cells. *Human molecular genetics* 9**,** 2799-2809.

Trottier, Y., Devys, D., Imbert, G., Saudou, F., An, I., Lutz, Y., Weber, C., Agid, Y., Hirsch, E.C., and Mandel, J.L. (1995). Cellular localization of the Huntington's disease protein and discrimination of the normal and mutated form. *Nature genetics* 10**,** 104-110.

Trushina, E., Dyer, R.B., Badger, J.D., 2nd, Ure, D., Eide, L., Tran, D.D., Vrieze, B.T., Legendre-Guillemin, V., Mcpherson, P.S., Mandavilli, B.S., Van Houten, B., Zeitlin,

S., Mcniven, M., Aebersold, R., Hayden, M., Parisi, J.E., Seeberg, E., Dragatsis, I., Doyle, K., Bender, A., Chacko, C., and Mcmurray, C.T. (2004). Mutant huntingtin impairs axonal trafficking in mammalian neurons in vivo and in vitro. *Molecular and cellular biology* 24**,** 8195-8209.

Tydlacka, S., Wang, C.E., Wang, X., Li, S., and Li, X.J. (2008). Differential activities of the ubiquitin-proteasome system in neurons versus glia may account for the preferential accumulation of misfolded proteins in neurons. *The Journal of neuroscience : the official journal of the Society for Neuroscience* 28**,** 13285-13295.

Underwood, B.R., Broadhurst, D., Dunn, W.B., Ellis, D.I., Michell, A.W., Vacher, C., Mosedale, D.E., Kell, D.B., Barker, R.A., Grainger, D.J., and Rubinsztein, D.C. (2006). Huntington disease patients and transgenic mice have similar pro-catabolic serum metabolite profiles. *Brain : a journal of neurology* 129**,** 877-886.

Vacher, C., Garcia-Oroz, L., and Rubinsztein, D.C. (2005). Overexpression of yeast hsp104 reduces polyglutamine aggregation and prolongs survival of a transgenic mouse model of Huntington's disease. *Human molecular genetics* 14**,** 3425-3433.

Valenza, M., Carroll, J.B., Leoni, V., Bertram, L.N., Bjorkhem, I., Singaraja, R.R., Di Donato, S., Lutjohann, D., Hayden, M.R., and Cattaneo, E. (2007a). Cholesterol biosynthesis pathway is disturbed in YAC128 mice and is modulated by huntingtin mutation. *Human molecular genetics* 16**,** 2187-2198.

Valenza, M., Leoni, V., Tarditi, A., Mariotti, C., Björkhem, I., Di Donato, S., and Cattaneo, E. (2007b). Progressive dysfunction of the cholesterol biosynthesis pathway in the R6/2 mouse model of Huntington's disease. *Neurobiology of disease* 28**,** 133-142.

Valenza, M., Rigamonti, D., Goffredo, D., Zuccato, C., Fenu, S., Jamot, L., Strand, A., Tarditi, A., Woodman, B., Racchi, M., Mariotti, C., Di Donato, S., Corsini, A., Bates, G., Pruss, R., Olson, J.M., Sipione, S., Tartari, M., and Cattaneo, E. (2005). Dysfunction of the cholesterol biosynthetic pathway in Huntington's disease. *The Journal of neuroscience : the official journal of the Society for Neuroscience* 25**,** 9932-9939.

Van Raamsdonk, J., Hayden, M.R., and Leavitt, B.R. (2005). Experimental models of Huntington's disease. *Drug Discovery Today: Disease Models* 2**,** 291-297.

Van Raamsdonk, J.M., Pearson, J., Rogers, D.A., Lu, G., Barakauskas, V.E., Barr, A.M., Honer, W.G., Hayden, M.R., and Leavitt, B.R. (2006). Ethyl-EPA treatment improves motor dysfunction, but not neurodegeneration in the YAC128 mouse model of Huntington disease. *Experimental Neurology,* 196**,** 266-272.

Velier, J., Kim, M., Schwarz, C., Kim, T.W., Sapp, E., Chase, K., Aronin, N., and Difiglia, M. (1998). Wild-type and mutant huntingtins function in vesicle trafficking in the secretory and endocytic pathways. *Experimental neurology* 152**,** 34-40.

Venkatraman, P., Wetzel, R., Tanaka, M., Nukina, N., and Goldberg, A.L. (2004). Eukaryotic proteasomes cannot digest polyglutamine sequences and release them during degradation of polyglutamine-containing proteins. *Molecular cell* 14**,** 95-104.

Verhoef, L.G., Lindsten, K., Masucci, M.G., and Dantuma, N.P. (2002). Aggregate formation inhibits proteasomal degradation of polyglutamine proteins. *Human molecular genetics* 11**,** 2689-2700.

Verlinsky, Y., Strelchenko, N., Kukharenko, V., Rechitsky, S., Verlinsky, O., Galat, V., and Kuliev, A. (2005). Human embryonic stem cell lines with genetic disorders. *Reproductive biomedicine online* 10**,** 105-110.

Visvanathan, J., Lee, S., Lee, B., Lee, J.W., and Lee, S.K. (2007). The microRNA miR-124 antagonizes the anti-neural REST/SCP1 pathway during embryonic CNS development. *Genes & development* 21**,** 744-749.

Vo, N., Klein, M.E., Varlamova, O., Keller, D.M., Yamamoto, T., Goodman, R.H., and Impey, S. (2005). A cAMP-response element binding protein-induced microRNA regulates neuronal morphogenesis. *Proceedings of the National Academy of Sciences of the United States of America* 102**,** 16426-16431.

Von Horsten, S., Schmitt, I., Nguyen, H.P., Holzmann, C., Schmidt, T., Walther, T., Bader, M., Pabst, R., Kobbe, P., Krotova, J., Stiller, D., Kask, A., Vaarmann, A., Rathke-Hartlieb, S., Schulz, J.B., Grasshoff, U., Bauer, I., Vieira-Saecker, A.M., Paul, M., Jones, L., Lindenberg, K.S., Landwehrmeyer, B., Bauer, A., Li, X.J., and Riess, O. (2003). Transgenic rat model of Huntington's disease. *Human molecular genetics* 12**,** 617-624.

Vuillaume, I., Vermersch, P., Destee, A., Petit, H., and Sablonniere, B. (1998). Genetic polymorphisms adjacent to the CAG repeat influence clinical features at onset in Huntington's disease. *Journal of neurology, neurosurgery, and psychiatry* 64**,** 758-762.

Waelter, S., Boeddrich, A., Lurz, R., Scherzinger, E., Lueder, G., Lehrach, H., and Wanker, E.E. (2001). Accumulation of mutant huntingtin fragments in aggresome-like inclusion bodies as a result of insufficient protein degradation. *Molecular biology of the cell* 12**,** 1393-1407.

Wang, J., Wang, C.-E., Orr, A., Tydlacka, S., Li, S.-H., and Li, X.-J. (2008). Impaired ubiquitin-proteasome system activity in the synapses of Huntington's disease mice. *The Journal of Cell Biology* 180**,** 1177-1189.

Weiss, A., Klein, C., Woodman, B., Sathasivam, K., Bibel, M., Regulier, E., Bates, G.P., and Paganetti, P. (2008). Sensitive biochemical aggregate detection reveals aggregation onset before symptom development in cellular and murine models of Huntington's disease. *Journal of neurochemistry* 104**,** 846-858.

Wexler, N.S., Lorimer, J., Porter, J., Gomez, F., Moskowitz, C., Shackell, E., Marder, K., Penchaszadeh, G., Roberts, S.A., Gayan, J., Brocklebank, D., Cherny, S.S., Cardon, L.R., Gray, J., Dlouhy, S.R., Wiktorski, S., Hodes, M.E., Conneally, P.M., Penney, J.B., Gusella, J., Cha, J.H., Irizarry, M., Rosas, D., Hersch, S., Hollingsworth, Z., Macdonald, M., Young, A.B., Andresen, J.M., Housman, D.E., De Young, M.M., Bonilla, E., Stillings, T., Negrette, A., Snodgrass, S.R., Martinez-Jaurrieta, M.D., Ramos-Arroyo, M.A., Bickham, J., Ramos, J.S., Marshall, F., Shoulson, I., Rey, G.J., Feigin, A., Arnheim, N., Acevedo-Cruz, A., Acosta, L., Alvir, J., Fischbeck, K., Thompson, L.M., Young, A., Dure, L., O'brien, C.J., Paulsen, J., Brickman, A., Krch, D., Peery, S., Hogarth, P., Higgins, D.S., Jr., and Landwehrmeyer, B. (2004). Venezuelan kindreds reveal that genetic and environmental factors modulate Huntington's disease age of onset. *Proceedings of the National Academy of Sciences of the United States of America* 101**,** 3498-3503.

Yamamoto, A., Lucas, J.J., and Hen, R. (2000). Reversal of Neuropathology and Motor Dysfunction in a Conditional Model of Huntington's Disease. *Cell* 101**,** 57-66.

Yang, S.-H., Cheng, P.-H., Banta, H., Piotrowska-Nitsche, K., Yang, J.-J., Cheng, E.C.H., Snyder, B., Larkin, K., Liu, J., Orkin, J., Fang, Z.-H., Smith, Y., Bachevalier, J., Zola,

S.M., Li, S.-H., Li, X.-J., and Chan, A.W.S. (2008). Towards a transgenic model of Huntington's disease in a non-human primate. *Nature* 453**,** 921-924.

Young, A.B., Greenamyre, J.T., Hollingsworth, Z., Albin, R., D'amato, C., Shoulson, I., and Penney, J.B. (1988). NMDA receptor losses in putamen from patients with Huntington's disease. *Science* 241**,** 981-983.

Zala, D., Benchoua, A., Brouillet, E., Perrin, V., Gaillard, M.-C., Zurn, A.D., Aebischer, P., and Déglon, N. (2005). Progressive and selective striatal degeneration in primary neuronal cultures using lentiviral vector coding for a mutant huntingtin fragment. *Neurobiology of disease* 20**,** 785-798.

Zeron, M.M., Hansson, O., Chen, N., Wellington, C.L., Leavitt, B.R., Brundin, P., Hayden, M.R., and Raymond, L.A. (2002). Increased sensitivity to N-methyl-D-aspartate receptor-mediated excitotoxicity in a mouse model of Huntington's disease. *Neuron* 33**,** 849-860.

Zeron, M.M., Fernandes, H.B., Krebs, C., Shehadeh, J, Wellington, C.L., Leavitt, B.R., Baimbridge, K.G., Hayden, M.R., Raymond, L.A. (2004). Potentiation of NMDA receptor-mediated excitotoxicity linked with intrinsic apoptotic pathway in YAC transgenic mouse model of Huntington's disease. *Molecular and Cellular Neuroscience* 25, 469-479.

Zhang, S., Feany, M.B., Saraswati, S., Littleton, J.T., and Perrimon, N. (2009). Inactivation of Drosophila Huntingtin affects long-term adult functioning and the pathogenesis of a Huntington's disease model. *Disease models & mechanisms* 2**,** 247-266.

Zhou, H., Cao, F., Wang, Z., Yu, Z.-X., Nguyen, H.-P., Evans, J., Li, S.-H., and Li, X.-J. (2003). Huntingtin forms toxic NH2-terminal fragment complexes that are promoted by the age-dependent decrease in proteasome activity. *The Journal of Cell Biology* 163**,** 109-118.

Zimbelman, J.L., Paulsen, J.S., Mikos, A., Reynolds, N.C., Hoffmann, R.G., and Rao, S.M. (2007). fMRI detection of early neural dysfunction in preclinical Huntington's disease. *Journal of the International Neuropsychological Society : JINS* 13**,** 758-769.

Zuccato, C. (2001). Loss of Huntingtin-Mediated BDNF Gene Transcription in Huntington's Disease. *Science* 293**,** 493-498.

Zuccato, C., Belyaev, N., Conforti, P., Ooi, L., Tartari, M., Papadimou, E., Macdonald, M., Fossale, E., Zeitlin, S., Buckley, N., and Cattaneo, E. (2007). Widespread disruption of repressor element-1 silencing transcription factor/neuron-restrictive silencer factor occupancy at its target genes in Huntington's disease. *The Journal of neuroscience : the official journal of the Society for Neuroscience* 27**,** 6972-6983.

Zuccato, C., and Cattaneo, E. (2007). Role of brain-derived neurotrophic factor in Huntington's disease. *Progress in neurobiology* 81**,** 294-330.

Zuccato, C., Liber, D., Ramos, C., Tarditi, A., Rigamonti, D., Tartari, M., Valenza, M., and Cattaneo, E. (2005). Progressive loss of BDNF in a mouse model of Huntington's disease and rescue by BDNF delivery. *Pharmacological research : the official journal of the Italian Pharmacological Society* 52**,** 133-139.

Zuccato, C., Marullo, M., Conforti, P., Macdonald, M.E., Tartari, M., and Cattaneo, E. (2008). Systematic assessment of BDNF and its receptor levels in human cortices affected by Huntington's disease. *Brain pathology* 18**,** 225-238.

Zuccato, C., Valenza, M., and Cattaneo, E. (2010). Molecular mechanisms and potential therapeutical targets in Huntington's disease. *Physiological Reviews* 90**,** 905-981.

CHAPTER 2

Huntington's Disease Mutations In Human Embryonic Stem Cell Lines

2.0 Declaration

Monash University
Declaration for Thesis Chapter 2

Declaration by candidate

In the case of Chapter 2, the nature and extent of my contribution to the work was the following:

Nature of contribution	Extent of contribution (%)
I performed all experimental procedures and prepared the manuscript (writing the text, generated the figures, formatted)	90%

The following co-authors contributed to the work. Co-authors who are students at Monash University must also indicate the extent of their contribution in percentage terms:

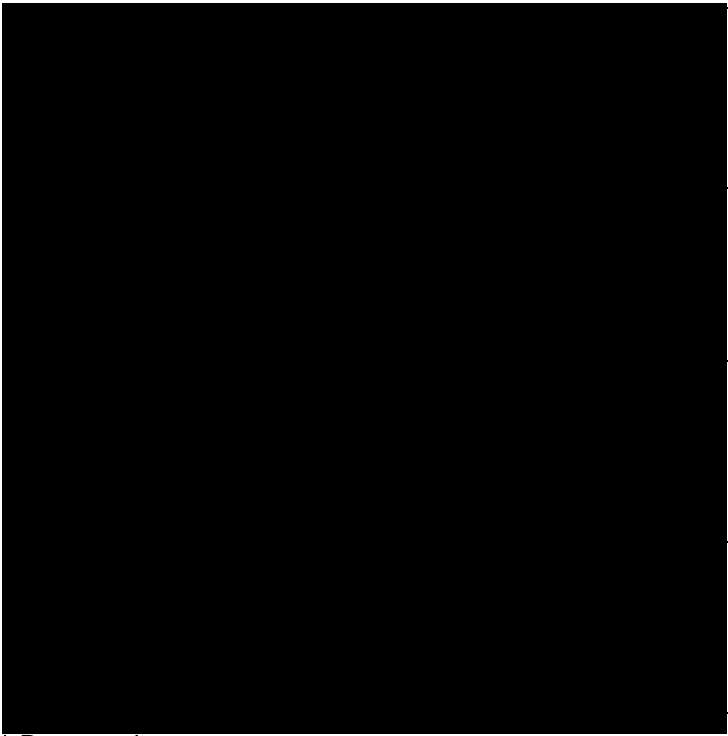| Name	Nature of contribution	Extent of contribution (%) for student co-authors only
Prof Alan Trounson	Professor Trounson provided supervision	
Dr Mirella Dottori	Dr Dottori provided supervision and technical guidance	
Dr Andrew Ellisdon	Dr Ellisdon provided technical assistance	
Dr Stephen Bottomley	Dr Bottomley provided supervision	
Dr Yury Verlinsky	Dr Verlinsky provided reagents	
Dr David Cram	Dr Cram provided supervision and contributed to the preparation of the manuscript for publication	

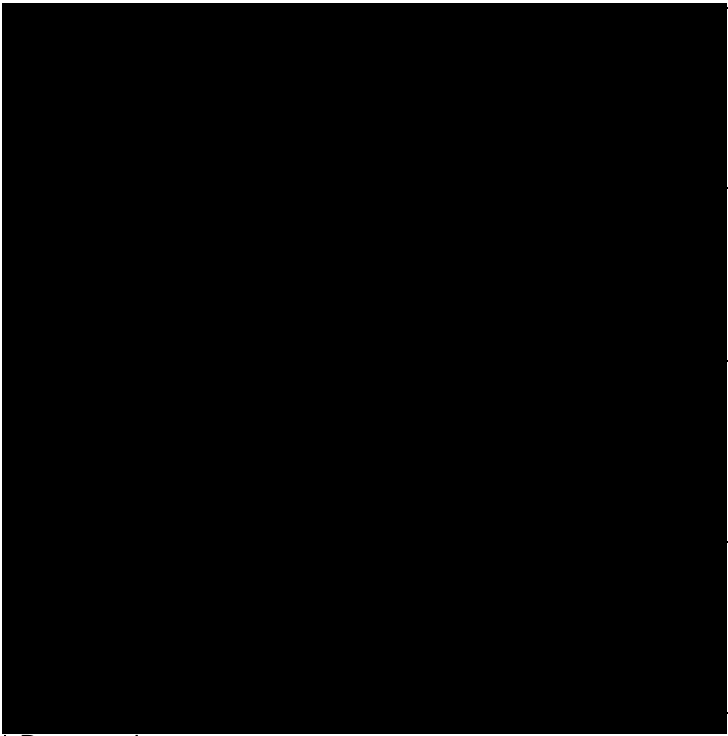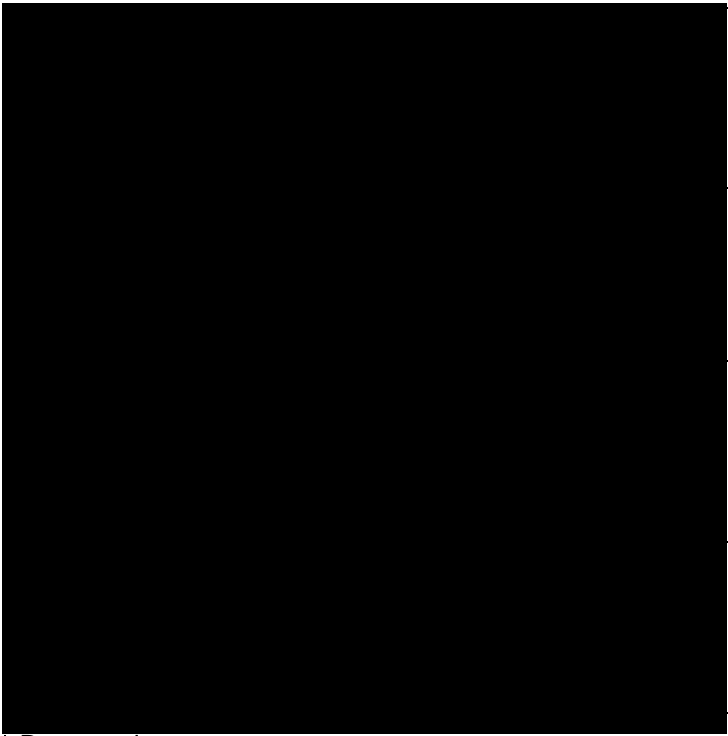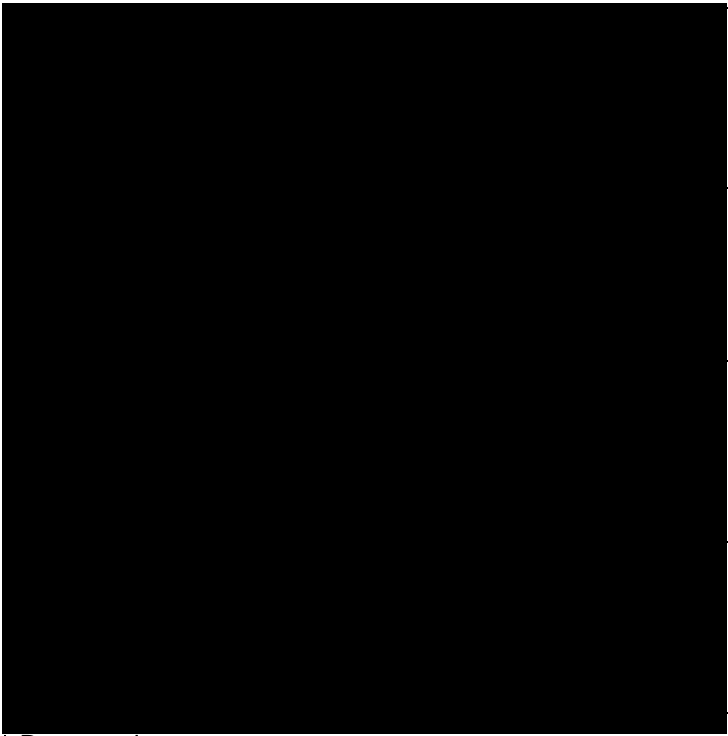| Candidate's Signature		Date **20.04.2014**

Declaration by co-authors

The undersigned hereby certify that:

(1) the above declaration correctly reflects the nature and extent of the candidate's contribution to this work, and the nature of the contribution of each of the co-authors.
(2) they meet the criteria for authorship in that they have participated in the conception, execution, or interpretation, of at least that part of the publication in their field of expertise;
(3) they take public responsibility for their part of the publication, except for the responsible author who accepts overall responsibility for the publication;
(4) there are no other authors of the publication according to these criteria;

(5) potential conflicts of interest have been disclosed to (a) granting bodies, (b) the editor or publisher of journals or other publications, and (c) the head of the responsible academic unit; and

(6) the original data are stored at the following location(s) and will be held for at least five years from the date indicated below:

Location(s)	Department of Anatomy and Developmental Biology

		Date
Signature 1		02.07.2013
Signature 2		13.08.2013
Signature 3		07.07.2013
Signature 4		04.07.2013
Signature 5	Deceased	N/A
Signature 6		24.07.2013

2.1 Introduction

Recent investigations of genetic animal models of HD and of human patients, demonstrate significant pathological dysfunction precedes overt clinical onset at cellular and physiological levels **(See Chapter 1)**. Early perturbations may represent crucial targets for unravelling the complex pathological tapestry of HD and reveal viable therapeutic targets. hESC models of HD provide the capacity to investigate pre-onset disease stages and pathological progress in an amenable *in vitro* system.

Three HD hESC lines, SI-186, SI-187 and SI-194, were developed from pre-implantation diagnosis embryos by the Reproductive Genetics Institute in Chicago and made available to researchers world wide through Stemride International (Verlinsky et al., 2005). Two lines (SI-186 and SI-194) were derived from the same maternal donor and possess a CAG_{37} repeat expansions, while SI-187 was derived from separate donors and harbours a larger CAG_{51} repeat expansion.

This chapter describes primary characterisation of two of these three hESC lines, SI-186 and SI-187, which were acquired by our institute for the purpose of establishing human *in vitro* models of HD. The re-establishment of these lines at Monash Immunology and Stem Cell Laboratories was performed and followed by the confirmation of stem cell identity and the presence of expanded HD alleles that were transcribed and translated.

For the first time, this chapter reports neural differentiation performed on hESCs carrying mutations for Huntington's disease. Further, utilising an established ectodermal differentiation protocol (Reubinoff et al., 2001), evidence of CAG repeat instability was observed in HD neural progeny.

2.2 Manuscript

2.2.1 Huntington's Disease mutation validation in human embryonic stem cell lines

The following publication to which I contributed details the first investigations into the two HD hESC lines, SI-186 and SI-187. The aims of this publication were to validate the pluripotent properties of these hESC lines after their establishment within our laboratory, confirm their disease status and assess neural differentiation capacities utilising an established noggin induction and neurosphere based protocol for the investigation of disease phenotypes.

Article

Human embryonic stem cell models of Huntington disease

In 2006 Jonathan Niclis completed a BSc degree with Honours at Monash Immunology and Stem Cell Laboratories (MISCL), Monash University, Melbourne, Australia. He is currently undertaking a PhD at MISCL within a research group focused on the development of stem cell therapies for reproductive and genetic disorders. His current project aims to characterize human embryonic stem cells which carry the Huntington disease mutation to determine their suitability as human in-vitro models of neurodegeneration.

Mr Jonathan C Niclis

JC Niclis[1], AO Trounson[1,2], M Dottori[3], AM Ellisdon[4], SP Bottomley[4], Y Verlinsky[5], DS Cram[1,6]
[1]Monash Immunology and Stem Cell Laboratories, Monash University, Victoria, Australia; [2]California Institute of Regenerative Medicine, California, USA; [3]Centre for Neuroscience and Department of Pharmacology, University of Melbourne, Victoria, Australia; [4]Department of Biochemistry, Monash University, Victoria, Australia; [5]Reproductive Genetics Institute, Chicago, USA
[6]Correspondence: e-mail: david.cram@med.monash.edu.au

Abstract

Huntington disease (HD) is an incurable late-onset neurodegenerative disorder caused by a CAG repeat expansion in exon 1 of the HD gene *(HTT)*. The major hallmark of disease pathology is neurodegeneration in the brain. Currently, there are no useful in-vitro human models of HD. Recently, two human embryonic stem cell (hESC) lines carrying partial (CAG_{37}) and fully (CAG_{51}) penetrant mutant alleles have been derived from affected IVF embryos identified following preimplantation genetic diagnosis (PGD). Fluorescence polymerase chain reaction (F-PCR) and Genescan analysis confirmed the original embryonic HD genotypes. Reverse transcription PCR (RT-PCR) analysis confirmed the expression of mutant transcripts and western blot analysis demonstrated expression of mutant huntingtin protein (HTT). After treatment with noggin, HD hESC formed neurospheres, which could be further differentiated into cells susceptible to neurodegeneration in HD, namely primary neurones and astrocytes. Small pool PCR analysis of neurosphere cells revealed instability of disease-length CAG repeats following differentiation. The presence of active *HTT* genes, neural differentiation capabilities and evidence of CAG repeat instability indicates these HD hESC lines may serve as valuable in-vitro human models of HD to better understand the mechanisms of neurodegeneration in patients, and for drug screening to identify new therapies for human clinical trials.

Keywords: CAG repeats, human embryonic stem cells, Huntington disease, neural differentiation

Introduction

Huntington disease (HD) is an autosomal dominant neurological disorder that is caused by an expanded CAG repeat region in exon 1 of the *HTT* gene (Huntington's Disease Collaborative Research Group, 1993). HD is the most common of the nine polyglutamine (polyQ) disorders, affecting approximately 1 in 10,000 individuals worldwide. Disease onset usually occurs between 40 and 50 years of age. There are no effective treatments and death usually occurs 10–20 years after clinical onset. Studies of post-mortem brain tissue from HD patients has shown that underlying neurodegeneration is a consequence of selective neuronal loss, particularly γ-aminobutyric acid (GABA)ergic medium spiny neurones (Vonsattel *et al.*, 1985; Ferrante *et al.*, 1991).

Mutant *HTT* alleles $(CAG_{\geq 35})$ exhibit an age-dependent penetrance. The lowest disease range $(CAG_{36–39})$ is associated with partial penetrance and a later age of onset (Snell *et al.*, 1993; McNeil *et al.*, 1997) whereas CAG_{40+} alleles are associated with full penetrance. Although wild-type repeat alleles $(CAG_{<35})$ are stable *in vivo*, mutant alleles can exhibit CAG repeat instability. Small-scale contractions of mutant alleles occur in the female germ line, whereas large expansions are commonly observed in the male germ line (Telenius *et al.*, 1993; Leeflang *et al.*, 1995). Mutant alleles also exhibit a propensity for CAG expansion within somatic cells. Expansions have been detected in the most severely affected brain regions of HD patients, with some exceeding 1000 CAG repeats (Telenius *et al.*, 1994; Kennedy

106

et al., 2003). Furthermore, analysis of individual laser-captured micro-dissected neurones has shown that CAG repeat gains are more prominent in susceptible neurones compared with those that are spared (Shelbourne *et al.*, 2007).

The *HTT* gene encodes a 350 kDa ubiquitously expressed protein called huntingtin (HTT). Mutant HTT proteins generate intranuclear and intracytoplasmic aggregates throughout the brain, including within axons and dendrites (Davies *et al.*, 1997; DiFiglia *et al.*, 1997; Scherzinger *et al.*, 1997; Becher *et al.*, 1998; Gutekunst *et al.*, 1999; Lunkes *et al.*, 2002; Shin *et al.*, 2005). Although the role of aggregates as a cell defence mechanism or as a perpetrator of pathology is debatable, it is clear that they are a major hallmark of HD. Aggregates have also been identified in a wide range of non-central nervous system tissue types that are seemingly unaffected (Sathasivam *et al.*, 1999). Another major pathological process observed in striatal neurones is the dysregulation of the transcriptome (Thomas, 2006). Mutant cytoplasmic HTT is cleaved by caspase activity to form monomeric N-terminal polyQ peptides with increased toxicity (Lunkes *et al.*, 2002; Wellington *et al.*, 2002; Graham *et al.*, 2006; Pattison *et al.*, 2006). Following translocation to the nucleus, the mutant polyQ peptide is believed to aberrantly modulate transcription via abnormal protein interactions with various transcription factors such as Sp1 (Dunah *et al.*, 2002; Chen-Plotkin *et al.*, 2006) and other polyglutamine-containing proteins such as wild-type huntingtin and TATA-binding protein (Huang *et al.*, 1998).

Mutant HTT or N-terminal polyQ isoforms have been expressed in a range of species such as *Caenorhabditis elegans*, *Drosophila melanogaster* and *Mus musculus*, and most recently *Macaca mulatta*, to generate different transgenic and knock-in models of HD (Sipione and Cattaneo, 2001; García-Ramos *et al.*, 2007; Yang *et al.*, 2008). Animal models have added valuable knowledge to the understanding of HD pathogenesis and continue to be of great importance; however, studies to date demonstrate that these models do not precisely reflect all HD pathologies, and so far they have not led to successful human therapies. There remains a need for new in-vitro human HD models. Alternative models yet to be explored are HD human embryonic stem cells (hESC). Recently, disease-specific hESC lines have been established from affected preimplantation genetic diagnosis (PGD) embryos (Pickering *et al.*, 2005; Verlinsky *et al.*, 2005, 2006; Mateizel *et al.*, 2006), including those carrying a mutant *HTT* gene (Verlinsky *et al.*, 2005, 2006; Mateizel *et al.*, 2006). These HD hESC may be useful in-vitro disease models that replicate key HD pathologies. This paper reports on the initial characterization of two HD hESC lines (SI-186 and SI-187) carrying mutant alleles with 37 and 51 CAG repeats, respectively.

Materials and methods

hESC lines

HD-positive stem cell lines SI-186 and SI-187 were derived from IVF embryos following PGD. Details of the IVF and PGD cycles that led to the identification of the HD embryos, as well as information on the generation and maintenance of the HD hESC lines, have been previously published (Verlinsky *et al.*, 2005). Both lines were obtained as frozen stocks from

Stemride International (http://www.stemride.com) under a materials transfer agreement with Monash University. Research on these lines at Monash University was approved by the Standing Committee on Ethics in Research Involving Humans (2006/063EA). Following derivation, SI-186 and SI-187 had normal female karyotypes and expressed the hESC pluripotency markers SSEA-3, SSEA-4, Oct-4, TRA-2–39, TRA-1–60 and TRA-1–80 (Verlinsky *et al.*, 2005). Genotyping revealed that the lines were heterozygous for mutant alleles of CAG_{38} and CAG_{51}, respectively (Verlinsky *et al.*, 2005). SI-186 and SI-187 were re-established at Monash University Immunology and Stem Cell Laboratories. HD-negative female control hESC lines HES2 and HES3 were derived previously from human blastocysts (Reubinoff *et al.*, 2000).

Culture of hESC lines

All hESC lines were cultured as colonies in Falcon centre-well organ culture dishes (BD Biosciences, USA) in 1 ml of human embryonic stem cell (HES) medium. Base stocks of HES medium were made by combining 400 ml knockout Dulbecco's modified Eagle's medium (DMEM), 100 ml knockout serum replacement, and 5 ml non-essential amino acids (GIBCO-Invitrogen). A more complex medium for routine stem cell culture included the following supplements: Glutamax (1.9 ng/mol), β-mercaptoethanol (0.1 mg/mol), penicillin (24.1 units/ml), streptomycin (24.1 μg/ml), insulin–transferrin–selenium-X (ITS-X; insulin at 9.65 μg/l, transferrin at 5.3 μg/l and selenium at 0.00646 μg/l) and basic fibroblast growth factor (bFGF; 4 ng/ml). All components were purchased from Gibco-Invitrogen, Australia. The HES3 line was grown on mouse embryonic fibroblasts, which were derived from MTK/NEO CD1 mice, Monash University Physiology Department, whereas HES2, SI-186 and SI-187 lines were grown on human mammary fibroblast feeder cells (CCD919SK, ATCC Corporation). Feeder cells were metabolically inactivated by mitomycin C (10 μg/ml) treatment for 3–4 min and plated at a density of 1.65 × 10^5 cells/cm². hESC were cultured for 7 days and colonies were mechanically passaged by cutting pieces of approximately 0.5–1.0 mm² and seeding 8–12 pieces onto fresh organ culture dishes, marking a single passage. The 'centre button' of colonies and other regions which displayed obvious signs of spontaneous differentiation were excluded from mechanical passaging. Colonies were grown at 37°C in 5% CO_2/air and HES medium was changed daily.

Neural differentiation

Neural differentiation was achieved by treatment of hESC colonies with 500 ng/ml noggin (kindly gifted from Green Chemistry, Monash University) and transfer of treated colony pieces to 96-well plates containing specific culture medium to generate neurospheres, according to protocols previously established (Pera *et al.*, 2004). A proportion of neurospheres was plated and cultured for 3 days in the absence of specific growth factors on combined poly-D-lysine-coated (1:100; Sigma, MO, USA) and fibronectin-coated (1:100; Sigma) wells and immunostained for the early neuroectoderm marker PAX6 (Pera *et al.*, 2004). The remaining neurospheres were differentiated in the presence of specific growth factors by plating on laminin-coated wells to produce primary neurones or plating on fibronectin-coated wells to produce astrocytes (Reubinoff *et*

107

al., 2001). Immunostaining for β-III-tubulin and microtubule-associated protein 2ab (MAP2ab) was used to identify primary neurones, whereas immunostaining for glial fibrillary acidic protein (GFAP) was used to identify astrocytes.

Immunostaining for neural markers

Cells were fixed for 15 min on ice using 4% paraformaldehyde in phosphate-buffered saline containing calcium and magnesium (PBS+; Invitrogen). Cells were then permeabilized with washes of PBT (1% Triton X-100/PBS+), blocked for 1 h at room temperature in 10% fetal calf serum/PBT (Invitrogen), and then incubated with primary antibodies overnight at 4°C. Mouse monoclonal anti-PAX6 immunoglobulin (Ig)G primary antibody (1:50; Developmental Studies Hybridoma Bank, USA) was used for PAX6 neurosphere staining. Primary neurones were simultaneously stained with rabbit anti-β-III-tubulin antibodies (1:500; Chemicon, USA) and mouse anti-MAP2ab antibodies (1:200; Lab Vision Corporation, USA). Astrocytes were stained with rabbit anti-GFAP antibodies (1:500; Dako, Denmark). Isotype-matched antibodies were used as negative controls. Secondary antibodies, either Alexa Fluor goat anti-mouse IgM (568) (1:500; Invitrogen) or Alexa Fluor goat anti-rabbit IgG (488) (1:1000; Invitrogen), were applied for 1 h at room temperature. Slides were then washed and cell nuclei were stained with 4,(6-diamidino-2-phenylindole) (1:1000; Sigma). Coverslips were placed onto glass slides with Vectashield mounting medium (Australian Lab Services, Australia) and sealed with nail polish. Bound fluorescence was detected using an Olympus BX51 microscope and ULH100HG fluorescence system with appropriate filters for each fluorescence wavelength. Slides were photographed using a DP70 camera.

Flow-activated cell sorting

Colonies of hESC were harvested from organ culture dishes and placed in TrypLE Express (Invitrogen) at 37°C for 10 min to generate a disassociated cell suspension. Samples were resuspended in PBS– (containing no calcium or magnesium; Invitrogen) and divided into three aliquots. Aliquot 1 was stained with a GCTM-2 IgM primary monoclonal antibody (Pera *et al.*, 1988), aliquot 2 was stained with a matched IgM negative control antibody (1:125; BD Biosciences) and aliquot 3 was left unstained. All three aliquots were left at 4°C for 30 min. Aliquots were then resuspended in 10% normal goat serum/HES medium, and Alexa Fluor goat anti-mouse IgM (647) (1:500; Invitrogen) was added to aliquots 1 and 2. Aliquots were left for 30 min at 4°C, protected from light. Aliquot 3 was resuspended in PBS+, while aliquots 1 and 2 were resuspended in propidium iodide (PI; 1:2000; Sigma). Cells were sorted using a FC500 flow cytometer, (Cytomics FC500; Beckman Coulter, USA). Sorting was performed for a PI-negative population and GCTM-2-positive population, with the threshold set to sort five cells directly into 200 µl polymerase chain reaction (PCR) tubes containing 2.5 µl lysis buffer (400 mmol/l KOH, 100 mmol/l dithiothreitol). Sorting was also conducted on neurosphere cells, stained with PI (1:2000). The PI-negative population was directly sorted into 200 µl PCR tubes containing 2.5 µl lysis buffer, with the threshold set for one cell per tube. Samples were frozen at –80°C prior to PCR analysis.

Purification of genomic DNA

Genomic DNA (gDNA) from each hESC line was extracted and purified from 15–25 colonies using a DNeasy Tissue Kit (Qiagen, Germany). The yield of gDNA was determined by UV spectrometry using a NanoDrop spectrometer (NanoDrop Spectrophotometer, ND-1000; BioLab, Australia).

Fluorescent PCR

The CAG repeat region in exon 1 of the *HTT* gene was amplified by fluorescence-PCR (F-PCR) using HU3 and HU4 primers (Sermon *et al.*, 1995). The HU4 sense primer was labelled with 6-carboxyfluorescein (6-FAM; Applied Biosystems, USA). Each F-PCR reaction master mix (total volume 45 µl) comprised 27.6 µl H_2O, 10 µl GC Rich Solution, 5 µl 10× $MgCl_2$ buffer, 0.4 µl Fast Start *Taq* Polymerase, 1 µl dNTP (Fast Start *Taq* Polymerase Kit; Roche Diagnostics, Australia) and 1 µl of a 20 pmol/l HU3 and HU4 primer solution. The DNA template in the F-PCR reaction was either 1 µl gDNA (≈200 ng) or fluorescence-activated cell sorted (FACS) samples. FACS cells collected in 2.5 µl lysis buffer were prepared by heating at 65°C for 10 min and then neutralized with 2.5 µl neutralization buffer (0.27 mol/ml Tris–HCl, 0.11 mol/ml KCl, 1 mol/ml HCl). F-PCR thermocycling conditions were as follows: reactions were initiated with one cycle at 95°C for 3 min, followed by 50 cycles at 95°C for 45 s, 61°C for 60 s, 72°C for 90 s, and they were terminated with one cycle at 72°C for 5 min. Aliquots (10 µl) of the F-PCR reaction products were analysed on 2% ethidium bromide agarose gels to visualize amplified DNA products.

Calculation of CAG repeat numbers

F-PCR reactions were also analysed on an ABI Prism 3100 DNA Sequencer (Applied Biosystems). Following Genescan software analysis (Applied Biosystems), labelled F-PCR product fragment sizes were automatically calculated using the internal 6-carboxy-X-rhodamine (ROX) size standards. The number of the CAG repeats (Δ) was then calculated using the formula $\Delta = (\delta$–flanking conserved regions)/3, where δ = F-PCR product length.

Reverse transcription PCR

Total RNA was extracted from 15–20 hESC colonies using the RNeasy Mini Kit (Qiagen) following the protocols recommended by the manufacturer. RNA samples (80 ng) were converted to cDNA in two separate reactions, one containing reverse transcriptase (RT+) the other without reverse transcriptase (RT–), as per manufacturer guidelines (SuperScript III First Strand Synthesis System for RT-PCR; Invitrogen). A 2 µl aliquot (10%) of the cDNA product from RT+ and RT– reactions was subjected to PCR as described above, and reaction products were separated on 2% ethidium bromide agarose gels.

Western blotting

Approximately 60 hESC colonies from each line were centrifuged at 15,500 *g* for 10 min at 4°C and resuspended in 30 µl radio-immunoprecipitation assay (RIPA) buffer (98.4%

PBS–, 1% Nonidet P-40/Igepal CA-630, 0.5% sodium deoxycholate, 0.1% sodium dodecyl sulphate (SDS)), and 3 µl protease inhibitors (Roche EDTA-free Complete Inhibitor; Roche Diagnostics) was added immediately. Samples were sonicated and incubated for 45 min on ice. Following centrifugation at 15,500 *g* for 10 min at 4°C, the supernatants were collected. A BCA Protein Assay (Thermo Scientific, Australia) estimated sample protein concentrations and 100 µg total protein was mixed with an equal volume of 2× sample buffer (0.125 mol/l Tris-HCl, 4% SDS, 20% v/v glycerol, 0.2 mol/l dithiothreitol, 0.02% bromophenol blue, pH 6.8) and then denatured at 98°C for 5 min. Samples were loaded onto a 3–8% gradient polyacrylamide Tris–acetate gel (Invitrogen) and electrophoresed for 2 h at 150 V at 4°C.

The polyacrylamide Tris–acetate gel was then placed in contact with a nitrocellulose membrane (Protran 0.45 µm pore size; Whatman, Schleicher and Schuell BioScience, Germany) and blotting was performed for 2 h at 250 V at 4°C. The nitrocellulose membrane was blocked in blocking buffer (Tris-buffered saline + 5% low fat milk powder) for 1 h. and incubated overnight at 4°C with a 1:20,000 dilution of anti-mouse 1C2 antibody (Chemicon) that only binds to disease-length polyQ tracts (Trottier *et al.*, 1995). A 1:5000 dilution of horseradish-peroxidase-conjugated secondary antibody (Chemicon) was applied for 1 h at room temperature to detect bound 1C2 antibody and conjugates were revealed by enzymatic chemiluminescence (ECL+; GE Healthcare, Australia).

Results

Molecular characterization of HD hESC lines

HD hESC lines SI-186 and SI-187 were re-established at Monash University Immunology and Stem Cell Laboratories on CCD feeder cells at passages 24 and 4, respectively. All studies were performed on hESC colonies from relatively early passages (SI-187, passages 6–28; SI-186, passages 24–44; hES2/3, passages 28–64). Karyotypes were firstly assessed in lines SI-186 and SI-187 to determine whether chromosome abnormalities had occurred in early undifferentiated cultures. At passage 6 all 20 SI-187 cells analysed had a normal female 46,XX karyotype. For SI-186 however, at passage 29, 6/16 cells tested had a normal female 46,XX karyotype whereas the remaining 10 cells were trisomic for chromosome 12 (data not shown). Despite differences in karyotype, SI-186 and SI-187 colonies displayed normal stem cell morphology and exhibited similar growth rates following continuous passage. Control HES2 and HES3 lines exhibited normal 46,XX female karyotypes.

Using F-PCR and Genescan analysis, all hESC lines and the CCD feeder cells were genotyped at the *HTT* locus to confirm their allelic CAG repeat sizes (**Figure 1**). As expected, SI-186 (CAG$_{37/15}$) and SI-187 (CAG$_{51/19}$) were heterozygous carrying both a wild-type and a mutant allele. The SI-187 genotype at
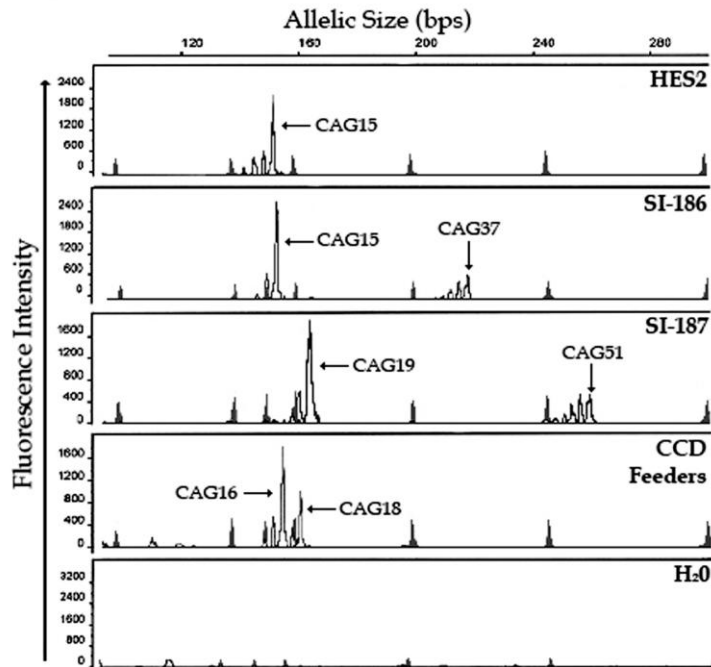
Figure 1. Genescan fluorescence polymerase chain reaction (F-PCR) product readouts. Alleles are represented by a series of open peaks of decreasing intensity to the left, with the true allele represented by the rightmost peak (arrow); remainder peaks represent artificial stutter alleles. CAG repeat numbers labelled on arrows were calculated from F-PCR product lengths. Closed peaks common to all profiles indicate Genescan internal standards; bps = base pairs.

RBMOnline®

the *HTT* locus was identical to that of the original IVF embryo. The genotype of SI-186 at the *HTT* locus was almost identical to the original IVF embryo, varying by one CAG repeat. The minor discrepancy between the CAG repeat lengths between the original embryo and resulting stem cell line was probably due to different Genescan sizing methods used by the two laboratories. The wild-type status of CCD feeder cells ($CAG_{16/18}$) and HES2 ($CAG_{15/15}$) and HES3 ($CAG_{15/15}$) control lines was also confirmed. Apart from the normal allelic stutter patterns there was no evidence in the SI-186 or SI-187 Genescan profiles of variability in the fluorescence peaks representing the mutant alleles, indicating CAG repeat stability.

Neural differentiation of HD hESC lines

Differentiation of the HD lines SI-186 and SI-187 was assessed by culturing cells in standard neural differentiation conditions. Neural differentiation via neurosphere intermediates was specifically directed towards the formation of mature neurones and astrocytes that are known to be associated with HD pathology. Both SI-186 and SI-187 lines were capable of producing spherical neurospheres of similar morphological quality to those formed by the wild-type lines HES2/HES3 (**Figure 2A–C**). Under the light microscope, neurospheres derived from SI-186, SI-187 and wild-type HES2/HES3 lines displayed characteristic 'rosette' structures (**Figure 2A–C**). In addition SI-187 and HES2 neurospheres stained positive for the expression of PAX6, an early neuroectodermal marker (**Figure 2D, G**). SI-186 and wild-type-derived neurospheres plated on a laminin substrate with specific growth factors formed primary neurones that stained positive for β-III-tubulin and MAP2ab (**Figure 3**). Levels and spatial distribution of β-III-tubulin and MAP2ab staining were similar between the mutant and wild-type lines (**Figure 3C, G**). SI-186 and HES2 neurospheres plated on a fibronectin substrate with specific growth factors generated GFAP-positive astrocytes of similar morphology and number (**Figure 4**).

Expression of the *HTT* gene

The transcriptional status of the *HTT* gene was assessed by qualitative RT-PCR and gel electrophoresis (**Figure 5A**). Both SI-186 and SI-187 RT+ reactions produced two distinct bands of the expected sizes: one representing the mutant allele and the other representing the wild-type allele, indicating transcription of the *HTT* gene in undifferentiated cultures. Control hESC lines HES2 and HES3 and the CCD feeders produced a single band, representing similar-sized wild-type alleles and demonstrating expression of only wild-type transcripts. Western blot assays were used to further evaluate expression of the mutant HTT protein. Total soluble protein fractions separated using gel electrophoresis were probed with the 1C2 antibody which only reacts with proteins containing expanded polyQ tracts. Consequently, only the mutant length HTT was detectable. SI-187 undifferentiated cells produced a strong band at the expected size of 360 kDa, indicating expression of mutant HTT protein (**Figure 5B**). In preliminary studies, slot blot filter retardation assays (Scherzinger *et al.*, 1997) using the 1C2 antibody were unable to detect the presence of insoluble HTT aggregates in undifferentiated SI-186 or SI-187 cells (data not shown).

Stability of the mutant CAG repeat allele

The 200 ng of starting DNA template used for genotyping (**Figure 1**) may mask detection of any low-level CAG repeat instability. Consequently, small pool F-PCR (SP F-PCR) was conducted on undifferentiated SI-186 cells (31 pools of five cells) and SI-187 cells (27 pools of five cells). No changes at the single cell level were observed in the wild-type or mutant allele CAG repeat lengths in either undifferentiated cell line (**Figure 6A, B**). CAG repeat stability was assessed further in SI-186 neurosphere cells using SP F-PCR. Of six pooled samples analysed, one pool displayed a six CAG repeat expansion (data not shown) and a second pool displayed a five CAG repeat expansion in the mutant allele (**Figure 6C**).

Discussion

This report describes what is thought to be the first characterization studies of two HD hESC lines derived from affected PGD embryos. Both lines were shown to express the *HTT* gene at the mRNA and protein levels, and thus have the genetic potential to develop HD pathology *in vitro*. In addition, the HD hESC lines were capable of neuronal differentiation into two neural lineages that are known to be affected by the disease process. Chromosomal analysis demonstrated a normal female karyotype (46,XX) for the fully penetrant SI-187 line and a mosaic female karyotype (46,XX, 47,XX +12) for the partially penetrant SI-186 line. Trisomy 12 is a recurrent abnormality in hESCs which is believed to provide a selective growth advantage *in vitro* (Draper *et al.*, 2004). Nevertheless, both SI-186 and SI-187 undifferentiated colonies displayed stem cell morphologies similar to those of the well-characterized control lines HES2 and HES3 (Reubinoff *et al.*, 2000). Further, the karyotypic abnormality in the SI-186 line did not hinder neural differentiation capabilities; however, investigations involving SI-186 beyond this initial characterization will require the derivation of a euploid clonal line.

The capacity of different hESC lines to undergo neural differentiation as a default pathway is well recognized (Reubinoff *et al.*, 2001). In a recent study of neural differentiation (Wu *et al.*, 2007), variation in the efficiency of neurosphere formation, quality and rosette formation was observed across a number of independently isolated hESC lines. These observations suggest inherent pluripotency differences exist between individual hESC lines, and may originate from different genetic and epigenetic backgrounds, the quality of the original blastocyst from which a line was derived, the stem cell protocol used, variation in fibroblast feeder layer cells or even extended passage. Importantly in this study, both HD hESC lines produced neurospheres of similar morphology (spherical and containing rosettes) to that of the wild-type HES2 and HES3 lines, and positive staining was observed for the neuroectodermal maker PAX6. Further, the SI-186 line produced primary neurones and astrocytes at a similar frequency to the control HES3 line. These findings suggest that the HD mutation does not prevent HD hESC lines from undergoing induced neural differentiation *in vitro*. On the basis of these observations, it is likely that these HD hESC lines will be useful models to generate specific neuronal subtypes, such as GABAergic medium spiny neurones that are susceptible to neurodegeneration or dopaminergic neurones that are more resistant to neurodegeneration. The

110
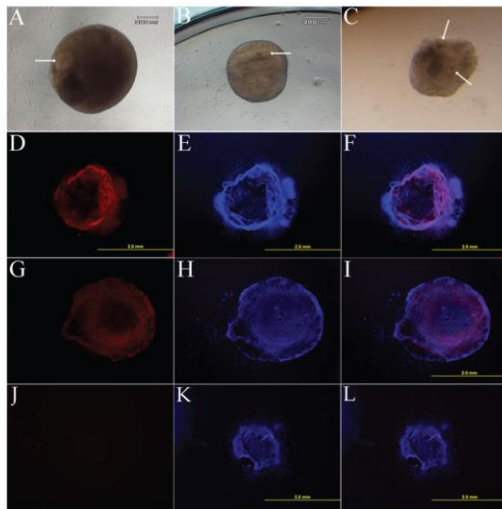
Figure 2. Neurosphere formation. Neurospheres generated in suspension from the wild-type HES2 (**A**), Huntington disease (HD) SI-186 (**B**), and HD SI-187 lines (**C**), containing rosettes (arrows). Pax-6 immunostaining (red) detected neuroectodermal cells in HD SI-187 (**D**) and wild-type (**G**) plated neurospheres, with corresponding 4,(6-diamidino-2-phenylindole) (blue) staining (**E, H**) and overlays (**F, I**). (**J–L**) Isotype negative controls. For images A–C, bar = 200 μm, for D–L, bar = 2 mm.
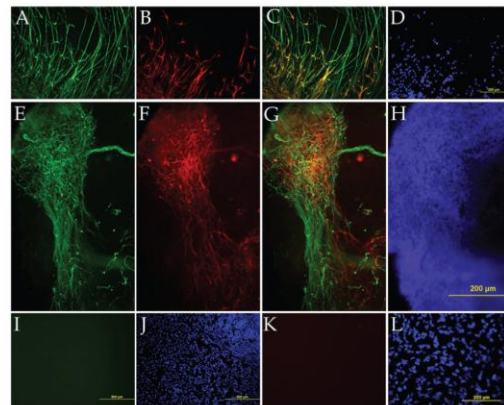
Figure 3. Neuronal differentiation. Neural-directed wild-type HES3 (**A–D**) and Huntington disease (HD) SI-186 (**E–H**) plated neurospheres immunostained to detect primary neurones using β-III-tubulin (green) and microtubule-associated protein 2ab (MAP2ab) (red), and nuclei stained using 4,(6-diamidino-2-phenylindole) (blue). (**C, G**) Overlays illustrate the co-localization of MAP2ab and β-III-tubulin within primary neurones. (**I–L**) Negative controls. For images A–H, K, L, bar = 200 μm, for I, J, bar = 500 μm,
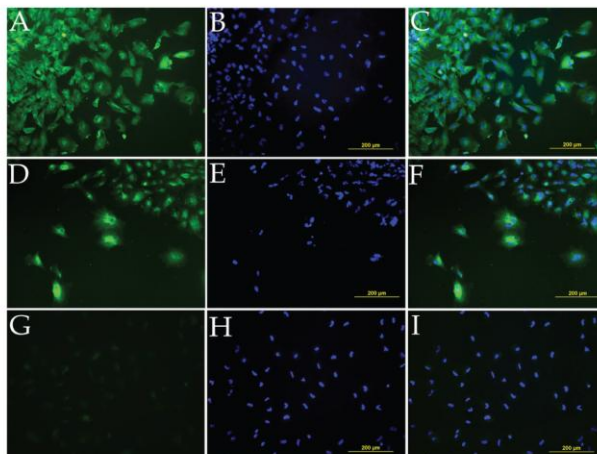
Figure 4. Glial differentiation. Glial-directed wild-type HES3 (**A–C**) and Huntington disease (HD) SI-186 (**D–F**) plated neurospheres immunostained to detect astrocytes using glial fibrillary acidic protein (green) and nuclei stained using 4,(6-diamidino-2-phenylindole) (blue). (**C, F**) Overlays illustrate the cytoplasmic location of GFAP. (**G–I**) Negative controls. For all images, bar = 200 μm.
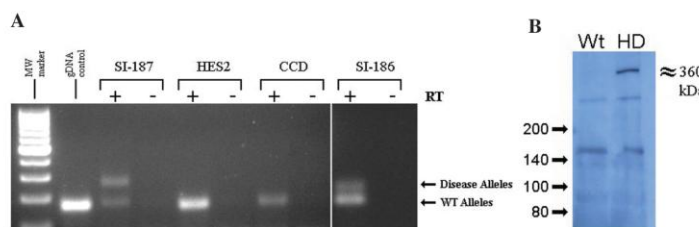
Figure 5. Reverse transcriptase-polymerase chain reaction and western blot. (**A**) Reverse transcriptase RT+ and RT– *HTT* mRNA samples visualized on a 2% agarose gel. Positions of wild-type (WT; ≈170 base pairs) and disease (>210 base pairs) alleles are indicated. (**B**) Western blot chemiluminescence staining using the 1C2 antibody demonstrates exclusive expression of the mutant protein in the Huntington disease (HD) positive SI-187 cells. Molecular mass markers (kDa) are indicated on the left. CCD = human mammary fibroblast feeder cells; gDNA = genomic DNA.

111
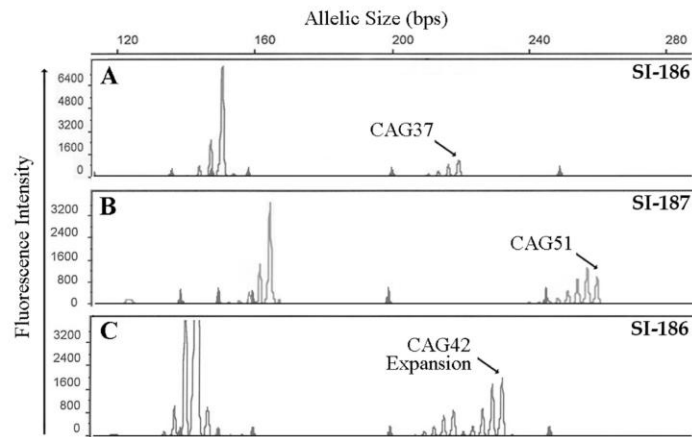
Figure 6. CAG repeat instability assessment. (**A**) Small pool fluorescent polymerase chain reaction (SP F-PCR) of SI-186 and (**B**) SI-187 undifferentiated cells shows no change in mutant allele length from progenitor length. (**C**) SP F-PCR of neurosphere differentiated SI-186 cells detects an expansion of five CAG repeats in the mutant allele. Closed peaks common to all profiles indicate Genescan internal standards. True product sizes are indicated by arrows; bps = base pairs.

ability to generate sufficient numbers of these neuronal cell types will provide the basis for detailed functional studies to investigate the mechanism(s) of HD pathogenesis *in vitro*.

Given the progressive nature and late age of onset of clinical HD, it could be argued that the relatively early passages of the undifferentiated HD hESC makes them unlikely to display the major hallmarks of disease pathology such as CAG expansion, transcriptome dysregulation or HTT aggregate formation. In this regard, analysis of SI-186 and SI-187 single cells by SP F-PCR did not detect any variation in their mutant allele CAG repeat tracts. Interestingly, however, when HD hESC were differentiated to neural progenitors, there was a high incidence of minor CAG expansions of the mutant allele at the single-cell level. Although the CAG repeat expansions were short compared with the very large CAG expansions seen in neurones of patients with HD (Kennedy *et al*., 2003; Shelbourne *et al*., 2007), this finding indicates that the neural progenitors derived from these HD hESC may be more prone to CAG repeat instability within the *HTT* gene. So far, even though the *HTT* gene was shown to be transcribed and translated in undifferentiated HD hESC, no HTT aggregates have been detected by slot blot analysis. Further studies of neuronal cultures using more sensitive techniques such as electron and confocal microscopy are warranted to establish the conditions that favour the formation of HTT aggregates.

This study provides the first example of two novel in-vitro human stem cell models of HD that will complement existing animal HD models to further the understanding of the pathways that lead to neurodegeneration in human patients. Further investigation of CAG repeat expansion and the identification transcriptional dysregulation and/or aggregate formation will also enable detailed molecular and cellular manipulation of the model to identify the underlying mechanism(s) that initiate and perpetuate these disease pathologies. Due to the innate ability of hESC lines to differentiate into any cell of the body, it will

be possible to use these HD stem cell models to address the conundrum as to why some neural cell types are particularly susceptible to apoptosis while other neural and non-central nervous system cells which express mutant *HTT* and form aggregates are resilient to disease. The availability of well-characterized HD hESC in-vitro models, which closely reflect clinical HD pathology, will also allow high-throughput drug screening which is currently precluded in animal models due to high costs. Many novel libraries containing small molecules, peptides or small inhibitory RNAs will in the future be screened to identify those that either reduce or prevent the initiation of HD pathology. By this approach, it will be possible to identify more potent drugs or new therapeutic strategies for human clinical trials.

Acknowledgements

References

Becher MW, Kotzuk JA, Sharp AH *et al*. 1998 Intranuclear neuronal inclusions in Huntington's disease and dentatorubral and pallidoluysian atrophy: correlation between the density of inclusions and IT15 CAG triplet repeat length. *Neurobiology of Disease* **4**, 387–397.

Chen-Plotkin AS, Sadri-Vakili G, Yohrling GJ *et al*. 2006 Decreased association of the transcription factor Sp1 with genes downregulated in Huntington's disease. *Neurobiology of Disease* **22**, 233–241.

Davies SW, Turmaine M, Cozens BA *et al*. 1997 Formation of neuronal intranuclear inclusions underlies the neurological dysfunction in mice transgenic for the HD mutation. *Cell* **90**, 537–548.

112

DiFiglia M, Sapp E, Chase KO *et al.* 1997 Aggregation of huntingtin in neuronal intranuclear inclusions and dystrophic neurites in brain. *Science* **277**, 1990–1993.

Draper JS, Smith K, Gokhale P *et al.* 2004 Recurrent gain of chromosomes 17q and 12 in cultured human embryonic stem cells. *Nature Biotechnology* **22**, 53–54.

Dunah AW, Jeong H, Griffin A *et al.* 2002 Sp1 and TAFII130 transcriptional activity disrupted in early Huntington's disease. *Science* **296**, 2238–2243.

Ferrante RJ, Kowall NW, Richardson EP Jr. 1991 Proliferative and degenerative changes in striatal spiny neurons in Huntington's disease: a combined study using the section-Golgi method and calbindin D28k immunocytochemistry. *Journal of Neuroscience* **11**, 3877–3887.

García-Ramos R, del Val-Fernández J, Catalán-Alonso MJ *et al.* 2007 Experimental models of Huntington's disease. *Revista de Neurologia* **45**, 437–441.

Graham RK, Deng Y, Slow EJ *et al.* 2006 Cleavage at the caspase-6 site is required for neuronal dysfunction and degeneration due to mutant huntingtin. *Cell* **125**, 1179–1191.

Gutekunst CA, Li SH, Yi H *et al.* 1999 Nuclear and neuropil aggregates in Huntington's disease: relationship to neuropathology. *Journal of Neuroscience* **19**, 2522–2534.

Huang CC, Faber PW, Persichetti F *et al.* 1998 Amyloid formation by mutant huntingtin: threshold, progressivity and recruitment of normal polyglutamine proteins. *Somatic Cell Molecular Genetics* **24**, 217–233.

Kennedy L, Evans E, Chen CM *et al.* 2003 Dramatic tissue-specific mutation length increases are an early molecular event in Huntington disease pathogenesis. *Human Molecular Genetics* **12**, 3359–3367.

Leeflang EP, Zhang L, Tavare S *et al.* 1995 Single sperm analysis of the trinucleotide repeats in the Huntington's disease gene: quantification of the mutation frequency spectrum. *Human Molecular Genetics* **4**, 1519–1526.

Lunkes A, Lindenberg KS, Ben-Haiem L *et al.* 2002 Proteases acting on mutant huntingtin generate cleaved products that differentially build up cytoplasmic and nuclear inclusions. *Molecular Cell* **10**, 259–269.

Mateizel I, De Temmerman N, Ullmann U *et al.* 2006 Derivation of human embryonic stem cell lines from embryos obtained after IVF and after PGD for monogenic disorders. *Human Reproduction* **21**, 503–511.

McNeil SM, Novelletto A, Srinidhi J *et al.* 1997 Reduced penetrance of the Huntington's disease mutation. *Human Molecular Genetics* **6**, 775–779.

Pattison LR, Kotter MR, Fraga D, Bonelli RM 2006 Apoptotic cascades as possible targets for inhibiting cell death in Huntington's disease. *Journal of Neurology* **253**, 1137–1342.

Pera MF, Andrade J, Houssami S *et al.* 2004 Regulation of human embryonic stem cell differentiation by BMP2 and its antagonist noggin. *Journal of Cell Science* **117**, 1–12.

Pera MF, Blasco-Lafita MJ, Cooper S *et al.* 1988 Analysis of cell-differentiation lineage in human teratomas using new monoclonal antibodies to cytostructural antigens of embryonal carcinoma cells. *Differentiation* **39**, 139–149.

Pickering SJ, Minger SL, Patel M *et al.* 2005 Generation of a human embryonic stem cell line encoding the cystic fibrosis mutation deltaF508, using preimplantation genetic diagnosis. *Reproductive BioMedicine Online* **10**, 390–397.

Reubinoff BE, Itsykon P, Turetsky T *et al.* 2001 Neural progenitors from human embryonic stem cells. *Nature* **19**, 1134–1140.

Reubinoff BE, Pera MF, Fong CY *et al.* 2000 Embryonic stem cell lines from human blastocysts: somatic differentiation *in vitro*. *Nature Biotechnology* **18**, 399–404.

Sathasivam K, Hobbs C, Turmaine M *et al.* 1999 Formation of polyglutamine inclusions in non-CNS tissue. *Human Molecular Genetics* **8**, 813–822.

Scherzinger E, Lurz R, Turmaine M *et al.* 1997 Huntingtin-encoded polyglutamine expansions form amyloid-like protein aggregates *in vitro* and *in vivo*. *Cell* **90**, 549–558.

Sermon K, Goossens V, Seneca S *et al.* 1995 Preimplantation diagnosis for HD: clinical application and analysis of the HD expansion in affected embryos. *Prenatal Diagnosis* **18**, 1427–1436.

Shelbourne PF, Keller-McGandy C, Bi WL *et al.* 2007 Triplet repeat mutation length gains correlate with cell-type specific vulnerability in Huntington disease brain. *Human Molecular Genetics* **16**, 1133–1142.

Shin JY, Fang ZH, Yu ZX *et al.* 2005 Expression of mutant huntingtin in glial cells contributes to neuronal excitotoxicity. *Journal of Cell Biology* **171**, 1001–1012.

Sipione S, Cattaneo E 2001 Modeling Huntington's disease in cells, flies and mice. *Molecular Neurobiology* **23**, 21–51.

Snell RG, MacMillan JC, Cheadle JP *et al.* 1993 Relationship between trinucleotide repeat expansion and phenotypic variation in Huntington's disease. *Nature Genetics* **4**, 393–397.

Telenius H, Kremer B, Goldberg YP *et al.* 1994 Somatic and gonadal mosaicism of the Huntington disease gene CAG repeat in brain and sperm. *Nature Genetics* **6**, 409–414.

Telenius H, Kremer HP, Theilmann J *et al.* 1993. Molecular analysis of juvenile Huntington disease: the major influence on (CAG)n repeat length is the sex of the affected parent. *Human Molecular Genetics* **2**, 1535–1540.

The Huntington's Disease Collaborative Research Group. 1993 A novel gene containing a trinucleotide repeat that is expanded and unstable on Huntington's disease chromosomes. *Cell* **72**, 971–983.

Thomas EA 2006 Striatal specificity of gene expression dysregulation in Huntington's Disease. *Journal of Neuroscience Research* **84**, 1151–1164.

Trottier Y, Lutz Y, Stevanin G *et al.* 1995 Polyglutamine expansion as a pathological epitope in Huntington's disease and four dominant cerebellar ataxias. *Nature* **378**, 403–406.

Verlinsky Y, Strelchenko N, Kukharenko V *et al.* 2006 Repository of human embryonic stem cell lines and development of individual specific lines using stembrid technology. *Reproductive BioMedicine Online* 13, 547–550.

Verlinsky Y, Strelchenko N, Rechitsky S *et al.* 2005 Human embryonic stem cell lines with genetic disorders. *Reproductive BioMedicine Online* **10**, 105–110.

Vonsattel JP, Myers RH, Steven TJ *et al.* 1985 Neuropathological classification of Huntington's disease. *Journal of Neuropathology and Experimental Neurology* **44**, 559–577.

Wellington CL, Ellerby LM, Gutekunst CA *et al.* 2002 Caspase cleavage of mutant huntingtin precedes neurodegeneration in Huntington's disease. *Journal of Neuroscience* **22**, 7862–7872.

Yang, SH, Cheng PH, Banta H *et al.* 2008 Towards a transgenic model of Huntington's disease in a non-human primate. *Nature* **453**, 921–924.

Wu H, Xu J, Pang ZP *et al.* 2007 Integrative genomic and functional analyses reveal neuronal subtype differentiation bias in human embryonic stem cell lines. *Proceedings of the National Academy of Sciences of the USA* **104**, 13821–13826.

113

2.3 Additional Methods

2.3.1 Establishment of SI-186 and SI-187 HD cell lines

Stem cell derivation of lines SI-186 and SI-187 from HD positive IVF embryos was originally performed at the Reproductive Genetics Institute in Chicago and made available from Stemride International through a Materials Transfer Agreement. Frozen colony pieces from each cell line were delivered from Stemride International and thawed as per reverse vitrification methods **(Section 2.3.4)**. Cell lines were initially cultured in media standardised for Stemride International for 2-4 passages until cell line growth rates and morphologies recovered from the thawing process, after which cells were transferred to the HES media and feeders utilised within our laboratory, as described in **Section 2.1**.

2.3.2 Vitrification

All hESC lines (HES2, SI-186, SI-187) were vitrified routinely every 6 months to ensure backup stocks were stored in the event of karyotypic abnormalities developing with extended culture. Five principle solutions are required for the vitrification of hESC colonies, DMEM-HEPES media (0.5mL 1M HEPES media, 19.5mL DMEM/F12; Invitrogen), ES-HEPES media (8mL DMEM-HEPES media, 2mL FBS; Invitrogen), 1M sucrose solution (3.42g sucrose added to 6mL of DMEM-HEPES media and dissolved for 15 minutes at 37°C, 2mL FBS; SigmaAldrich), 10% vitrification solution (4mL ES-HEPES media, 0.5mL ethylene glycol, 0.5mL DMSO; Sigma) and 20% vitrification solution (1.5mL ES-HEPES media, 1.5mL 1M sucrose solution, 1mL ethylene glycol, 1mL DMSO).

hESC colonies were manually dissected into quarters or sixths and 12 pieces transferred to ES-HEPES media for 5 minutes. Pieces were transferred using a p20 pipette to 10% vitrification solution and incubated for 60 seconds before being transferred to 20% vitrification solution for 25 seconds. Pieces were then collected in 20ml and transferred to a sterilised plastic plate, producing a single droplet. All pieces were then collected in a 3ul volume using a p20 pipette and drawn into a vitrification straw (Gytech). The vitrification straw was immediately placed into a 5mL cyrovial

and submerged in LN$_2$. Cryovials were sealed and placed into liquid phase LN$_2$ tanks for long-term storage.

2.3.3 Reverse vitrification

Where necessary hESC lines were reverse vitrified, or thawed, from LN$_2$ stocks. Five principle solutions were prepared, DMEM-HEPES media, ES-HEPES media, 1M sucrose solution, 0.2M sucrose solution (2mL ES-HEPES media, 0.5mL 1M sucrose solution) and 0.1M sucrose solution (2.25mL ES-HEPES media, 0.25mL 1M sucrose solution). Vitrification straws containing frozen pieces of the required hESC line were removed from cryovials using forceps and the narrow end immediately plunged into a well containing 0.2M sucrose solution. Frozen hESC pieces diffused out of vitrification straws and after 60 seconds were transferred to 0.1M sucrose solution. After 5 minutes of incubation pieces were transferred to ES-HEPES media for 5mins and then again to a fresh well containing ES-HEPES media for a further 5 minutes. hESC pieces were then transferred to a standard centre well organ culture dish (BD Biosciences) and placed in a 37°C incubator to attach overnight, after which hESC were maintained as per standard colony culture methods.

2.3.4 Neural differentiation

Differentiation was performed according to the protocol utilised in **Section 2.1** which was first described in 2001 (Reubinoff et al., 2001). Two independent culture replicate differentiation experiments were performed at passages 28 and 34 (SI-187), 45 and 51 (SI-186) and 44 and 50 (HES2). Approximately 200 neurospheres in total were generated for each cell line, 100 for each culture replicate.

2.3.5 Neurosphere morphological assessment

Morphological evaluations were made four weeks after neural differentiation induction at the end of the neurosphere stage to determine the differentiation capabilities of each line. Three scoring categories were devised to assess neurosphere quality and each well was assigned one grade:

Grade 0 = Complete apoptosis or sphere formation failure

Grade 1 = Aggregate structure of irregular morphology and/or cystic structures

Grade 2 = Spherical sphere formation without cystic structures

The total score was calculated by the following equation:

(0 x number of grade 1) + (1 x number of grade 2) + (2 x number of grade 2)

2.3.6 Immunocytochemistry

Immunocytochemistry labelling of HTT was performed and analysed according to methods described in **Section 2.1**. A primary rabbit anti-human N-terminal HTT antibody (Millipore) was used at 1:100, and visualisation illuminated with goat anti-rabbit AlexaFluor 555 (BD) secondary antibodies at 1:200.

2.4 Additional Results

2.4.1 Resolution of SI-186 karyotypic mosaicism

A mosaic karyotype in the SI-186 line at passage 29 was identified in **Section 2.2**, where 62.5% of the otherwise normal cell population was trisomic (47,XX +12; **Figure 2.1A**). Given that a majority of SI-186 cell produce discrepant levels of chromosome 12 genes which may infuse stochastic elements throughout undifferentiated and differentiated culture systems and obfuscate experimental results, preventing the resolution of disease specific phenotypes, correction of this genetic anomaly was critical for future investigations.

Earlier passage aliquots of the SI-186 line were thus obtained from StemRide International. Subsequent to the adaptation and establishment of early passage SI-186 cells to colony culture conditions, SI-186 cells were again subjected to Giemsa staining that reported a normal 46,XX karyotype in 100% of the mitotically active cells assessed at passage 17 **(Figure 2.1B)**. As a result, all experimental assays utilising the SI-186 line beyond **Section 2.1** were obtained utilising cells from the euploid (46, XX) derivative.

2.4.2 Neural differentiation of 46,XX SI-186 cells

Confirmation of the neural differentiation capacity of the 46,XX SI-186 line was required prior to comparisons between HD and wildtype lines. Representative morphological images of efficacious differentiation replicates from all three cell lines, including SI-186, at all three principle differentiation stages are provided in **Figure 2.1C.** Morphological images demonstrate the capacity of all lines, particularly the re-established SI-186 line, to differentiate to neuronal cells in a robust manner.

Noggin treated hESC colonies at d7 **(Figure 2.1Ci)** and d14 **(Figure 2.1Cii)** reveal similar morphology across all lines, all colonies contain regions indicative of spontaneous differentiation by two weeks and are avoided during manual selection for neurosphere formation **(Figure 2.1Cii, arrows)**. Indeed, little variation between control and HD lines in terms of noggin treated colony growth and morphology were

observed. All lines possessed the capacity to generate some neurospheres of high morphological quality from noggin treated colony pieces as shown at d21 and d28 **(Figure 2.1Ciii-iv)**. Further differentiation of neurospheres on laminin coated surfaces to neurons was successful with the re-established karyotypically normal SI-186 line as well as the SI-187 and HES2 lines; each line produced neurospheres that exhibited a strong propensity to generating significant neurite outgrowth **(Figure 2.1Cv-vi)**.

The generation of neurospheres is a particularly robust technique, with the successful formation of a neurosphere from 97% of HES2 and 94% SI-186 and SI-187 noggin treated colony pieces **(Figure 2.2C)**. Both wildtype control and HD cell lines exhibited the capacity to generate neurospheres of high morphological quality (grade = 2) that were symmetrical in nature and contained neural rosettes **(Figure 2.2A)**, and further each line produced numerous neurospheres of poor quality (grade = 1), that were typically asymmetric bodies with cystic structures and cell debris **(Figure 2.2B)**.

Intriguingly, reduced frequencies of grade 2 neurospheres were generated from noggin treated cultures in SI-186 (-57.7%) and SI-187 (-73.1%) cells compared to HES2 controls **(Figure 2.2C)**. Reduced grade 2 neurosphere formation in both disease lines was accompanied by concomitant increases in lower quality grade 1 spheres, with little difference in the number of failed, grade 0 neurospheres **(Figure 2.2C)**. Overall grade values of HD neurospheres were reduced compared to controls by 27.4% and 32.4% for SI-186 and SI-187 cultures respectively **(Figure 2.2C)**.

Karyotypically normal SI-186 cells were seen to differentiate into neurons as evaluated by immunocytochemistry staining for the pan-neuronal cytoskeletal marker β-iii-tubulin **(Figure 2.3F).** Simultaneous neuronal differentiation of SI-187 and HES2 was also performed and confirmed with β-iii-tubulin immunostaining **(Figure 2.3C & I)**. Equivalent across all cell lines, β-iii-tubulin immunostaining show strong antibody binding within neurites and cell bodies but not within nuclei **(Figure 2.3A, D, G)**. No aberrant loss of HTT arises during differentiation or extended culture, with protein expression observed with anti-HTT N-terminal antibodies binding to neurons derived from all lines **(Figure 2.3B, E, H)**.
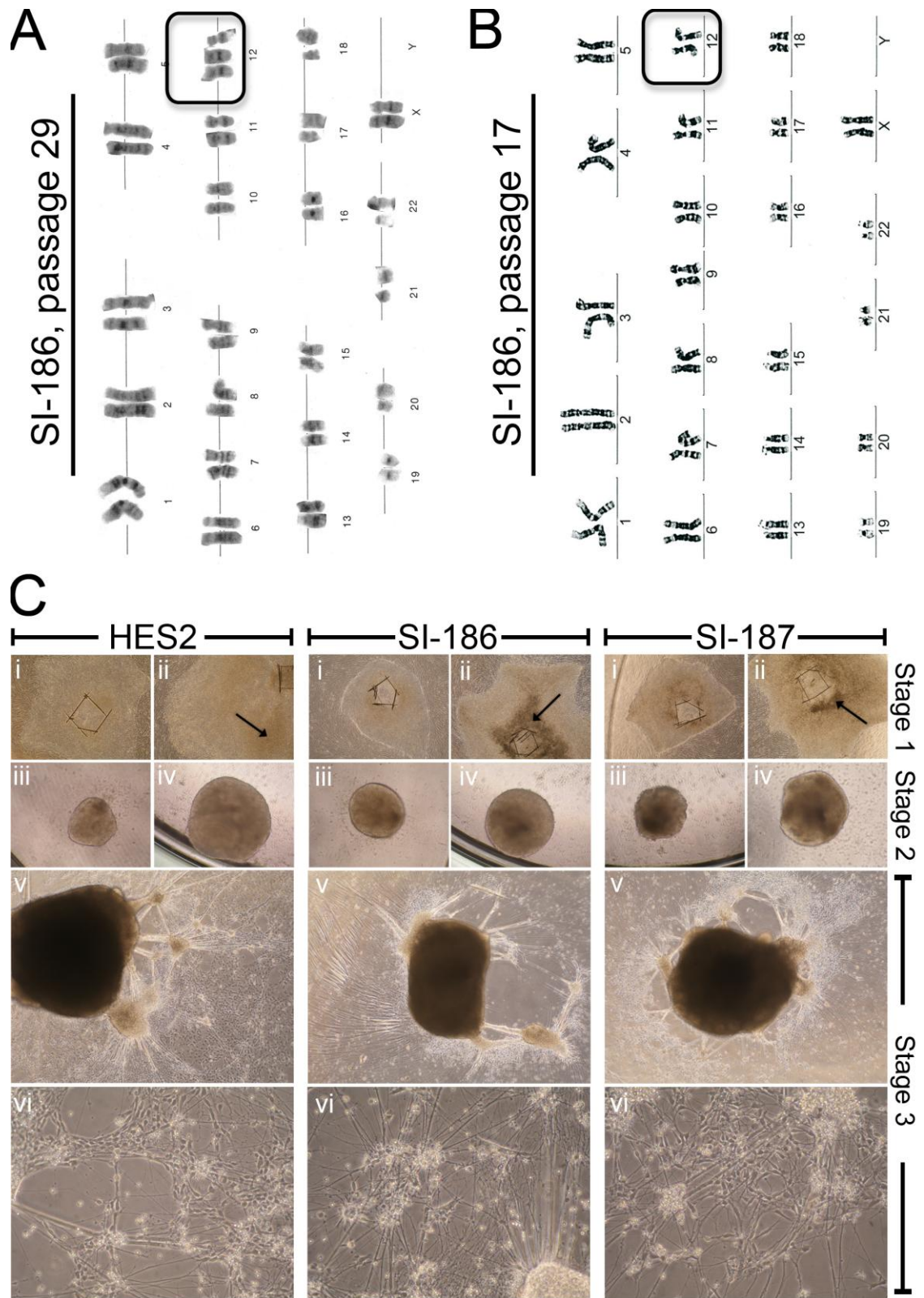
Figure 2.1: Giemsa staining of SI-186 cells with the karyotype of a representative cell with chromosome 12 trisomy **(A, circled)**. Karyotype results SI-186 cells with a normal 46, XX human karyotype **(B)**. Morphological images of karyotypically normal HES2, SI-186 and SI-187 lines at all three neural differentiation stages **(C)**. Noggin treatment stage at d7 **(Ci)** and d14 **(Cii)**, arrow regions denote spontaneous differentiation and are were avoided for neurosphere generation. Neurosphere development stage at d21 **(Ciii)** and d28 **(Civ)**, neuronal differentiation stage at d42 at 4x magnification **(Cv)** and 20x magnification **(Cvi)**.
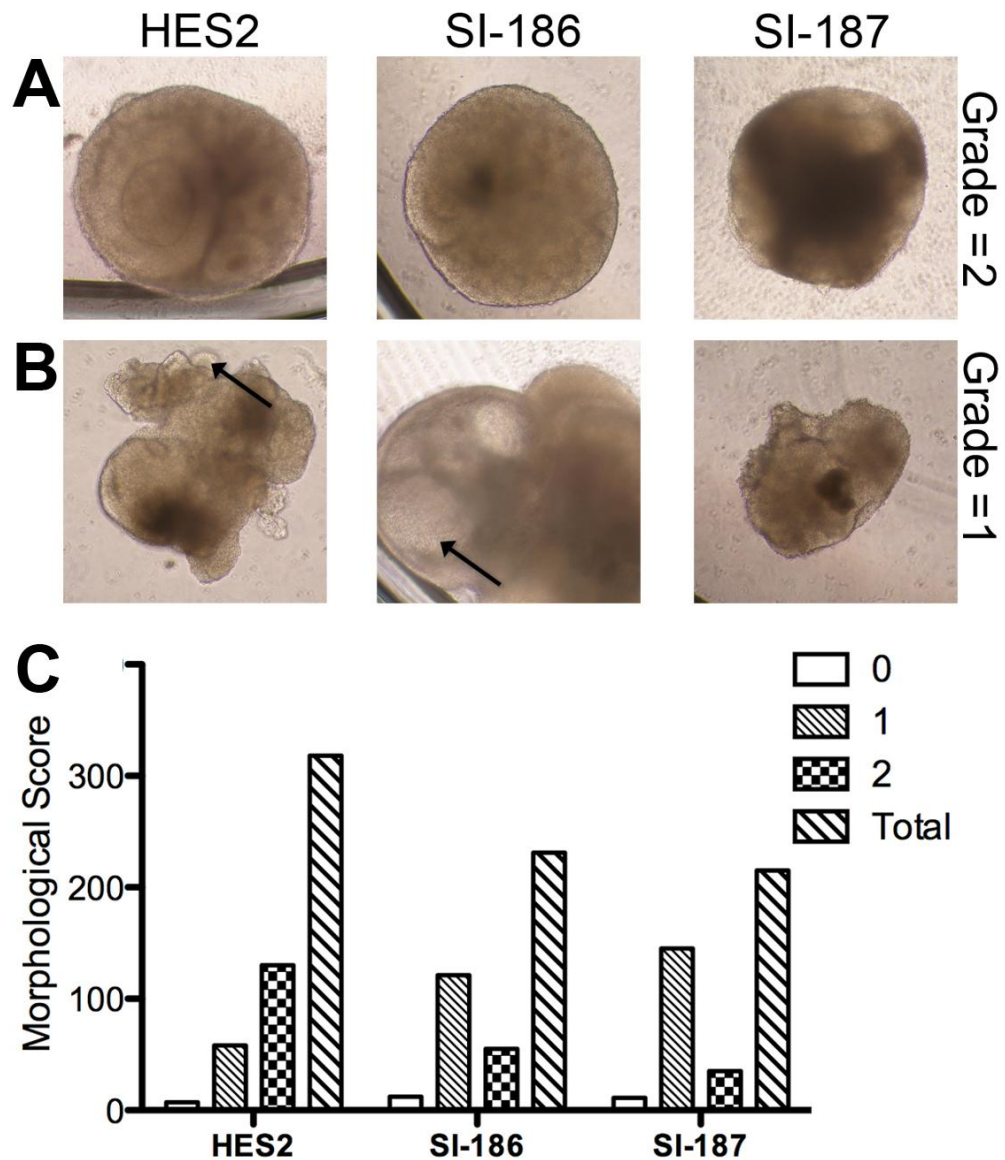
Figure 2.2: Representative images of HES2, SI-186 and SI-187 neurospheres of morphological quality grade 1 **(A)** and grade 2 **(B)**. Arrows indicate cystic structures. Total numbers of neurospheres that received each scoring grade are graphically represented and compared to a total score **(C)**. Brightfield neurosphere images at 4x magnification.
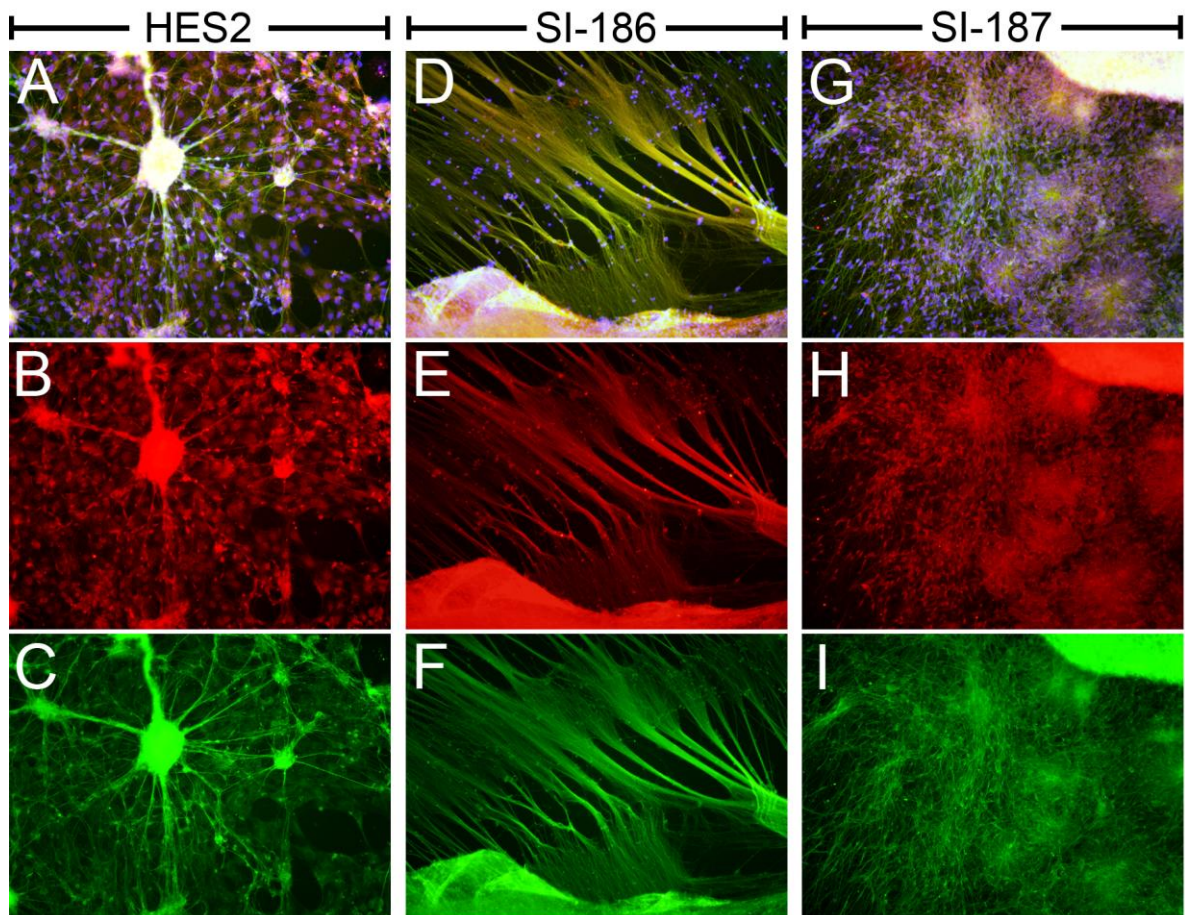
Figure 2.3: Immunochemistry staining of neuronal progeny antibodies targeting β-iii-tubulin **(green)** and HTT **(red)** in control cell line HES2 **(A-C)**, and HD cell lines SI-186 **(D-F)** and SI-187 **(G-I)**. Merged images **(A, D, G)** include DAPI nuclear staining (blue), images at 20x magnification.

2.5 Additional Discussion

This chapter investigates two hESC lines heterozygous for CAG repeat expansions within exon 1 of the *HTT* loci. Validation of CAG repeat mutations and allelic expression in undifferentiated and neural differentiated cells confirm these cell lines produce the causative protein required for HD pathology at relevant stages.

2.5.1 Trisomic mosaicism

A majority of SI-186 cells were found to harbour an abnormal trisomic karyotype. Early studies of the genomic integrity of hESCs were reliant upon low-resolution karyotypic assessments, such as Geimsa staining, and have produced conflicting results. Reports of stability within hESC cultures (Brimble et al., 2004;Buzzard et al., 2004;Rosler et al., 2004) contrast those detecting trisomies and whole-arm duplications, particularly of chromosomes 12 and 17 in many hESCs lines (Draper et al., 2004;Mitalipova et al., 2005;Baker et al., 2007). Today, it is well established that karyotypic instability is an intractable feature of hESC culture, and novel comparative genomic hybridisation studies have even located 'hotspots' of several megabases that are preferentially duplicated, particularly at 20q11.21 (Maitra et al., 2005;Lefort et al., 2008;Spits et al., 2008;Wu et al., 2008;Narva et al., 2010;Initiative et al., 2011)

Such changes are postulated to provide a pro-survival and/or proliferative advantage within an *in vitro* environment and steadily accumulate with progressive passaging and freeze/thaw cycles (Loring and Rao, 2006;Initiative et al., 2011), and therefore it is not surprising that a chromosome 12 abnormality arose in the SI-186 lines utilised. Chromosome 12 contains approximately 1200 – 1400 genes and their aberrant cellular loadings introduces innumerable variability that compromises the ability to accurately contrast disease and wildtype hESC lines.

Validation of a normal 46,XX karyotype in an earlier passage SI-186 sample delivered from Stemride International subsequent to the identification of a trisomic karyotype provided appropriate euploid cellular material for comparative analysis between HD and wildtype lines for all future experimentation.

2.5.2 Interline neuronal differentiation variability

Successful *in vitro* neuronal differentiation of both SI-186 and SI-187 lines demonstrate mHTT does not significantly inhibit this process, consistent with HD rodent and human patients whose nervous system develops fully. However, morphological observations of impaired neurosphere formation in SI-186 and SI-187 lines compared to the control HES2 line ostensibly suggests a correlation between mHTT expression and reduced *in vitro* neural differentiation capacity. While such perturbations have not been reported *in vivo*, the simplistic microenvironment of *in vitro* differentiation may lack crucial trophic cues, to exacerbate or emphasise underlying dysfunction.

Further, two issues prohibit a definitive attribution of impaired neurosphere formation to mHTT expression and may account for the observations recorded; namely interline differentiation variation and the presence of stochastic elements present within the neural differentiation protocol employed.

Interline variation is a pernicious and widespread phenomenon, occurring upon hESC differentiation that occurs spontaneously (Mikkola et al., 2006;Osafune et al., 2008;Tavakoli et al., 2009), towards non-neural lineges (Burridge et al., 2007;Chang et al., 2008;Osafune et al., 2008;Pekkanen-Mattila et al., 2009;Grigoriadis et al., 2010) and neural lineages (Wu et al., 2007;Tavakoli et al., 2009;Lappalainen et al., 2010).

The avant-garde protocol developed by Ben Reubinoff and Martin Pera represents one of the earliest demonstrations of hESC *in vitro* differentiation to neurons (Reubinoff et al., 2001). Arguably however, requisite stages of the protocol presented difficulties upon their application to a disease-modelling scenario that relies on the resolution of potentially subtle disease phenotypes. Specifically, hESC must be cultured as colonies for noggin-mediated differentiation induction and neurosphere generation, a culture system that inherently carries substantial variations (Laslett et al., 2007;Kolle et al., 2009;Ho et al., 2011). Colony heterogeneity is an area subjected to active research and it is uncertain whether it translates to inconsistency in neural and neuronal differentiation propensities. Manual selection of colony regions for neurosphere formation may exacerbate this phenomenon as morphological assessment cannot

distinguish heterogeneous populations, and neurosphere seeding densities are not controlled and has been shown to affect sub-lineage commitment (Goulburn et al., 2011).

In conclusion, this chapter describes initial characterisation hESC lines carrying HD mutations. Subjecting these cells to neural inducing conditions with the BMP inhibitor Noggin and promotion of neural identity with FGFβ and EGF, generated neuronal cells despite the presence of mHTT. Karyotypic abnormalities within the partially penetrant SI-186 line were resolved and neural differentiation reassessed. Future studies will benefit from the use of multiple wildtype control lines and emerging or novel differentiation protocols that emphasise a reduction in stochastic elements to ensure the accurate discrimination of disease phenotypes that may be present. These lines aim to provide an informative tool for understanding pre-onset HD etiology and uniquely throughout stages equivalent to early human development in the context of an *in vitro* format.

2.6 References

Baker, D.E., Harrison, N.J., Maltby, E., Smith, K., Moore, H.D., Shaw, P.J., Heath, P.R., Holden, H., and Andrews, P.W. (2007). Adaptation to culture of human embryonic stem cells and oncogenesis in vivo. *Nature biotechnology* 25**,** 207-215.

Brimble, S.N., Zeng, X., Weiler, D.A., Luo, Y., Liu, Y., Lyons, I.G., Freed, W.J., Robins, A.J., Rao, M.S., and Schulz, T.C. (2004). Karyotypic stability, genotyping, differentiation, feeder-free maintenance, and gene expression sampling in three human embryonic stem cell lines derived prior to August 9, 2001. *Stem cells and development* 13**,** 585-597.

Burridge, P.W., Anderson, D., Priddle, H., Barbadillo Muñoz, M.D., Chamberlain, S., Allegrucci, C., Young, L.E., and Denning, C. (2007). Improved Human Embryonic Stem Cell Embroid Body Homogeneity and Cardiomyocyte Differentiation from a Novel V-96 Plate Aggregation System Highlights Interline Variability. *Stem Cells* 25**,** 929-938.

Buzzard, J.J., Gough, N.M., Crook, J.M., and Colman, A. (2004). Karyotype of human ES cells during extended culture. *Nature biotechnology* 22**,** 381-382; author reply 382.

Chang, K.-H., Nelson, A.M., Fields, P.A., Hesson, J.L., Ulyanova, T., Cao, H., Nakamoto, B., Ware, C.B., and Papayannopoulou, T. (2008). Diverse hematopoietic potentials of five human embryonic stem cell lines. *Experimental cell research* 314**,** 2930-2940.

Draper, J.S., Smith, K., Gokhale, P., Moore, H.D., Maltby, E., Johnson, J., Meisner, L., Zwaka, T.P., Thomson, J.A., and Andrews, P.W. (2004). Recurrent gain of chromosomes 17q and 12 in cultured human embryonic stem cells. *Nature biotechnology* 22**,** 53-54.

Goulburn, A.L., Alden, D., Davis, R.P., Micallef, S.J., Ng, E.S., Yu, Q.C., Lim, S.M., Soh, C.-L., Elliott, D.A., Hatzistavrou, T., Bourke, J., Watmuff, B., Lang, R.J., Haynes, J.M., Pouton, C.W., Giudice, A., Trounson, A.O., Anderson, S.A., Stanley, E.G., and Elefanty, A.G. (2011). A Targeted NKX2.1 Human Embryonic Stem Cell Reporter Line Enables Identification of Human Basal Forebrain Derivatives. *Stem Cells* 29**,** 462-473.

Grigoriadis, A.E., Kennedy, M., Bozec, A., Brunton, F., Stenbeck, G., Park, I.H., Wagner, E.F., and Keller, G.M. (2010). Directed differentiation of hematopoietic precursors and functional osteoclasts from human ES and iPS cells. *Blood* 115**,** 2769-2776.

Ho, M.S.H., Fryga, A., and Laslett, A.L. (2011). Flow cytometric analysis of human pluripotent stem cells. *Methods in molecular biology (Clifton, N.J.)* 767**,** 221-230.

Initiative, T.I.S.C., Amps, K., Andrews, P.W., Anyfantis, G., Armstrong, L., Avery, S., Baharvand, H., Baker, J., Baker, D., Munoz, M.B., Beil, S., Benvenisty, N., Ben-Yosef, D., Biancotti, J.-C., Bosman, A., Brena, R.M., Brison, D., Caisander, G., Camarasa, M.V., Chen, J., Chiao, E., Choi, Y.M., Choo, A.B.H., Collins, D., Colman, A., Crook, J.M., Daley, G.Q., Dalton, A., De Sousa, P.A., Denning, C., Downie, J., Dvorak, P., Montgomery, K.D., Feki, A., Ford, A., Fox, V., Fraga, A.M., Frumkin, T., Ge, L., Gokhale, P.J., Golan-Lev, T., Gourabi, H., Gropp, M., Guangxiu, L., Hampl, A., Harron, K., Healy, L., Herath, W., Holm, F., Hovatta, O., Hyllner, J., Inamdar, M.S., Irwanto, A.K., Ishii, T., Jaconi, M., Jin, Y., Kimber, S., Kiselev, S., Knowles, B.B., Kopper, O., Kukharenko, V., Kuliev, A., Lagarkova, M.A., Laird, P.W., Lako,

M., Laslett, A.L., Lavon, N., Lee, D.R., Lee, J.E., Li, C., Lim, L.S., Ludwig, T.E., Ma, Y., Maltby, E., Mateizel, I., Mayshar, Y., Mileikovsky, M., Minger, S.L., Miyazaki, T., Moon, S.Y., Moore, H., Mummery, C., Nagy, A., Nakatsuji, N., Narwani, K., Oh, S.K.W., Oh, S.K., Olson, C., Otonkoski, T., Pan, F., Park, I.-H., Pells, S., Pera, M.F., Pereira, L.V., Qi, O., Raj, G.S., Reubinoff, B., Robins, A., Robson, P., Rossant, J., et al. (2011). Screening ethnically diverse human embryonic stem cells identifies a chromosome 20 minimal amplicon conferring growth advantage. *Nature biotechnology* 29**,** 1132-1144.

Kolle, G., Ho, M., Zhou, Q., Chy, H.S., Krishnan, K., Cloonan, N., Bertoncello, I., Laslett, A.L., and Grimmond, S.M. (2009). Identification of Human Embryonic Stem Cell Surface Markers by Combined Membrane-Polysome Translation State Array Analysis and Immunotranscriptional Profiling. *Stem Cells* 27**,** 2446-2456.

Lappalainen, R.S., Salomäki, M., Ylä-Outinen, L., Heikkilä, T.J., Hyttinen, J.A., Pihlajamäki, H., Suuronen, R., Skottman, H., and Narkilahti, S. (2010). Similarly derived and cultured hESC lines show variation in their developmental potential towards neuronal cells in long-term culture. *Regenerative Medicine* 5**,** 749-762.

Laslett, A.L., Grimmond, S., Gardiner, B., Stamp, L., Lin, A., Hawes, S.M., Wormald, S., Nikolic-Paterson, D., Haylock, D., and Pera, M.F. (2007). Transcriptional analysis of early lineage commitment in human embryonic stem cells. *BMC Developmental Biology* 7**,** 12.

Lefort, N., Feyeux, M., Bas, C., Féraud, O., Bennaceur-Griscelli, A., Tachdjian, G., Peschanski, M., and Perrier, A.L. (2008). Human embryonic stem cells reveal recurrent genomic instability at 20q11.21. *Nature biotechnology* 26**,** 1364-1366.

Loring, J.F., and Rao, M.S. (2006). Establishing standards for the characterization of human embryonic stem cell lines. *Stem Cells* 24**,** 145-150.

Maitra, A., Arking, D.E., Shivapurkar, N., Ikeda, M., Stastny, V., Kassauei, K., Sui, G., Cutler, D.J., Liu, Y., Brimble, S.N., Noaksson, K., Hyllner, J., Schulz, T.C., Zeng, X., Freed, W.J., Crook, J., Abraham, S., Colman, A., Sartipy, P., Matsui, S.-I., Carpenter, M., Gazdar, A.F., Rao, M., and Chakravarti, A. (2005). Genomic alterations in cultured human embryonic stem cells. *Nature genetics* 37**,** 1099-1103.

Mikkola, M., Olsson, C., Palgi, J., Ustinov, J., Palomaki, T., Horelli-Kuitunen, N., Knuutila, S., Lundin, K., Otonkoski, T., and Tuuri, T. (2006). Distinct differentiation characteristics of individual human embryonic stem cell lines. *BMC Developmental Biology* 6**,** 40.

Mitalipova, M.M., Rao, R.R., Hoyer, D.M., Johnson, J.A., Meisner, L.F., Jones, K.L., Dalton, S., and Stice, S.L. (2005). Preserving the genetic integrity of human embryonic stem cells. *Nature biotechnology* 23**,** 19-20.

Narva, E., Autio, R., Rahkonen, N., Kong, L., Harrison, N., Kitsberg, D., Borghese, L., Itskovitz-Eldor, J., Rasool, O., Dvorak, P., Hovatta, O., Otonkoski, T., Tuuri, T., Cui, W., Brustle, O., Baker, D., Maltby, E., Moore, H.D., Benvenisty, N., Andrews, P.W., Yli-Harja, O., and Lahesmaa, R. (2010). High-resolution DNA analysis of human embryonic stem cell lines reveals culture-induced copy number changes and loss of heterozygosity. *Nature biotechnology* 28**,** 371-377.

Osafune, K., Caron, L., Borowiak, M., Martinez, R.J., Fitz-Gerald, C.S., Sato, Y., Cowan, C.A., Chien, K.R., and Melton, D.A. (2008). Marked differences in differentiation propensity among human embryonic stem cell lines. *Nature biotechnology* 26**,** 313-315.

Pekkanen-Mattila, M., Kerkelä, E., Tanskanen, J.M.A., Pietilä, M., Pelto-Huikko, M., Hyttinen, J., Skottman, H., Suuronen, R., and Aalto-Setälä, K. (2009). Substantial variation in the cardiac differentiation of human embryonic stem cell lines derived and propagated under the same conditions—a comparison of multiple cell lines. *Annals of Medicine* 41**,** 360-370.

Reubinoff, B.E., Turetsky, T., and Pera, M.F. (2001). Neural progenitors from human embryonic stem cells. *Nature biotechnology* 19**,** 1134-1140.

Rosler, E.S., Fisk, G.J., Ares, X., Irving, J., Miura, T., Rao, M.S., and Carpenter, M.K. (2004). Long-term culture of human embryonic stem cells in feeder-free conditions. *Developmental dynamics : an official publication of the American Association of Anatomists* 229**,** 259-274.

Spits, C., Mateizel, I., Geens, M., Mertzanidou, A., Staessen, C., Vandeskelde, Y., Van Der Elst, J., Liebaers, I., and Sermon, K. (2008). Recurrent chromosomal abnormalities in human embryonic stem cells. *Nature biotechnology* 26**,** 1361-1363.

Tavakoli, T., Xu, X., Derby, E., Serebryakova, Y., Reid, Y., Rao, M.S., Mattson, M.P., and Ma, W. (2009). Self-renewal and differentiation capabilities are variable between human embryonic stem cell lines I3, I6 and BG01V. *BMC Cell Biology* 10**,** 44.

Verlinsky, Y., Strelchenko, N., Kukharenko, V., Rechitsky, S., Verlinsky, O., Galat, V., and Kuliev, A. (2005). Human embryonic stem cell lines with genetic disorders. *Reproductive biomedicine online* 10**,** 105-110.

Wu, H., Kim, K.J., Mehta, K., Paxia, S., Sundstrom, A., Anantharaman, T., Kuraishy, A.I., Doan, T., Ghosh, J., Pyle, A.D., Clark, A., Lowry, W., Fan, G., Baxter, T., Mishra, B., Sun, Y., and Teitell, M.A. (2008). Copy Number Variant Analysis of Human Embryonic Stem Cells. *Stem Cells* 26**,** 1484-1489.

Wu, H., Xu, J., Pang, Z.P., Ge, W., Kim, K.J., Blanchi, B., Chen, C., Südhof, T.C., and Sun, Y.E. (2007). Integrative genomic and functional analyses reveal neuronal subtype differentiation bias in human embryonic stem cell lines. *Proceedings of the National Academy of Sciences of the United States of America* 104**,** 13821-13826.

CHAPTER 3

Robust Defined Forebrain Differentiation Of Human Pluripotent Stem Cells

3.1 Introduction

The first study to compare neural differentiation outcomes of an individual protocol across multiple hESC lines demonstrated significant interline variation (Wu et al., 2007). Despite strict control of *in vitro* parameters such as media components and an avoidance of co-culture stages, prominent variations between lines HSF1 and HSF were reported at key neural developmental stages, including the presence or absence of neural epithelial-like rosette structures (Wu et al., 2007). Investigations by Tavakoli and others in 2009 on two separate hESC lines (I3 and I6) have corroborated rosette variation (Tavakoli et al., 2009). Indeed, reported interline variation arises across a broad range of parameters, including gene expression timing, cell responses to growth factor administration and functional profiles of derived neurons (Wu et al., 2007;Tavakoli et al., 2009;Lappalainen et al., 2010).

Studies that aim to evaluate wildtype and disease hESCs lines during neural differentiation require comprehensive understandings of gene expression profiles in combination with robust differentiation protocols. Numerous surface protein antigens have been characterised and found to frequently present as unique combinations on discrete cell types, and has led to the high-throughput evaluation of live cells by fluorescent activated cell sorting (FACS) and analysis. The fastidious and comprehensive characterisation of surface antigen expression profiles of cells that comprise the hematopoietic lineage stand in stark contrast to the limited and often contradictory studies performed on cells during neural differentiation (Pruszak et al., 2007;Pruszak et al., 2009;Sundberg et al., 2009;Yuan et al., 2011).

An early candidate for a neural cell surface antigen was CD24, as this protein showed upregulation upon neural differentiation (Pruszak et al., 2007), however, later studies found expression levels were equivalent between neural cells and pluripotent cells (Sundberg et al., 2009;Yuan et al., 2011). A subsequent study utilised CD24 in combination with CD15 and CD29, to isolate three distinct neural groups including proliferative NSCs and neurons with reduced proliferation and an elimination of tumour formation (Pruszak et al., 2009). Oddly, high and low CD24 expressing populations were not observed separately in similar cellular populations highlighting

the lack of certainty in this field (Yuan et al., 2011). Another surface antigen to receive similar attention, CD184 has yielded conflicting results, with Sundberg and colleagues identifying CD184-positive selection to define a population biased to neuronal differentiation whereas Yuan and colleagues found CD184-negative selection was required (Sundberg et al., 2009;Yuan et al., 2011).

An additional surface antigen is CD56, which may be valuable during neural differentiation as FACS sorting and enrichment is beneficial for promoting neuronal differentiation (Pruszak et al., 2007). Further, later findings found high CD56+ expression correlates with strong neuronal differentiation potential (Sundberg et al., 2009). Later studies do suggest however, that CD56 may act as an identifier of proliferative multi-potent NSCs in addition to neurons (Sundberg et al., 2009;Yuan et al., 2011).

The glycoprotein CD133 represents another potential candidate and is well established as a marker of NSCs differentiated from hESCs (Golebiewska et al., 2009;Peh et al., 2009;Pruszak et al., 2007) and NSCs isolated from CNS tissue (Uchida et al., 2000; Schwartz et al., 2003). CD133 however also demonstrates significant expression on hESCs (Sundberg et al., 2009;Yuan et al., 2011). Nevertheless, downregulation of this marker during neural differentiation is indicative of reduced cell proliferation capacity and a loss of hPSCs and NSCs within cultures (Pruszak et al., 2007;Sundberg et al., 2009).

Antibodies raised to FORSE-1 also appears promising for the selection of neural subpopulations, strongly labelling the telencephalon in the developing rodent CNS and exhibiting limited expression and brief temporal range in the diencephalon (Tole et al., 1995). Immunolabelling of rat embryos with FORSE-1 antibodies first identifies expression at E9.5, with the strong expression throughout the telencephalon that does not wane throughout development (Tole et al., 1995;Tole and Patterson, 1995). Furthermore, the forkhead box G1 (FOXG1) transcription factor is highly restricted to the developing telencephalon (Tao and Lai, 1992;Murphy et al., 1994), and exhibits a striking overlap with the expression regions and boundaries of FORSE-1 expression throughout the telencephalon (Tole et al., 1995;Tole and Patterson, 1995).

FORSE-1 was found to recognise a carbohydrate moiety, Le^X, believed to be widely involved in adhesive and proliferative roles (Allendoerfer et al., 1995) and fittingly is shown to demarcate germinal zones of the developing murine telencephalon (Capela and Temple, 2002). The Le^X surface epitope is also known as CD15, FAL and SSEA-1 (Allendoerfer et al., 1995;Allendoerfer et al., 1999;Capela and Temple, 2002). While it is uncertain as to whether FORSE-1 demarcates the developing human forebrain and telencephalon with the precision seen in rodents, FORSE-1+ fractions of hESC neural differentiation cultures have shown striking correlation with FOXG1 expression (Pruszak et al., 2007;Goulburn et al., 2011), and further, FORSE-1+ fractions appear to possess strong neural and neuronal differentiation potential (Elkabetz et al., 2008).

Numerous surface antigens are also found to identify hPSCs, in particular SSEA-3, SSEA-4, TRA-1-60, TRA-1-80, GCTM2 and CD9. A glycoprotein identified at the Karolinska Institute, epithelial cell adhesion molecule (EpCAM, also known as CD326), was also recently found to be a marker of undifferentiated hPSCs, with several hESC lines expressing robust levels of this antigen which were downregulated in parallel with TRA-1-81 upon neural differentiation (Sundberg et al., 2009), and this has since been corroborated by a separate research laboratory (Kolle et al., 2009). Combinations of the existing and emerging pluripotent surface antigens is crucial for ensuring the exit of cells from a pluripotent state that is associated with tumorgenicity.

To address crucial aspects of neural differentiation such as protocol efficacy, transcription factor and surface antigen expression profiles, interline variation and to discern relevant phenotypes of disease hPSC lines, a robust and defined differentiation system is prudent. A defined suspension based system that does not utilise serum has been developed for hESC neural differentiation (Schulz et al., 2004). However, manual dissection of hESC cultures is required for this system and the individual aggregates formed initially appear to coalesce into large structures prohibitive to the diffusion of essential nutrients and patterning factors.

This Chapter details the development and validation of a robust forebrain differentiation protocol, termed the neural directed EB (NDEB) system. The aim of this protocol is to provide an improved methodology for neural differentiation, and specifically for application in the proceeding chapter to HD hESC lines SI-186 and SI-187 to enable resolution of potentially subtle disease phenotypes that may exist. The inclusion of spin embryoid body (EB) aggregation techniques, that have been principally applied to mesendodermal differentiation contexts, provides a synchronised and high throughput platform for investigating hESC differentiation (Ng, 2005;Burridge et al., 2007;Davis et al., 2008;Eiraku et al., 2008;Ng et al., 2008a;Ng et al., 2008b;Burridge et al., 2011;Elliott et al., 2011;Goulburn et al., 2011). Further, this Chapter emphasises the utility of surface antigens for evaluating neural differentiation efficacy, focusing on the traditional NSC marker CD133, NSC/neuronal marker CD56 (PSA-NCAM), forebrain marker FORSE1, glial marker CD140α (PDGFRα), as well as pluripotent markers TRA-1-60, CD9 and EpCAM. The efficacy of this novel neural differentiation system is further evaluated across hESC and iPSC lines.

3.2 Methods

3.2.1 hESC maintenance and culture conditions

All five hESC lines (HES3, H9, MEL1, SI-186 and SI-187) were routinely maintained as colony cultures passaged manually and monolayer cultures passaged enzymatically in TrypLE Select (Invitrogen) by the author to avoid potential user-specific variability. Undifferentiated hESCs were maintained as previously described, in HES media supplemented with 10 ng/ml bFGF (R&D Systems) (Costa et al., 2008). Importantly HES media was changed daily to ensure the robust maintenance of pluripotent states. Morphological assessment of the wildtype HES3 line over 4 passages on each batch of human fibroblasts was performed to ensure a sufficient capacity for maintaining pluripotency. All MEF batches were tested for their ability to maintain the wildtype HES3 line at an appropriate morphology, with correct expression levels of SSEA-3, SSEA-4 and CD9 assayed by flow cytometry at StemCore Australia.

A robust protocol for the conversion of hESC colonies to a bulk culture system has been described previously (Ng et al., 2008a). Typically, mechanical dissection and removal of any regions of spontaneous differentiation from hESC colonies was performed first. Subsequently, each hESC colony was cut 15-20 times vertically and horizontally to produce dozens of colony pieces. After 10 colonies have been dissected, all pieces were transferred to a T25 cm^2 culture flask (BD Biosciences) pre-coated with irradiated MEFs (0.02×10^6/cm^2). This was repeated until 70-100 colonies had been harvested and transferred to a T25 cm^2 culture flask. Pieces were left to attach overnight, after which HES media was changed every day for $\approx$4-6 days, prior to the majority of pieces growing into contact with each other. The culture was then passaged enzymatically at a 1:1 ratio, as described in 3.3.3.4 Methods and previously (Costa et al., 2008). The first 3 passages were split at a 1:1 ratio and increased to a 1:4 ratio by the 5th passage, with each passage requiring approximately 3-4 days of growth to reach 100% confluence. All culturing was performed in an incubator at 37°C with 5% CO_2/air.

For freezing hESC bulk cultures, a 100% confluent T25 cm² flask of cells was passaged at a 1:1 ratio onto a T25cm² flask pre-coated with 0.01×10^6/cm² irradiated MEFs and incubated for 24 hours at 37°C with 5% CO_2/air. hESCs were then made to a single cell suspension by treatment with TrypLE Select, collected with PBS- into a 15ml Falcon tube and centrifuged for 3min at 1500rpm at 4°C. After the removal of the supernatant, cells were resuspended in hESC freezing media (10ml FBS, 7ml DMEM/F12, 2ml Ethylene Glycol [Sigma], 1ml DMSO) and stored at -80°C for 24 hours before being transferred to LN_2 for long term storage.

For thawing hESC bulk cultures, cryovials were removed from LN_2 and placed within a 37°C water bath for approximately 5 minutes and removed when 10% of the frozen pellet remained. Slowly 0.5ml of HES media was added to the cryovial and contents then transferred to a 15ml Falcon tube (BD Biosciences), containing 9ml of HES media. The cells were centrifuged for 3min at 1500rpm at 4°C, the supernatant was aspirated and cells resuspended in 4ml of HES media for seeding in a T25 culture flask. Cells were pipetted gently 3-5 times before transfer to remove cell aggregates. Cells were left to attach overnight in an incubator at 37°C with 5% CO_2/air.

All five hESC lines were routinely karyotyped (every 12 months at a minimum), with analysis performed by Southern Cross Pathology, Monash Medical Centre, Melbourne. To avoid potentially significant delays that would ensue if non-euploid karyotypes were detected, all lines were frozen as backup stocks on a quarterly basis.

An Olympus IX51 brightfield microscope and Olympus Camedia C-7070 wide zoom camera were utilised to image undifferentiated hESCs and neural progeny. Images were taken at 4, 10, 20 or 40x magnification.

3.2.2 Neural differentiation

Neural differentiation was performed according to the methodologies outlined in **Section 3.3.3.4**. PVA and ROCK inhibitor assays were conducted using the HES3 wildtype hESC line, while noggin titrations were performed with H9, HES3 and MEL1 hESC lines.

For the passaging of NDEBs, 12 were collected after 14 days of growth and transferred to a 2mL tube filled with 0.5mL PBS-. Cell aggregates were centrifuged for 2 minutes at 1500rpms, supernatant aspirated and cells resuspended in 200ul TrypLE Select. Samples were incubated for 5 minutes and pipetted ~10 times to disassociate to a near single cell suspension. The sample was again centrifuged for 2 minutes at 1500rpms, the supernatant was aspirated and cells were resuspended in 3.6ml NBM supplemented with 20ng/ml EGF and FGF for a 1 in 3 passage ratio. A total of 100ul of cell suspension was pipetted into the wells of a round bottom 96-well plate and centrifuged for 5 minutes at 1500rpm. Passaged spheres were cultured for a further 14 days before the passaging process was repeated.

3.2.3 FACS processing of hESCs and neural progeny

hESCs and NDEBs were washed once with PBS- and collected as single cell suspensions by treatment with TrypLE Select for 5 - 10 minutes as required at 37°C. Cells were then centrifuged at 480g for 3min at 4°C, supernatants aspirated and cells were resuspended in 1ml of FACS Wash (2% FCS/PBS-, Invitrogen) and then passed through a 35μm filter capped FACS tube (BD Biosciences). Cells were counted and 0.1×10^6 added to separate v-bottom FACS tubes for antibody staining.

V-bottom tubes were then centrifuged at 480g for 3min at 4°C and cells resuspended in primary cell surface antibodies diluted in FACS Wash and incubated in the dark at 4°C for 15min. Tubes were then flooded with 1ml of FACS wash and centrifuged at 480g for 3min at 4°C. Supernatants were aspirated and cell pellets resuspended in a solution of FACS Wash containing secondary cell surface antibodies and incubated at 4°C for 15 mins in the dark. Tubes were flooded with 1ml of FACS wash and centrifuged at 480g for 3min at 4°C. Supernatants were aspirated and cell pellets resuspended by flicking tubes. 5ul of mouse serum was added to tubes for 5min at 4°C and then conjugated cell surface antibodies diluted in FACS Wash solution and incubated at 4°C for 15 mins in the dark. Tubes were flooded with 2ml of FACS wash and centrifuged at 480g for 3min at 4°C. Supernatants were aspirated and cells resuspended in 200ul of FACS Wash containing DAPI (4',6-diamidino-2-phenylindole, Sigma) at 0.4ug/ml for the negative selection of dead cells.

All antibodies were individually titrated to determine their optimal working concentration using either SH-SY5Y neuroblastoma cells, undifferentiated hESCs or neural differentiated hESCs, as antigen. Antibody details are summarised in **Table 3.1**.

Table 3.1: Primary antibodies utilised within this study

Target	Antibody	Ig	Conjugate Fluoro-phore	Dilut-ion	Company	Secondary Utilised
hESCs	Mouse anti-CD9	IgG1,κ	FITC	1:30	BD Biosciences	N/A
hESCs	Mouse anti-TRA-1-60	IgM,κ	APC	1:25	BD Biosciences	N/A
hESCs/ Neural	Mouse anti-EpCAM	IgG1,λ	FITC	1:30	BD Biosciences	N/A
Neural	Mouse anti-CD133	IgG1	PE	1:300	BD Biosciences	N/A
Neural	Mouse anti-CD56 (NCAM)	IgG1,κ	PerCP-Cy5.5	1:50	BD Biosciences	N/A
Neural	Mouse anti-FORSE1	IgM	N/A	1:100	DSHB	APC goat-anti mouse Ig(multi-affinity), 1:100
Neural	Mouse anti-CD140α (PDGFRα)	IgG2,aκ	N/A	1:100	BD Biosciences	

3.2.4 FACS analysis and data representation

FACS samples were run and analysed as described in **Section 4.2.5**. All combinatorial FACS experiments were compensated utilising single stain antibody controls for each fluorphore, and gates established in relation to concentration-matched isotype control antibodies. Flow cytometric analysis was partitioned into two separate groupings, the

first targeting pluripotent antigens assessed at d0, d3 and d7, with a second group targeting neural antigens assessed at d0, d7, d14 and d21.

Noggin titration experiments were performed once across three wildtype hESC cell lines, H9, HES3 and MEL1. Three noggin treatment groups of 0ng/ml, 100ng/ml and 400ng/ml for each cell line were examined. Where statistical analysis was performed each noggin treatment group comprised of three independent replicates of each wildtype hESC line. Subsequent experimentation was performed with 100ng/ml noggin treatment. Statistical analysis was performed on gene expression curves using a two-way ANOVA for each surface antigen, with significance equivalent to a p value of <0.05. Error bars denote the SEM.

Venn diagrams were produced using PowerPoint (Microsoft). Graphs and statistical analysis were performed using GraphPad PRISM (GraphPad Software), and where statistical analysis was performed with a two-way ANOVA and a Bonferroni post-test. The p value was set to <0.05, with data from independent biological triplicates plotted as means and scale bars denoting the mean ± SEM.

3.3 Results

## 3.3.1 Neural directed spin EB calibrations

At the commencement of these studies the spin EB system was established for mesendodermal differentiation and had not been adapted to generate neural cell types (Burridge et al., 2007;Davis et al., 2008;Ng et al., 2008a;Ng et al., 2008b;Burridge et al., 2011;Elliott et al., 2011). Adaptation of this technology for neural differentiation initially focused on determining the necessity of several aspects used in mesendodermal differentiation protocols, specifically, cell seeding density, polyvinyl alcohol (PVA) and Y-27632, an inhibitor of p160-Rho-associated coiled-coil kinase (ROCKi). Additionally, the effects of the patterning factor Noggin, used to inhibit SMAD signalling and promote neural fate determination, were evaluated in a spin EB system using the HES3 cell line.

When incorporated into spin EB methods, PVA by increasing viscosity and is used to promote initial hESC aggregation and typically at a concentration of 0.125% (Ng et al., 2008a;Ng et al., 2008b;Elliott et al., 2011;Goulburn et al., 2011). The presence or absence of PVA at 0.125% was compared at several cell densities with striking contrast in NDEB formation capacity clearly apparent within 24 hours and was not rescued by extended *in vitro* culture **(Figure 3.1A)**. All wells without PVA produced cell suspensions that failed to aggregate into a single cluster with dozens of minor cellular aggregates observed **(Figure 3.1A)**. Similar observations were made at 10,000 cell seeding density, although frequently one larger aggregate was observed in these cultures **(Figure 3.1A, arrows)**. In contrast, PVA containing wells produced a single rounded embryoid body per well with high symmetry and was thus PVA was included in all subsequent experiments **(Figure 3.1A)**. Seeding densities below 3,000 cells/well displayed embryoid body formation even in the presence of PVA, but the efficiency was consistently below 100% (data not shown).

The efficacy of ROCKi and Noggin displayed minor morphological differences in early stages of culture (d3), with the addition of 10uM ROCKi demonstrating more dense and spherical NDEBs **(Figure 3.1B)**. In contrast, in the absence of ROCKi, spheres of

lower density with bulbous surface structures were produced. Maturation of the NDEB cultures resulted in the attenuation of these differences after two weeks of culture **(Figure 3.1B)**. The addition of ROCKi was maintained in subsequent assays due to the minor improvement in neurosphere structure.

Morphological consistency was observed with and without the presence of the neural signalling molecule Noggin (200ng/ml; **Figure 3.1B**). Cell seeding densities did not create variability in the morphological quality in the presence or absence of noggin or ROCKi **(Figure 3.1B)**. Results indicate NDEBs are viable at the lowest seeding density of 3,000 cells per well, and future assays utilised this density to maximize culture yield and economy and additionally provide a structure with the lowest volume for greatest diffusion rates for media components.
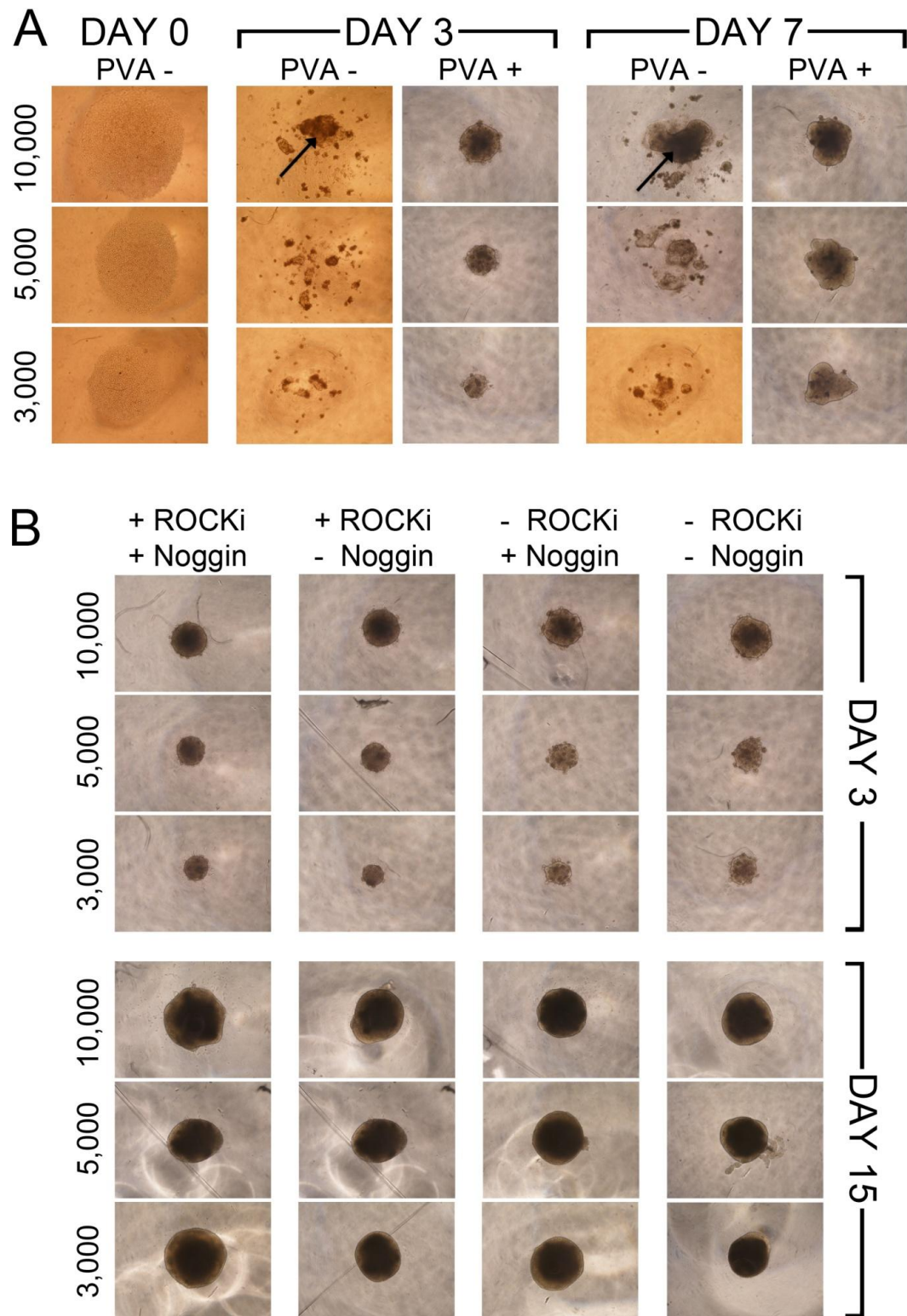
**Figure 3.1:** HES3 bulk cultures seeded into wells of a 96 well plate at three separate seeding densities, with or without PVA supplemented to the media **(A)**. PVA- wells only produced single aggregates at the highest cell density **(A, arrows)**. HES3 bulk cultures seeded into wells of a 96 well plate at three separate seeding densities, with or without ROCKi and/or Noggin supplemented to the media **(B)**.

3.3.2 Differentiation outcomes in response to noggin treatment

The neural functionality of the signalling molecule Noggin was first described in *Xenopus* (Smith & Harland 1992) and has been shown to be essential for embryonic neural tube fusion (Schwartz et al., 2008). Noggin is an inhibitor of the TGF-β superfamily of growth factors, and specifically antagonises BMPs to prevent the downstream activity of SMAD proteins and results in the differentiation of hPSCs towards a neural fate (Pera et al., 2004;Itsykson et al., 2005;Denham and Dottori, 2009). The inhibition of BMPs by noggin and other factors is a key requirement for neural-fate acquisition (Munoz-Sanjuan and Brivanlou 2002). To gauge the role noggin plays in lineage and patterning specification of hESCs within this NDEB system, noggin treatment at 0ng/ml, 100ng/ml and 400ng/ml were compared.

3.3.2.1 Pluripotency downregulation across a noggin gradient

Two traditional hPSC surface antigens, TRA-1-60 and CD9, whose co-expression is an essential requirement for pluripotency, were evaluated in conjunction with a recently discovered hESC surface marker, EpCAM on the three control hESC lines H9. HES and MEL1. Before differentiation initiation, at day 0, all three hESC lines expressed high levels (>90%) of these antigens **(Figure 3.2A)**. Expression of TRA-1-60 and EpCAM did not fall between d0 and d3, as opposed to CD9, which was downregulated rapidly to between 15-39% of the total live sample in this same period **(Figure 3.2B)**. By d8 substantial downregulation of CD9 had extended, with <15% of all samples expressing this antigen. Similarly, expression of TRA-1-60 had dropped dramatically, to within 23-31% for all but one sample group by d8 **(Figure 3.2B)**. Downregulation of EpCAM was also evident between d3 and d8, however, minor interline variability was observed with EpCAM expression, that ranged between 51-72% for all H9 and HES3 sample groups but exhibited greater downregulation in all MEL1 sample groups to ~28% **(Figure 3.2B)**. Overall no discernable correlation was observed between pluripotency surface antigen expression and noggin concentrations in the three hESC lines assessed **(Figure 3.2)**, and this was also reflected in NDEB formation and growth morphology consistency across Noggin concentrations **(Figure 3.2C)**.
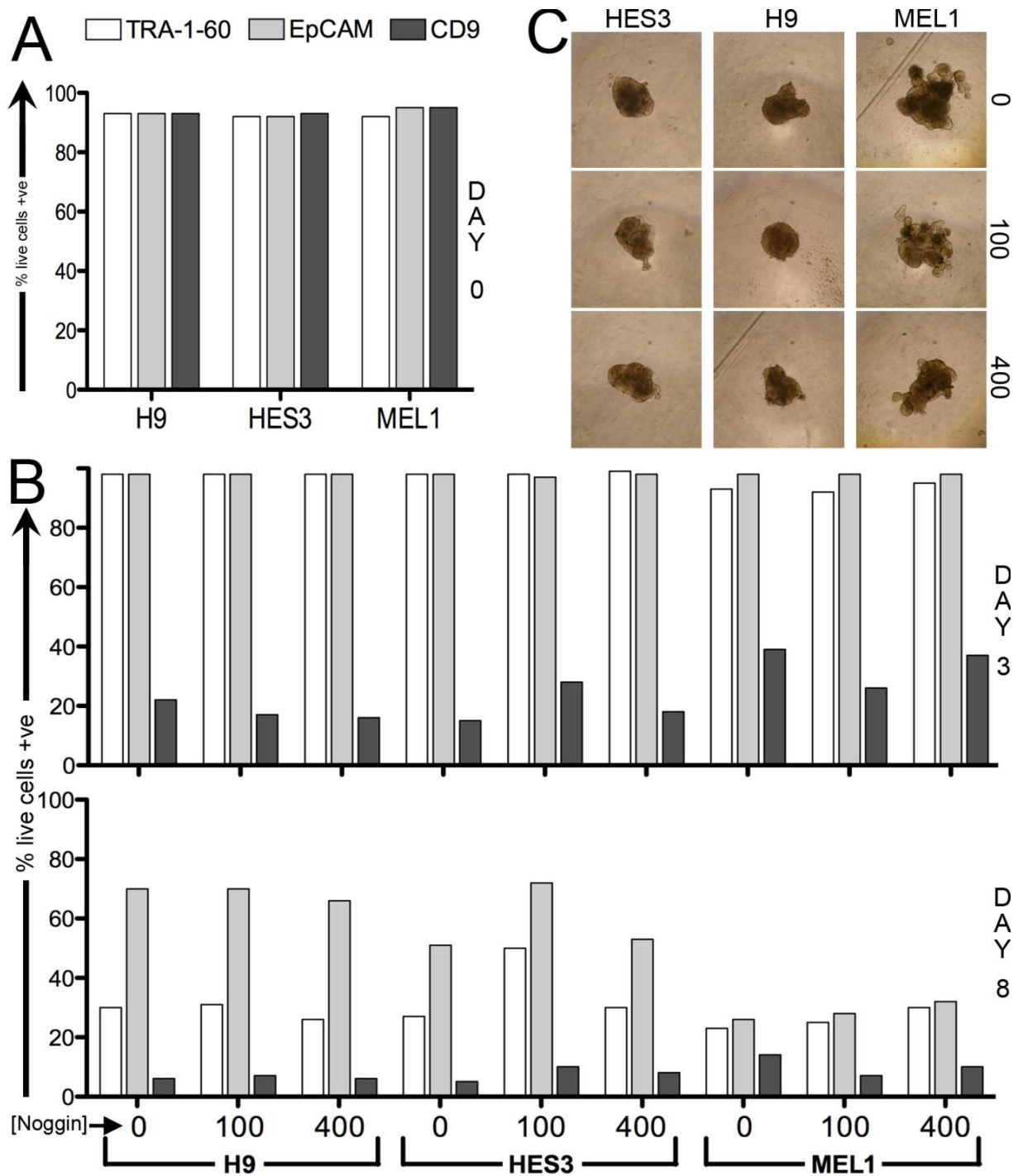
Figure 3.2: Graphical representations of flow cytometry data of hESC pluripotent surface antigen expression within three wildtype hESCs lines while undifferentiated (day 0) and following exposure to three noggin concentrations during neural differentiation at day 3 and day 8 **(A)**. Representative morphological images of NDEBs at day 8 for all hESC lines and across all noggin concentrations **(B)**.

90

3.3.2.2 Noggin titration and neural surface antigens

The kinetics of hESC neural differentiation in relation to alternate noggin concentrations was evaluated by the combinatorial analysis of five key neural development surface antigens, EpCAM, CD133, CD56, FORSE1 and CD140α using flow cytometry throughout differentiation **(Figure 3.3)**.

Changes in surface antigen expression over three weeks of neural differentiation were significant for two markers of hESCs and NSCs, EpCAM and CD133. Total EpCAM+ and CD133+ cell fractions across all noggin concentrations decreased in parallel from d7 to d14. Between d14 and d21 a moderate upregulation of EpCAM expression between 30 and 54% was observed in the 100ng/ml and 400ng/ml noggin treatment groups compared to 0ng/ml samples which fell by 10%, however, these changes were not significant. All noggin treatment groups demonstrated consistent moderate upregulation of CD133 between d14 and d21.

Significant increases in the percentage of CD56+ cells from d7 to d14 were observed but were not affected by noggin treatment. A discrepancy between noggin treatment groups was noticed at d21, with CD56+ cells maintained at 77% from d14 to d21 under 0ng/ml noggin exposure, whereas an attenuation between ~15-20% was observed in the 100ng/ml and 400ng/ml groups **(Figure 3.3)**. This change at d21 indicates a potential influence of noggin treatment on CD56 expression.

Neural cells generated within the first week of differentiation appeared to possess an immature neural precursor phenotype based on these observations, and no indication of forebrain specification was seen based on FORSE-1 antibody staining, however, continued differentiation produced FORSE-1+ cells by d14 and this population increased with further differentiation **(Figure 3.3)**. At d14 no differences in FORSE-1 expression across noggin treatment groups was observed, although from d14 to d21 the 0ng/ml treatment group exhibited a trend to an increase in FORSE-1 expression when compared with 100ng/ml and 400ng/ml treatment groups, although this was not statistically significant **(Figure 3.3)**. No detectable CD140α expression was found on NDEB cells at d7 and d14 across all noggin treatment groups **(Figure 3.3)**, and a minor increase observed at d21 was not affected by noggin titration.
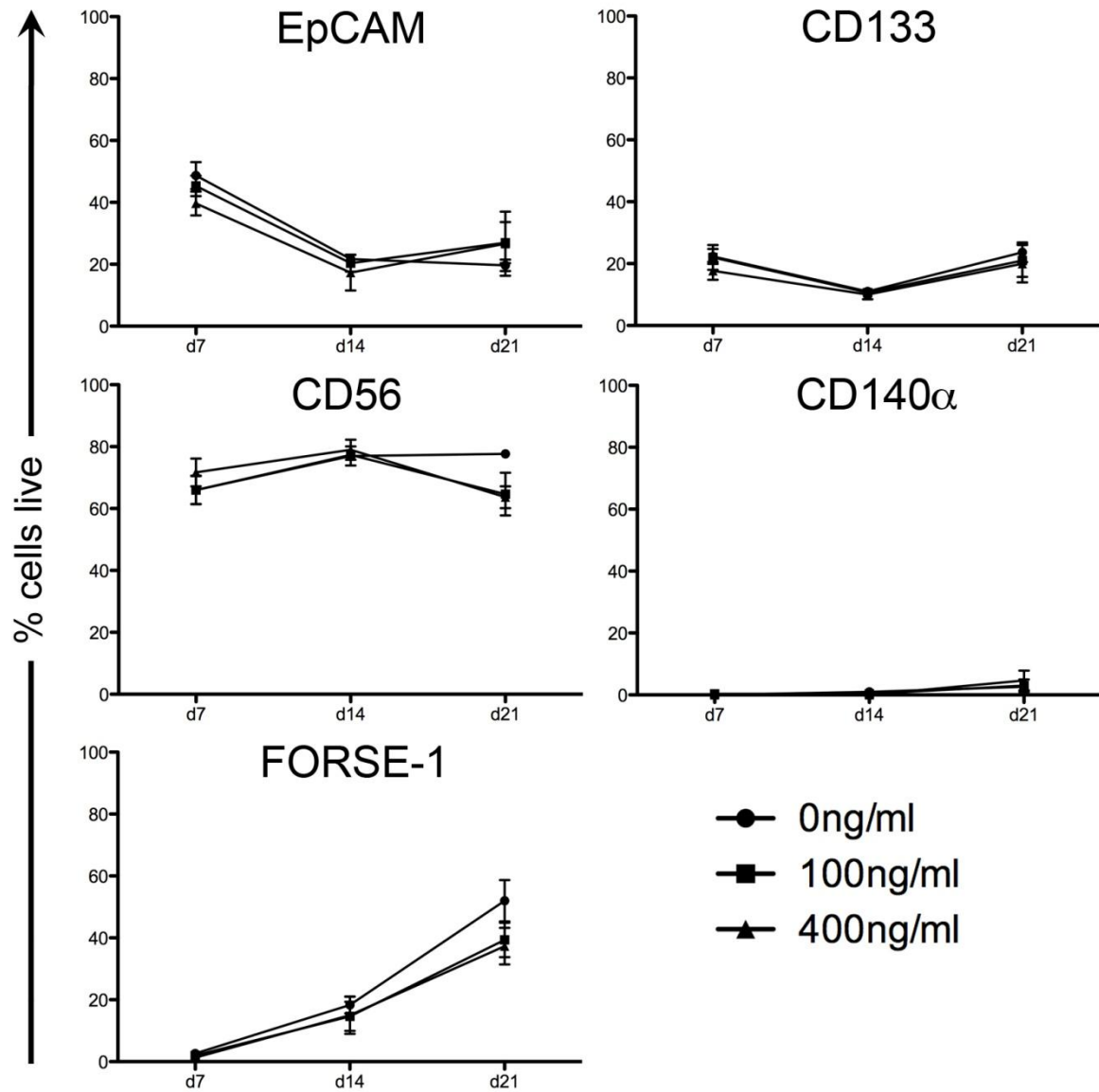
Figure 3.3: Surface antigen expression curves of EpCAM+, CD133+, CD56+, CD140α+ and FORSE-1+ populations from differentiation d7 to d21. Separate noggin treatment groups are plotted over time, with each data point representing averaged values from three wildtype hESC lines. Two-way ANOVAs were performed for each surface antigen, significance is equivalent to a p value of 0.05. Error bars denote the SEM.

3.3.3 NDEB differentiation kinetics

3.3.3.1 Pluripotent surface antigen relationships during NDEB differentiation

Downregulation of pluripotent genes is of crucial importance for the robust differentiation of hESCs into desired somatic cell types and was evaluated with the surface antigens TRA-1-60, CD9 and the more recently described EpCAM. Robust downregulation of TRA-1-60 and CD9 expression is demonstrated within this protocol during the first week of differentiation for all three hESC lines HES3, H9 and MEL1 (**Figure 3.4A, C, E**). A decline in TRA-1-60 expression was observed, falling from 92-98% at d3 to 23-50% by d7, and a parallel yet potentiated trend was noted with CD9 which was downregulated rapidly within the initial three days to 18-32% and fell by d7 to 7-10% (**Figure 3.4A, C, E**).

The downregulation of TRA-1-60 and CD9 was similar, yet moderated in comparison to the adhesion molecule EpCAM over the observed period falling to 26-66% by d7 (**Figure 3.4A, C, E**). Furthermore, a substantial proportion of cells remained TRA-1-60-/EpCAM+/CD9-, particularly in the H9 and HES3 samples to between 25-40% (**Figure 3.4B, D, F**).

Rapid downregulation of CD9 across cell lines is observed, decreasing from ~94% at d0 to 15-39% at d3 and further decreasing to 5-14% by d7 (**Figure 3.4A, C, E**). Intriguingly >98% of CD9+ cells at all time-points studied co-expressed TRA-1-60 and EpCAM, suggesting the CD9 population represents a minor yet residual pluripotent pool (**Figure 3.4**). Importantly, neural differentiation with this protocol resulted in robust and consistent downregulation of the total number of triple positive TRA-1-60+/EpCAM+/CD9+ cells across all cell lines by d7 (**Figure 3.4**), and likely represents a robust loss of pluripotency in this system.

Combinatorial surface maker analysis further revealed ~ 9% of the total live cell population at d0 did not express any pluripotent antigens, being TRA-1-60-/EpCAM-/CD9- (**Figure 3.4B, D, F**). This population is likely to represent irradiated MEFs, a crucial co-culture requirement for the maintenance of pluripotency in d0 cultures. Increases from d0 to d3 in the percentage of TRA-1-60 and EpCAM expression was evident across all cell lines and is likely indicative of irradiated MEF apoptosis (**Figure 3.4B, D, F**).
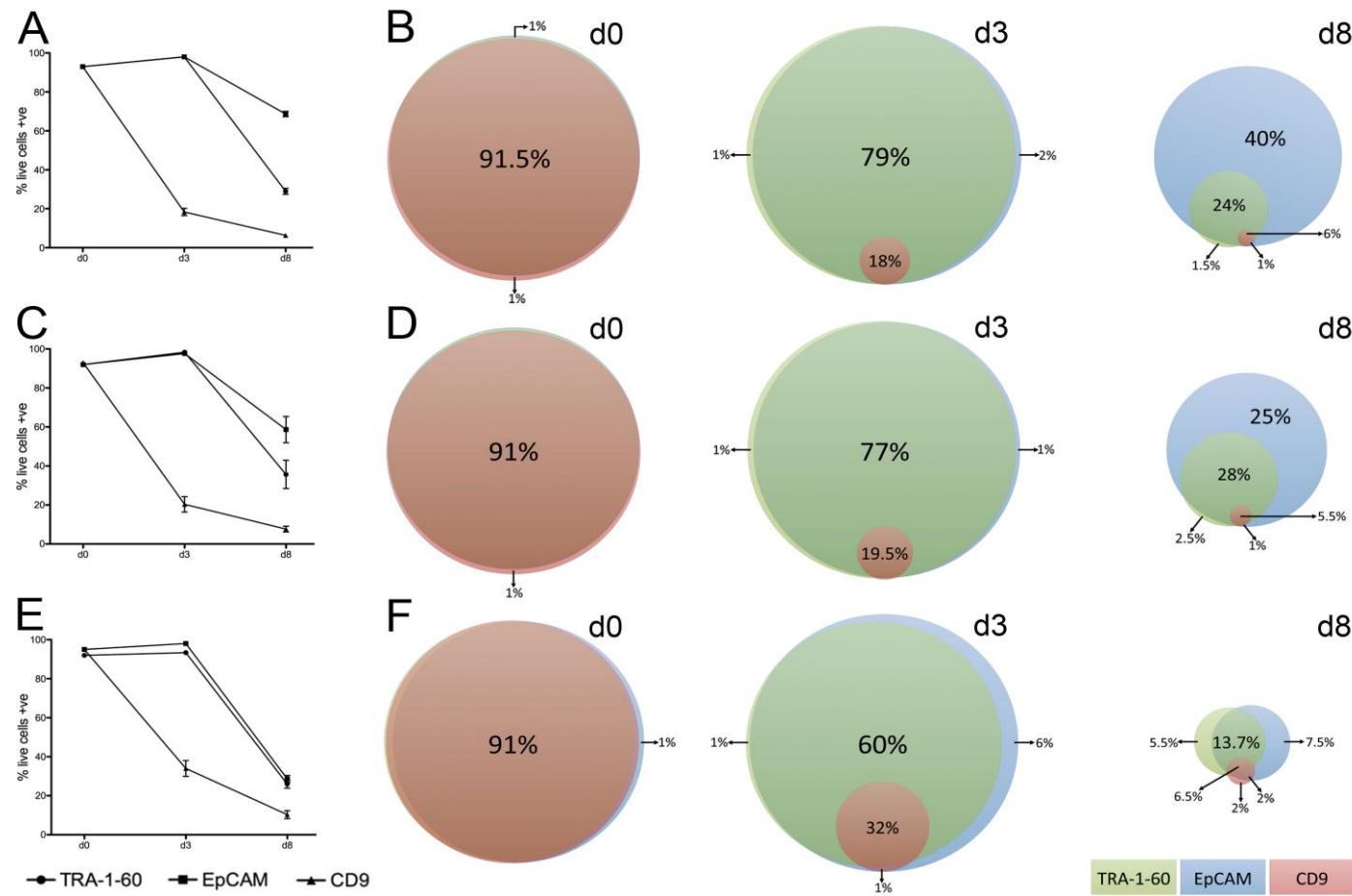
Figure 3.4: Surface antigen expression curves of TRA-1-60+, EpCAM+ and CD9+ during the first week of neural differentiation for hESC lines H9 **(A)**, HES3 **(C)**, MEL1 **(E)**. Expression curve data points reflect the mean of independent biological triplicates with error bars denoting the SEM. Venn diagram representations of pluripotent antigen co-expression during the first week of neural differentiation for hESC lines H9 **(B)**, HES3 **(D)** and MEL1 **(F)**. Venn diagram expression levels are presented for TRA-1-60 **(green)**, EpCAM **(blue)** and CD9 **(red)**. TRA-1-60-/EpCAM-/CD9- cells are not represented, values are of live cell fraction percentages as determined by DAPI flow cytometry exclusion.

94

3.3.3.2 Germ layer specification and NSC identity

Germ layer lineage specification of the NDEB protocol was measured with the differentiation with the MIXL1$^{GFP/w}$ knockin reporter hESC line (Davis et al., 2008). During embryogenesis MIXL1, a marker of primitive mesendoderm, is transiently expressed in the primitive streak and during the first 3-4 days of hematopoietic ESC differentiation (Davis et al., 2008). Co-expression of MIXL1 with epithelial markers such as E-cadherin or EpCAM and CD140α are indicative of early mesodermal cells (Davis et al., 2008). Culture for one week of the MIXL1$^{GFP/w}$ hESC line in the NDEB protocol did not produce any detectable expression of either MIXL1 (GFP) or CD140α, and no co-expression of either of these markers with EpCAM was observed, definitively demonstrating this protocol does not produce any detectable mesendodermal contaminants **(Figure 3.5)**.

Adult striatal extracts were shown to generate spherical structures *in vitro* termed neurospheres from single cell cultures that expressed nestin and exhibited multipotentiality (Reynolds and Weiss, 1992). The hESC derived NDEBs of this protocol are believed to comprise NSCs and represent an analogy to neurospheres. Indeed, d14 NDEBs plated on laminin were shown to produce prodigious quantities of cells expressing the intermediate NSC filament protein nestin **(refer to Section 3.3.3.4, Figure 4H, I)**. Neurospheres are also characterised by the capacity to passage such cells, a feature shared by d14 NDEBs that were successfully passaged up to three times at 1:3 ratios, forming perfectly spherical progeny upon each passage (data not shown).
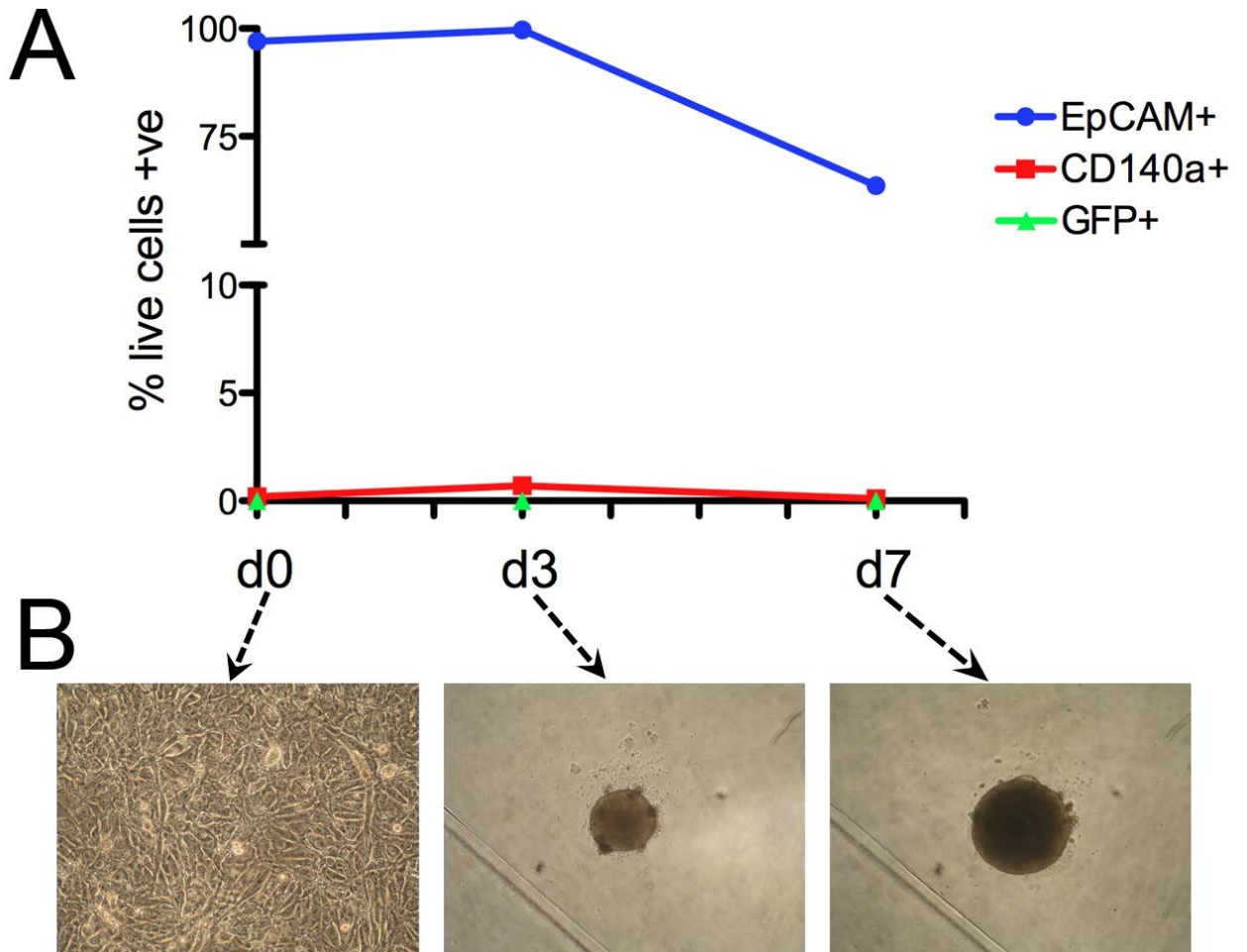
Figure 3.5: Expression curves of EpCAM+, CD140α+ and GFP+ populations demonstrating no detectable levels of GFP expression in the MIXL1 reporter hESC line **(A)**. Bright field images of undifferentiated MIXL1 hESCs at d0 that were successfully differentiated to NDEBs as shown at d3 and d7 **(B)**.

3.3.3.3 Neural surface antigen expression relationships

Evaluation of neurodevelopmental surface antigens was next performed, and in conjunction with the antigen EpCAM due to significant expression of this marker remaining after a week of neural differentiation in comparison to other candidate pluripotency antigens **(Section 3.3.3.1)**. EpCAM is related to another epithelial adhesion molecule, E-cadherin, that is expressed on undifferentiated hESC but not embryoid bodies (Cai et al., 2005; Ullmann et al., 2007). The presence of this surface antigen on primitive endodermal hESC derivatives (Lim et al., 2011) and the importance of neuroepithelial attachments for the equipoise between self-renewal of NSCs and differentiation in the developing CNS (Rousso et al., 2012), rationalised the assessment of this marker's expression profile during neural differentiation.

Interline differentiation consistency was demonstrated by this neural differentiation protocol and is shown by equivalent FACS histogram plots between cell lines throughout 3 weeks of *in vitro* culture **(Figure 3.6B)**. Further, consistent antigen expression levels are observed between H9 and HES3 samples over multiple culture replicates (n=3), with a two-way ANOVA analysis demonstrating no significant expression differences between neural surface antigens EpCAM, CD133, CD56 and FORSE1 at each analysis time-point **(Figure 3.6A)**. One significant difference in expression between H9 and HES3 was observed for the surface antigen CD140α **(Figure 3.6)**, a change in a non-neuronal population that was not of interest for this study and was detected only at d21 with maximal expression found to be 5% and 19% in H9 and HES3 cultures respectively.

The kinetics of this differentiation system are readily visualised by surface marker expression curves of combined H9 and HES3 sample groups **(Figure 3.6C)**. A trend was observed throughout the majority of the differentiation protocol for a decrease at d0, 7 and 14 in the hESC/NSC marker CD133, which fell from 70% at d0 to <20% by d14, with an unexplained slight upregulation by d21 potentially reflecting a residual neural precursor subpopulation. Intriguingly, this decreasing expression trend seen with CD133 was closely mirrored by EpCAM, which was seen to decrease from >90% in hESCs to <15% by d21 **(Figure 3.6C)**, conflicting with reports of EpCAM denoting pluripotent cells alone.

Importantly the neural/neuronal marker CD56 demonstrates rapid upregulation within the first week of differentiation, with >60% of NDEB cells expressing this marker, indicating rapid acquisition of a neural phenotype **(Figure 3.6C)**. The proportion of CD56+ cells continued to increase with differentiation, reaching a mean peak of 72% detected at d14, before a moderate attenuation at d21.

From d0 to d7 inclusive, undifferentiated hESCs were negative for FORSE1 expression, and this epitope is first detected at d14 on 22% of the live cell population **(Figure 3.6C)**. Upregulation of FORSE1 continued with mean expression levels elevated by +108% to a total of 46% of the live cell fraction by d21, indicating robust patterning of cells to a telecephalic phenotype.
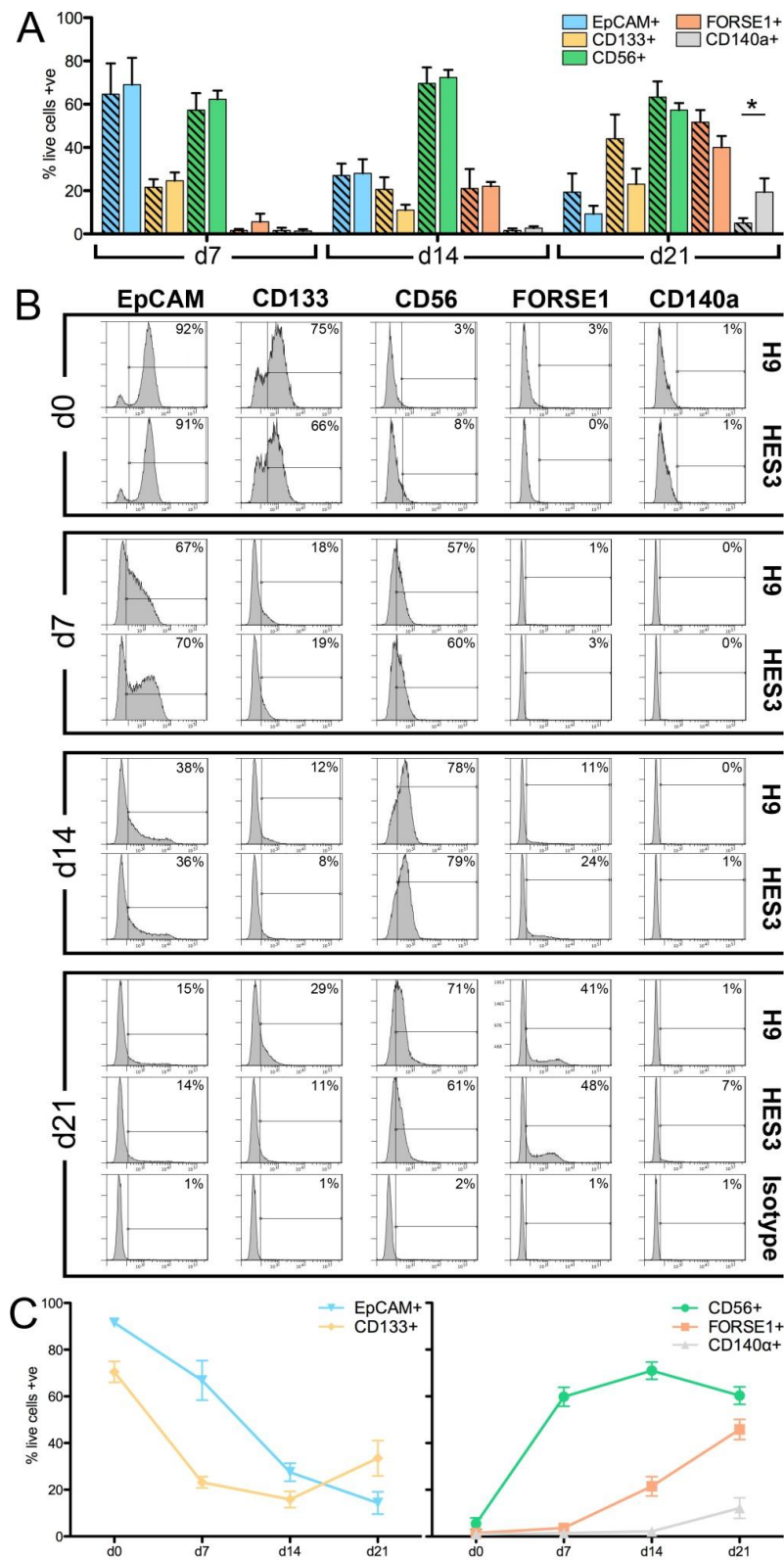
Figure 3.6: H9 (dashed bars) and HES3 (open) neural differentiation surface antigen analysis from single positive histograms from d7 to d21, data analysed with a two-way ANOVA and Bonferroni post test, n=3 independent biological culture replicates, mean ± SEM, with p(*)<0.05 **(A)**. Representative histogram plots for each surface antigen assessed and isotype controls from d0 to d21 of neural differentiation **(B)**. Surface marker expression curves of EpCAM+, CD133+, CD56+, FORSE-1+ and CD140α+ populations from d0 to d21 of neural differentiation, values at d0 n=2 cell line replicates and from d7 to d21 n=6 with 3 independent biological culture replicates from both H9 and HES3, mean ± SEM **(C)**.

Interline consistency is further observed in the relationship between single and double positive surface marker expression profiles. Highly correlating CD56+/FORSE-1+ levels are observed from d7 to d21 in both cell lines and while minor divergences in absolute values between lines are noticeable at d21, expression trends and ratios of single to double positive cells are consistent **(Figure 3.7A)**. Further, the majority of FORSE-1+ cells co-express CD56 throughout the 3 weeks of neurosphere culture reinforcing the neural identity of this forebrain subpopulation **(Figure 3.7B & 3.8A)**.

Throughout differentiation an extremely low co-expression of EpCAM was observed in FORSE-1+ population, with <4% of the total population double positive at all stages analysed **(Figure 3.7F)**. Indeed, a negative correlation is seen between the expression levels of EpCAM and FORSE-1 expression. A greater proportion, although still a minority, of FORSE-1+ cells co-express the traditional NSC marker CD133 at d14 (27%) and d21 (41%) **(Figure 3.7D and Figure 3.8A & B)**. Together, this data suggests FORSE-1 expression correlates better with increased neural maturity than does either CD133 or EpCAM expression and may be useful for the isolation of cells with reduced multipotentiality.

Combinatorial gene expression profiles further highlight and provide additional depth to this proposition. Populations of FORSE-1+/CD56- cells increase with continued differentiation, and possess lower co-expression of both hESC/NSC markers EpCAM and CD133 than FORSE-1+/CD56+ fractions **(Figure 3.8A & B)**. While CD133 and EpCAM are reported to be present on similar cell types, such as pluripotent cells, co-staining found these populations did not consistently overlap. Singularly positive EpCAM+/CD133- and EpCAM-/CD133+ populations existed throughout differentiation **(Figure 3.8C)**, suggesting that these two markers concomitantly delineate similar and discrete progenitor subtypes and to avoid such proliferative subtypes negative selection would be required. Taken together, this data suggests a FORSE1+/CD56-/CD133-/EpCAM- population may represent a forebrain committed subpopulation with limited mulitpotentiality.

Robust upregulation of CD56 occurs within one week of differentiation, with a majority (67%) co-expressing EpCAM and a significant proportion (26%) co-

expressing CD133 at d7 **(Figure 3.7E)**. Throughout differentiation the association between these two markers and CD56 was strong and consistent, with the majority of EpCAM+ cells (~55-65%) and CD133+ cells (~60-80%) co-expressing CD56 **(Figure 3.7C, E)**. Despite substantial decreases in EpCAM expression with progressive differentiation, three weeks of culture did not result in the separation of these two populations entirely, with ~15% of the total CD56+ population still co-expressing EpCAM at d21 **(Figure 3.7E and 3.8A)**. Similarly, there remained a significant proportion of CD56+ cells (~40%) which co-express CD133 by d21 **(Figure 3.7C & 3.8B)**. This data together reinforces the proposition that CD56+ cells do not represent terminally differentiated neuronal cells. Supporting the theory that CD56 expression exists on multipotent neural precursors, the development of a glial precursor CD140α+ population (while rare and variable between cell lines), predominantly exists within the CD56+ population **(Figure 3.8D)**.
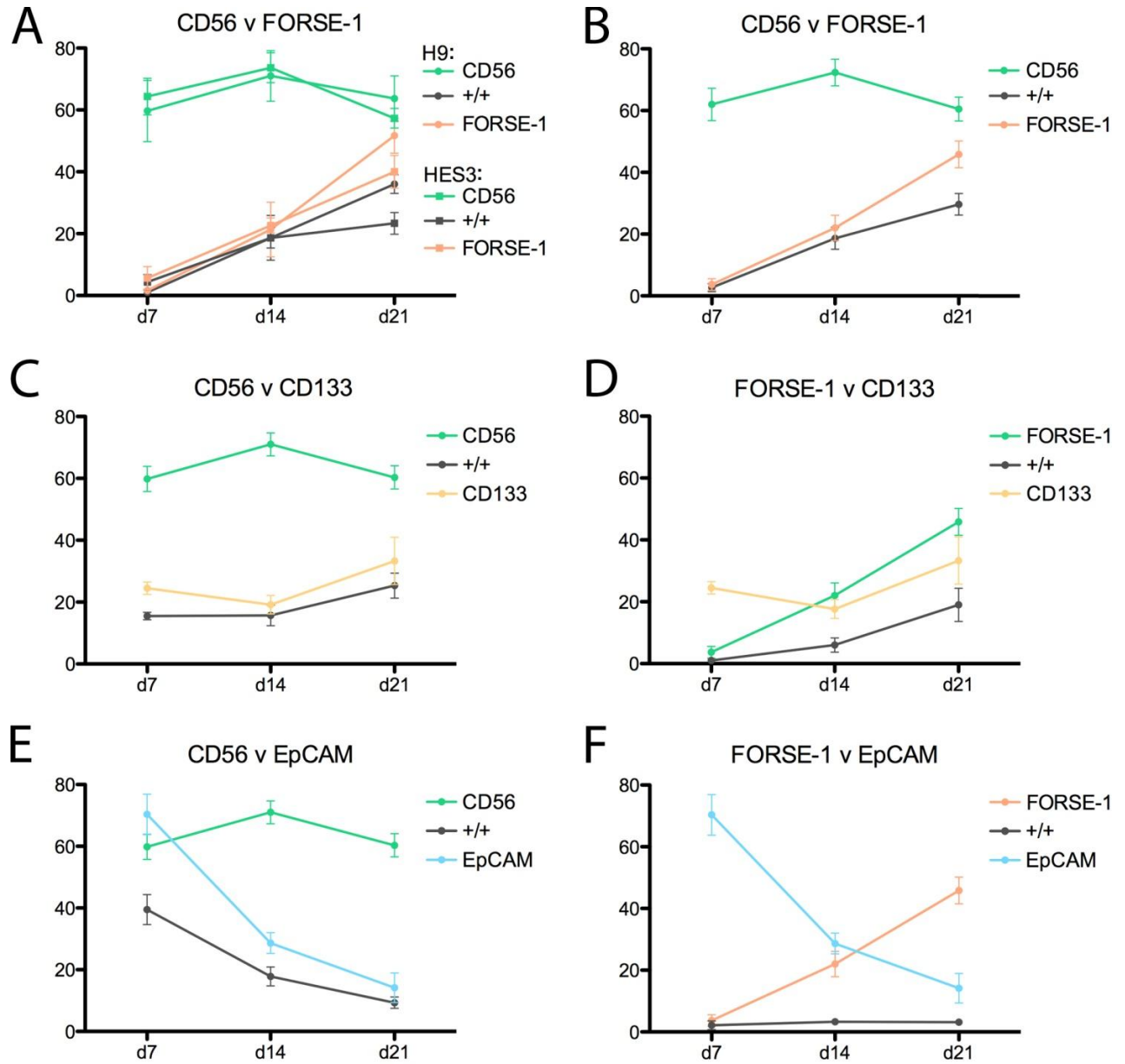
Figure 3.7: Trend graph representations of neural surface marker expression percentages in relation to each other and the proportion of double positive cells from differentiation day 7 to 21. Each data point represents averaged values of independent biological triplicates for each cell line **(A)**. Data points represent mean values, n=6 with 3 independent biological culture replicates from both H9 and HES3 **(B-F)**. Error bars denote the SEM.
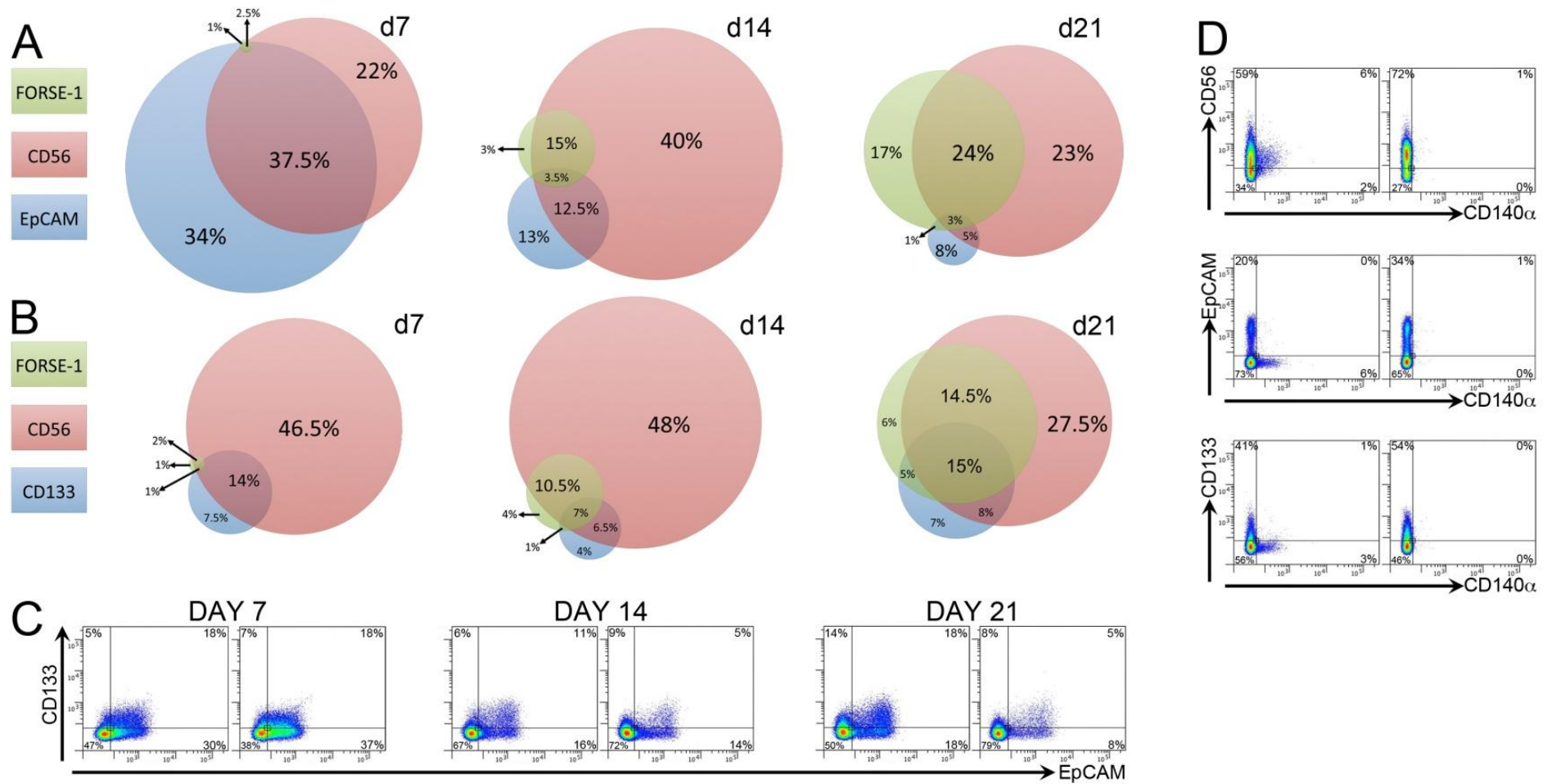
Figure 3.8: Venn diagram representations of neural surface marker co-expression at d7, 14 and 21 of neural differentiation. Expression levels are presented for FORSE-1 **(green)** and CD56 **(red) (A, B)**. Expression levels are presented for EpCAM **(blue) (A),** and CD133 **(red) (B)**. Triple negative cells are not represented. Values are of live cell fraction percentages as determined by DAPI flow cytometry exclusion. FACS scatter plots of HES3 CD133 and EpCAM co-expression at d7, 14 and 21 **(C)**, as well as CD140α and EpCAM/CD133/CD56 co-expression at d7, 14 and 21 **(D)**.

3.3.3.4 Terminal differentiation of NDEBs and application to hiPSCs

Appendix I comprises a published paper detailing the successful application of the developed NDEB protocol to a hiPSC line derived from a non-ectodermal lineage, specifically kidney mesangial cells. The successful differentiation of kidney-derived hiPSCs demonstrates the robust nature of this protocol particularly as hiPSCs frequently exhibit reduced differentiation propensities as a consequence of harbouring residual epigenetic profiles from their cells of origin. Further, the neural stem cell identity of intermediate NDEBs is demonstrated within this publication, with d14 NDEBs shown to readily generate a monolayer of nestin+ cells. Importantly, the generation of terminally differentiated neuronal cell types from both hESCs and hiPSCs, based on key neuronal cytoskeletal immunostaining, is demonstrated subsequent to growth factor restriction and the attachment of NDEBs to laminin and poly-D-lysine coated culture surfaces.

3.4 Discussion

Several protocols have been described recently to differentiate bulk cultured hESCs to mesendodermal lineages with a spin EB method, specifically of cardiac and heamatopoietic lineages (Burridge et al., 2007;Davis et al., 2008;Ng et al., 2008a;Ng et al., 2008b;Burridge et al., 2011;Elliott et al., 2011). The adaptation of this system for neural differentiation purposes was undertaken to overcome stochastic elements within existing protocols and produce a suitable system for discerning minor variations cellular physiology that may arise as a consequence of mutant *HTT* transcript expression in hESCs.

3.4.1 Protocol optimization

Differentiation of hESCs using spin-EB methodologies have regularly reported an optimal seeding density of 3,000 cells per well (Ng, 2005;Burridge et al., 2007;Goulburn et al., 2011) and this was utilised by this study upon titration experiments. Further optimizations assessed PVA in the NDEB system. The addition of PVA has been shown to improve the proliferation of undifferentiated hESC cultures (Burridge et al., 2007;Vallier et al., 2009). It was theorized that PVA would be critical during the initial formation of NDEBs. Evidence supports this theory as PVA has been shown to be critical for single cell suspensions to aggregate successfully in mesendoderm directed spin-EBs (Ng et al., 2008b;Elliott et al., 2011). Conversely, the Denning laboratory has observed PVA addition at cell seeding densities ≤3,000 elicited an inhibitory or attenuating effect to sphere formation (Burridge et al., 2007). This study clearly supports the evidence from the Elefanty and Stanley laboratories that PVA is a necessity for seeding of NDEBs, and this finding corroborates a recent neural differentiation report that utilises PVA at similar concentrations for the neural differentiation of an Nkx2.1 hESC reporter line (Goulburn et al., 2011).

Strong evidence that the ROCKi diminishes disassociation-induced apoptosis in hESC and EB cultures (Watanabe et al., 2007) is supported by more recent studies affirming the utility of this small molecule in neural differentiated spin-EBs (Eiraku et al.,

2008;Goulburn et al., 2011). Our study corroborates these findings, with robust spheres preferentially observed within ROCKi sample groups.

The actions of the signalling molecule Noggin (and small molecule analogues) in promoting ectodermal lineage specification via SMAD inhibition, stands as a cornerstone of numerous neural differentiation protocols (Reubinoff et al., 2001;Banin et al., 2006;Sonntag et al., 2007;Chambers et al., 2009;Kriks et al., 2011;Carri et al., 2012). Counter intuitively, within the NDEB system Noggin did not have an effect on the differentiation of hESC to primitive neuroepithelial cell types denoted by TRA-1-60, CD9, EpCAM and CD133 expression. Additionally, noggin treatment does not influence relevant neural surface antigens such as the forebrain marker FORSE1 or neural/neuronal marker CD56. Indications of minor modulation of CD56 and FORSE-1 expression in response to noggin were observed but were not significant and warrant further evaluation to discern whether these indicative trends represent stochastic or credible responses.

Potentially hESCs produce sufficient levels of endogenous noggin to render exogenous addition redundant, a scenario that could be discerned by gene expression assays to measure endogenous noggin production, and the comparison of present differentiation outcomes with those from hESCs in which noggin has been silenced. Noggin redundancy may be further explained by the mechanics of a spin-EB system, where enzymatic disassociation of pluripotent cultures and transfer to neural differentiation conditions induces the senescence of irradiated MEFs, the principle source of BMPs and major rational for noggin addition in numerous protocols (Reubinoff et al., 2001). The possibility still remains that noggin may influence downstream neural pathways not assessed by this study, specifically the commitment of NSCs to various neuronal neurotransmitter and/or regional subtypes, and requires investigation in future studies. Supplementation with 100ng/ml noggin was however maintained throughout all assays based on the heavily documented neural promoting actions reported throughout the literature, and the potential that these may not have been detected within the scope of this study.

Observed neural specification of hESCs in the NDEB system is thus corollary to other components of the culture milieu, several of which are known to promote and sustain ectodermal lineage specification. This includes the base media NBM-A, developed originally for the culture of forebrain neurons from the hippocampus, cortex and other regions (Invitrogen http://products.invitrogen.com/ivgn/product/0050128DJ). Further, the administration of the growth factors FGF2 and EGF that are known to promote neural stem cell growth and maintenance (Reynolds and Weiss, 1992;Reubinoff et al., 2001;Schulz et al., 2004;Iacovitti et al., 2007;Lee et al., 2007;Cohen et al., 2010). FGF2 in particular has been shown to critically influence the ectodermal patterning and induction in vertebrates (Mason, 2007). Additionally, the supplements N2 (http://products.invitrogen.com/ivgn/product/17502048) and B27 (Invitrogen http://products.invitrogen.com/ivgn/product/17504044) contain numerous components (i.e. Vitamin A) specifically tailored for supporting growth and proliferation of neural precursors and the development and maintenance of post-mitotic neurons (Niederreither and Dolle, 2008).

3.4.2 Differentiation outcomes

Combinatorial FACS analysis of pluripotency markers TRA-1-60, CD9 and EpCAM, as well as key neurodevelopmental surface antigens CD133, FORSE-1, CD56 and CD140α, enabled the evaluation of the differentiation kinetics of this novel protocol during critical induction and specification stages. Further, this approach provides additional information to the nascent and conflicting body of scientific literature associated with the spatial and temporal relationships between neural surface antigens.

3.4.2.1 Differentiation outcomes on pluripotency

The activity of two classical hESC markers, TRA-1-60, CD9 and the recently ascribed EpCAM, were assessed to ensure downregulation of pluripotent cells during differentiation. Within the NDEB system hESCs exit rapidly from a pluripotent state, with pluripotent cells, denoted by CD9+/TRA-1-60+/EpCAM+ expression, decreasing in >80% of the total population within 3 days and >90% within one week. The robust nature of this protocol is seen by consistent downregulation of each surface antigen across several hESC lines.

This study confirms EpCAM represents a strong marker of hESCs, sharing near absolute co-expression with established pluripotency markers CD9 and TRA-1-60 in undifferentiated cultures, and reports this observation across three hESC lines derived from separate institutions, all of which are distinct from the institution of the first reported study by Sundberg and colleagues in 2009.

CD9 is a robust marker of pluripotency with antibodies targeting this surface antigen registering high binding affinities across a cohort of hESC lines (Initiative et al., 2007). Further, CD9 is utilised in positive selection techniques for purifying genuine pluripotent sub-populations from hESC cultures (Kolle et al., 2009;Zhou et al., 2009). While this study confirms the strong expression of CD9 on hESCs, novel observations of this antigen are suggestive of a similar role in identifying pluripotent sub-populations during early stages of neural differentiation and may provide a single surface antigen for the negative selection of residual hESC contaminants from neural differentiating cultures. Such a possibility seems unattainable for other hESC surface antigens assessed such as TRA-1-60 and EpCAM which were shown to co-express numerous neural surface antigens and thus mark large proportions of early neural progeny. Future studies may FACS sort from early 7 day neural cultures to purify CD9+/TRA+/EpCAM+ and compare their ability to re-establish hESC colonies compared with CD9+ cells alone, to assess whether CD9 alone is sufficient to isolate hESCs from mixed, immature differentiation populations. Further studies are also warranted to determine whether negative selection of CD9+ cells produces a neural population with reduced tumorigenic capacity upon transplantation and define where other pluripotent surface epitopes (i.e. SSEA-3, SSEA-4, GCTM2) and intracellular markers (i.e. nanog, OCT-4), lie in relation to those investigated.

3.4.2.2 Differentiation outcomes on neural specification

Limited characterisations of EpCAM activity during hESC differentiation have been performed in previous studies of this surface antigen (Kolle et al., 2009;Sundberg et al., 2009). Temporal and combinatorial observations from this study indicate that EpCAM possesses a role beyond pluripotency and demonstrates novel roles for EpCAM under neural differentiation conditions. Firstly we have shown that EpCAM, despite identical expression to traditional pluripotent surface antigens on hESCs, is

downregulated at a far slower rate during neural differentiation with expression remaining high (>70%) at one week of differentiation. Combinatorial FACS studies of TRA-160, CD9 and EpCAM identified a window arises during neural differentiation where a substantial proportion (~10-40%) of live cells are solely EpCAM+ and thus cannot continue to mark pluripotent cell types.

Through further analysis of EpCAM by combinatorial FACS analysis of neural differentiation samples, significant co-expression with markers of neural developmental, including the NSC/neuronal marker CD56, NSC marker CD133 and NSC/forebrain marker FORSE-1 was observed. EpCAM is a member of the Cadherin family of cell surface adhesion molecules that are crucial for cell-to-cell interactions (Simon et al., 1990). The early neural tube and primitive ectoderm are epithelial in nature, a class of tissues that are known to express various Cadherin proteins, and this information combined with high co-expression between EpCAM and early neural markers suggests EpCAM+ cells equate to cells within the primitive ectoderm.

These results attenuate the conclusions by Kolle and others in 2009 that EpCAM can be used to isolate or enrich for undifferentiated cells from differentiated cell types. The deployment of EpCAM for such a purpose may only apply to the hESC colony culture conditions utilised within that study, where spontaneously differentiated cells may not be of an ectodermal lineage. Clearly, the significant overlap between EpCAM, CD133 and particularly CD56 (which is an antigen with low expression on pluripotent cells), cautions against the use of EpCAM-positive selection for hESC enrichment. Simultaneously these findings caution against the proposal of EpCAM-negative selection for the removal of hESC contaminants in neural differentiation systems proposed by Sundberg and colleagues in 2009, as the data from this study demonstrates this would exclude significant numbers of cells that no longer remain pluripotent and may exhibit a primitive ectodermal phenotype.

Importantly, strong expression of the forebrain NSC marker FORSE-1 was shown to arise several days after the pluripotent/proliferative-NSC markers CD133 and EpCAM achieve peak expression, indicating FORSE-1 positive cells may represent NSCs of greater maturity than those detected with either EpCAM or CD133. Cells with FORSE-

1 affinity were predominantly CD56+ indicating a neural phenotype, and interestingly FORSE-1+/CD56+ cells co-expressed CD133 in greater proportions compared to EpCAM, further reinforcing the notion that EpCAM marks cells of greater immaturity.

Future studies are required to describe the role of EpCAM, specifically whether EpCAM+/CD56+ or EpCAM+/CD133+ cells denote populations with variable downstream differentiation potentials, and the relationship between this adhesion molecule and other neurodevelopmental markers that have been highlighted recently, such as CD24, CD44, CD184 and CD217.

The importance of understanding cell maturation during the early stages of differentiation cannot be overstated. One principle reason being that hESC derived neural and neuronal populations frequently contain an unacceptable proportion of proliferative NSCs that possess a capacity to overpopulate *in vitro* cultures and *in vivo* grafts (Roy et al., 2006;Aubry et al., 2008;Doi et al., 2012). Recently, the transplantation of hESC-derived neurospheres into PD primates produced tumour overgrowths from cultures differentiated for 14 and 28 days, however, neurospheres of greater maturity (>d35) demonstrated no tumour formation (Doi et al., 2012). Similarly, reports have shown prolonged neural differentiation of many weeks were required to downregulate surface antigens associated with proliferative NSCs, such as CD133 (Sundberg et al., 2009). Our study corroborates these findings, demonstrating progressive downregulation of markers such as EpCAM and CD133+ with time.

While culturing neural cells *in vitro* for extended periods may provide a solution to remove undesirable proliferative cell types, it may simultaneously extend cultures beyond the optimal transplantation stages for the desired neuronal subtypes, and bias or restrict differentiation potential with extended culture within a specific cellular milieu. FACS purification based on surface antigens could provide a more optimal alternative and concomitantly enhance neuronal differentiation by enriching cultures with desired cell types. Interestingly, the combinatorial surface antigen analysis performed in this study has identified a promising population of FORSE1+/CD56+/CD133-/EpCAM- cells that increases with continued differentiation. As shown, the CD133+ population does not entirely encompass the EpCAM+ population or vice versa, thus negative selection of either marker in isolation would

not sufficiently exclude proliferative NSCs. Future studies are warranted to resolve whether FORSE1+/CD56+/CD133-/EpCAM- purification enables the isolation of live neural progenitor cells committed to neuronal differentiation, which would be useful in transplantation scenarios that seek to attenuate the propensity of grafts to proliferate uncontrollably.

Subsequent to the initiation of this study, alternative spin embryoid body protocols for neural differentiation have emerged (Eiraku et al., 2008;Kim et al., 2011). However, these incorporate undesirable aspects prone to batch variability, with extended culture in knockout serum replacement media used by Eiraku and colleagues, or growth on an extracellular matrix harvested from mouse sarcoma cells by Kim and colleagues. While these comparable techniques involve spin aggregation the protocol developed by Kim and others reverts to a monolayer system within 48 hours and later requires manual isolation of neural rosettes countering the technical initiation advantage. These studies corroborate the utility of ROCKi to improve sphere formation and the ability of Neurobasal media with N2 and B27 supplements as well as SMAD inhibition to support neural differentiation. A further report describes the spin aggregation of hESC and their neural differentiation in the presence of an alternative fully defined media, however, dissimilar to most protocols in this field utilises high doses of FGF-2 and RA in the absence of SMAD inhibitors (Goulburn et al., 2011). Further, the protocol described by Goulburn and colleagues was tailored to generate high proportions of ventral telencephalic, medial ganglionic eminence NKX2.1+ cells. Future studies would benefit from comparisons of these emergent studies with the NDEB protocol established here to determine whether comparable neural induction and plasticity are achieved.

A system for the directed differentiation of hESCs under defined conditions to primitive neuroepithelial cells and subsequently a telencephalic phenotype has been developed in this chapter. Investigations of this NDEB system confirmed differentiation proceeded holistically towards an ectodermal fate with the use of a MIXL1$^{GFP/w}$ mesendodermal reporter line. Differentiation outcomes were highly uniform across hESC and iPSC lines, and this has enabled the elucidation of novel gene expression patterns in early stages of neurogenesis. The robustness of this system

indicates a platform suitable for the investigation of hESC lines carrying neurodegenerative diseases where the elucidation of subtle phenotypes requires strict differentiation synchronisation and uniformity.

Importantly, the combination of spin aggregation techniques and fully defined conditions provides a controlled and scalable platform for the administration of desired agonists and antagonists to pattern primitive neuroectodermal tissue to desired cell types. Indeed, Eiraku and colleagues administer patterning factors DKK-1 and LEFTY-1 in a spin aggregation format although the efficacy of the addition of these and other factors remains to be determined (Eiraku et al., 2008). Future studies may substantially extend this system by evaluating the capacity of NDEBs to be directed towards neurotransmitter and regional specific neuronal subtypes, as well as non-neuronal lineages such as astrocyte and oligodendrocytes, in response to various doses of relevant patterning factors.

3.5 References

Allendoerfer, K.L., Durairaj, A., Matthews, G.A., and Patterson, P.H. (1999). Morphological domains of Lewis-X/FORSE-1 immunolabeling in the embryonic neural tube are due to developmental regulation of cell surface carbohydrate expression. *Developmental Biology* 211**,** 208-219.

Allendoerfer, K.L., Magnani, J.L., and Patterson, P.H. (1995). FORSE-1, an antibody that labels regionally restricted subpopulations of progenitor cells in the embryonic central nervous system, recognizes the Le(x) carbohydrate on a proteoglycan and two glycolipid antigens. *Molecular and cellular neurosciences* 6**,** 381-395.

Aubry, L., Bugi, A., Lefort, N., Rousseau, F., Peschanski, M., and Perrier, A.L. (2008). Striatal progenitors derived from human ES cells mature into DARPP32 neurons in vitro and in quinolinic acid-lesioned rats. *Proceedings of the National Academy of Sciences of the United States of America* 105**,** 16707-16712.

Banin, E., Obolensky, A., Idelson, M., Hemo, I., Reinhardtz, E., Pikarsky, E., Ben-Hur, T., and Reubinoff, B. (2006). Retinal incorporation and differentiation of neural precursors derived from human embryonic stem cells. *Stem Cells* 24**,** 246-257.

Burridge, P.W., Anderson, D., Priddle, H., Barbadillo Muñoz, M.D., Chamberlain, S., Allegrucci, C., Young, L.E., and Denning, C. (2007). Improved Human Embryonic Stem Cell Embryoid Body Homogeneity and Cardiomyocyte Differentiation from a Novel V-96 Plate Aggregation System Highlights Interline Variability. *Stem Cells* 25**,** 929-938.

Burridge, P.W., Thompson, S., Millrod, M.A., Weinberg, S., Yuan, X., Peters, A., Mahairaki, V., Koliatsos, V.E., Tung, L., and Zambidis, E.T. (2011). A Universal System for Highly Efficient Cardiac Differentiation of Human Induced Pluripotent Stem Cells That Eliminates Interline Variability. *PloS one* 6**,** e18293.

Cai, J., Olson, J.M., Rao, M.S., Stanley, M., Taylor, E., and Ni, H.T. (2005). Development of antibodies to human embryonic stem cell antigens. *BMC Developmental Biology* 5**,** 26.

Capela, A., and Temple, S. (2002). LeX/ssea-1 is expressed by adult mouse CNS stem cells, identifying them as nonependymal. *Neuron* 35**,** 865-875.

Carri, A.D., Onorati, M., Lelos, M.J., Castiglioni, V., Faedo, A., Menon, R., Camnasio, S., Vuono, R., Spaiardi, P., Talpo, F., Toselli, M., Martino, G., Barker, R.A., Dunnett, S.B., Biella, G., and Cattaneo, E. (2012). Developmentally coordinated extrinsic signals drive human pluripotent stem cell differentiation toward authentic DARPP-32+ medium-sized spiny neurons. *Development (Cambridge, England)* 140**,** 301-312.

Chambers, S.M., Fasano, C.A., Papapetrou, E.P., Tomishima, M., Sadelain, M., and Studer, L. (2009). Highly efficient neural conversion of human ES and iPS cells by dual inhibition of SMAD signaling. *Nature biotechnology* 27**,** 275-280.

Cohen, M.A., Itsykson, P., and Reubinoff, B.E. (2010). The role of FGF-signaling in early neural specification of human embryonic stem cells. *Developmental Biology***,** 1-9.

Costa, M., Sourris, K., Hatzistavrou, T., Elefanty, A.G., and Stanley, E.G. (2008). Expansion of human embryonic stem cells in vitro. *Current protocols in stem cell biology* Chapter 1**,** Unit 1C.1.1-1C.1.7.

Davis, R.P., Ng, E.S., Costa, M., Mossman, A.K., Sourris, K., Elefanty, A.G., and Stanley, E.G. (2008). Targeting a GFP reporter gene to the MIXL1 locus of human

embryonic stem cells identifies human primitive streak-like cells and enables isolation of primitive hematopoietic precursors. *Blood* 111, 1876-1884.

Denham, M., and Dottori, M. (2009). Signals Involved in Neural Differentiation of Human Embryonic Stem Cells. *Neurosignals* 17, 234-241.

Doi, D., Morizane, A., Kikuchi, T., Onoe, H., Hayashi, T., Kawasaki, T., Motono, M., Sasai, Y., Saiki, H., Gomi, M., Yoshikawa, T., Hayashi, H., Shinoyama, M., Refaat, M.M., Suemori, H., Miyamoto, S., and Takahashi, J. (2012). Prolonged Maturation Culture Favors a Reduction in the Tumorigenicity and the Dopaminergic Function of Human ESC-Derived Neural Cells in a Primate Model of Parkinson's Disease. *Stem Cells* 30, 935-945.

Eiraku, M., Watanabe, K., Matsuo-Takasaki, M., Kawada, M., Yonemura, S., Matsumura, M., Wataya, T., Nishiyama, A., Muguruma, K., and Sasai, Y. (2008). Self-Organized Formation of Polarized Cortical Tissues from ESCs and Its Active Manipulation by Extrinsic Signals. *Stem Cell* 3, 519-532.

Elkabetz, Y., Panagiotakos, G., Al Shamy, G., Socci, N.D., Tabar, V., and Studer, L. (2008). Human ES cell-derived neural rosettes reveal a functionally distinct early neural stem cell stage. *Genes &amp; Development* 22, 152-165.

Elliott, D.A., Braam, S.R., Koutsis, K., Ng, E.S., Jenny, R., Lagerqvist, E.L., Biben, C., Hatzistavrou, T., Hirst, C.E., Yu, Q.C., Skelton, R.J.P., Ward-Van Oostwaard, D., Lim, S.M., Khammy, O., Li, X., Hawes, S.M., Davis, R.P., Goulburn, A.L., Passier, R., Prall, O.W.J., Haynes, J.M., Pouton, C.W., Kaye, D.M., Mummery, C.L., Elefanty, A.G., and Stanley, E.G. (2011). NKX2-5eGFP/w hESCs for isolation of human cardiac progenitors and cardiomyocytes. *Nature Methods* 8, 1037-1040.

Golebiewska, A., Atkinson, S.P., Lako, M., and Armstrong, L. (2009). Epigenetic landscaping during hESC differentiation to neural cells. *Stem Cells* 27, 1298-1308.

Goulburn, A.L., Alden, D., Davis, R.P., Micallef, S.J., Ng, E.S., Yu, Q.C., Lim, S.M., Soh, C.-L., Elliott, D.A., Hatzistavrou, T., Bourke, J., Watmuff, B., Lang, R.J., Haynes, J.M., Pouton, C.W., Giudice, A., Trounson, A.O., Anderson, S.A., Stanley, E.G., and Elefanty, A.G. (2011). A Targeted NKX2.1 Human Embryonic Stem Cell Reporter Line Enables Identification of Human Basal Forebrain Derivatives. *Stem Cells* 29, 462-473.

Iacovitti, L., Donaldson, A.E., Marshall, C.E., Suon, S., and Yang, M. (2007). A protocol for the differentiation of human embryonic stem cells into dopaminergic neurons using only chemically defined human additives: Studies in vitro and in vivo. *Brain research* 1127, 19-25.

Initiative, I.S.C., Adewumi, O., Aflatoonian, B., Ahrlund-Richter, L., Amit, M., Andrews, P.W., Beighton, G., Bello, P.A., Benvenisty, N., Berry, L.S., Bevan, S., Blum, B., Brooking, J., Chen, K.G., Choo, A.B.H., Churchill, G.A., Corbel, M., Damjanov, I., Draper, J.S., Dvorak, P., Emanuelsson, K., Fleck, R.A., Ford, A., Gertow, K., Gertsenstein, M., Gokhale, P.J., Hamilton, R.S., Hampl, A., Healy, L.E., Hovatta, O., Hyllner, J., Imreh, M.P., Itskovitz-Eldor, J., Jackson, J., Johnson, J.L., Jones, M., Kee, K., King, B.L., Knowles, B.B., Lako, M., Lebrin, F., Mallon, B.S., Manning, D., Mayshar, Y., Mckay, R.D.G., Michalska, A.E., Mikkola, M., Mileikovsky, M., Minger, S.L., Moore, H.D., Mummery, C.L., Nagy, A., Nakatsuji, N., O&Apos;Brien, C.M., Oh, S.K.W., Olsson, C., Otonkoski, T., Park, K.-Y., Passier, R., Patel, H., Patel, M., Pedersen, R., Pera, M.F., Piekarczyk, M.S., Pera, R.a.R., Reubinoff, B.E., Robins, A.J., Rossant, J., Rugg-Gunn, P., Schulz, T.C., Semb, H., Sherrer, E.S., Siemen, H., Stacey, G.N., Stojkovic, M., Suemori, H., Szatkiewicz, J., Turetsky, T., Tuuri, T., Van Den Brink, S., Vintersten, K., Vuoristo, S., Ward, D., Weaver, T.A., Young,

L.A., and Zhang, W. (2007). Characterization of human embryonic stem cell lines by the International Stem Cell Initiative. *Nature biotechnology* 25**,** 803-816.

Itsykson, P., Ilouz, N., Turetsky, T., Goldstein, R.S., Pera, M.F., Fishbein, I., Segal, M., and Reubinoff, B.E. (2005). Derivation of neural precursors from human embryonic stem cells in the presence of noggin. *Molecular and Cellular Neuroscience* 30**,** 24-36.

Kim, J.-E., O&Apos;Sullivan, M.L., Sanchez, C.A., Hwang, M., Israel, M.A., Brennand, K., Deerinck, T.J., Goldstein, L.S.B., Gage, F.H., Ellisman, M.H., and Ghosh, A. (2011). Investigating synapse formation and function using human pluripotent stem cell-derived neurons. *Proceedings of the National Academy of Sciences of the United States of America* 108**,** 3005-3010.

Kolle, G., Ho, M., Zhou, Q., Chy, H.S., Krishnan, K., Cloonan, N., Bertoncello, I., Laslett, A.L., and Grimmond, S.M. (2009). Identification of Human Embryonic Stem Cell Surface Markers by Combined Membrane-Polysome Translation State Array Analysis and Immunotranscriptional Profiling. *Stem Cells* 27**,** 2446-2456.

Kriks, S., Shim, J.-W., Piao, J., Ganat, Y.M., Wakeman, D.R., Xie, Z., Carrillo-Reid, L., Auyeung, G., Antonacci, C., Buch, A., Yang, L., Beal, M.F., Surmeier, D.J., Kordower, J.H., Tabar, V., and Studer, L. (2011). Dopamine neurons derived from human ES cells efficiently engraft in animal models of Parkinson's disease. *Nature***,** 1-7.

Lappalainen, R.S., Salomäki, M., Ylä-Outinen, L., Heikkilä, T.J., Hyttinen, J.A., Pihlajamäki, H., Suuronen, R., Skottman, H., and Narkilahti, S. (2010). Similarly derived and cultured hESC lines show variation in their developmental potential towards neuronal cells in long-term culture. *Regenerative Medicine* 5**,** 749-762.

Lee, H., Shamy, G.A., Elkabetz, Y., Schofield, C.M., Harrsion, N.L., Panagiotakos, G., Socci, N.D., Tabar, V., and Studer, L. (2007). Directed Differentiation and Transplantation of Human Embryonic Stem Cell-Derived Motoneurons. *Stem Cells* 25**,** 1931-1939.

Lim, S.M., Li, X., Schiesser, J., Holland, A.M., Elefanty, A.G., Stanley, E.G., and Micallef, S.J. (2011). Temporal Restriction of Pancreatic Branching Competence During Embryogenesis Is Mirrored In Differentiating Embryonic Stem Cells. *Stem cells and development***,** 111216132119003.

Mason, I. (2007). Initiation to end point: the multiple roles of fibroblast growth factors in neural development. *Nature reviews. Neuroscience* 8**,** 583-596.

Munoz-Sanjuan, I., and Brivanlou, A.H. (2002). Neural induction, the default model and embryonic stem cells. *Nature reviews. Neuroscience* 3**,** 271-280.

Murphy, D.B., Wiese, S., Burfeind, P., Schmundt, D., Mattei, M.G., Schulz-Schaeffer, W., and Thies, U. (1994). Human brain factor 1, a new member of the fork head gene family. *Genomics* 21**,** 551-557.

Ng, E.S. (2005). Forced aggregation of defined numbers of human embryonic stem cells into embryoid bodies fosters robust, reproducible hematopoietic differentiation. *Blood* 106**,** 1601-1603.

Ng, E.S., Davis, R., Stanley, E.G., and Elefanty, A.G. (2008a). A protocol describing the use of a recombinant protein-based, animal product-free medium (APEL) for human embryonic stem cell differentiation as spin embryoid bodies. *Nature protocols* 3**,** 768-776.

Ng, E.S., Davis, R.P., Hatzistavrou, T., Stanley, E.G., and Elefanty, A.G. (2008b). Directed differentiation of human embryonic stem cells as spin embryoid bodies and a

description of the hematopoietic blast colony forming assay. *Current protocols in stem cell biology* Chapter 1, Unit 1D.3.

Niederreither, K., and Dolle, P. (2008). Retinoic acid in development: towards an integrated view. *Nature reviews. Genetics* 9, 541-553.

Peh, G.S., Lang, R.J., Pera, M.F., and Hawes, S.M. (2009). CD133 expression by neural progenitors derived from human embryonic stem cells and its use for their prospective isolation. *Stem cells and development* 18, 269-282.

Pera, M.F., Andrade, J., Houssami, S., Reubinoff, B., Trounson, A., Stanley, E.G., Ward-Van Oostwaard, D., and Mummery, C. (2004). Regulation of human embryonic stem cell differentiation by BMP-2 and its antagonist noggin. *Journal of cell science* 117, 1269-1280.

Pruszak, J., Ludwig, W., Blak, A., Alavian, K., and Isacson, O. (2009). CD15, CD24 and CD29 Define a Surface Biomarker Code for Neural Lineage Differentiation of Stem Cells. *Stem Cells*, N/A-N/A.

Pruszak, J., Sonntag, K.-C., Aung, M.H., Sanchez-Pernaute, R., and Isacson, O. (2007). Markers and Methods for Cell Sorting of Human Embryonic Stem Cell-Derived Neural Cell Populations. *Stem Cells* 25, 2257-2268.

Reubinoff, B.E., Turetsky, T., and Pera, M.F. (2001). Neural progenitors from human embryonic stem cells. *Nature biotechnology* 19, 1134-1140.

Reynolds, B.A., and Weiss, S. (1992). Generation of neurons and astrocytes from isolated cells of the adult mammalian central nervous system. *Science* 255, 1707-1710.

Rousso, D.L., Pearson, C.A., Gaber, Z.B., Miquelajauregui, A., Li, S., Portera-Cailliau, C., Morrisey, E.E., and Novitch, B.G. (2012). Foxp-Mediated Suppression of N-Cadherin Regulates Neuroepithelial Character and Progenitor Maintenance in the CNS. *Neuron* 74, 314-330.

Roy, N.S., Cleren, C., Singh, S.K., Yang, L., Beal, M.F., and Goldman, S.A. (2006). Functional engraftment of human ES cell-derived dopaminergic neurons enriched by coculture with telomerase-immortalized midbrain astrocytes. *Nature Medicine* 12, 1259-1268.

Schulz, T.C., Noggle, S.A., Palmarini, G.M., Weiler, D.A., Lyons, I.G., Pensa, K.A., Meedeniya, A.C., Davidson, B.P., Lambert, N.A., and Condie, B.G. (2004). Differentiation of human embryonic stem cells to dopaminergic neurons in serum-free suspension culture. *Stem Cells* 22, 1218-1238.

Schwartz, P.H., Bryant, P.J., Fuja, T.J., Su, H., O'dowd, D.K., and Klassen, H. (2003). Isolation and characterization of neural progenitor cells from post-mortem human cortex. *Journal of Neuroscience Research* 74, 838-851.

Schwartz, P.H., Brick, D.J., Stover, A.E., Loring, J.F., and Müller, F.-J. (2008). Differentiation of neural lineage cells from human pluripotent stem cells. *Methods (San Diego, Calif)* 45, 142-158.

Simon, B., Podolsky, D.K., Moldenhauer, G., Isselbacher, K.J., Gattoni-Celli, S., and Brand, S.J. (1990). Epithelial glycoprotein is a member of a family of epithelial cell surface antigens homologous to nidogen, a matrix adhesion protein. *Proceedings of the National Academy of Sciences of the United States of America* 87, 2755-2759.

Smith, W.C., and Harland, R.M. (1992). Expression cloning of noggin, a new dorsalizing factor localized to the Spemann organizer in Xenopus embryos. *Cell* 70, 829-840.

Sonntag, K.C., Pruszak, J., Yoshizaki, T., Van Arensbergen, J., Sanchez-Pernaute, R., and Isacson, O. (2007). Enhanced yield of neuroepithelial precursors and midbrain-

like dopaminergic neurons from human embryonic stem cells using the bone morphogenic protein antagonist noggin. *Stem Cells* 25**,** 411-418.

Sundberg, M., Jansson, L., Ketolainen, J., Pihlajamäki, H., Suuronen, R., Skottman, H., Inzunza, J., Hovatta, O., and Narkilahti, S. (2009). CD marker expression profiles of human embryonic stem cells and their neural derivatives, determined using flow-cytometric analysis, reveal a novel CD marker for exclusion of pluripotent stem cells. *Stem Cell Research* 2**,** 113-124.

Tao, W., and Lai, E. (1992). Telencephalon-restricted expression of BF-1, a new member of the HNF-3/fork head gene family, in the developing rat brain. *Neuron* 8**,** 957-966.

Tavakoli, T., Xu, X., Derby, E., Serebryakova, Y., Reid, Y., Rao, M.S., Mattson, M.P., and Ma, W. (2009). Self-renewal and differentiation capabilities are variable between human embryonic stem cell lines I3, I6 and BG01V. *BMC Cell Biology* 10**,** 44.

Tole, S., Kaprielian, Z., Ou, S.K., and Patterson, P.H. (1995). FORSE-1: a positionally regulated epitope in the developing rat central nervous system. *The Journal of neuroscience : the official journal of the Society for Neuroscience* 15**,** 957-969.

Tole, S., and Patterson, P.H. (1995). Regionalization of the developing forebrain: a comparison of FORSE-1, Dlx-2, and BF-1. *The Journal of neuroscience : the official journal of the Society for Neuroscience* 15**,** 970-980.

Uchida, N., Buck, D.W., He, D., Reitsma, M.J., Masek, M., Phan, T.V., Tsukamoto, A.S., Gage, F.H., and Weissman, I.L. (2000). Direct isolation of human central nervous system stem cells. *Proceedings of the National Academy of Sciences of the United States of America* 97**,** 14720-14725.

Ullmann, U., In't Veld, P., Gilles, C., Sermon, K., De Rycke, M., Van De Velde, H., Van Steirteghem, A., and Liebaers, I. (2007). Epithelial-mesenchymal transition process in human embryonic stem cells cultured in feeder-free conditions. *Molecular Human Reproduction* 13**,** 21-32.

Vallier, L., Touboul, T., Chng, Z., Brimpari, M., Hannan, N., Millan, E., Smithers, L.E., Trotter, M., Rugg-Gunn, P., Weber, A., and Pedersen, R.A. (2009). Early cell fate decisions of human embryonic stem cells and mouse epiblast stem cells are controlled by the same signalling pathways. *PloS one* 4**,** e6082.

Watanabe, K., Ueno, M., Kamiya, D., Nishiyama, A., Matsumura, M., Wataya, T., Takahashi, J.B., Nishikawa, S., Nishikawa, S.-I., Muguruma, K., and Sasai, Y. (2007). A ROCK inhibitor permits survival of dissociated human embryonic stem cells. *Nature biotechnology* 25**,** 681-686.

Wu, H., Xu, J., Pang, Z.P., Ge, W., Kim, K.J., Blanchi, B., Chen, C., Südhof, T.C., and Sun, Y.E. (2007). Integrative genomic and functional analyses reveal neuronal subtype differentiation bias in human embryonic stem cell lines. *Proceedings of the National Academy of Sciences of the United States of America* 104**,** 13821-13826.

Yuan, S.H., Martin, J., Elia, J., Flippin, J., Paramban, R.I., Hefferan, M.P., Vidal, J.G., Mu, Y., Killian, R.L., Israel, M.A., Emre, N., Marsala, S., Marsala, M., Gage, F.H., Goldstein, L.S.B., and Carson, C.T. (2011). Cell-Surface Marker Signatures for the Isolation of Neural Stem Cells, Glia and Neurons Derived from Human Pluripotent Stem Cells. *PloS one* 6**,** e17540.

Zhou, H., Wu, S., Joo, J.Y., Zhu, S., Han, D.W., Lin, T., Trauger, S., Bien, G., Yao, S., Zhu, Y., Siuzdak, G., Schöler, H.R., Duan, L., and Ding, S. (2009). Generation of induced pluripotent stem cells using recombinant proteins. *Cell stem cell* 4**,** 381-384.

CHAPTER 4

Characterisation Of Forebrain Neurons Derived From Late-Onset Huntington's Disease Human Embryonic Stem Cell Lines

4.0 Declaration

Monash University
Declaration for Thesis Chapter 4

Declaration by candidate

In the case of Chapter 4, the nature and extent of my contribution to the work was the following:

Nature of contribution	Extent of contribution (%)
I was central to the development of the experimental design, performed the vast majority of experimentation and supervised most co-authors who performed experimentation and/or data collection. I also prepared the manuscript (writing the text, generated the figures, formatted)	85%

The following co-authors contributed to the work. Co-authors who are students at Monash University must also indicate the extent of their contribution in percentage terms:

Name	Nature of contribution	Extent of contribution (%) for student co-authors only
Pinar, A	Ms Pinar contributed to the execution of experiments and collection of data while under supervision by Mr Niclis & Dr Cram	10%
Haynes, JM	Dr Haynes contributed to the execution of experiments and collection of data	
Alsanie, W	Mr Alsanie contributed to the collection of data	
Jenny, R	Dr Jenny contributed to the execution of experiments	
Dottori, M	Dr Dottori provided supervision and contributed to the preparation of the manuscript for publication	
Cram, DS	Dr Cram provided supervision and contributed to the preparation of the manuscript for publication	

Candidate's Signature		Date 20.04.2014

Declaration by co-authors
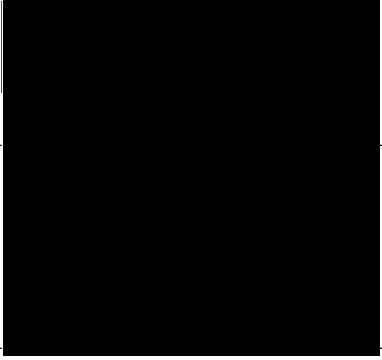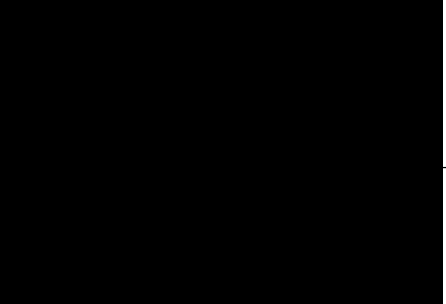
The undersigned hereby certify that:

(7) the above declaration correctly reflects the nature and extent of the candidate's contribution to this work, and the nature of the contribution of each of the co-authors.
(8) they meet the criteria for authorship in that they have participated in the conception, execution, or interpretation, of at least that part of the publication in their field of expertise;
(9) they take public responsibility for their part of the publication, except for the responsible author who accepts overall responsibility for the publication;
(10) there are no other authors of the publication according to these criteria;

(11)   potential conflicts of interest have been disclosed to (a) granting bodies, (b) the editor or publisher of journals or other publications, and (c) the head of the responsible academic unit; and

(12)   the original data are stored at the following location(s) and will be held for at least five years from the date indicated below:

Location(s)	Department of Anatomy and Developmental Biology

		Date
Signature 1		07.08.2013
Signature 2		14.08.2013
Signature 3		
Signature 4		
Signature 5		13.08.2013
Signature 6		24.07.2013

4.1 Introduction

The onset of Huntington's disease occurs after extended periods of concealed perturbation and degeneration in a variety of cellular components and pathways. The temporal initiation of the various HD pathological mechanisms and their relationship to one another remains to be elucidated, particularly because of the technological limitations in studying pre-onset human patients. The embryonic nature of hPSCs and their differentiated derivatives provide the only practicable opportunity to answer these fundamental questions by providing a window into the stages of human development.

A plethora of molecular pathologies, including intracellular aggregates, transcriptome disruption, vesicular trafficking alterations and autophagy-lysosomal impairment are dominant features of HD **(See Chapter 1)**. Tantalisingly, several of these pathologies are detectable in related *in vitro* embryonic HD models such as mHTT knockin hECCs and transgenic R6/2 miPSCs (Gaughwin et al., 2011;Castiglioni et al., 2012). Specifically, aggregates were observed at differentiated stages and altered lysosome numbers. Gene expression alterations were seen at both pluripotent and neural stages for each *in vitro* model system, and from one of these *in vitro* models a novel patient biomarker was identified. These studies strongly validate the principle of analysing developmentally early stages of HD for furthering knowledge of HD pathology.

Earlier experimental outcomes within this thesis using HD hESC lines found the presence of an expanded CAG tract within the *HTT* gene did not prevent differentiation to neural lineages (**Chapter 2**). To elucidate whether these outcome were a direct consequence of *mHTT* alleles or the stochasticity of the differentiation protocol involved, a novel spin-embryoid body neural differentiation protocol **(described in Chapter 3)**, was developed. The robust nature of the NDEB system, with trivial interline gene expression variation and a high differentiation output capacity, provided an ideal platform for meaningful investigation of SI-186 and SI-187 HD hESC line growth properties, differentiation capabilities, neuronal function and transcriptome assessment.

A robust differentiation system is of critical importance, as the late-onset nature of HD may eventuate as only subtle phenotypes in the non-transgenic hESC lines utilised for this study. Indeed, related studies of similar model systems fit this assumption, finding that the entire repertoire of HD hallmarks were not recapitulated at early developmental stage equivalents (Gaughwin et al., 2011;Castiglioni et al., 2012).

The manuscript describes for the first time comparisons between typical late-onset HD hESCs lines carrying mutations within the CAG_{35-59} repeat range. Investigations are performed against two wildtype hESC lines, H9 and HES3, and utilise the NDEB system developed in Chapter 3. Cell growth, survival and forebrain neural differentiation were found to be unperturbed by the presence of mutant *HTT* transcripts. Gene expression of key markers dysregulated in HD were found to be unaltered in HD samples across a neural differentiation timeframe, however, functional analyses revealed a disturbance in intracellular calcium signalling in neuronal cultures.

4.2 Manuscript

Characterization of forebrain neurons derived from late-onset Huntington's disease human embryonic stem cell lines

Jonathan C. Niclis[1,2]*[†], Anita Pinar[1†], John M. Haynes[3], Walaa Alsanie[1], Robert Jenny[1], Mirella Dottori[4] and David S. Cram[1]

[1] *Monash Immunology and Stem Cell Laboratories, Monash University, Clayton, VIC, Australia*
[2] *The Florey Institute of Neuroscience and Mental Health, University of Melbourne, Parkville, VIC, Australia*
[3] *Monash Institute of Pharmaceutical Sciences, Monash University, Parkville, VIC, Australia*
[4] *Department of Anatomy and Neuroscience, Centre of Neuroscience Research, University of Melbourne, Parkville, VIC, Australia*

Huntington's disease (HD) is an incurable neurodegenerative disorder caused by a CAG repeat expansion in exon 1 of the Huntingtin (HTT) gene. Recently, induced pluripotent stem cell (iPSC) lines carrying atypical and aggressive (CAG60+) HD variants have been generated and exhibit disparate molecular pathologies. Here we investigate two human embryonic stem cell (hESC) lines carrying CAG_{37} and CAG_{51} typical late-onset repeat expansions in comparison to wildtype control lines during undifferentiated states and throughout forebrain neuronal differentiation. Pluripotent HD lines demonstrate growth, viability, pluripotent gene expression, mitochondrial activity and forebrain specification that is indistinguishable from control lines. Expression profiles of crucial genes known to be dysregulated in HD remain unperturbed in the presence of mutant protein and throughout differentiation; however, elevated glutamate-evoked responses were observed in HD CAG_{51} neurons. These findings suggest typical late-onset HD mutations do not alter pluripotent parameters or the capacity to generate forebrain neurons, but that such progeny may recapitulate hallmarks observed in established HD model systems. Such HD models will help further our understanding of the cascade of pathological events leading to disease onset and progression, while simultaneously facilitating the identification of candidate HD therapeutics.

Keywords: Huntington's disease, human embryonic stem cells, neuronal differentiation, GABAergic neurons

INTRODUCTION

Huntington's disease (HD) is an autosomal dominant neurodegenerative disorder caused by an expanded CAG repeat tract in exon 1 of the *HTT* gene (Group, 1993). Disease alleles ($CAG_{>35}$) exhibit an age-dependent penetrance, with the lowest disease range ($CAG_{36−39}$) associated with a later onset (McNeil et al., 1997). CAG_{40+} alleles are associated with full penetrance, while larger expansions (CAG_{60+}) result in juvenile or infantile onset (Andrew et al., 1993; Squitieri et al., 2006). Substantial correlation of ∼50% exists between CAG repeat length and age of onset, with secondary contributions from known and unknown genetic and environmental factors (Andrew et al., 1993; Wexler et al., 2004). HD affects approximately 1 in 10,000 individuals worldwide, with onset of disease usually in the fourth or fifth decade of life. HD culminates in death 15–20 years after persistent, irreversible and debilitating clinical symptoms (Naarding et al., 2001). To date, there is no cure for HD and consequently, there is an unmet clinical need for more effective therapeutics.

The *HTT* gene comprises 67 exons and encodes a ubiquitously expressed protein of approximately 350 kDa called Huntingtin (HTT). HTT plays a critical role in early embryogenesis with homozygous *HTT* null mouse embryos exhibiting incomplete neural development and lethality at embryonic day 8.5 and 10.5 of gestation (Zeitlin et al., 1995). HTT has been extensively studied in relation to its interacting partners, sub-cellular localization and effects on gene expression, and acts in a variety of cellular systems (Zuccato et al., 2010). The clinical symptoms of HD seen in patients can largely be classified as either neural, such as behavior and cognitive alterations, or motor, such as involuntary movements and abnormalities of voluntary movements. Underlying neurodegeneration is most prominent within the GABAergic medium spiny neurons of the striatum although widespread neuronal loss occurs with disease progression (Graveland et al., 1985; Vonsattel et al., 1985).

Understanding the molecular nature of HD is critical to the development of novel and efficacious therapies. Numerous animal models such as the R6/2 transgenic mouse (Mangiarini et al., 1996) together with post mortem patient tissues have proven valuable resources for identifying and elucidating major CNS cellular mechanisms and hallmarks that contribute to HD pathology; these are comprehensively reviewed in Zuccato et al. (2010) and include transcriptional dysregulation, CAG repeat expansion, excitotoxic stress, autophagy-lysosomal, and proteasome-ubiquitin system perturbation, anterograde and

124

retrograde transport interference, mitochondrial dysfunction and cholesterol biosynthesis alteration.

The hierarchical relationship between the disparate mechanisms/hallmarks and their degree of individual contribution to the overall HD phenotype still remains uncertain. New human HD models such as pluripotent stem cells (PSCs) may provide an alternative system to shed light on this etiological question. Studies investigating hPSC lines, specifically human embryonic stem cell (hESC) lines, carrying pathogenic CAG repeat mutations have provided limited data in relation to the consequences of disease allele expression (Niclis et al., 2009; Bradley et al., 2011; Seriola et al., 2011). More recently, mouse and human induced pluripotent stem cell (iPSC) lines have been analysed for the appearance of HD hallmarks (Camnasio et al., 2012; Castiglioni et al., 2012; HDIPSCC, 2012; Jeon et al., 2012) and several phenotypes have been observed, including transcriptional dysregulation, CAG repeat instability, mutant HTT aggregates, cholesterol biosynthesis perturbation, lysosomal dysfunction and neuronal vulnerability. However, phenotypes reported from the various HD iPSC studies differ significantly and rarely correlate, for example CAG repeat instability is seen in human but not R6/2 iPSCs. A further caveat is that the HD iPSC lines studied to date either carry rare homozygous HD mutations or alleles with egregious repeat tracts (CAG_{60-180}) indicative of juvenile and infantile onset and may represent atypical disease scenarios.

Limited studies assess the appearance of HD phenotypes in hPSC lines with clinically relevant trinucleotide expansions (CAG_{35-60}) that correlate with late ages of onset. To this end, we have extended an earlier study by Niclis et al. (2009) using two HD hESC lines SI-187 ($CAG_{51/19}$) and SI-186 ($CAG_{37/15}$) that were generated from embryos identified with pre-implantation genetic detection (PGD). Here we show that the HD hESC lines are indistinguishable from control hESCs with respect to pluripotent characteristics, mitochondrial function, forebrain neural differentiation capabilities, relevant cellular phenotypes and with no evidence of a dysregulated transcriptome in key HTT associated genes. However, the larger of the two CAG repeat cell lines showed an altered responsiveness to the neurotransmitter glutamate. Overall, these results are informative for establishing a human neuronal cellular model of HD.

MATERIALS AND METHODS
CULTURE AND NEURAL DIFFERENTIATION OF hESC LINES
Two HD hESC lines SI-186 ($CAG_{37/15}$) and SI-187 ($CAG_{51/19}$) (Niclis et al., 2009) as well as two wildtype control hESC lines, HES3 and H9 (Thomson et al., 1998; Reubinoff et al., 2000) were used. All hESC lines were screened for karyotypic abnormalities using Geisma staining and found to maintain euploid 46 XX karyotypes (data not shown). All four hESC lines were grown as bulk cultures on γ-irradiated mouse embryonic fibroblasts (MEFs) according to previously described conditions (Costa et al., 2008); briefly, cells were grown in DMEM/ F-12, supplemented with 0.1 mM β-mercaptoethanol, 1% non-essential amino acids, 1% Glutamax, 25 U/ml penicillin, 25 U/ml streptomycin, and 20% knockout serum replacement (all Invitrogen).

hESC neural differentiation was performed as previously described (Song et al., 2011a). Briefly, ~3000 hESCs

were distributed to each well of a round-bottom ultra-low attachment 96-well plate (Corning) containing 100 μl of Differentiation Medium (Neurobasal A, 5% ITS-X, 2.5% Penicillin/Streptomycin, 5% Glutamax, 5% B27 and 5% N2; Invitrogen). From d0–d21 cells were grown as neurospheres at 37°C in 5% CO_2 in air, with 0.125% polyvinyl alcohol and 10 μM Roh-Associated Coil Kinase (ROCK) inhibitor Y-27632 at d0–4. From d0–d21 media was supplemented with 20 ng/ml epidermal growth factor (EGF) and 20 ng/ml fibroblast growth factor (FGFb) (R&D Systems), and 100 ng/ml of Noggin (R&D Systems) from d0–8. Neurospheres were passaged at d14 by manual sectioning in half. To promote neuronal differentiation neurospheres were plated at d21 in Differentiation Medium onto 24-well plates (BD Biosciences) coated with 20 μg/ml poly-D-lysine and 20 μg/ml laminin (Invitrogen) in the absence of growth factors and media changed every 4 days for up to 24 days.

FLOW CYTOMETRY
Cells were harvested using TrypLE Select (Invitrogen), passed through a 70 μm filter and 1×10^5 cells stained with various antibodies listed in **Table 1**. Samples were analysed using a BD Canto II flow cytometer with data analyses performed using GateLogic. All samples were gated to assess only single cells as determined by forward scatter area vs. height channels and live cells as determined by negative DAPI selection. Background fluorescence was subtracted using unlabeled cells. A total of 50,000 events (~40,000 live cells) were recorded, compensations were performed using single label antibody controls; positive gates were designated on concentration-matched isotype control antibodies.

GENOTYPING
Genotyping was performed as previously described (Niclis et al., 2009). Briefly, HU3 and HU4 primers (Sermon et al., 1998) were used to amplify the CAG repeat expansion region in exon 1 of *HTT*. The HU4 sense primer was labeled with 6-carboxyfluorescein (6-FAM) and sizing of amplicons performed with an ABI Prism 3100 DNA sequencer coupled with GeneScan Software according to previously described methods (Cram et al., 2000). The number of CAG repeats was accurately calculated to ±1 bp from GeneScan sized F-PCR products, using

Table 1 | Antibodies and dilutions utilized for flow cytometry and immunocytochemistry.

Antibody target	Species	Conjugate	Dilution	Company
CD9	Mouse	FITC	1:30	BD
TRA-1-60	Mouse	APC	1:25	BD
FORSE-1	Mouse	N/A	1:1000	DSHB
CD56	Mouse	PerCPcy5.5	1:50	BD
β-III-TUBULIN	Mouse	N/A	1:500	Millipore
Huntingtin	Rabbit	N/A	1:100	Millipore
SOX2	Goat	N/A	1:200	ABcam
OTX2	Rabbit	N/A	1:1000	Millipore
GABA	Rabbit	N/A	1:500	Millipore
FOXG1	Rabbit	N/A	1:50	ABCam

the formula: CAG repeat number = (size of PCR product – size of non-CAG repeat region)/3.

IMMUNOCYTOCHEMISTRY

Neurospheres were collected at d10 or 21 and fixed for 15 min at room temperature with 4% paraformaldehyde, cryoprotected in sucrose (20% w/v in 0.1 M PBS) and embedded in OCT compound (Tissue–Tek) before serial sectioning ($6 \times 10\,\mu m$ thick sections) on a cryostat (Leica). Neuronal cultures were fixed at d35 or 45 for 15 min at room temperature with 4% paraformaldehyde, permeabilized with 1% Triton X-100 (Ameresco), blocked using 10% normal donkey serum (Invitrogen) and incubated with primary antibodies described in **Table 1** at 4°C overnight. Species-specific AlexaFluor (Invitrogen) or Dyelight (Jackson Laboratories) 488 and 555 secondary antibodies (all 1:200) were added for 2 h at room temperature and then counterstained with 0.1 μg/ml DAPI (SIGMA). Coverslips were mounted onto glass slides using Fluorescent Mounting Media (DAKO). Bound fluorescence was detected using an Olympus BX51 microscope coupled to the ULH100HG fluorescence system. Images were captured using a DP70 camera.

CELL GROWTH AND VIABILITY ASSAYS

Duplicate MEF coated T25 culture flasks were seeded with 1×10^6 hESCs for each line. Cells were harvested at 24 and 72 h. FACS analysis of DAPI, CD9, and TRA-1-60 staining was used to distinguish live hESCs (DAPI–/CD9+/TRA1–60+) and MEFs (DAPI–/CD9–/TRA1–60–). Doubling rates were calculated based on hESC and live cells only, according to the following formulae: $[Log_2(\beta/\alpha)]/2$; $\alpha = 24$ h count and $\beta = 72$ h count. Viability assays were performed similarly on hESCs 24 h after passage but with DAPI live and dead cell gating performed by FACS after CD9 and TRA-1–60 gating. Neurosphere growth rates were determined by measuring area sizes using Adobe Photoshop CS5, the average value for 12 neurospheres equated a single replicate, with three averaged values analysed at each time point for each line. Data values at d21 were doubled to account for passaging in half of spheres at d14. Data was statistically analysed with PRISM, using a One-Way ANOVA with a Kruskal–Wallis Test and Dunn's post test. Means were graphed with the SEM and a p-value (*) of < 0.05 considered significantly different.

NEURONAL FUNCTIONAL ANALYSIS

Neurons were cultured as described above. For intracellular Ca^{2+} $[(Ca^{2+})_i]$ imaging, neurons were loaded with Fluo4-AM ($2\,\mu M$, for 45 min at 37°C, as previously described (Watmuff et al., 2012). Media was then replaced with HEPES buffer (of composition, mM, NaCl 145; $MgSO_4$ 1; KCl 5; glucose 10; $CaCl_2$ 2.5; HEPES 10; pH 7.4) containing bovine serum albumin (0.3% w:v) and placed on a heated (37°C) stage. Neurons were viewed using a Nikon A1R confocal microscope and excited with a 488 nm laser, emission was recorded at 525/50 nm at two image frames per second. After 2 min of baseline recording glutamate ($30\,\mu M$) or vehicle was added to each well and imaging continued for 90 s as previously described (Raye et al., 2007; Khaira et al., 2011; Watmuff et al., 2012). After this time KCl (30 mM) was added to each well and imaging continued for a further 60 s. For analysis,

background emission light was subtracted from analysis regions defined within each cell body and emission intensity within each region calculated using Nikon Elements software. The maximal elevation of intracellular $[Ca^{2+}]_i$ in response to vehicle or glutamate is expressed as the net fraction of the KCl-induced maximal increase in $[Ca^{2+}]_i$.

QUANTITATIVE REAL-TIME PCR

Total RNA was extracted from $\sim 1 \times 10^6$ cells using the commercially available RNeasy Mini Kit (Qiagen) as per the manufacturer's instructions and treated with RNase-Free DNase (Qiagen). RNA was quantitated using a ND-1000 Spectrophotometer (NanoDrop Technologies). Purified RNA (0.4–2 μg) was reverse transcribed to single stranded cDNA with SuperScript III reverse transcriptase using the First Strand Synthesis System Kit (Invitrogen) and treated with RNase H to remove contaminating RNA.

cDNA products were subjected to qRT-PCR of selected genes (**Table 2**) using TaqMan® Universal PCR Master Mix and the inventoried TaqMan® Gene Expression Assay Kit (Applied Biosystems) according to manufacturer's recommendations. Glyceraldehyde 3-phosphate dehydrogenase (*GAPDH*) was used for normalization of RNA input, two independent reactions were prepared for each sample. Reaction plates were run on the 7500 Real Time PCR System (Applied Biosystems) at the following thermocycler conditions: stage 1, 50°C for 2 min; stage 2, 95°C for 10 min and stage 3, 40 cycles of 95°C for 15 s and 60°C for 1 min. The relative quantification (RQ) of gene expression in each sample was analysed using SDS Software version 1.3 (Applied Biosystems). The Ct value for each sample was measured in duplicate and the average normalized against the endogenous control *GAPDH* to determine the ΔCt value. The ΔCt values were then standardized against the calibrator's ΔCt (wildtype HES3 line) to yield the ΔΔCt. The RQ was then calculated as $2^{-\Delta\Delta Ct}$. Statistical analysis for qRT-PCR data was performed using GraphPad Prism with a one-way ANOVA analysis of each gene at each specific time point. A Kruskal–Wallis test was performed on the non-matched, non-parametric data. The p-value was set to <0.05 and a Dunn's post-test performed with RQ data from three culture replicates plotted as a mean and scale bars denoting the mean ± SEM.

Table 2 | TaqMan gene expression assay details used for qRT-PCR.

Gene symbol	Amplicon length (bp)	Gene bank number	Assay ID
GAPDH	93	NM_002046.3	Hs99999905_m1
HTT	66	NM_002111.6	Hs00918134_m1
PGC1a	74	NM_013261.3	Hs01016719_m1
DRP1	88	NM_005690.3	Hs00247147_m1
BDNF	116	NM_170733.3	Hs00380947_m1
DRD2	64	NM_000795.3	Hs00241436_m1
PENK	56	NM_001135690.1	Hs00175049_m1
SREBP1	90	NM_001005291.2	Hs01088691_m1
β-III-TUBULIN	82	N/A	Hs00964967_g1

All primers were purchased from Applied Biosystems.

126

WESTERN BLOTTING

1×10^6 cells were lysed in $500\,\mu l$ of Cell Lysis Buffer (Cell Signaling) and protein concentrations determined using a BCA assay (Pierce, Thermo Scientific). Protein samples $(10\,\mu g)$ in $1\times$ SDS sample buffer containing 10% β-mercaptoethanol were electrophoresed on 4–12% NuPAGE gels (Invitrogen). Proteins were transferred to immobilon PVDF transfer membranes (Millipore), blocked in TBS-T containing 5% non-fat dry milk powder and then immunoblotted with either monoclonal antibody 1HU-4C8 (Millipore, 1:2000) specific for epitopes within amino acids 181–810 on wildtype and mutant HTT or monoclonal antibody 5TF1-1C2 (Millipore, 1:5000) which has a high avidity for long polyglutamine epitopes (>15 polyglutamine residues). A secondary anti-mouse HRP antibody (Calbiochem) in combination with an ECL kit was finally used to illuminate HTT protein.
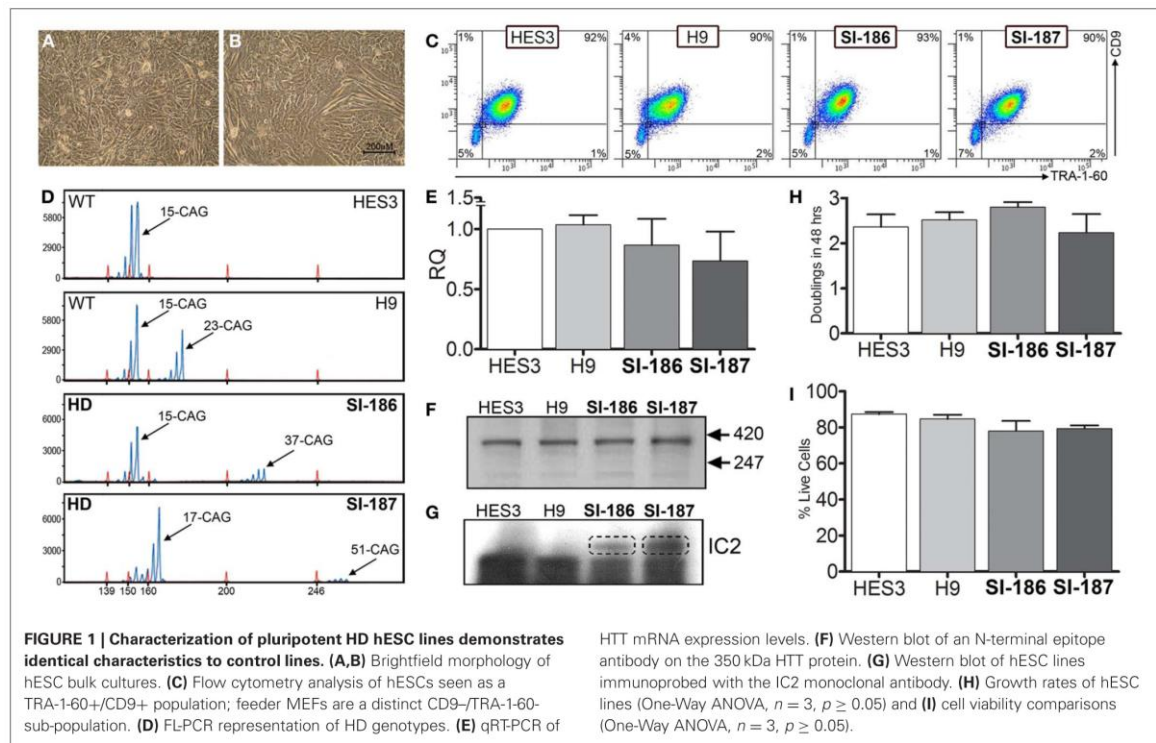
JC-1 MITOCHONDRIAL STAINING

JC-1 a cationic dye that undergoes a fluorescence emission shift from green (529 nm) to red (590 nm) upon accumulation in the mitochondrial matrix (Simeonova et al., 2004), was employed to measure changes in the mitochondrial membrane potential (MMP). Undifferentiated hESCs (1×10^6) prepared from bulk cultures were incubated in media containing $2\,\mu M$ of JC-1 for 30 min, washed twice in PBS and then analysed using a BD FACS Canto II flow cytometer 488 nm excitation and emission detection dually from both FITC and PE channels. Compensations were performed with hESC specific CD9 and EpCAM antibodies,

conjugated to FITC and PE respectively. Data analysis was conducted using FACS Diva software (BD).

RESULTS

CHARACTERIZATION OF PLURIPOTENT HD hESC LINES

HD and control hESC lines were originally derived as colony cultures that intrinsically comprise significant heterogeneity with differential degrees of pluripotency and differentiation capacities across a gradient of isolatable sub-fractions (Laslett et al., 2007; Hough et al., 2009; Kolle et al., 2009). To eliminate this stochasticity, HD hESC lines were adapted to an enzymatically passaged bulk culture system to provide homogenous cultures amenable to stringent molecular and functional comparative evaluations. Of note, adaptation rates of HD lines were commensurate with controls, requiring ∼3–5 passages, and produced morphologically identical bulk culture monolayers of hESCs with low cytoplasmic-to-nuclear ratios (**Figures 1A,B**). Robust homogeneity was achieved with hESC bulk culture conditions, evidenced by a tightly clustered population of TRA-1-60+/CD9+ pluripotent cells and an absence of single positive cells indicating that the hESCs were maintained in a pluripotent state (**Figure 1C**). Both HD hESC lines exhibited FACS profiles with pluripotent markers similar to control lines verifying stable undifferentiated states (**Figure 1C**). Further, no significant differences in cell growth rates (doublings/48 h) were observed between HD and control hESC lines (SI-187 2.24, SI-186 2.8, HES3 2.36, and H9 2.52, $p > 0.05$; **Figure 1H**) or cell viability during enzymatic

FIGURE 1 | Characterization of pluripotent HD hESC lines demonstrates identical characteristics to control lines. (A,B) Brightfield morphology of hESC bulk cultures. **(C)** Flow cytometry analysis of hESCs seen as a TRA-1-60+/CD9+ population; feeder MEFs are a distinct CD9–/TRA-1-60– sub-population. **(D)** FL-PCR representation of HD genotypes. **(E)** qRT-PCR of HTT mRNA expression levels. **(F)** Western blot of an N-terminal epitope antibody on the 350 kDa HTT protein. **(G)** Western blot of hESC lines immunoprobed with the IC2 monoclonal antibody. **(H)** Growth rates of hESC lines (One-Way ANOVA, $n = 3$, $p \geq 0.05$) and **(I)** cell viability comparisons (One-Way ANOVA, $n = 3$, $p \geq 0.05$).

passaging (SI-187 79.3%, SI-186 78.0%, HES3 84.7%, and H9 87.3%, $p > 0.05$; **Figure 1I**).

Analysis of FL-PCR products confirmed correct CAG repeat genotypes for HD lines SI-187 (CAG$_{51/19}$) and SI-186 (CAG$_{37/15}$) and control lines HES3 (CAG$_{15/15}$) and H9 (CAG$_{23/15}$) (**Figure 1D**). qRT-PCR using primers specific for conserved sequences on both wildtype and mutant alleles confirmed *HTT* mRNA was expressed at similar levels in HD and control hESC lines (**Figure 1E**). Western blot analysis using a polyclonal antibody reactive to an N-terminal epitope on the 350 kDa HTT protein (**Figure 1F**) confirmed HTT protein expression in all four hESC lines. Further immunoprobing using the IC2 monoclonal antibody that specifically reacts with long polyglutamine epitopes >15–20 residues (Trottier et al., 1995) detected a ∼350 kDa band exclusively within SI-187 and SI-186 cells confirming mutant HTT expression in both HD lines (**Figure 1G**).
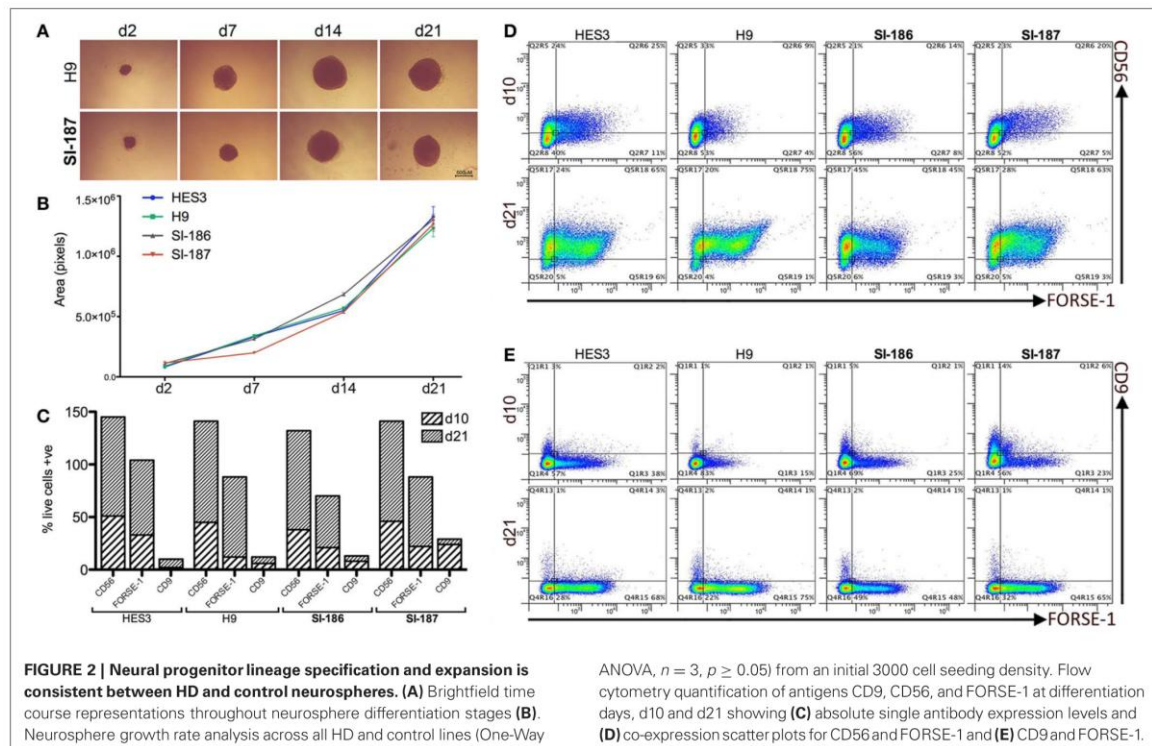
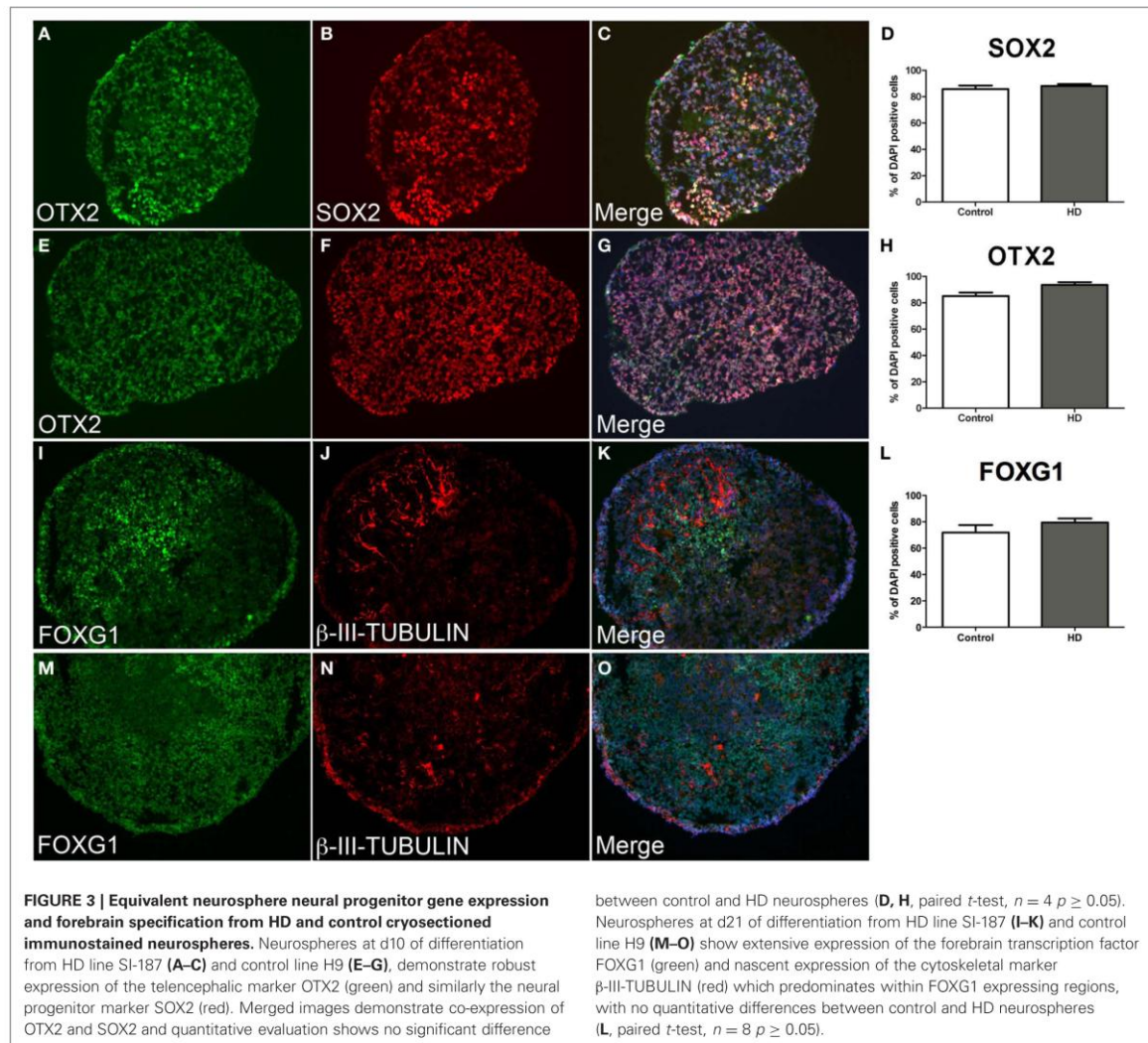### NEURAL DIFFERENTIATION IS UNPERTURBED BY AN EXPANDED CAG TRACT

HD neurodegeneration emerges within the forebrain and progresses to whole-brain atrophy. Differentiation of HD hESC lines to a regionally relevant forebrain phenotype was achieved using the spin aggregation neurosphere system we have previously reported (Song et al., 2011a). Seeding 3000 hESCs per well resulted in morphologically similar neurospheres within 24 h and throughout the neurosphere differentiation stage between HD and control lines (**Figure 2A**). Neural growth rates were

equivalent between HD and control lines indicating the presence of mHTT does not interfere with neural precursor division and differentiation ($p > 0.05$; **Figure 2B**).

Quantitative flow cytometric assessment throughout neurosphere stages demonstrated highly analogous expression profiles across HD and control lines. All lines progress early to a neural fate and near total expression (>90%) of the pan-neural marker CD56 is observed by d21 (**Figure 2C**). Neural differentiation exhibited an anterior identity with >50% of cells expressing the forebrain surface antigen FORSE-1 (**Figure 2C**). The forebrain population was confirmed as neural in character with >90% of the FORSE-1+ population co-staining with CD56 by d21 (**Figure 2D**), and all FORSE-1+ cells separating from minor CD9+ fractions (**Figure 2E**). All hESCs rapidly exit a pluripotent state with low levels of the hESC marker CD9 d10 which falls to ∼2% by d21 (**Figure 2E**). Intriguingly, a delay in CD9 downregulation is observed in the fully penetrant SI-187 line at d10, although by d21 CD9 expression is consistent across all lines (**Figure 2E**). Overall, these findings suggest that pathogenic HD mutations do not perturb neural progenitor generation, expansion or specification to an anterior identity.

Control and HD neurospheres exhibited equivalent progenitor phenotypes at d10 (**Figures 3A–H**). Strong expression of the multipotent neural stem cell transcription factor SOX2 was observed in control (85.8%) and HD (88.2%) cells equally (**Figure 3D**, data not significant $p = 0.05$). This was concomitant with a rostral

FIGURE 2 | Neural progenitor lineage specification and expansion is consistent between HD and control neurospheres. (A) Brightfield time course representations throughout neurosphere differentiation stages **(B)**. Neurosphere growth rate analysis across all HD and control lines (One-Way

ANOVA, $n = 3$, $p \geq 0.05$) from an initial 3000 cell seeding density. Flow cytometry quantification of antigens CD9, CD56, and FORSE-1 at differentiation days, d10 and d21 showing **(C)** absolute single antibody expression levels and **(D)** co-expression scatter plots for CD56 and FORSE-1 and **(E)** CD9 and FORSE-1.

128

FIGURE 3 | Equivalent neurosphere neural progenitor gene expression and forebrain specification from HD and control cryosectioned immunostained neurospheres. Neurospheres at d10 of differentiation from HD line SI-187 **(A–C)** and control line H9 **(E–G)**, demonstrate robust expression of the telencephalic marker OTX2 (green) and similarly the neural progenitor marker SOX2 (red). Merged images demonstrate co-expression of OTX2 and SOX2 and quantitative evaluation shows no significant difference between control and HD neurospheres **(D, H**, paired t-test, $n = 4$ $p \geq 0.05$). Neurospheres at d21 of differentiation from HD line SI-187 **(I–K)** and control line H9 **(M–O)** show extensive expression of the forebrain transcription factor FOXG1 (green) and nascent expression of the cytoskeletal marker β-III-TUBULIN (red) which predominates within FOXG1 expressing regions, with no quantitative differences between control and HD neurospheres **(L**, paired t-test, $n = 8$ $p \geq 0.05$).
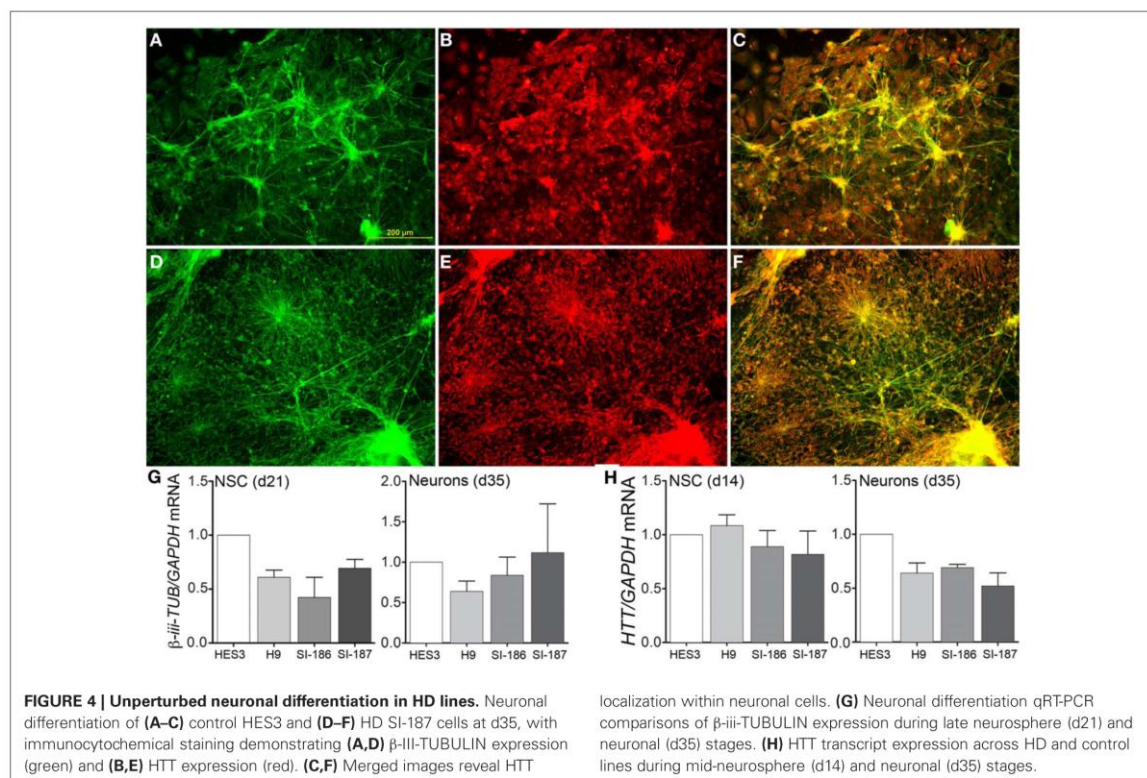
fate seen by the robust expression of the telencephalic marker OTX2 in comparable proportions between control (88.0%) and HD (92.4%) cells (**Figure 3H**, data not significant $p = 0.05$), and by co-localization of both proteins (**Figures 3C,G**). Importantly, continued differentiation to d21 facilitated robust expression of the forebrain specific transcription factor FOXG1 within the majority of neurosphere cells in both control and HD sections (**Figures 3I–O**). Expression levels of FOXG1 were not significantly different between control (71.9%) and HD (79.4%) neurospheres (**Figure 3L**, $p = 0.05$). Limited numbers of neuronal cells were seen at the end of neurosphere culture, detected by β-III-TUBULIN expression (**Figures 3J,N**). FOXG1 expressing regions preferentially co-localize with β-III-TUBULIN expression indicating maturation of anterior cells to a post-mitotic neuronal fate (**Figures 3K,O**).

Subsequent to neurosphere plating on extracellular matrices, neuronal differentiation disseminated throughout cultures in control (**Figure 4A**) and HD neurons (**Figure 4D**) as shown by cytoskeletal β-III-TUBULIN immunostaining. Quantitative validation was made of these observations during late neurospheres (d21) and neuronal (d35) differentiation stages by β-*III-TUBULIN* transcript expression comparisons (**Figure 4G**). Antibody staining against an N-terminal HTT epitope revealed cytoplasmic and nuclear protein localization (**Figures 4B,E**) and specifically preferential nuclear reactivity within the nuclei of neurons with no discernable differences between control (**Figure 4C**) and HD neurons (**Figure 4F**). Further, quantitative *HTT* transcript expression levels were equal across all HD and control lines during neural precursor and neuronal differentiation stages (**Figure 4H**). Crucially, neuronal differentiation

129

FIGURE 4 | Unperturbed neuronal differentiation in HD lines. Neuronal differentiation of **(A–C)** control HES3 and **(D–F)** HD SI-187 cells at d35, with immunocytochemical staining demonstrating **(A,D)** β-III-TUBULIN expression (green) and **(B,E)** HTT expression (red). **(C,F)** Merged images reveal HTT localization within neuronal cells. **(G)** Neuronal differentiation qRT-PCR comparisons of β-iii-TUBULIN expression during late neurosphere (d21) and neuronal (d35) stages. **(H)** HTT transcript expression across HD and control lines during mid-neurosphere (d14) and neuronal (d35) stages.

of anterior neurosphere cells culminated in robust detection of the neurotransmitter GABA, which was observed in equal proportions throughout the elaborate neuronal networks produced from control HES3 (**Figures 5A–C**) and H9 (**Figures 5D–F**) as well as HD SI-186 (**Figures 5G–I**) and SI-187 (**Figures 5J–L**) cell lines. Co-staining for β-III-TUBULIN and GABA demonstrate the majority of neuronal cells possess a GABAergic identity (**Figures 5C,F,I,L**).
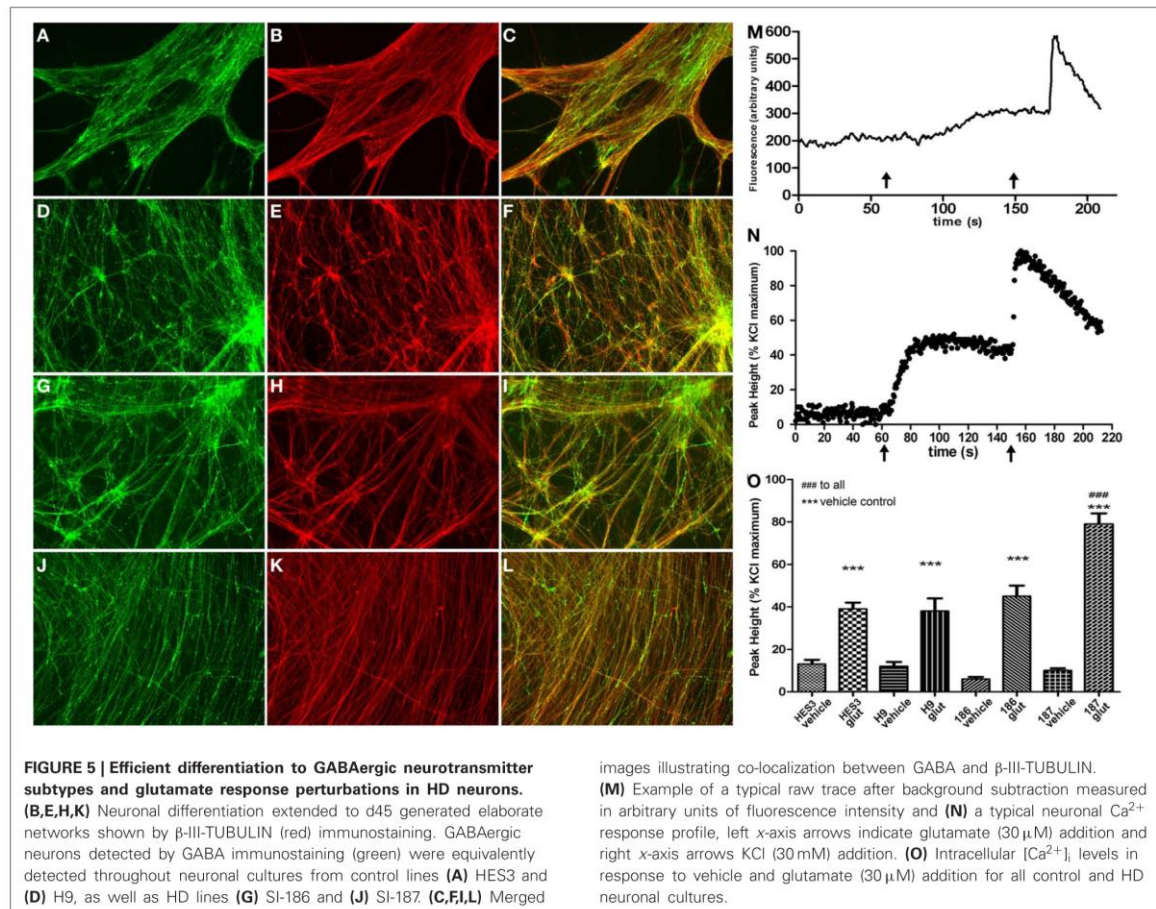
FUNCTIONAL RESPONSES OF NEURONAL CULTURES

Neurons derived from this culture protocol were compared to their respective vehicle control wells with all four hESC derived neuronal cultures responding to glutamate ($30\,\mu$M) with a significant elevations of $[Ca^{2+}]_i$, **Figure 5M** for a typical raw trace after background subtraction and **Figure 5N** for a typical response profile (One-Way ANOVA with *post-hoc* Tukey test). Interestingly, neurons derived from the fully penetrant SI-187 cell line responded to glutamate with a significantly greater elevation of $[Ca^{2+}]_i$ than neurons from the wildtype HES3 and H9 lines, or the partially penetrant SI-186 line ($p < 0.05$, One-Way ANOVA with *post-hoc* Tukey test, **Figure 5O**).

TRANSCRIPTIONAL ANALYSIS OF MUTANT HTT MODULATED GENES

Recent studies of HD human embryonic carcinoma cells (hECCs) and iPSC lines demonstrate *in vitro* gene expression alterations (Gaughwin et al., 2011; Castiglioni et al., 2012). Whether similar

transcriptome disruptions are evident in late-onset CAG length hESC lines remains uncertain. Expression levels of critical transcripts identified in previous studies and those with direct paths from mHTT expression to gene disruption were assessed by qRT-PCR in undifferentiated HD and control lines (day 0), within neurospheres derivatives at day 14 and at neuronal promoting stages (day 35) (**Figure 6**). Selected for assessment were neural-specific genes Brain-Derived Neurotrophic Factor (*BDNF;* Zuccato and Cattaneo, 2007, 2009), dopamine receptor D2 (*DRD2*) and proenkephalin (*PENK*) (Luthi-Carter et al., 2000; Dunah et al., 2002; Hodges et al., 2006). Also assessed were the cholesterol biosynthesis transcripts 7-Dehydrocholesterol reductase (*7-DHCR*) and sterol regulatory element-binding protein 1 (*SREBP1*) (Valenza et al., 2005; Valenza and Cattaneo, 2011), as well as transcription factor EB (*TFEB*) a master regulator of lysosomal biogenesis (Sardiello et al., 2009; Settembre et al., 2011; Camnasio et al., 2012). At day 0 and 14 significant downregulation of *PENK* mRNA expression was observed in SI-187 cells compared to HES3 cells ($p < 0.05$; **Figure 6C**) and *SREBP1* was significantly up-regulated in SI-187 compared to HES3 at day 0 ($p < 0.05$; **Figure 6D**). Nevertheless, significant gene expression changes in *PENK* and *SREBP1* mRNA of HD SI-187 cells were not corroborated when compared to the second control line H9 ($p >$ 0.05), suggesting these discrepancies are a consequence of interline variation as opposed to CAG repeat length. mRNA expression levels of the remaining genes *BDNF, DRD2, 7-DHCR7,* and *TFEB*

130

FIGURE 5 | Efficient differentiation to GABAergic neurotransmitter subtypes and glutamate response perturbations in HD neurons. **(B,E,H,K)** Neuronal differentiation extended to d45 generated elaborate networks shown by β-III-TUBULIN (red) immunostaining. GABAergic neurons detected by GABA immunostaining (green) were equivalently detected throughout neuronal cultures from control lines **(A)** HES3 and **(D)** H9, as well as HD lines **(G)** SI-186 and **(J)** SI-187. **(C,F,I,L)** Merged images illustrating co-localization between GABA and β-III-TUBULIN. **(M)** Example of a typical raw trace after background subtraction measured in arbitrary units of fluorescence intensity and **(N)** a typical neuronal Ca^{2+} response profile, left x-axis arrows indicate glutamate (30 μM) addition and right x-axis arrows KCl (30 mM) addition. **(O)** Intracellular $[Ca^{2+}]_i$ levels in response to vehicle and glutamate (30 μM) addition for all control and HD neuronal cultures.

were similar across HD and control lines at days 0, 14, and 35 ($p > 0.05$) (**Figures 6A,B,E,F**).

ASSESSMENT OF MITOCHONDRIAL GENE EXPRESSION AND FUNCTION

Mitochondrial dysfunction comprises a robust hallmark of HD pathology, measurable by cellular dysregulation of key transcripts, deficits in mitochondrial energy capacities, and fusion/fission events (Cantuti-Castelvetri et al., 2005; Cui et al., 2006; Knott et al., 2008; Song et al., 2011b). qRT-PCR analysis of mitochondrial genes *PGC-1α*, a master regulator of mitochondrial biogenesis and energy metabolism and *DRP1*, a regulator of mitochondrial fusion and fission showed no consistent differences in transcript levels between both control and HD hESCs or neural differentiated derivatives (**Figures 7A,B** respectively). Intriguingly, significant ($p < 0.05$) downregulation of SI-187 *PGC-1α* mRNA levels compared to H9 samples were observed at d14 and a similar yet non-significant trend was seen with SI-186 at d14 and both HD lines at d21 compared to wildtype controls (**Figure 6B**). Mitochondrial functional JC-1 assays that directly

measure MMP found all hESC lines demonstrated similar populations of cells exhibiting dual red and green fluorescence (HES3 95%, H9 68%, SI-186 86%, and SI-187 81%; **Figure 7C**), indicative of an active MMP. Remaining green fluorescent cells from each line represented a sub-population of cells with less active mitochondria.

DISCUSSION

Human PSCs provide a unique window to investigate the ramifications of mutant HTT within the intracellular milieu from the earliest stages of human development until the specification of relevant neuronal subtypes. This study assesses two HD hESCs carrying expanded CAG repeat lengths representative of those harbored by individuals with archetypal late clinical onset. For the first time, we report detailed quantitative evaluations of the pluripotent properties and neural differentiation capabilities of these HD hESC lines using two wildtype control hESC lines as biological comparisons. Our studies of undifferentiated hESCs show expanded CAG repeat tracts have no adverse effects on stem cell parameters that were assessed, such as viability, mitochondrial

FIGURE 6 | qRT-PCR transcriptional analysis of relevant HD related transcripts modulated by mutant HTT. Relative transcript quantification for all four lines are normalized to the control HES3 line and were evaluated across a differentiation time course at the undifferentiated stage (d0), mid-neurosphere stage (d14) and neuronal differentiation stage (d35). Transcripts are assessed for **(A)** BDNF, **(B)** DRD2, **(C)** PENK, **(D)** SREPB1, **(E)** 7-DHCR, and **(F)** TFEB. One-Way ANOVA, $*p < 0.05$.

function, proliferation, and pluripotency markers. These findings are in agreement with recent pluripotent HD studies that observe no disturbance to similar parameters (Gaughwin et al., 2011; Camnasio et al., 2012; Castiglioni et al., 2012; HDIPSCC, 2012; Jeon et al., 2012).

Further, we demonstrate for the first time that neural differentiation of hESCs with HD mutations is equivalent to wildtype controls. Expression of neural markers CD56 and SOX2 and equivalent growth rates of neurospheres show unaltered differentiation in the presence of mutant HTT. Transient lag in the downregulation of the pluripotency marker CD9 was however, observed in one HD line, and corroborates findings of HD hECCs (Gaughwin et al., 2011). Crucially anterior specification assessed by key markers OTX2, FOXG1, and FORSE-1 were equivalent across all lines irrespective of CAG repeat length, and further extended differentiation produced consistent neuronal networks with similar acquisition of GABAergic identities upon *in vitro* maturation. These findings are consistent with mouse and human HD iPSC studies (Camnasio et al., 2012; Castiglioni et al., 2012; HDIPSCC, 2012).

HD patients and animal models are characterized by corticostriatal synaptic dysfunction and profligate excitotoxicity (Raymond, 2003; Estrada Sanchez et al., 2008). A major component of this pathological mechanism is glutamate receptor hypersensitivity on postsynaptic GABAergic striatal neurons. Striatal neurons receive essential glutamate signaling from cortical axons and mutant HTT is directly responsible for excessive Ca^{2+} influx downstream of glutamate stimulation, as seen in YAC128 (Tang et al., 2005) and R6/2 (Cepeda et al., 2001) transgenic models. Mutant HTT aberrantly binds endoplasmic reticulum $InsP_3R1$ receptors that are critical for Ca^{2+} release. This in turn increases the responsiveness of $InsP_3R1$ receptors to upstream glutamate receptor agonists and induces abnormal Ca^{2+} release (Tang et al., 2003, 2005).

In our studies we identified increased neuronal Ca^{2+} elevation in the fully penetrant HD line SI-187 upon glutamate stimulation that suggests late-onset HD hESCs are be capable of recapitulating some neuronal pathologies that characterize established HD model systems. Detectable alterations in Ca^{2+} glutamate responses are not unexpected with evidence of this phenotype in GABAergic neurons from pre-onset HD mice (Cepeda et al., 2001; Laforet et al., 2001) and even within neurons isolated as early as post-natal day 0-1 (Zeron et al., 2004). Together, these findings suggest increased Ca^{2+} responses may occur in early human stages of HD and thus represent a potentially valuable therapeutic target. The absence of such observations in the partially penetrant SI-186 line may correspond with the lesser pathological intensity of mutant proteins comprising 35–39 polyglutamine tracts and prolonged neuronal culture may be necessary to manifest this functional state.

FIGURE 7 | Assessment of mitochondrial gene expression and function. Relative transcript quantification for all four lines are normalized to the control HES3 line for mitochondrial genes **(A)** DRP1 and **(B)** PGC-1α at the undifferentiated (d0), neurosphere (d14) and neuronal (d35) stages of differentiation. **(C)** Mitochondrial functional JC-1 assay quantifying activity of the mitochondrial membrane potential (MMP) between control and HD hESCs. One-Way ANOVA, $*p < 0.05$.

Extensive mutant HTT dysregulation of the cellular transcriptomes is a dominant hallmark seen in post-mortem brain tissue from HD patients and across animal models, reportedly affecting ∼1–2% of total cellular transcripts (Cha, 2000; Luthi-Carter et al., 2002a,b; Hodges et al., 2006). Transcript alteration has emerged as a focal point across HD pluripotent cell studies of aggressive HD subclasses, though little consensus appears to date. Exemplifying this are contrary observations of BDNF transcript stability and downregulation compared to controls in generated neural cultures (Gaughwin et al., 2011; Castiglioni et al., 2012; HDIPSCC, 2012). This contradiction is surprising considering clear evidence from model systems of the process by which mutant HTT instigates reduced BDNF expression via nuclear translocation of the transcriptional repressor REST (Zuccato and Cattaneo, 2007; Zuccato et al., 2007). Our study found BDNF is not altered in neural and neuronal derivatives of HD hESCs carrying typical late-onset ranges, suggesting BDNF may not be dysregulated unless significant pathology has progressed.

None of the remaining transcripts analysed in the HD hESC lines were significantly changed at either pluripotent or neural differentiated time points when compared to both control hESC lines. SREBP1, a cholesterol biosynthesis regulator, was significantly upregulated in pluripotent SI-187 cells compared to one control and approached significance to the second control line; a finding consistent with overt cholesterol biosynthesis disruption in HD models (Valenza et al., 2007a,b), patients (Markianos

et al., 2008) and undifferentiated HD iPSC lines (Castiglioni et al., 2012). Further, there was a transient downregulation of the mitochondrial gene PGC-1α at d14 in SI-187 neural derivatives which continued to d21 although the trend was not statistically significant at the latter time-point. To corroborate this finding, we undertook functional studies of MMP activity, which is reduced when PGC-1α is down-regulated. In both undifferentiated cells and in d14 neurospheres from SI-186 and SI-187 (data not shown) we found no evidence of altered MMP. Together these findings in conjunction with those of other pluripotent systems imply transcript disturbances in this class of in vitro models may be a phenomenon that predominates in lines equivalent to juvenile and infantile disease subclasses, warranting array based studies to scrutinize cellular transcriptomes across a range of lines carrying different CAG repeat lengths.

In summary we have provided detailed characterization of HD hESCs and also those that harbor typical CAG repeat expansions. We demonstrate for the first time that pluripotent dynamics and forebrain neuronal differentiation are unhindered but that glutamate signaling perturbations indicative of Huntington's pathology are observable subsequent to extended in vitro culture and cellular acquisition of a forebrain GABAergic neuron identity. These late-onset hESC lines demonstrate the potential of such model systems to provide a platform to interrogate disease mechanisms and hallmarks. Advances describing the efficient generation of DARPP32+ medium spiny neurons provide an

133

opportunity for probing HD etiology within a more relevant cell type (Ma et al., 2012) and could be coupled with proteasomal inhibition or oxidative stress to exacerbate disease phenotypes as demonstrated recently (HDIPSCC, 2012; Jeon et al., 2012).

Emergent studies of HD iPSCs describe lines that possess atypical alleles representative of rare juvenile/infantile (CAG_{60+}) or homozygous subclasses that are poorly studied in human patients (Camnasio et al., 2012; Castiglioni et al., 2012; HDIPSCC, 2012; Jeon et al., 2012). The observation of some HD specific phenotypes in these lines demonstrate their potential value as *in vitro* human models, however, such phenotypes rarely correlate across lines and some are seen as contradictory. Existing HD iPSC lines may not faithfully represent the molecular perturbations of late-onset HD since they potentially exhibit unknown consequences by the reprogramming somatic cells exposed to mutant HTT proteins for considerable durations, and hence PGD isolated hESCs described in this study provide a more "natural" cellular alternative.

Late-onset HD alleles appear to provide a unique system to probe pre-onset changes at the molecular level and within a neurological context, as attested by observations of elevated Ca^{2+} glutamate responses. Understanding pre-onset HD alterations could elucidate the hierarchical relationship between various HD hallmarks, yet is presently restricted primarily to non-invasive imaging methodologies (Tabrizi et al., 2009; Nopoulos et al., 2011) and peripheral blood analysis (Borovecki et al., 2005; Runne et al., 2007; Bjorkqvist et al., 2008). The application of late-onset hESC to long-term *in vitro* neuronal cultures or cellular challenges that mimic *in vivo* conditions (i.e., oxidative or proteasomal stressors) may provide a system to delineate the thresholds that mark clinical onset that is otherwise difficult in extreme CAG repeat variants. Nevertheless, future work must simultaneously evaluate differing model systems to identify those which most faithfully recapitulate human HD, to steer prospective *in vitro* therapeutic activity toward models with the highest potential.

REFERENCES

Andrew, S. E., Goldberg, Y. P., Kremer, B., Telenius, H., Theilmann, J., Adam, S., et al. (1993). The relationship between trinucleotide (CAG) repeat length and clinical features of Huntington's disease. *Nat. Genet.* 4, 398–403.

Bjorkqvist, M., Wild, E. J., Thiele, J., Silvestroni, A., Andre, R., Lahiri, N., et al. (2008). A novel pathogenic pathway of immune activation detectable before clinical onset in Huntington's disease. *J. Exp. Med.* 205, 1869–1877.

Borovecki, F., Lovrecic, L., Zhou, J., Jeong, H., Then, F., Rosas, H. D., et al. (2005). Genome-wide expression profiling of human blood reveals biomarkers for Huntington's disease. *Proc. Natl. Acad. Sci. U.S.A.* 102, 11023–11028.

Bradley, C. K., Scott, H. A., Chami, O., Peura, T. T., Dumevska, B., Schmidt, U., et al. (2011). Derivation of Huntington's disease-affected human embryonic stem cell lines. *Stem Cells Dev.* 20, 495–502.

Camnasio, S., Carri, A. D., Lombardo, A., Grad, I., Mariotti, C., Castucci, A., et al. (2012). The first reported generation of several induced pluripotent stem cell lines from homozygous and heterozygous Huntington's disease patients demonstrates mutation related

enhanced lysosomal activity. *Neurobiol. Dis.* 46, 41–51.

Cantuti-Castelvetri, I., Lin, M. T., Zheng, K., Keller-McGandy, C. E., Betensky, R. A., Johns, D. R., et al. (2005). Somatic mitochondrial DNA mutations in single neurons and glia. *Neurobiol. Aging* 26, 1343–1355.

Castiglioni, V., Onorati, M., Rochon, C., and Cattaneo, E. (2012). Induced pluripotent stem cell lines from Huntington's disease mice undergo neuronal differentiation while showing alterations in the lysosomal pathway. *Neurobiol. Dis.* 46, 30–40.

Cepeda, C., Ariano, M. A., Calvert, C. R., Flores-Hernandez, J., Chandler, S. H., Leavitt, B. R., et al. (2001). NMDA receptor function in mouse models of Huntington disease. *J. Neurosci. Res.* 66, 525–539.

Cha, J. H. (2000). Transcriptional dysregulation in Huntington's disease. *Trends Neurosci.* 23, 387–392.

Costa, M., Sourris, K., Hatzistavrou, T., Elefanty, A. G., and Stanley, E. G. (2008). Expansion of human embryonic stem cells *in vitro*. *Curr. Protoc. Stem Cell Biol.* [Chapter 1: Unit 1C.1.1–1C.1.7].

Cram, D. S., Song, B., McLachlan, R. I., and Trounson, A. O. (2000). CAG trinucleotide repeats in the androgen receptor gene of infertile men exhibit stable inheritance in female

offspring conceived after ICSI. *Mol. Hum. Reprod.* 6, 861–866.

Cui, L., Jeong, H., Borovecki, F., Parkhurst, C. N., Tanese, N., and Krainc, D. (2006). Transcriptional repression of PGC-1alpha by mutant huntingtin leads to mitochondrial dysfunction and neurodegeneration. *Cell* 127, 59–69.

Dunah, A. W., Jeong, H., Griffin, A., Kim, Y. M., Standaert, D. G., Hersch, S. M., et al. (2002). Sp1 and TAFII130 transcriptional activity disrupted in early Huntington's disease. *Science* 296, 2238–2243.

Estrada Sanchez, A. M., Mejia-Toiber, J., and Massieu, L. (2008). Excitotoxic neuronal death and the pathogenesis of Huntington's disease. *Arch. Med. Res.* 39, 265–276.

Gaughwin, P. M., Ciesla, M., Lahiri, N., Tabrizi, S. J., Brundin, P., and Bjorkqvist, M. (2011). Hsa-miR-34b is a plasma-stable microRNA that is elevated in pre-manifest Huntington's disease. *Hum. Mol. Genet.* 20, 2225–2237.

Graveland, G. A., Williams, R. S., and Difiglia, M. (1985). Evidence for degenerative and regenerative changes in neostriatal spiny neurons in Huntington's disease. *Science* 227, 770–773.

Group, H. C. R. (1993). A novel gene containing a trinucleotide repeat that is expanded and unstable on Huntington's disease chromosomes.

The Huntington's disease collaborative research group. *Cell* 72, 971–983.

HDIPSCC. (2012). Induced pluripotent stem cells from patients with Huntington's disease show CAG-repeat-expansion-associated phenotypes. *Cell Stem Cell* 11, 264–278.

Hodges, A., Strand, A. D., Aragaki, A. K., Kuhn, A., Sengstag, T., Hughes, G., et al. (2006). Regional and cellular gene expression changes in human Huntington's disease brain. *Hum. Mol. Genet.* 15, 965–977.

Hough, S. R., Laslett, A. L., Grimmond, S. B., Kolle, G., and Pera, M. F. (2009). A continuum of cell states spans pluripotency and lineage commitment in human embryonic stem cells. *PLoS ONE* 4:e7708. doi: 10.1371/journal.pone.0007708

Jeon, I., Lee, N., Li, J. Y., Park, I. H., Park, K. S., Moon, J., et al. (2012). Neuronal properties, *in vivo* effects, and pathology of a Huntington's disease patient-derived induced pluripotent stem cells. *Stem Cells* 30, 2054–2062.

Khaira, S. K., Nefzger, C. M., Beh, S. J., Pouton, C. W., and Haynes, J. M. (2011). Midbrain and forebrain patterning delivers immunocytochemically and functionally similar populations of neuropeptide Y containing GABAergic neurons. *Neurochem. Int.* 59, 413–420.

Knott, A. B., Perkins, G., Schwarzenbacher, R., and Bossy-Wetzel, E. (2008). Mitochondrial fragmentation in neurodegeneration. *Nat. Rev. Neurosci.* 9, 505–518.

Kolle, G., Ho, M., Zhou, Q., Chy, H. S., Krishnan, K., Cloonan, N., et al. (2009). Identification of human embryonic stem cell surface markers by combined membrane-polysome translation state array analysis and immunotranscriptional profiling. *Stem Cells* 27, 2446–2456.

Laforet, G. A., Sapp, E., Chase, K., McIntyre, C., Boyce, F. M., Campbell, M., et al. (2001). Changes in cortical and striatal neurons predict behavioral and electrophysiological abnormalities in a transgenic murine model of Huntington's disease. *J. Neurosci.* 21, 9112–9123.

Laslett, A., Grimmond, S., Gardiner, B., Stamp, L., Lin, A., Hawes, S., et al. (2007). Transcriptional analysis of early lineage commitment in human embryonic stem cells. *BMC Dev. Biol.* 7:12. doi: 10.1186/1471-213X-7-12

Luthi-Carter, R., Hanson, S. A., Strand, A. D., Bergstrom, D. A., Chun, W., Peters, N. L., et al. (2002a). Dysregulation of gene expression in the R6/2 model of polyglutamine disease: parallel changes in muscle and brain. *Hum. Mol. Genet.* 11, 1911–1926.

Luthi-Carter, R., Strand, A. D., Hanson, S. A., Kooperberg, C., Schilling, G., La Spada, A. R., et al. (2002b). Polyglutamine and transcription: gene expression changes shared by DRPLA and Huntington's disease mouse models reveal context-independent effects. *Hum. Mol. Genet.* 11, 1927–1937.

Luthi-Carter, R., Strand, A., Peters, N. L., Solano, S. M., Hollingsworth, Z. R., Menon, A. S., et al. (2000). Decreased expression of striatal signaling genes in a mouse model of Huntington's disease. *Hum. Mol. Genet.* 9, 1259–1271.

Ma, L., Hu, B., Liu, Y., Vermilyea, S. C., Liu, H., Gao, L., et al. (2012). Human embryonic stem cell-derived GABA neurons correct locomotion deficits in quinolinic acid-lesioned mice. *Cell Stem Cell* 10, 455–464.

Mangiarini, L., Sathasivam, K., Seller, M., Cozens, B., Harper, A., Hetherington, C., et al. (1996). Exon 1 of the HD gene with an expanded CAG repeat is sufficient to cause a progressive neurological phenotype in transgenic mice. *Cell* 87, 493–506.

Markianos, M., Panas, M., Kalfakis, N., and Vassilopoulos, D. (2008). Low plasma total cholesterol in patients with Huntington's disease and first-degree relatives. *Mol. Genet. Metab.* 93, 341–346.

McNeil, S. M., Novelletto, A., Srinidhi, J., Barnes, G., Kornbluth, I., Altherr, M. R., et al. (1997). Reduced penetrance of the huntington's disease mutation. *Hum. Mol. Genet.* 6, 775–779.

Naarding, P., Kremer, H. P., and Zitman, F. G. (2001). Huntington's disease: a review of the literature on prevalence and treatment of neuropsychiatric phenomena. *J. Eur. Psychiatry* 16, 439–445.

Niclis, J. C., Trounson, A. O., Dottori, M., Ellisdon, A. M., Bottomley, S. P., Verlinsky, Y., et al. (2009). Human embryonic stem cell models of Huntington disease. *Reprod. Biomed. Online* 19, 106–113.

Nopoulos, P. C., Aylward, E. H., Ross, C. A., Mills, J. A., Langbehn, D. R., Johnson, H. J., et al. (2011). Smaller intracranial volume in prodromal Huntington's disease: evidence for abnormal neurodevelopment. *Brain* 134, 137–142.

Raye, W. S., Tochon-Danguy, N., Pouton, C. W., and Haynes, J. M. (2007). Heterogeneous population of dopaminergic neurons derived from mouse embryonic stem cells: preliminary phenotyping based on receptor expression and function. *Eur. J. Neurosci.* 25, 1961–1970.

Raymond, L. A. (2003). Excitotoxicity in Huntington disease. *Clin. Neurosci. Res.* 3, 121–128.

Reubinoff, B. E., Pera, M. F., Fong, C. Y., Trounson, A., and Bongso, A. (2000). Embryonic stem cell lines from human blastocysts: somatic differentiation *in vitro*. *Nat. Biotechnol.* 18, 399–404.

Runne, H., Kuhn, A., Wild, E. J., Pratyaksha, W., Kristiansen, M., Isaacs, J. D., et al. (2007). Analysis of potential transcriptomic biomarkers for Huntington's disease in peripheral blood. *Proc. Natl. Acad. Sci. U.S.A.* 104, 14424–14429.

Sardiello, M., Palmieri, M., Di Ronza, A., Medina, D. L., Valenza, M., Gennarino, V. A., et al. (2009). A gene network regulating lysosomal biogenesis and function. *Science* 325, 473–477.

Seriola, A., Spits, C., Simard, J. P., Hilven, P., Haentjens, P., Pearson, C. E., et al. (2011). Huntington's and myotonic dystrophy hESCs: down-regulated trinucleotide repeat instability and mismatch repair machinery expression upon differentiation. *Hum. Mol. Genet.* 20, 176–185.

Sermon, K., Goossens, V., Seneca, S., Lissens, W., De Vos, A., Vandervorst, M., et al. (1998). Preimplantation diagnosis for Huntington's disease (HD): clinical application and analysis of the HD expansion in affected embryos. *Prenat. Diagn.* 18, 1427–1436.

Settembre, C., Di Malta, C., Polito, V. A., Garcia Arencibia, M., Vetrini, F., Erdin, S., et al. (2011). TFEB links autophagy to lysosomal biogenesis. *Science* 332, 1429–1433.

Simeonova, E., Garstka, M., Koziol-Lipinska, J., and Mostowska, A. (2004). Monitoring the mitochondrial transmembrane potential with the JC-1 fluorochrome in programmed cell death during mesophyll leaf senescence. *Protoplasma* 223, 143–153.

Song, B., Niclis, J. C., Alikhan, M. A., Sakkal, S., Sylvain, A., Kerr, P. G., et al. (2011a). Generation of induced pluripotent stem cells from human kidney mesangial cells. *J. Am. Soc. Nephrol.* 22, 1213–1220.

Song, W., Chen, J., Petrilli, A., Liot, G., Klinglmayr, E., Zhou, Y., et al. (2011b). Mutant huntingtin binds the mitochondrial fission GTPase dynamin-related protein-1 and increases its enzymatic activity. *Nat. Med.* 17, 377–382.

Squitieri, F., Frati, L., Ciarmiello, A., Lastoria, S., and Quarrell, O. (2006). Juvenile Huntington's disease: does a dosage-effect pathogenic mechanism differ from the classical adult disease? *Mech. Ageing Dev.* 127, 208–212.

Tabrizi, S. J., Langbehn, D. R., Leavitt, B. R., Roos, R. A., Durr, A., Craufurd, D., et al. (2009). Biological and clinical manifestations of Huntington's disease in the longitudinal TRACK-HD study: cross-sectional analysis of baseline data. *Lancet Neurol.* 8, 791–801.

Tang, T. S., Slow, E., Lupu, V., Stavrovskaya, I. G., Sugimori, M., Llinas, R., et al. (2005). Disturbed Ca2+ signaling and apoptosis of medium spiny neurons in Huntington's disease. *Proc. Natl. Acad. Sci. U.S.A.* 102, 2602–2607.

Tang, T. S., Tu, H., Chan, E. Y., Maximov, A., Wang, Z., Wellington, C. L., et al. (2003). Huntingtin and huntingtin-associated protein 1 influence neuronal calcium signaling mediated by inositol-(1, 4, 5) triphosphate receptor type 1. *Neuron* 39, 227–239.

Thomson, J. A., Itskovitz-Eldor, J., Shapiro, S. S., Waknitz, M. A., Swiergiel, J. J., Marshall, V. S., et al. (1998). Embryonic stem cell lines derived from human blastocysts. *Science* 282, 1145–1147.

Trottier, Y., Lutz, Y., Stevanin, G., Imbert, G., Devys, D., Cancel, G., et al. (1995). Polyglutamine expansion as a pathological epitope in Huntington's disease and four dominant cerebellar ataxias. *Nature* 378, 403–406.

Valenza, M., Carroll, J. B., Leoni, V., Bertram, L. N., Bjorkhem, I., Singaraja, R. R., et al. (2007a). Cholesterol biosynthesis pathway is disturbed in YAC128 mice and is modulated by huntingtin mutation. *Hum. Mol. Genet.* 16, 2187–2198.

Valenza, M., Leoni, V., Tarditi, A., Mariotti, C., Bjorkhem, I., Di Donato, S., et al. (2007b). Progressive dysfunction of the cholesterol biosynthesis pathway in the R6/2 mouse model of Huntington's disease. *Neurobiol. Dis.* 28, 133–142.

Valenza, M., and Cattaneo, E. (2011). Emerging roles for cholesterol in Huntington's disease. *Trends Neurosci.* 34, 474–486.

Valenza, M., Rigamonti, D., Goffredo, D., Zuccato, C., Fenu, S., Jamot, L., et al. (2005). Dysfunction of the cholesterol biosynthetic pathway in Huntington's disease. *J. Neurosci.* 25, 9932–9939.

Vonsattel, J. P., Myers, R. H., Stevens, T. J., Ferrante, R. J., Bird, E. D., and Richardson, E. P. Jr. (1985). Neuropathological classification of Huntington's disease. *J. Neuropathol. Exp. Neurol.* 44, 559–577.

Watmuff, B., Pouton, C. W., and Haynes, J. M. (2012). *In vitro* maturation of dopaminergic neurons derived from mouse embryonic stem cells: implications for transplantation. *PLoS ONE* 7:e31999. doi: 10.1371/journal.pone.0031999

Wexler, N. S., Lorimer, J., Porter, J., Gomez, F., Moskowitz, C., Shackell, E., et al. (2004). Venezuelan kindreds reveal that genetic and environmental factors modulate Huntington's disease age of onset. *Proc. Natl. Acad. Sci. U.S.A.* 101, 3498–3503.

Zeitlin, S., Liu, J. P., Chapman, D. L., Papaioannou, V. E., and Efstratiadis, A. (1995). Increased apoptosis and early embryonic lethality in mice nullizygous for the Huntington's disease gene homologue. *Nat. Genet.* 11, 155–163.

Zeron, M. M., Fernandes, H. B., Krebs, C., Shehadeh, J., Wellington, C. L., Leavitt, B. R., et al. (2004). Potentiation of NMDA receptor-mediated excitotoxicity linked with intrinsic apoptotic pathway

135

in YAC transgenic mouse model of Huntington's disease. *Mol. Cell Neurosci.* 25, 469–479.

Zuccato, C., Belyaev, N., Conforti, P., Ooi, L., Tartari, M., Papadimou, E., et al. (2007). Widespread disruption of repressor element-1 silencing transcription factor/neuron-restrictive silencer factor occupancy at its target genes in Huntington's disease. *J. Neurosci.* 27, 6972–6983.

Zuccato, C., and Cattaneo, E. (2007). Role of brain-derived neurotrophic

factor in Huntington's disease. *Prog. Neurobiol.* 81, 294–330.

Zuccato, C., and Cattaneo, E. (2009). Brain-derived neurotrophic factor in neurodegenerative diseases. *Nat. Rev. Neurol.* 5, 311–322.

Zuccato, C., Valenza, M., and Cattaneo, E. (2010). Molecular mechanisms and potential therapeutical targets in Huntington's disease. *Physiol. Rev.* 90, 905–981.

Conflict of Interest Statement: The authors declare that the research

was conducted in the absence of any commercial or financial relationships that could be construed as a potential conflict of interest.

136

CHAPTER 5

General Discussion

5.1 Introduction

This thesis describes the characterisation and evaluation of two clinically relevant HD hESC lines, SI-186 and SI-187, carrying CAG37 and CAG51 repeat expansions respectively. Importantly this work evaluates lines expressing disease alleles with late onset CAG repeat ranges associated with the majority of HD incidences, thus enabling the study of typical disease etiology. Pursuant to this aim, a robust forebrain neural differentiation protocol was developed and validated across multiple hPSC lines. Both HD hESC lines were shown to be equivalent to wildtype controls with respect to numerous parameters including pluripotency, growth rates, viability, neural differentiation efficiency and patterning. Hallmarks of HD were however identified, including minor transcriptional disturbances, CAG repeat instability and abnormal neuronal calcium signalling. This study evaluated two hESC lines that were derived from affected PGD embryos (Verlinsky et al., 2005) and were specifically chosen as HD models because they were free from any genetic manipulation. While hiPSCs lines represent an emerging and competing HD model system, they had not reached technological maturity at the initiation of this study. Furthermore, there are still concerns with some hiPSC lines regarding their differentiation capacity due to biased epigenetic profiles and/or constitutive activity of reprogramming factors.

5.2 Development of an in vitro neural differentiation protocol for stem cell modelling of neurological disorders

The interconnected and fragile nature of the CNS renders it intolerant to invasive investigation and manipulation. Directing hPSCs into assorted cell types enables researchers to probe human neurons at an unprecedented depth. Coupling this technology with cell lines that harbour genetic determinants for neurological disorders, an equally unrivalled analysis of human disease pathways and mechanisms can be performed *in vitro*.

Numerous methodologies have been devised for coaxing pluripotent cells towards different neural cell types however, many render comparative assessment between disease and control cells difficult due to stochastic elements such as subjective manual

selection or variable seeding densities. The emergence in recent years of a spin aggregation system for neural differentiation (Eiraku et al., 2008;Kim et al., 2011) provides an improved platform for comparative evaluation of disease and control cells, seeding specific quantities of more homogeneous cells in multiple chambers. These protocols are, however, dependent upon batch-variable knockout serum replacement medium or extracellular matrices. The NDEB system developed within this study by contrast is a scalable system that can be controlled in defined conditions allowing differentiation with precise cell numbers to simultaneously yield robust and uniform neural progeny across multiple hPSC lines. This differentiation system provided a platform suitable for investigating hPSC HD lines in order to identify pre-clinical or clinical HD alterations in disease neural progeny.

As HD neurodegeneration is particularly acute within striatal GABAergic neurons that arise from the LGE, it is important for future studies to resolve where on the dors-ventral axis the forebrain GABAergic neurons generated by this neural differentiation system lie. Dorsal and cortical specification would be indicated by co-expression of broad telencephalic markers FORSE-1, OTX2 or FOXG1 **(Figure 5.1,A)** with transcription factors PAX6, PAX7 or mature cortex proteins such as Cux1 or Ctip2 (Denham et al., 2012b; **Figure 5.1,B)**. Co-expression of broad telencephalic markers with GSH2/GSX2 would imply an LGE phenotype (Carri et al., 2012; **Figure 5.1,B)** while co-expression with NKX2.1 would indicate a ventral MGE identity. Further, FOXG1-/NKX2.1+ populations would be indicative of a diencephalic floor plate specification (Maroof et al., 2013; **Figure 5.1,B).** Depending upon these expression results, administration of additional patterning factors to the NDEB system could alter the fate of these forebrain GABAergic neurons, to increase the proportion of LGE precursors, i.e. if a dorsal telencephalic phenotype is observed the addition of the ventralising morphogen SHH would be beneficial.
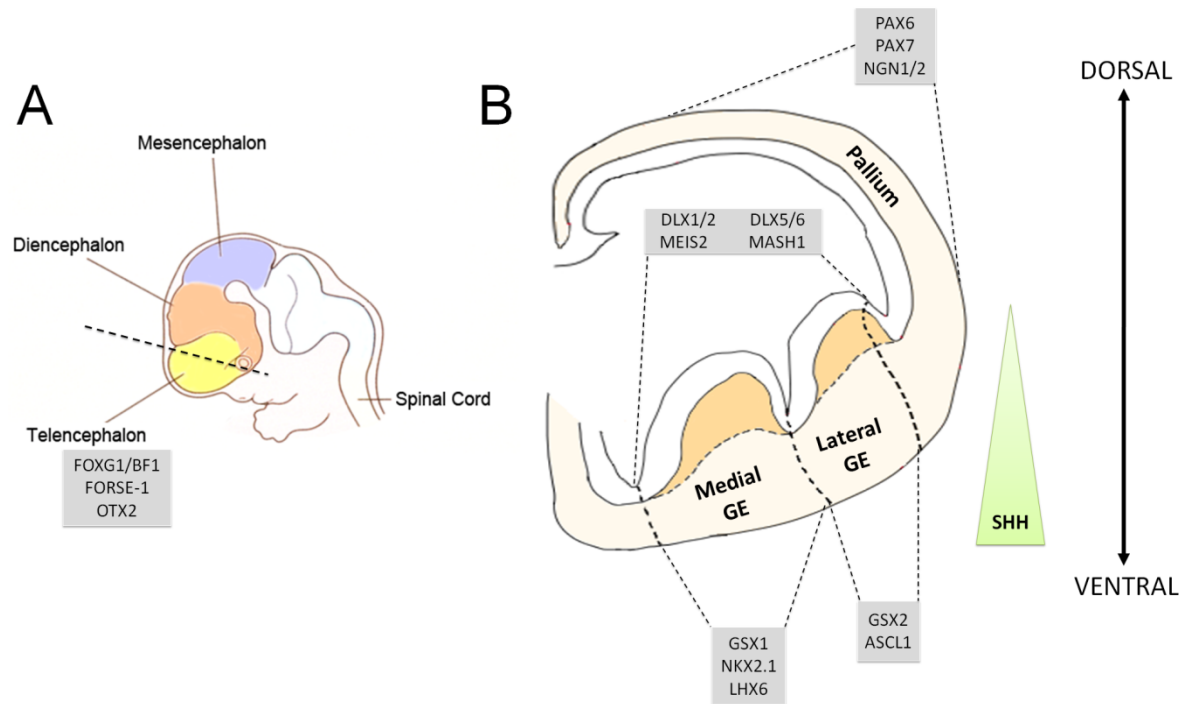
Figure 5.1: Depiction of an E12.5 mouse embryo, with major CNS regions highlighted and key markers of the telencephalon **(A)**. E12.5 coronal section of the telencephalon, cut at an angle approximate to the dashed line in A, with various regions and discriminating genes identified **(B)**.

Alternatively, existing protocols that claim to generate bona fide LGE GABAergic neurons could be applied to HD hPSCs. The first definitive generation of these neural cells was reported by Mark Perchansky's research group in Paris (Aubry et al., 2008). While this seminal work represented a significant milestone towards a viable cell transplantation option for HD, it was restricted in its ability to produce GABAergic striatal neurons with only ≈11% of cells DARPP32+. Furthermore, the protocol incorporated numerous variable factors and cells exhibited excessive tumour growth upon transplantation. More recently, publication of two protocols in 2011 and 2012, produced significantly higher proportions of GABAergic striatal neurons, avoided transplantation overgrowth and lead to behavioural improvements in HD models (Carri et al., 2012;Ma et al., 2012). These protocols present an opportunity to generate HD neurons with the precise regional and neurotransmitter subtypes, a powerful tool perfectly poised to decipher the rich tapestry of molecular dysfunction that underlies neuropathology and, an optimal platform for screening novel therapeutic compounds.

The NDEB methodology may further prove useful for studying lines carrying genetic insults associated with other forebrain neuropathologies such as epilepsy, Alzheimer's disease and related polyglutame expansion disorders, where the elucidation of subtle phenotypes would benefit tremendously from strict differentiation synchronisation and uniformity. Pursuant to these aims, future studies could extend the spin aggregation system described here with the addition of patterning factors that antagonise or agonise relevant signalling pathways for appropriate regionalisation and sub-type specification to generate the specific subsets of neurons associated with the aforementioned disorders. Contemporary protocols indicate optimal patterning is achieved with very early administration of signalling factors (Kriks et al., 2011;Carri et al., 2012;Denham et al., 2012a;Maroof et al., 2013), and as such, primitive neuroectodermal cells within d1-7 NDEBs appear a logical target window. For example, ventralisation could be achieved by the early addition of SHH and/or small molecule agonist purmorphamine to generate floor plate diencephalic or MGE populations as previously shown (Maroof et al., 2013;Nicholas et al., 2013). In addition, extended SMAD inhibition could be used to promote a default rostral-dorsal identity as shown recently (Nicoleau et al., 2013).

5.3 HD stem cell models and future research possibilities

Recently, mouse and human iPSC lines harbouring HD mutations have been assessed for disease hallmarks (Camnasio et al., 2012;Castiglioni et al., 2012;HDIPSCC, 2012;Jeon et al., 2012), and some classical HD phenotypes have been observed in these models, including transcriptional dysregulation, CAG repeat instability, mutant HTT aggregates, cholesterol biosynthesis perturbation, lysosomal dysfunction and neuronal vulnerability. Importantly, similar phenotypic observations were noted in this thesis from the SI-186 and SI-187 lines, such as gene expression alterations, CAG repeat instability and aberrant calcium signalling.

It is unsurprising that the greatest success in detecting disease phenotypes in HD hPSCs have arisen from the interrogation of lines carrying CAG repeats equivalent to egregious early onset sub-types (CAG180; HDIPSCC, 2012). These repeat ranges are equivalent to juvenile and infantile HD onset which may exhibit different mechanisms not truly reflective of clinically typical HD patients (Squitieri et al., 2006). Therefore, lines harbouring repeat ranges such as those assessed within this thesis may represent a more informative model of HD. If however typical late-onset lines do not exhibit HD at a level necessary for investigating pathology due to the embryonic nature of these lines, future experiments may need to accelerate or exacerbate disease pathology. Extended *in vitro* culture protocols, such as those recently developed by Elena Cattaneo's laboratory (Carri et al., 2012), could achieve this by prolonging neuronal maturation of HD cells, whereas lactacystin administration presents another more drastic option as an inhibitor of the ubiquitin-proteasome system and autophagy-lysosomal system which therefore antagonises the cellular ability for mHTT clearance (Ravikumar et al., 2002). Future studies could also utilise techniques with greater sensitivity for detecting post-onset, and particularly, pre-onset HD hallmarks, such as mRNA and microRNA arrays for measuring gene dysregulation or transmission X-ray spectroscopy for identifying aggregate precursors.

Unfortunately, HD ascribed phenotypes in the hESC lines of this study and emergent iPSC models demonstrate considerable interline variability in both individual HD hallmarks (i.e. differential gene dysregulation) and even outright contradictory observations in the variety of hallmarks observed (i.e. CAG repeat instability presence vs absence). Interestingly HD

143

phenotypic variation was also observed across the two lines of this study; with neural progeny of the SI-187 expansion line demonstrating aberrant calcium signalling, while progeny of the SI-186 line displayed minor repeat instability.

Indeed, overall the phenotypic picture that has emerged from studies of HD hPSC lines is conflicting and the underlying factors remain unclear. From a speculative point of view, two factors are likely. The first being the existence of a pathological gradient across the vast CAG repeat ranges of the lines utilised throughout the research community (CAG37-CAG181), with various repeat lengths eliciting a differential degree of pathological mechanisms and hallmarks. Secondly, an inevitable corollary of isolating lines from individuals/embryos with unique genetic backgrounds is a variety of uncontrollable genetic modifiers that interact either directly with mHTT or indirectly with a perturbed system, and account for over 30% of the age of onset (reviewed in Gusella and MacDonald, 2009).

To address these potential factors, comparisons of lines spanning the full gamut of CAG repeat lengths is warranted and should incorporate tracts associated with distinct human phenotypes (i.e. CAG35-39/late onset, CAG40-59/typical onset, CAG60-79/juvenile onset, CAG80+/infantile onset). Such a study would also benefit immensely by simultaneously overcoming the 'noise' of interline variation by developing this spectrum of CAG expansions in a cohort of isogenic hPSC lines generated with the knockin of CAG expansions into one specific wildtype line. Emerging genome-editing methodologies, such as TALENs (Beurdeley et al., 2013) are a precise and rapid technology that could be readily adapted for this task so that more meaningful comparative studies of defined HD lines can be undertaken.

Eliminating inherent cell line variability with a cohort of isogenic HD lines encompassing a range of CAG expansions would represent a significant milestone by providing the most optimal system for modelling human HD. This would yield particularly valuable information to determine the number of CAG repeat expansions that accurately and efficaciously reflect clinical HD and provide a focus for prospective research efforts. This focus could enable concerted and fastidious dissection of the relationship between various pathological mechanisms and contributing weight of each in a universally accepted gold standard system and hopefully advance the development of efficacious and novel therapeutic strategies.

5.4 Conclusion

This thesis presents a detailed characterisation of HD hESCs which carry typical CAG repeat expansions. By expressing the sole mutant protein responsible for this devastating disease, these HD cell lines are primed to activate a cascade of negative molecular events and eventually neurodegeneration. This provide a unique system to probe both pre- and post-onset changes in a human *in vitro* molecular and neurological context, The results described in this thesis demonstrate the potential of such HD model systems to provide a platform to interrogate the chronology and hierarchy of disease mechanisms and hallmarks. This work and future studies utilising disease hPSC lines will hopefully advance our understanding HD's complex pathological tapestry and facilitate the identification of candidate therapeutics.

5.5 References

Aubry, L., Bugi, A., Lefort, N., Rousseau, F., Peschanski, M., and Perrier, A.L. (2008). Striatal progenitors derived from human ES cells mature into DARPP32 neurons in vitro and in quinolinic acid-lesioned rats. *Proceedings of the National Academy of Sciences of the United States of America* 105, 16707-16712.

Beurdeley, M., Bietz, F., Li, J., Thomas, S., Stoddard, T., Juillerat, A., Zhang, F., Voytas, D.F., Duchateau, P., and Silva, G.H. (2013). Compact designer TALENs for efficient genome engineering. *Nature communications* 4, 1762.

Camnasio, S., Carri, A.D., Lombardo, A., Grad, I., Mariotti, C., Castucci, A., Rozell, B., Riso, P.L., Castiglioni, V., Zuccato, C., Rochon, C., Takashima, Y., Diaferia, G., Biunno, I., Gellera, C., Jaconi, M., Smith, A., Hovatta, O., Naldini, L., Di Donato, S., Feki, A., and Cattaneo, E. (2012). The first reported generation of several induced pluripotent stem cell lines from homozygous and heterozygous Huntington's disease patients demonstrates mutation related enhanced lysosomal activity. *Neurobiol Dis* 46, 41-51.

Carri, A.D., Onorati, M., Lelos, M.J., Castiglioni, V., Faedo, A., Menon, R., Camnasio, S., Vuono, R., Spaiardi, P., Talpo, F., Toselli, M., Martino, G., Barker, R.A., Dunnett, S.B., Biella, G., and Cattaneo, E. (2012). Developmentally coordinated extrinsic signals drive human pluripotent stem cell differentiation toward authentic DARPP-32+ medium-sized spiny neurons. *Development (Cambridge, England)* 140, 301-312.

Castiglioni, V., Onorati, M., Rochon, C., and Cattaneo, E. (2012). Induced pluripotent stem cell lines from Huntington's disease mice undergo neuronal differentiation while showing alterations in the lysosomal pathway. *Neurobiology of Disease* 46, 30-40.

Denham, M., Bye, C., Leung, J., Conley, B.J., Thompson, L.H., and Dottori, M. (2012a). GSK3β and Activin/Nodal Inhibition in Human Embryonic Stem Cells Induces a Pre-Neuroepithelial State that is Required for Specification to a Floor Plate Cell Lineage. *Stem Cells*.

Denham, M., Parish, C.L., Leaw, B., Wright, J., Reid, C.A., Petrou, S., Dottori, M., and Thompson, L.H. (2012b). Neurons derived from human embryonic stem cells extend long-distance axonal projections through growth along host white matter tracts after intra-cerebral transplantation. *Frontiers in cellular neuroscience* 6, 11.

Eiraku, M., Watanabe, K., Matsuo-Takasaki, M., Kawada, M., Yonemura, S., Matsumura, M., Wataya, T., Nishiyama, A., Muguruma, K., and Sasai, Y. (2008). Self-Organized Formation of Polarized Cortical Tissues from ESCs and Its Active Manipulation by Extrinsic Signals. *Stem Cell* 3, 519-532.

Gusella, J.F., and Macdonald, M.E. (2009). Huntington's disease: the case for genetic modifiers. *Genome medicine* 1, 80.

Hdipscc (2012). Induced pluripotent stem cells from patients with Huntington's disease show CAG-repeat-expansion-associated phenotypes. *Cell Stem Cell* 11, 264-278.

Jeon, I., Lee, N., Li, J.Y., Park, I.H., Park, K.S., Moon, J., Shim, S.H., Choi, C., Chang, D.J., Kwon, J., Oh, S.H., Shin, D.A., Kim, H.S., Do, J.T., Lee, D.R., Kim, M., Kang, K.S., Daley, G.Q., Brundin, P., and Song, J. (2012). Neuronal properties, in vivo effects,

and pathology of a Huntington's disease patient-derived induced pluripotent stem cells. *Stem Cells* 30**,** 2054-2062.

Kim, J.-E., O&Apos;Sullivan, M.L., Sanchez, C.A., Hwang, M., Israel, M.A., Brennand, K., Deerinck, T.J., Goldstein, L.S.B., Gage, F.H., Ellisman, M.H., and Ghosh, A. (2011). Investigating synapse formation and function using human pluripotent stem cell-derived neurons. *Proceedings of the National Academy of Sciences of the United States of America* 108**,** 3005-3010.

Kriks, S., Shim, J.-W., Piao, J., Ganat, Y.M., Wakeman, D.R., Xie, Z., Carrillo-Reid, L., Auyeung, G., Antonacci, C., Buch, A., Yang, L., Beal, M.F., Surmeier, D.J., Kordower, J.H., Tabar, V., and Studer, L. (2011). Dopamine neurons derived from human ES cells efficiently engraft in animal models of Parkinson's disease. *Nature* 480**,** 547-551.

Ma, L., Hu, B., Liu, Y., Vermilyea, S.C., Liu, H., Gao, L., Sun, Y., Zhang, X., and Zhang, S.-C. (2012). Human Embryonic Stem Cell-Derived GABA Neurons Correct Locomotion Deficits in Quinolinic Acid-Lesioned Mice. *Stem Cell***,** 1-10.

Maroof, A.M., Keros, S., Tyson, J.A., Ying, S.W., Ganat, Y.M., Merkle, F.T., Liu, B., Goulburn, A., Stanley, E.G., Elefanty, A.G., Widmer, H.R., Eggan, K., Goldstein, P.A., Anderson, S.A., and Studer, L. (2013). Directed differentiation and functional maturation of cortical interneurons from human embryonic stem cells. *Cell stem cell* 12**,** 559-572.

Nicholas, C.R., Chen, J., Tang, Y., Southwell, D.G., Chalmers, N., Vogt, D., Arnold, C.M., Chen, Y.J., Stanley, E.G., Elefanty, A.G., Sasai, Y., Alvarez-Buylla, A., Rubenstein, J.L., and Kriegstein, A.R. (2013). Functional maturation of hPSC-derived forebrain interneurons requires an extended timeline and mimics human neural development. *Cell stem cell* 12**,** 573-586.

Nicoleau, C., Varela, C., Bonnefond, C., Maury, Y., Bugi, A., Aubry, L., Viegas, P., Bourgois-Rocha, F., Peschanski, M., and Perrier, A.L. (2013). ES Cells Neural Differentiation Qualifies the Role of Wnt/beta-Catenin Signals in Human Telencephalic Specification and Regionalization. *Stem Cells*.

Ravikumar, B., Duden, R., and Rubinsztein, D.C. (2002). Aggregate-prone proteins with polyglutamine and polyalanine expansions are degraded by autophagy. *Human molecular genetics* 11**,** 1107-1117.

Squitieri, F., Frati, L., Ciarmiello, A., Lastoria, S., and Quarrell, O. (2006). Juvenile Huntington's disease: does a dosage-effect pathogenic mechanism differ from the classical adult disease? *Mechanisms of ageing and development* 127**,** 208-212.

Thenbsphdnbspipscnbspconsortium (2012). Induced Pluripotent Stem Cells from Patients with Huntington's Disease Show CAG-Repeat-Expansion-Associated Phenotypes. *Stem Cell* 11**,** 264-278.

Verlinsky, Y., Strelchenko, N., Kukharenko, V., Rechitsky, S., Verlinsky, O., Galat, V., and Kuliev, A. (2005). Human embryonic stem cell lines with genetic disorders. *Reproductive biomedicine online* 10**,** 105-110.

Appendix I

Generation of Induced Pluripotent Stem Cells from Human Kidney Mesangial Cells

Bi Song,* Jonathan C. Niclis,* Maliha A. Alikhan,* Samy Sakkal,* Aude Sylvain,*
Peter G. Kerr,[†] Andrew L. Laslett,[‡§] Claude A. Bernard,* and Sharon D. Ricardo*

*Monash Immunology and Stem Cell Laboratories, Monash University; [†]Department of Medicine, Monash Medical Centre, Australia, Clayton, Australia; [‡]CSIRO Materials Science and Engineering, Clayton, Australia; [§]Department of Anatomy and Developmental Biology, Monash University, Clayton, Australia

ABSTRACT

Glomerular injury and podocyte loss leads to secondary tubulointerstitial damage and the development of fibrosis. The possibility of genetically reprogramming adult cells, termed induced pluripotent stem cells (iPS), may pave the way for patient-specific stem-cell-based therapies. Here, we reprogrammed normal human mesangial cells to pluripotency by retroviral transduction using defined factors (*OCT4, SOX2, KLF4* and *c-Myc*). The kidney iPS (kiPS) cells resembled human embryonic stem-cell-like colonies in morphology and gene expression: They were alkaline phosphatase-positive; expressed OCT3/4, TRA-1 to 60 and TRA-1 to 81 proteins; and showed downregulation of mesangial cell markers. Quantitative (qPCR) showed that kiPS cells expressed genes analogous to embryonic stem cells and exhibited silencing of the retroviral transgenes by the fourth passage of differentiation. Furthermore, kiPS cells formed embryoid bodies and expressed markers of all three germ layers. The injection of undifferentiated kiPS colonies into immunodeficient mice formed teratomas, thereby demonstrating pluripotency. These results suggest that reprogrammed kidney induced pluripotent stem cells may aid the study of genetic kidney diseases and lead to the development of novel therapies.

Over two-thirds of patients with chronic kidney disease who progress to end-stage renal failure suffer from glomerular disorders.[1] Irreparable damage to glomerular cells leading to podocyte loss are common to a number of glomerulopathies that are responsible for the initiation and progression of tubulointerstitial fibrosis and impaired renal function.[2–5] The major challenge in renal regeneration involves replacing damaged glomerular cells to enable the spontaneous regeneration of damaged tubules.[6,7]

The cellular components of the glomerulus are developmentally derived from the mesenchyme and are considered highly terminally differentiated with a limited capacity to replicate *in situ*.[2,8,9] The location of progenitor cells within the kidney remains elusive.[10] However, recently, Ronconi *et al.*[11] reported a heterogenous subset of CD133$^+$CD24$^+$ progenitor cells capable of replacing both glomerular and tubular epithelial cells. These cells, located in the Bowman's capsule, may migrate to the glomerular tuft and differentiate into podocytes, leading to podocyte replacement following injury.[11] Mesangial cells that comprise specialized pericytes of the glomerulus represent another cell type important in maintaining normal glomerular structure and in regulating blood flow of the glomerular capillaries through their contractile activity.[12]

The direct reprogramming of somatic cells to produce induced pluripotent stem (iPS) cells is a prominent recent advance in stem cell biology[13] and has attracted considerable attention in disease modeling, drug screening and regenerative medicine.[14] Pluripotent cells can be derived from fibroblasts in the mouse[13] and human[15,16] by the induced expression of four transcription factors (*OCT4, SOX2, KLF4* and *c-Myc*). The derivation of iPS cell lines from patients with genetic disorders may be achieved by reprogramming somatic cells toward a pluripotent state.[17–20] A fundamental question is whether terminally

differentiated kidney cells can be reprogrammed to pluripotency, that is, generate stem cells that have the potential to differentiate into all three germ layers. Our study, for the first time, provides proof-of-concept for the direct nuclear reprogramming of adult human mesangial cells to generate kidney-derived iPS (kiPS) cells.

RESULTS

Normal human mesangial cells (NHMCs) were used to derive iPS cell lines using genetic programming that consisted of transfection of 293FT cells with retroviral vectors using the genes *OCT3/4*, *SOX2*, *KLF4* and *c-Myc*, as previously reported.[3,4] After 5 d of transfection, NHMCs were reseeded on mouse embryonic fibroblast (MEF) feeders (for timeline, see Figure 1A). Compared with cultured NHMCs (Figure 1B), as early as 12 days after retroviral transduction, distinct colonies were evident exhibiting morphology similar to human embryonic stem (hES) cells that contained spontaneous differentiation at colony centers, a morphologic trait of hES colonies (Figure 1C). From 5×10^4 NHMCs, an average of 40 iPS colonies were observed. These colonies stained alkaline phosphatase-positive, a phenotypic assessment of undifferentiated ES/iPS cells (Figure 1D). To confirm that kiPS cells had the characteristics of typical iPS cells, we examined stem cell marker expression. Immunofluorescence microscopy showed that kiPS cells localized for OCT3/4, TRA-1 to 60 and TRA-1 to 81 proteins (Figure 1E–M) after long-term culture at passage 22.

The NHMCs were negative for protein expression of Factor VIII Related Antigen, cytokeratin 18/19 and von Willebrand factor (Lonza Walkersville Inc., USA). Using qPCR, a panel of markers was screened to determine the phenotype of the starting population, including the mesangial specific gene megsin.[21] NHMCs were found to express megsin, Thy-1, desmin, α-smooth muscle actin (α-SMA) and RUNX1,
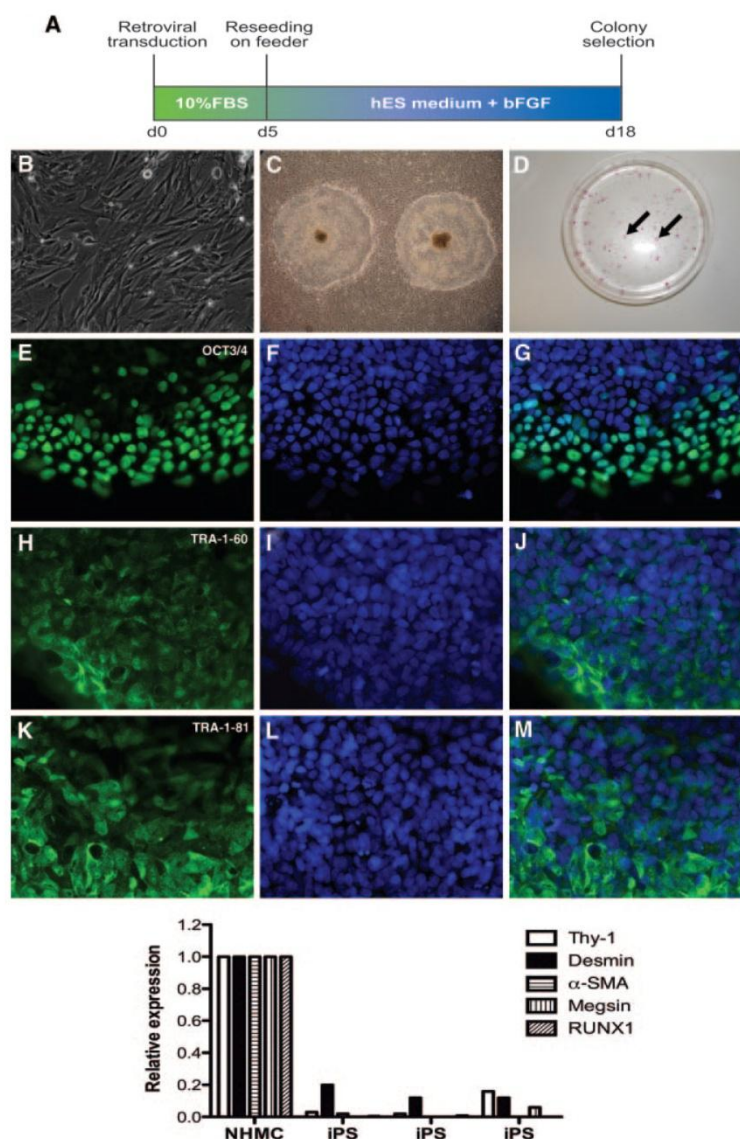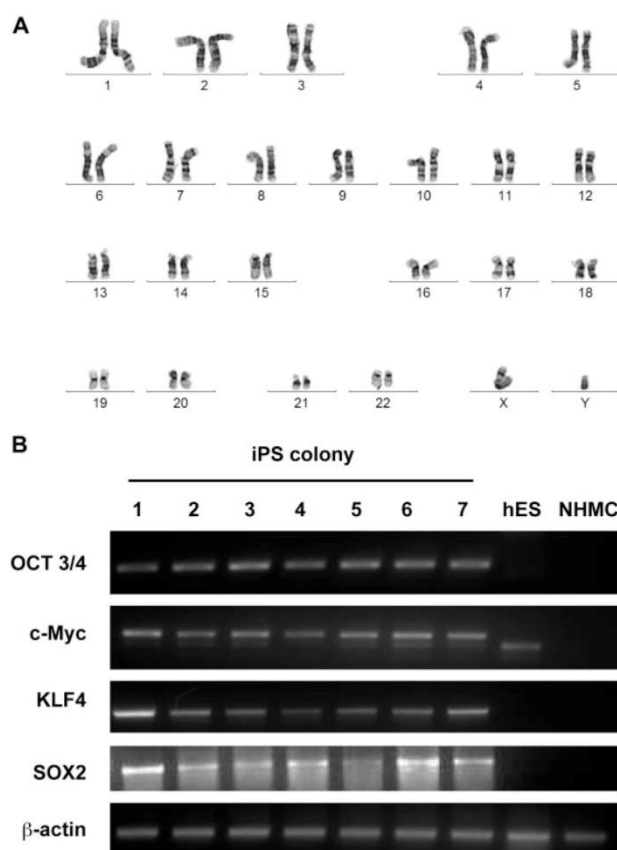

Figure 1. Kidney mesangial cell-derived iPS cells express stem cell markers. (A) The timeline of induction of iPS cells from human mesangial cells following retroviral transduction. (B) Representative images of normal cultured human mesangial cells reprogrammed to generate iPS colonies (C). (D) Alkaline phosphatase-positive iPS colonies (arrows). Immunofluorescence staining of mesangial cell-derived iPS colonies shows localization of OCT3/4 protein (E; green), with corresponding DAPI-stained nuclei (F; blue) and a merged image (G). TRA-1-60 (H–J) and TRA-1-81 (K–M) proteins are also expressed. Original magnifications (B, E–M ×400, C ×10). The graph in the lower panel shows qPCR of mesangial cell markers in NHMCs, with a downregulated expression in iPS cells from 3 separate colonies at passage 4. 120 × 189mm (600 × 600 DPI).

which were downregulated following differentiation to iPS cells at passage 4 (Figure 1).

The kiPS cells displayed a normal karyotype of 46XY (Figure 2A). PCR of genomic DNA confirmed the inte-

151

Figure 2. (A) The iPS colonies display a normal 46XY karyotype. (B) PCR of genomic DNA shows the integration of the target vectors in mesangial cell-derived iPS cells at passage 4. Lanes 1–7 show representative iPS cells following retroviral transduction, confirming the expression of OCT3/4, c-Myc, KLF4 and SOX2, compared to human embryonic stem (hES) cells (Lane 8) and normal cultured mesangial cells (NHMC; Lane 9). β-actin is shown as a loading control and for positive amplification. 154x218mm (600 × 600 DPI).

ferentiated EBs showed marker gene expression from endoderm (α-feto-protein; AFP), mesoderm (α-SMA) and ectoderm (neural cell adhesion molecule; NCAM), shown in Figure 4B. The expression of these genes was absent in undifferentiated cells from the same colonies (Figure 4B). RT-PCR confirmed that α-SMA was expressed in kiPS cells and NHMCs but not in hES cells (Figure 4B). Furthermore, immunofluorescence micros-copy of EBs at day 7 (Figure 4D,E) showed protein localization for desmin (mesoderm), Fox2 (endoderm) and nestin (ectoderm; not shown). To assess ectodermal lineage differentiation fur-ther, neural-directed EB differentiation was performed on hES and kiPS cells (Figure 4F and G) showing immunoflu-orescence staining of the neural stem cell marker nestin (Figure 4H, I) and β-iii-tubulin protein expression with microtubule-associated protein 2ab (MAP2ab) colocalization (Figure J, K) identifying neurons.

To test pluripotency *in vivo*, immu-nodeficient mouse recipients were in-jected with kiPS colonies. The forma-tion of encapsulated cystic teratomas (Figure 4L) were observed (3/3 mice) and showed differentiated tissues from all three germ layers (Figure 4M-S). Notably, the teratomas showed ev-idence of endoderm (respiratory epi-thelium, serous glands), mesoderm (muscle, nucleated red blood cells, car-tilage), and ectoderm (neural tis-sue). Taken together, our analyses of iPS colonies derived from retrovirally transduced human mesangial cells confirm pluripotent potential.

DISCUSSION

The culture of immortalized cell lines from kidney disease patients is an in-valuable resource for medical research but is largely limited to tumor cell lines or transformed derivatives of kidney tis-sue. Patient-derived iPS cell lines, using a reprogramming protocol of somatic cells from patients with genetic disor-ders,[22] will provide an opportunity to

gration of the target vectors in kiPS colonies (Figure 2B) but not in NHMCs. In addition, DNA genetic fingerprint analysis confirmed that the human iPS colonies were derived from the NHMC source and were not a result of cross contamination (Sup-plementary Figure 1). Reverse-tran-scriptase PCR (RT-PCR) analysis re-vealed that the kiPS cells expressed stem cell marker genes for OCT3/4, NANOG, SOX2, fibroblast growth factor (FGF)-4, reduced expression protein 1 (REX1), telomerase reverse transcriptase (hTERT), developmen-tal pluripotency-associated (DPPA)-2, DPPA4 and DPPA5. This was compa-rable to hES cells but different from

NHMCs (Figure 3A). qPCR using transgene-specific primers showed that the *OCT3/4*, *SOX2*, *KLF4* and *c-MYC* transgenes were absent in all 7 kiPS clones after four passages con-firming retroviral silencing (Figure 3B). In comparison, NHMCs at day 6 after retroviral transduction show an upregulated expression *OCT3/4*, *SOX2*, *KLF4* and *c-Myc* transgenes (Figure 3B). qPCR confirmed that rela-tive to hES cells, iPS cells expressed stem cell markers *OCT3/4*, *SOX2* and *NANOG*, with an absence of mRNA ex-pression in NHMCs (Figure 4A).
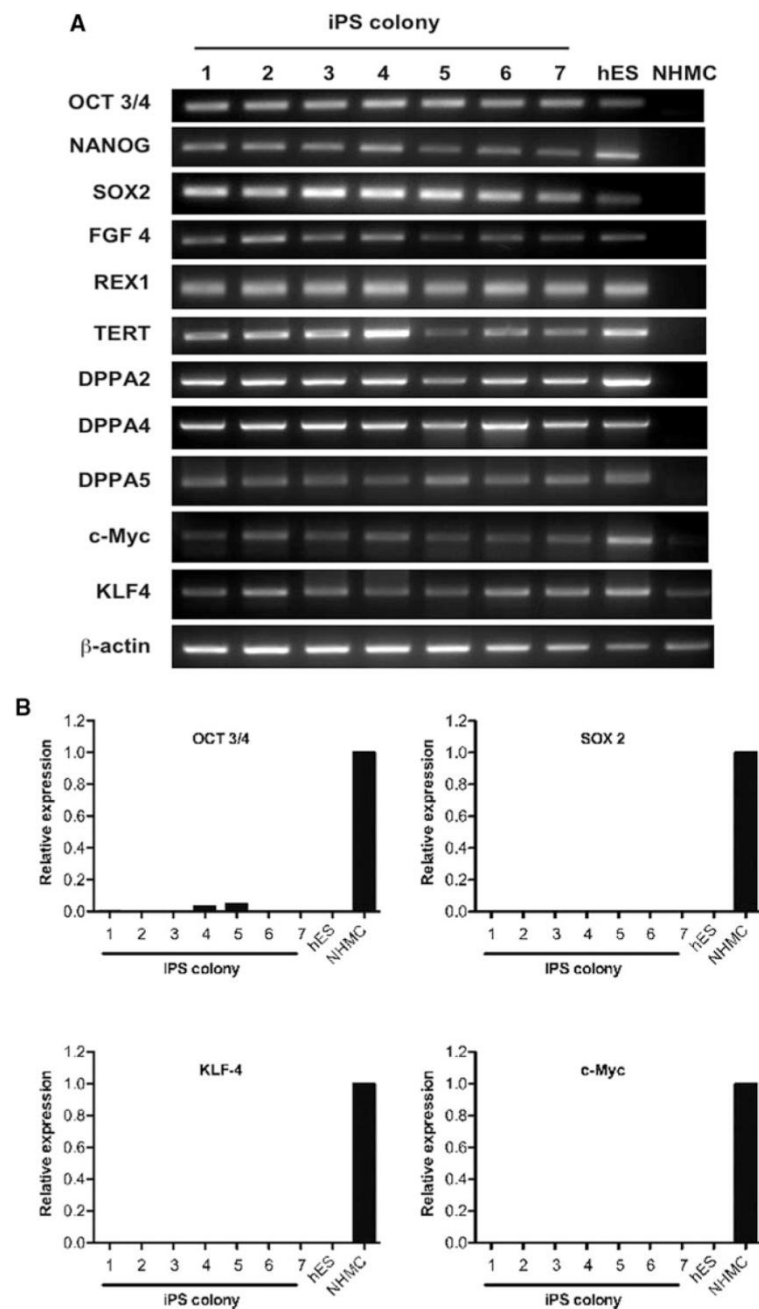
After 18 d in suspension culture, iPS cells had differentiated into em-bryoid bodies (EBs). RT-PCR of dif-

Figure 3. (A) RT-PCR analysis of stem cell marker genes in kiPS cells for expression of OCT3/4, NANOG, SOX2, FGF4, REX1, TERT, DPPA2, DPPA4, DPPA5, c-Myc and KLF4. Lanes 1–7 represent mesangial cell-derived iPS (kiPS) cells compared to hES cells (Lane 8) and the NHMC target cells at day 0 (Lane 9). The β-actin housekeeping gene is also shown. Panel (B) shows quantitative PCR using primers specific for the transgenes, and not detecting endogenous gene expression levels (shown in Panel A), which confirms retroviral transgene silencing in most kips colonies (passage 4). This is evidenced by a loss of OCT3/4, SOX2, KLF4 and c-Myc expression analogous to expression levels in hES cells. In comparison, an upregulated expression of OCT3/4, SOX2, KLF4 and c-Myc is observed in NHMCS at 6 days following retroviral induction. 112×196mm (150 × 150 DPI).

153
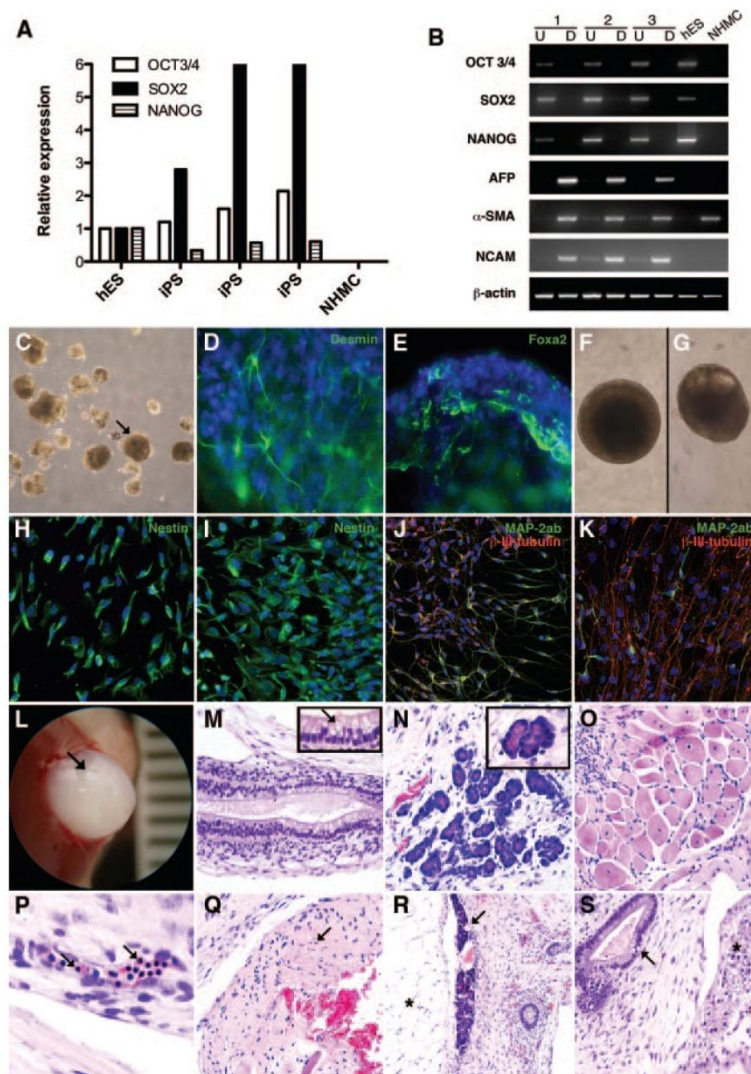
Figure 4. Kidney-derived iPS cells demonstrate pluripotency. (A) qPCR of stem cell markers OCT3/4, SOX2 and NANOG in kidney-iPS cells (kiPS) relative to human embryonic stem cells (hES), with an absence of expression in normal human mesangial cells (NHMCs). (B) RT-PCR shows undifferentiated iPS cells (U; Lanes 1, 3, 5) and hES expressed stem cell marker genes OCT3/4, SOX2 and NANOG. In comparison, differentiated embryoid bodies (EBs) (B; Lanes 2, 4, 6) expressed markers from all three germ layers, including α-fetoprotein (AFP; endoderm), α-smooth muscle actin (α-SMA; mesoderm) and neural cell adhesion molecule (NCAM; ectoderm), but did not express undifferentiated stem cell markers. kips formed EBs (C; arrow) with protein localization evident for desmin (D; mesoderm) and Foxa2 (E; endoderm) by immunofluorescence staining. Brightfield images of neural-directed EBs (NDEBs) from hES cells (F) and kiPS cells (G) at day 14. Immunofluorescence staining of NDEBs from hES cells show expression of nestin (H), β-iii-tubulin and MAP2ab (merged, J). In Panels D–K, DAPI-stained nuclei are evident in blue. Nestin (I), β-iii-tubulin and MAP2ab (merged, K) are also observed in NDEBs from kiPS. Original Magnifications C ×10; D, E ×400; F–K ×200. Teratomas are evident following the injection of undifferentiated kiPS cells into immunodeficient mice (L; arrow). Panels M–S show hematoxylin and eosin staining of tissues from all three germ layers, including endoderm; (M) pseudostratified ciliated respiratory epithelium with goblet cells (arrow inset Mag ×1000), (N) serous glands (acini shown in inset Mag ×1000), mesoderm; (O) muscle, (P) nucleated red blood cells (arrows); and endoderm: (Q) neural tissue. At lower power (Mag ×100), panels R and S show glandular tissue (arrows) in cystic teratomas adjacent to adipocytes (asterisk; R) and immature cartilage (asterisk; S). Original magnifications (K × 400; H–J, L ×200; M, N ×100). 120 × 173mm (600 × 600 DPI).

154

generate pluripotent cells for the facilitation of pharmaceutical development and small molecule screening specifically targeted at genetic disorders.[14] These cells could, in turn, be used for disease modeling and eventually autologous cell replacement therapies.

A fundamental question of reprogrammed somatic cells from patients with genetic kidney disease such as polycystic kidney disease [PKD[23,24]] and Alport Syndrome,[25] is whether the iPS cells can mimic the disease phenotype. iPS cells derived from patients with PKD and Alport Syndrome that maintain the disease genotype and phenotype indefinitely could be used for disease modeling[26] and screening compounds aimed at modifying epigenetic and/or transcriptional abnormalities,[27] important regulators of these genetic disorders.

Kim et al.[28] recently reported that iPS retain a lingering genome-wide epigenetic memory of their cell of origin.[28] Furthermore, histone methylation patterns and transcription profiles of genetically identical iPS cell lines derived from different somatic cell types were found to be distinctive to their tissue origin.[29] Our efficiency in generating iPS cells from human kidney mesangial cells was comparable to reports using human skin fibroblasts.[15,16] Further analysis will be necessary to determine the molecular and functional differences and differentiation potential of kidney-derived iPS cells to more efficiently generate mesoderm and kidney cells compared with iPS cells derived from fibroblasts and target cells from other sources.

A residual cellular epigenetic memory of mesangial cell-derived iPS cell lines may open a new avenue for the generation other glomerular cells, such as podocytes. The directed differentiation of mesangial cell-derived iPS lines to other kidney cell types must rely on the identification of antigenic and molecular markers to establish differentially upregulated genes important in podocyte development. We have recently used a FACS-based selective strategy underpinned by transcriptional profiling to isolate hES-derived cells that had differentiated toward a renal progenitor state.[30] A fraction of $CD24^+podocalyxin^+$ $GCTM2^{neg}$ differentiated hES cells were shown to express upregulated genes associated with metanephric mesenchyme in comparison to other cell lineages.[30]

In the long term, PKD and Alport patient-derived iPS lines could be generated to correct the genetic defect identified in the cells. A fundamental goal is to reprogram the somatic cells derived from genetic kidney disease patients and establish iPS cell lines that are indistinguishable from healthy individuals to be used in the development of cellular-based therapies, as has recently been reported in hematopoietic cells from patients with Fanconi anemia,[31] degenerative disorders including amyotrophic lateral sclerosis [ALS;[18]] and dyskeratosis congenita.[20] Ultimately, kiPS cell lines could become an essential tool for the exploration of high throughput screening of drugs, natural compounds and toxin screens for new drug discovery and pharmacologic testing, and to determine the potential of induced pluripotency as a therapeutic strategy.

CONCISE METHODS

Retroviral Transfection of Human Mesangial Cells

Primary normal human mesangial cells (NHMC) from an 18-yr-old male kidney (Lonza) were cultured in MsGM Mesangial Growth Media with 5% fetal bovine serum (FBS) at 37 °C. Retroviral vectors containing human *OCT3/4, SOX2, KLF4* and *c-Myc* were introduced into 293FT cells and the supernatant cultured with NHMCs for 24 h, as described previously.[16] After 5 d, the transduced NHMCs were reseeded onto MEF feeders in KO DMEM (Life Technologies Invitrogen, CA, USA) containing 20% KO (knockout) serum replacement and human basic FGF (10ng/ml). Eighteen days after transduction, colonies were mechanically dissociated for replating.

Embryoid Body Differentiation and Neural Staining

To test the differentiation capacity of iPS cells, floating suspension cultures were used to form EBs after 18 d of culture, as described previously.[15,16] For neural-directed EB differentiation, 3000 disassociated kiPS or HES3 cells were distributed to each well of a round-bottom ultra-low attachment 96-well plate (Corning, MA, USA) containing $100\mu l$ of Neurobasal Medium per well (Neurobasal A, 5% ITS-X, 2.5% Penicillin/Streptomycin, 5% Glutamax, 5% B27 and 5% N2; Invitrogen). Wells were also supplemented with 0.125% PVA, 1mM ROCK inhibitor Y-27632, 20ng/ml EGF and 20ng/ml FGF (R&D Systems, MN, USA) and incubated at 37 °C in 5% CO_2 in air. 100ng/ml of noggin per well (R&D Systems) was added at day 0 and 4. After 24 h, cell suspensions aggregated to form spheres or 'neural-directed embryoid bodies' (NDEBs). Media was changed at days 4 and 8, and every 2 d thereafter.

Aliquots of NDEBs were plated after 14 d in suspension onto glass cover slips coated with 10mg/ml Poly-D-Lysine and 5mg/ml Laminin (BD, NJ, USA), grown for a further 7 d in Neurobasal Medium containing 20ng/ml EGF and 20ng/ml FGF, and stained with antibodies for Nestin (ABcam, MA, USA). Further aliquots of NDEBs were plated after 21 d in suspension and grown for a further 14 d before staining with antibodies for β-iii-tubulin and MAP2ab (Millipore, MA, USA).

Alkaline Phosphatase Staining and Immunofluorescence Microscopy

Following 4% paraformaldehyde fixation, immunofluorescence for the hES-cell specific proteins TRA-1 to 60 and TRA-1 to 81 were performed using an ES cell characterization kit (Millipore) and an OCT-3/4 primary antibody (Santa Cruz Biotechnology, CA, USA). Antibodies for desmin (Dako, CA, USA), Foxa2 (Santa Cruz), Nestin (ABcam) were used for EB wholemount staining at day 7. Alkaline phosphatase staining for the phenotypic characterization of iPS cells was assessed using a Leukocyte Alkaline Phosphatase kit (Sigma Chem Co., USA).

PCR, Karyotype and Fingerprinting Analysis

RNA was extracted from iPS cells (passage 4), embryoid bodies (day 18 of differenti-

155

ation) and hES cells (H9 cell line obtained from the Australian Stem Cell Centre Core Laboratories, Monash University, Australia) using a Picopure RNA isolation kit (Bio-strategy, Victoria, Australia). PCR for endogenous stem cell marker genes was performed using platinum TaqDNA polymerase (Invitrogen) and a SuperScript III first-Strand Synthesis system (Invitrogen), according to the manufacturer's instructions, relative to a β-actin housekeeping gene. Quantitative PCR (qPCR) for mesangial cell and stem cell markers in NHMCs, iPS cells and hES (stem cell markers only) was performed using a Platinum Super-Mix-UDG (Invitrogen) with primers listed in Supplementary Figure 2. Transgene-specific PCR primers allowed for analysis of the quantitative expression of retrovirally expressed transgenes in iPS cells (passage 4) and NHMCS at 6 d following retroviral induction using a Platinum SYBR Green qPCR super-Mix-UDG (Invitrogen) and published primer sequences.[16]

Karyotype analysis was assessed in iPS cells at passage 5 (Southern Cross Pathology, Clayton, Australia). DNA was extracted using a DNase blood and Tissue Kit (Qiagen, CA, USA). Short tandem repeats-based DNA profiling was used for fingerprinting analysis to verify the genetic source of the iPS to their parent mesangial cells. An ABI Prism 3100 DNA sequencer was used with Genescan software (Applied Biosystems).

Teratoma Assay

Xenografts of undifferentiated mesangial cell-derived iPS colonies at passage 3 were transplanted under the kidney capsule of immune-compromised NOD-SCID mice (n = 3 animals). Teratoma formation was assessed after 8 wk in hematoxylin and eosin-stained paraffin sections.

ACKNOWLEDGMENTS

DISCLOSURES

None.

REFERENCES

1. Wiggins RC: The spectrum of podocytopathies: A unifying view of glomerular diseases. Kidney Int 71: 1205–1214, 2007
2. Kriz W: Progression of chronic renal failure in focal segmental glomerulosclerosis: Consequence of podocyte damage or of tubulointerstitial fibrosis? Pediatr Nephrol 18: 617–622, 2003
3. Ronconi E, Mazzinghi B, Sagrinati C, Angelotti ML, Ballerini L, Parente E, Romagnani P, Lazzeri E, Lasagni L: [The role of podocyte damage in the pathogenesis of glomerulosclerosis and possible repair mechanisms]. G Ital Nefrol 26: 660–669, 2009
4. Abbate M, Zoja C, Remuzzi G: How does proteinuria cause progressive renal damage? J Am Soc Nephrol 17: 2974–2984, 2006
5. Mundel P, Shankland SJ: Podocyte biology and response to injury. J Am Soc Nephrol 13: 3005–3015, 2002
6. Humphreys BD, Bonventre JV: The contribution of adult stem cells to renal repair. Nephrol Ther 3: 3–10, 2007
7. Humphreys BD, Valerius MT, Kobayashi A, Mugford JW, Soeung S, Duffield JS, McMahon AP, Bonventre JV: Intrinsic epithelial cells repair the kidney after injury. Cell Stem Cell 2: 284–291, 2008
8. Quaggin SE, Kreidberg JA: Development of the renal glomerulus: good neighbors and good fences. Development 135: 609–620, 2008
9. Shankland SJ: The podocyte's response to injury: Role in proteinuria and glomerulosclerosis. Kidney Int 69: 2131–2147, 2006
10. Little MH, Bertram JF: Is there such a thing as a renal stem cell? J Am Soc Nephrol 20: 2112–2117, 2009
11. Ronconi E, Sagrinati C, Angelotti ML, Lazzeri E, Mazzinghi B, Ballerini L, Parente E, Becherucci F, Gacci M, Carini M, Maggi E, Serio M, Vannelli GB, Lasagni L, Romagnani S, Romagnani P: Regeneration of glomerular podocytes by human renal progenitors. J Am Soc Nephrol 20: 322–332, 2009
12. Schlondorff D: The glomerular mesangial cell: An expanding role for a specialized pericyte. FASEB J 1: 272–281, 1987
13. Takahashi K, Yamanaka S: Induction of pluripotent stem cells from mouse embryonic and adult fibroblast cultures by defined factors. Cell 126: 663–676, 2006
14. Nishikawa S, Goldstein RA, Nierras CR: The promise of human induced pluripotent stem cells for research and therapy. Nat Rev Mol Cell Biol 9: 725–729, 2008
15. Park IH, Zhao R, West JA, Yabuuchi A, Huo H, Ince TA, Lerou PH, Lensch MW, Daley GQ: Reprogramming of human somatic cells to pluripotency with defined factors. Nature 451: 141–146, 2008
16. Takahashi K, Tanabe K, Ohnuki M, Narita M, Ichisaka T, Tomoda K, Yamanaka S: Induction of pluripotent stem cells from adult

17. Park IH, Arora N, Huo H, Maherali N, Ahfeldt T, Shimamura A, Lensch MW, Cowan C, Hochedlinger K, Daley GQ: Disease-specific induced pluripotent stem cells. Cell 134: 877–886, 2008
18. Dimos JT, Rodolfa KT, Niakan KK, Weisenthal LM, Mitsumoto H, Chung W, Croft GF, Saphier G, Leibel R, Goland R, Wichterle H, Henderson CE, Eggan K: Induced pluripotent stem cells generated from patients with ALS can be differentiated into motor neurons. Science 321: 1218–1221, 2008
19. Carvajal-Vergara X, Sevilla A, D'Souza SL, Ang YS, Schaniel C, Lee DF, Yang L, Kaplan AD, Adler ED, Rozov R, Ge Y, Cohen N, Edelmann LJ, Chang B, Waghray A, Su J, Pardo S, Lichtenbelt KD, Tartaglia M, Gelb BD, Lemischka IR: Patient-specific induced pluripotent stem-cell-derived models of LEOPARD syndrome. Nature 465: 808–812, 2010
20. Agarwal S, Loh YH, McLoughlin EM, Huang J, Park IH, Miller JD, Huo H, Okuka M, Dos Reis RM, Loewer S, Ng HH, Keefe DL, Goldman FD, Klingelhutz AJ, Liu L, Daley GQ: Telomere elongation in induced pluripotent stem cells from dyskeratosis congenita patients. Nature 464: 292–296, 2010
21. Inagi R, Nangaku M, Miyata T, Kurokawa K: Mesangial cell-predominant functional gene, megsin. Clin Exp Nephrol 7: 87–92, 2003
22. Park IH, Lerou PH, Zhao R, Huo H, Daley GQ: Generation of human-induced pluripotent stem cells. Nat Protoc 3: 1180–1186, 2008
23. Harris PC, Torres VE: Polycystic kidney disease. Annu Rev Med 60: 321–337, 2009
24. Torres VE, Harris PC: Autosomal dominant polycystic kidney disease: The last 3 years. Kidney Int 76: 149–168, 2009
25. Hudson BG, Tryggvason K, Sundaramoorthy M, Neilson EG: Alport's syndrome, Goodpasture's syndrome, and type IV collagen. N Engl J Med 348: 2543–2556, 2003
26. Osafune K: In vitro regeneration of kidney from pluripotent stem cells. Exp Cell Res 316: 2571–2577, 2010
27. Yang J, Cai J, Zhang Y, Wang X, Li W, Xu J, Li F, Guo X, Deng K, Zhong M, Chen Y, Lai L, Pei D, Esteban MA: Induced pluripotent stem cells can be used to model the genomic imprinting disorder Prader-Willi syndrome. J Biol Chem 285: 40303–40311, 2010
28. Kim K, Doi A, Wen B, Ng K, Zhao R, Cahan P, Kim J, Aryee MJ, Ji H, Ehrlich LI, Yabuuchi A, Takeuchi A, Cunniff KC, Hongguang H, McKinney-Freeman S, Naveiras O, Yoon TJ, Irizarry RA, Jung N, Seita J, Hanna J, Murakami P, Jaenisch R, Weissleder R, Orkin SH, Weissman IL, Feinberg AP, Daley GQ: Epigenetic memory in induced pluripotent stem cells. Nature 467: 285–290, 2010
29. Polo JM, Liu S, Figueroa ME, Kulalert W, Eminli S, Tan KY, Apostolou E, Stadtfeld M, Li Y, Shioda T, Natesan S, Wagers AJ, Mel-

156

nick A, Evans T, Hochedlinger K: Cell type
of origin influences the molecular and func-
tional properties of mouse induced pluri-
potent stem cells. *Nat Biotechnol* 28: 848–
855, 2010

30. Lin SA, Kolle G, Grimmond SM, Zhou Q,
Doust E, Little MH, Aronow B, Ricardo SD,
Pera MF, Bertram JF, Laslett AL: Subfrac-
tionation of differentiating human embry-
onic stem cell populations allows the isola-
tion of a mesodermal population enriched
for intermediate mesoderm and putative
renal progenitors. *Stem Cells Dev* 19:
1637–1648, 2010

31. Raya A, Rodriguez-Piza I, Guenechea G,
Vassena R, Navarro S, Barrero MJ, Con-
siglio A, Castella M, Rio P, Sleep E, Gon-
zalez F, Tiscornia G, Garreta E, Aasen T,
Veiga A, Verma IM, Surralles J, Bueren J,
Izpisua Belmonte JC: Disease-corrected
haematopoietic progenitors from Fanconi
anaemia induced pluripotent stem cells.
Nature 460: 53–59, 2009

Supplemental information for this article is available
online at http://www.jasn.org/.

157